A NON-INVASIVE ASSESMENT OF MOISTURE CONTENT OF MUNICIPAL SOLID WASTE IN A LANDFILL USING RESISTIVITY IMAGING

by

HUDA SHIHADA

Presented to the Faculty of the Graduate School of

The University of Texas at Arlington in Partial Fulfillment

of the Requirements

for the Degree of

DOCTOR OF PHILOSOPHY

THE UNIVERSITY OF TEXAS AT ARLINGTON

AUGUST 2011

ACKNOWLEDGEMENTS

I thank God for bestowing knowledge upon me and for giving me this great opportunity to pursue a doctoral degree. This work would have never been a success without the support of those who believed in me.

First, I would like to express my deepest gratitude to Dr. Sahadat Hossain, my mentor, for guiding me through this process with his experience and knowledge. I sincerely thank you for motivating me all the way during my doctoral journey and for allowing me to work at my own pace. Your constructive feedback strengthened the final product of my research.

I would like to thank Dr. Victoria Chen for guiding me through the statistical analysis portion of my research. I truly appreciate your timely response to all my questions. I thank Dr. Melanie Sattler, Dr. Laureano Hoyos, and Dr. Mohammad Najafi for devoting their time to serve in my committee. I really appreciate your valuable suggestions and advice.

I thank my husband and my life partner Eyad, whose patience, understanding, and support allowed me to accomplish my mission. I am deeply indebted and forever grateful. My precious boys, Jad and Majd, you are the most beautiful thing I have. I apologize for missing the many hours that I was supposed to spend with you.

Special thanks to my parents, who provided me with the best education opportunities, and to my sisters who are a great source of inspiration. You are all the reason for my success.

To my friends and colleagues with whom I had the pleasure working in the laboratory, thank you for your assistance and moral support throughout this process.

Finally, I would like to thank the City of Denton for funding this research, especially Vance Kemler (Director of Solid Waste) and David Dugger (Landfill Manager) for their support during all stages of this research.

July 1, 2011

ABSTRACT

A NON-INVASIVE ASSESMENT OF MOISTURE CONTENT OF MUNICIPAL SOLID WASTE IN A LANDFILL USING RESISTIVITY IMAGING

Huda Shihada, PhD

The University of Texas at Arlington, 2011

Supervising Professor: Sahadat Hossain

A bioreactor landfill is operated to enhance waste decomposition, gas production, and refuse stabilization. The fundamental aspect in the operation of a bioreactor landfill is the controlled addition of water and/or the recirculation of leachate into the landfill's waste mass. Since there is an increasing trend to operate landfills as bioreactor landfills, it is crucial to understand the moisture distribution within the landfill. Monitoring the moisture distribution within a bioreactor landfill is essential not only for the design and operation of leachate recirculation systems, but also to identify sites with non-uniform leachate distribution due to ponding and channeling.

In the recent years, there has been a huge interest in using electrical resistivity imaging (ERI) as a non-destructive tool to monitor the moisture distribution within a bioreactor landfill. ERI can detect variation in moisture content, because along with other

factors, resistivity varies with moisture content. ERI can produce detailed profiles of the subsurface, showing the spatial distribution of moisture within the landfill. However, these profiles do not give quantitative information about the moisture content of the waste.

The overall objective of this research is to develop a correlation between electrical resistivity and moisture content of waste, in order to be able to determine in situ moisture content of municipal solid waste (MSW) without any direct sampling and laboratory testing. Since electrical resistivity depends on several factors, an experimental program was developed to study the variation of electrical resistivity of MSW with moisture content, unit weight, stage of decomposition, temperature, composition of MSW, and composition of pore fluid. Fresh, landfilled, and degraded MSW samples were used for this study. Fresh and landfilled MSW samples were collected from the City of Denton landfill. Degraded MSW samples were prepared using laboratory scale reactors.

Laboratory results showed that resistivity is a complex property that depends on numerous factors. A trend of decreasing electrical resistivity with increasing moisture content was observed. For example, the resistivity of fresh MSW sample #1 decreased from 21.6 ohm-m at moisture content of 21.4% to 2.4 ohm-m at moisture content of 52.6%. Results showed that resistivity depends on unit weight. A trend of decreasing resistivity with increasing unit weight was observed. For example, the resistivity of fresh MSW sample #1 decreased from 21.6 ohm-m at unit weight of 35 lb/ft^3 to 14.9 ohm-m at unit weight of 55 lb/ft^3. Resistivity tests on decomposed MSW samples prepared in laboratory scale reactors indicated that electrical resistivity decreased with decomposition. Resistivity decreased from 8.98 ohm-m in phase 1 to 4.91 ohm-m in

phase 4. This decrease in is most probably caused by the increase in unit weight as a result of decomposition.

Results also showed that electrical resistivity of MSW decreases with increasing temperature. The resistivity of MSW decreased by about 2% per temperature increase of 1°C. MSW samples having same moisture content and same unit weight had different resistivity values, indicating that the composition of the waste itself affects resistivity. A decrease in electrical resistivity with increasing paper content was observed. On the other hand, an increase in electrical resistivity with increasing "others" (soil and fines) content was observed. Based on the experimental results, the effect of the pore fluid composition on the resistivity of MSW is not significant. Same MSW samples had almost identical resistivity values when prepared using tap water, leachate, or re-use water.

Multiple linear regression analysis was used to quantify the effect of the several factors that affect resistivity. Five predictor variables were considered: moisture content, unit weight, percentage paper, percentage "others" (fines), and organic content. The best model was selected using backward elimination method, best subsets selection method, and stepwise regression method. The developed model was validated using a second set of landfilled MSW samples. ERI was conducted at the same location from which the MSW samples were collected. Using the field resistivity values and the developed model, the moisture content was estimated. The estimated moisture content was then compared with the actual moisture content determined by oven drying the samples at the laboratory. Good agreement was found between the estimated moisture contents and the measured values. The percentage error ranged from 4.9 to 10.2 percent and from 0.5 to 13.8 percent for MSW samples from boreholes B70 and B72, respectively.

TABLE OF CONTENTS

LIST OF ILLUSTRATIONS

LIST OF TABLES

CHAPTER 1

INTRODUCTION

1.1 Background

Over the last few decades, the generation, recycling, and disposal of municipal solid waste (MSW) have changed substantially. In the United States, MSW generation has increased from 3.66 to 4.34 pounds per person per day between 1980 and 2009. About 243 million tons of municipal solid waste (MSW) was generated in 2009 (EPA, 2009). About 33.8% of MSW was recycled and composted, 11.9% was converted to energy, and 54.3% (about 132 million tons) was discarded in landfills. In the foreseeable future, landfilling is going to remain a major solid waste disposal method for MSW.

In conventional landfills that are designed and operated in accordance with Subtitle D of the Resource Conservation and Recovery Act (RCRA), efforts are typically made to minimize the moisture entering the landfill. The reason behind that is to minimize the generation of leachate and reduce the risk of groundwater contamination. However, the time required for the decomposition of waste in a dry tomb landfill ranges typically from 30 to 100 years. Also, the landfill gas is expected to be produced at a slow rate over a long period of time.

In the mid-1970s, Pohland (1975) proposed the idea of enhancing waste decomposition by recirculating the leachate and/or the addition of supplemental water. Additional moisture stimulates microbial activity by providing better contact between insoluble substrates, soluble nutrients, and microorganisms (Barlaz et al., 1990). As a

result, decomposition and biological stabilization of MSW can be reduced to years as compared to decades for traditional dry landfills. The fundamental aspect in the operation of a bioreactor landfill is the controlled addition of water and/or the recirculation of the generated leachate back into the landfill's waste mass. Several studies have pointed out the potential benefits of the bioreactor landfill approach (Barlaz et al., 1990; Reinhart and Townsend, 1998; Pacey, 1999; Warith, 2001), which include (1) increased rate of settlement of MSW which results in increasing the landfill's capacity, (2) increased rate of landfill gas production for energy recovery projects, (3) stabilization of waste occurs in a shorter time, reducing post closure monitoring cost, and (4) reduced leachate treatment and disposal costs. As a result of these benefits, there has been an increasing trend to operate landfills as bioreactor landfills, particularly in areas where landfill space is crucial.

According to the National Emissions Standards for Hazardous Air Pollutants (40 CFR 63.1990), a bioreactor landfill is defined as "a MSW landfill or a portion of a MSW landfill where any liquid, other than leachate or landfill gas condensate, is added in a controlled fashion into the waste mass (often in combination with recirculating leachate) to reach a minimum average moisture content of at least 40% by weight to accelerate or enhance the anaerobic biodegradation of the waste." Under current Texas regulations, MSW landfills are not allowed to operate as bioreactors. However, landfills are allowed to operate as Enhanced Leachate Recirculation (ELR) landfills as long as the average moisture content is maintained below 40% at all times.

1.2 Problem Statement

Since there is an increasing trend to operate landfills as bioreactor landfills, it is crucial to understand and monitor the moisture content and distribution within the landfill. Monitoring the moisture distribution within a bioreactor landfill is essential not only for the design and operation of leachate recirculation systems, but also to identify sites with non-uniform leachate distribution due to ponding and channeling as shown in Figure 1.1.

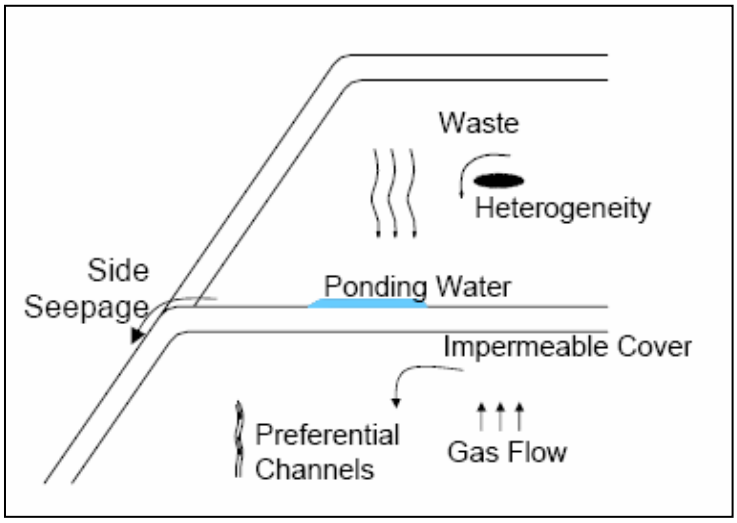

Figure 1.1 Processes Affecting Leachate Movement through a Landfill (ITRC, 2008)

Several methods have been developed and implemented to measure the moisture content of MSW (Imhoff et al. 2007). The most common methods are: (a) waste sampling using drilling (Figure 1.2), (b) moisture sensors, or (c) probe measurements, all of which are intrusive methods and provide data for localized waste. The major problems associated with these methods are:

(1) Although the direct method of waste sampling and determining the moisture content gravimetrically provides accurate waste moisture content, it is expensive to sample the waste and is intrusive to the containment of the waste. In addition, a large number of MSW samples are necessary for accurate determination of moisture distribution because of the waste heterogeneity.

(2) The moisture measuring probes such as time domain reflectometry (TDR) probes and sensors are commonly used to provide waste moisture. One of the limitations associated with using such probes is the poor contact between probes or sensors and waste.

(3) With time and solid waste decomposition, the moisture content of MSW is expected to change significantly. Also, solid waste materials are expected to settle considerably with time. Therefore, the possibility of sensors being lost or being short circuited during the leachate recirculation period is very high. This eventually leads to poor moisture content readings.

(4) The use of sensors is highly invasive and requires a lot of instrumentation. For example, a study conducted at the New River Regional Landfill in Florida (Figure 1.3) using the resistance based sensors method utilized approximately 65,000 ft of wiring.

(5) All of these methods provide localized information of moisture content, not a general view of the entire site.

Figure 1.2 Drilling Method to Collect MSW Samples

Figure 1.3 Resistance Sensors Study at New River Regional Landfill (Reinhart and Townsend, 2007)

Electrical Resistivity Imaging (ERI) is a non-destructive geophysical surveying method that provides large-scale coverage, compared to the drilling method that provides localized information only. Originating from the field of soil science, ERI is based on injecting current into the ground via an electrode pair and measuring the potential difference between another electrode pair (Dahlin, 2001). ERI has been widely used for environmental and geotechnical investigations. It has been used to investigate brownfield sites (Hobbs 1999), to investigate landslides (Drahor, 2006), to study a landfill cover (Carpenter et al., 1991), to map leachate plumes at landfills (Rosqvist et al., 2003), and to monitor leachate recirculation systems in landfills (Guerin et al., 2004;Grellier et al., 2008; Hossain et al., 2010).

ERI can detect variation in moisture content, because along with other factors, resistivity varies with moisture content. ERI can produce detailed profiles of the subsurface, showing the spatial distribution of moisture within the landfill. However, these profiles do not give quantitative information about the moisture content of the waste. Therefore, there is a need to develop a correlation between electrical resistivity and moisture content of waste, in order to be able to interpret field data without any direct sampling and laboratory testing.

Electrical resistivity is a physical property of the material and is affected by water content, temperature, porosity, particle size, pore fluid composition, and clay content (Ward, 1990). MSW samples in a landfill can have identical moisture contents, but still have different resistivity values because of different degrees of compaction and different stages of decomposition. Therefore, it is important to develop a correlation between electrical resistivity and moisture content, considering all the influencing factors.

1.3 Objectives

The overall objective of this research is to develop a correlation between electrical resistivity and moisture content of waste, in order to determine the in situ moisture content of MSW without any direct sampling and laboratory testing. Another objective of the current research is to develop a model to predict moisture content of MSW based on the resistivity imaging results. Finally the developed model will be validated using the actual field data.

The objective of this research is achieved by extensive literature review and laboratory testing. An experimental program was developed to study the variation of electrical resistivity of MSW with moisture content and with other factors that affect resistivity at the laboratory. The results from laboratory testing are then combined to develop a model that correlates electrical resistivity to the parameters that have a significant effect on resistivity of MSW in a bioreactor landfill. The specific tasks to achieve these objectives are:

1. Study the effect of moisture content on electrical resistivity of MSW.
2. Study the effect of unit weight on electrical resistivity of MSW.
3. Study the effect of decomposition on electrical resistivity of MSW.
4. Study the effect of temperature on electrical resistivity of MSW.
5. Study the effect of the composition of waste on electrical resistivity.
6. Study the effect of pore fluid composition on electrical resistivity of MSW.
7. Develop a statistical model using multiple linear regression (MLR) to correlate the electrical resistivity of MSW to the parameters that have a significant effect on resistivity of MSW.

8. Validate the developed model using electrical resistivity values obtained from field investigation.

1.4 Thesis Organization

This thesis is divided into six chapters as summarized below:

Chapter 1 provides an introduction and presents the problem statement and objectives of the research.

Chapter 2 presents a literature review of the characteristics of municipal solid waste, the stages of MSW decomposition, the different methods that have been used in the past to measure the moisture content of MSW, the theory behind electrical resistivity, the factors that affect electrical resistivity, and previous studies on MSW that utilized resistivity imaging.

Chapter 3 describes the experimental procedures followed to collect/prepare MSW samples, to determine the characteristics of the MSW, and to measure the resistivity of MSW as a function of several parameters.

Chapter 4 presents all the experimental results, discussion on the results, and comparison of the results with existing literature.

Chapter 5 presents the statistical modeling procedure using multiple linear regression. The developed model was then validated using resistivity values from field investigation.

Chapter 6 summarizes the main conclusions from the current research and provides some recommendations for future work.

CHAPTER 2

LITERATURE REVIEW

2.1 Characteristics of Municipal Solid Waste

The characteristics of MSW are very important for the design and operation of a bioreactor landfill. The reliable knowledge of MSW characteristics is important for the evaluation and prediction of landfill behavior. Determining the characteristics of MSW usually require physical sampling, drilling into the waste mass, and time-consuming laboratory testing. According to Manassero et al. (1996), determining the characteristics of MSW is challenging due to: 1) difficulties in collecting MSW samples which are representative of in situ condition, 2) lack of generally accepted sampling procedures, 3) change of MSW properties with time, and 4) heterogeneity of MSW within the landfill. The MSW characteristics of interest in this study are the physical composition, moisture content, unit weight, and organic content.

2.1.1 Physical Composition

Municipal solid waste (MSW) is the refuse consisting of everyday items that we consume and discard. It includes food waste, yard wastes, containers and product packaging, and other miscellaneous wastes from residential, institutional, and commercial sources. Physical composition refers to the individual components that make up a solid waste stream, commonly given as a percentage by weight. Information on the physical composition of MSW is necessary in the selection and operation of equipment at a

landfill, in assessing the feasibility of resource and energy recovery, and in the analysis and design of landfill disposal facilities (Tchobanoglous, 1993).

Municipal solid waste is heterogeneous in composition, reflecting the economic status and lifestyle of a community. According to EPA, the MSW generated in 2009 in the United States is comprised of the following: paper account for 28.2%; yard trimmings and food scraps account for another 27.8%; plastic make up 12.3%; metals make up 8.6%; leather and textile make up 8.3%; wood follows at around 6.5% and glass at 4.8%; and other miscellaneous wastes make up 3.5% as presented in Figure 2.1.

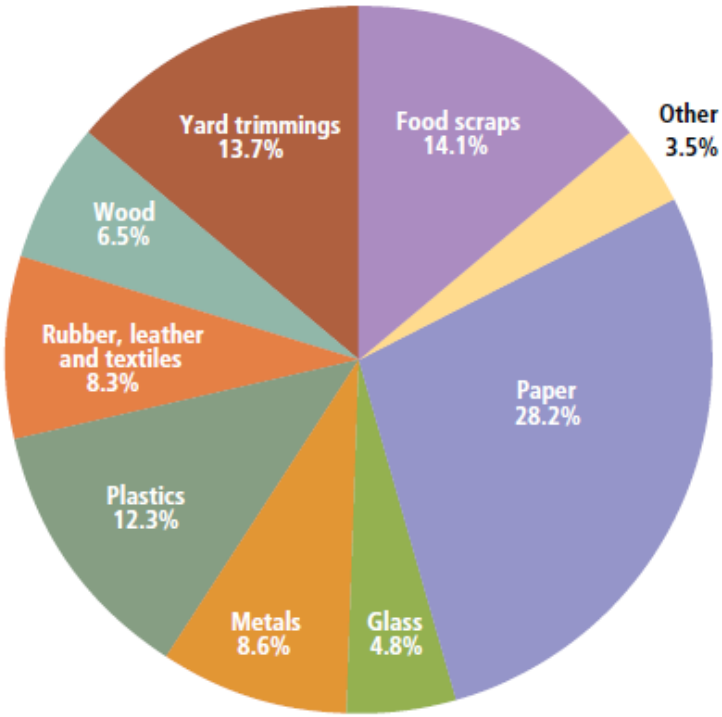

Figure 2.1 Total MSW Generation by Material Type (EPA, 2009)

2.1.2 Moisture Content

Moisture content is a measure of the amount of liquid within the waste. The moisture content can be defined in three different ways: (a) the ratio of the mass of liquid to the dry mass of the waste, (b) the ratio of the mass of liquid to the wet mass of the waste, or (c) the ratio of the volume of liquid to the volume of the waste (Reddy, 2006). The wet weight method is most commonly used in the solid waste field.

Several researchers determined that the control of the moisture content of MSW is the most important factor in accelerating waste decomposition in landfills (Pohland, 1975). The reason behind that is that increased moisture content enhances methanogenesis and stimulates microbial activity by providing better contact between insoluble substrates, soluble nutrients, and microorganisms (Barlaz et al., 1990).

A wide range of moisture content values of MSW have been reported in the literature. For most MSW in the United States, the moisture content will range from 15 to 40 percent, depending on the composition of the waste, the season of the year, humidity, and weather conditions (Tchobanoglous, 1993). Typically, higher moisture contents are reported when the samples are collected during the rainy season. According to Gabr and Valero (1995), there is a trend of increasing moisture content with depth. The authors reported that the moisture content varied from 30% for samples collected near surface to over 130% for samples collected at greater depths. Townsend et al. (1996) reported the moisture content of MSW at a landfill in North-Central Florida to be 31.3% before leachate recirculation compared with 45.7% after leachate recirculation. Gomes et al. (2005) reported moisture content ranging from 61% near the surface to over 117% at 11m depth for three years old waste at a landfill in Portugal.

Zornberg et al. (1999) estimated the gravimetric moisture content of 80 waste samples collected from boring from a landfill in southern California. According to the authors, the average moisture content (dry weight basis) was 28% and no significant trend of increasing moisture content with depth. An increasing trend of moisture with depth was observed when moisture contents results were expressed in terms of volumetric moisture contents. Reddy et al. (2009) estimated the dry gravimetric moisture content of fresh MSW collected from Orchard Hills Landfill in Illinois to be 44%.

2.1.3 Unit Weight

Unit weight is defined as the weight of waste per unit volume. Unit weight of MSW can vary widely depending mainly on the composition of the waste, the degree of compaction, the type of cover soil, and stage of decomposition. For bioreactor landfills, unit weight is a critical parameter because it affects the permeability of the waste, and thus affects the amount of leachate that needs to be recirculated and the amount of leachate that will be produced.

A wide range of unit weight values of MSW have been reported in literature. By in-situ unit weight measurements, Landva and Clark (1990) determined that the unit weight ranges from 6.8 to 16.2 kN/m^3 for MSW in landfills across Canada. Fassett et al. (1994) reported unit weights ranging from 3 to 9 kN/m^3 for fresh waste with poor compaction, 5 to 7.8 kN/m^3 for moderate compaction, and 8.8 to 10.5 kN/m^3 for good compaction.

Kavazanijan et al. (1996) reported MSW unit weights ranging from 10 to 13 kN/m^3 near the ground surface to 13 to 16 kN/m^3 at a depth of 30m based on a correlation with shear wave velocity measurements at six southern California landfills. According to

Kavazanijan (2001), the unit weight of MSW in a bioreactor landfill can sometimes approach or exceed 20 kN/m^3 due to the higher moisture contents. Zornberg et al. (1999) performed in-situ unit weight tests using the sand-cone method in a southern California landfill. The unit weight of the waste ranged from approximately 10 kN/m^{3}to 15 kN/m^3 between 8 m and 50 m below the landfill surface.

According to Zekkos et al. (2006), individual landfills have a characteristic MSW unit weight profile which is a function of waste composition, compaction, cover soil placement, liquids management, and confining stress. The authors proposed a hyperbolic model for MSW total unit weight as a function of depth as shown in Figure 2.2. This model is considered reasonable for typical conventional landfills with moisture contents at or below field capacity.

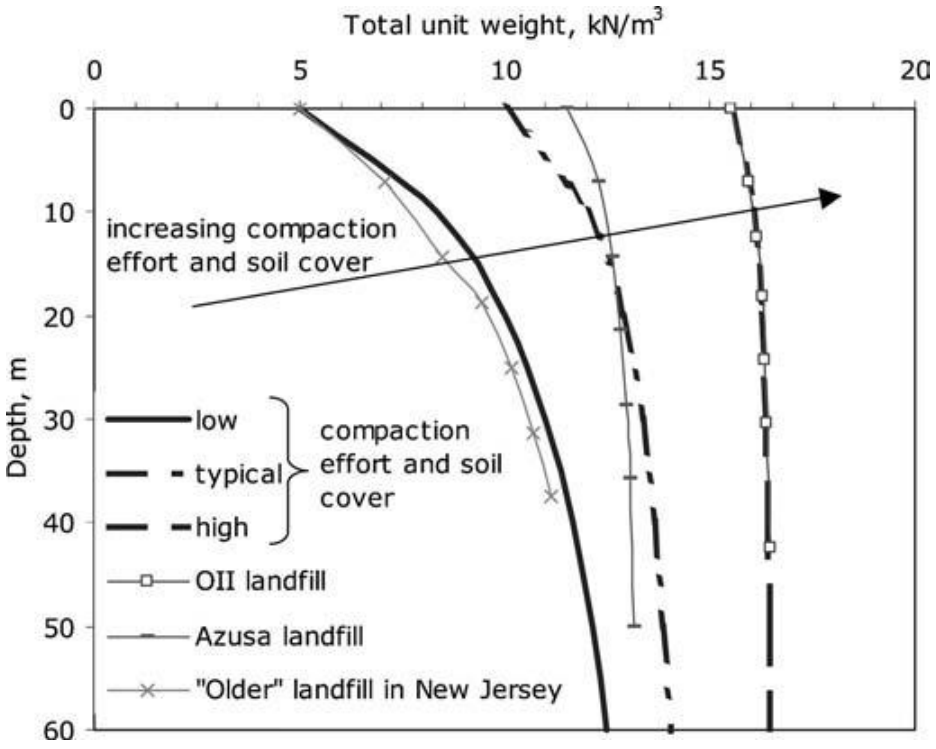

Figure 2.2 Unit Weight Profile with Depth for Conventional MSW Landfills (Zekkos et al., 2006)

2.1.4 Organic Content

Organic content is one of the main indicators of the state of decomposition of MSW. Decomposition results in a decrease in organic content. Organic content, also known as volatile solids (VS) and loss-on-ignition, is defined as the percent of weight loss on ignition at 550°C according to Standard Methods (APHA, 2005).

A wide range of organic content values have been reported in literature. Barlaz et al. (1990) reported an organic content of 79% for fresh MSW. Reddy et al. (2009) estimated the organic content of fresh MSW collected from Orchard Hills Landfill in Illinois to range from 76% to 84%.

Gabr and Valero (1995) determined the average organic content of aged waste from a depth of 19m to be 33%. Gomes et al. (2005) reported the variation of organic content with depth ranging from 43% to 63% near the surface and 56% at 11m depth at a landfill in Portugal. Hossain and Haque (2009) prepared degraded MSW samples in laboratory scale reactors. The authors determined that the organic content of MSW decreased from 94% in phase 1 of decomposition to 41% in phase 4.

Townsend et al. (1996) measured the organic content of MSW collected from a landfill in North-Central Florida in a four-year period, before and after the start of leachate recycle. The gross sample organic content decreased with sample age for the leachate recycle area and the control area, and both areas showed nearly identical fitted lines as shown in Figure 2.3.

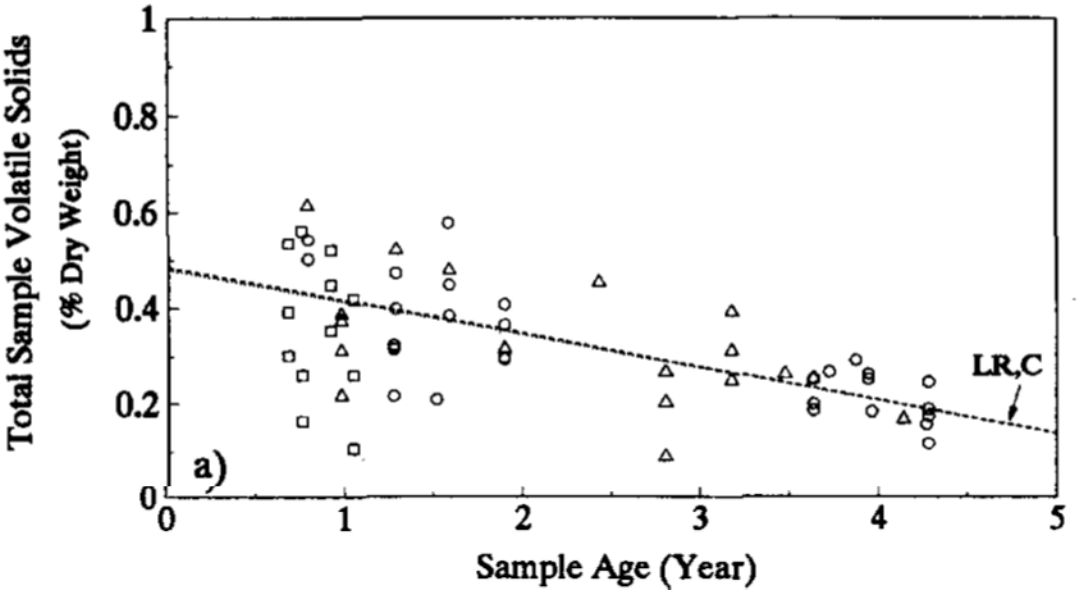

Figure 2.3 Organic Content vs. MSW Sample Age (Townsend et al., 1996)

Mehta et al. (2002) measured the organic content of MSW from two test cells at Yolo County, California to evaluate the effect of leachate recirculation on refuse decomposition. The authors found the average organic content in the control (without leachate recirculation) and enhanced (with leachate recirculation) samples to be 40.1% and 42.6%, respectively and this difference was not significant. This can be attributed to the inclusion of non-degradable components in the organic content test. According to the authors, the ratio of cellulose plus hemicellulose to lignin is a better indicator of the decomposition of MSW than the volatile solids test. Table 2.1 summarizes some of the organic content values of MSW as reported in the literature.

Table 2.1 Organic Contents of MSW as reported in Literature

Reference	Type of Waste and Age	Organic Content (%)
Barlaz (1990)	Fresh biodegradable waste	79
Gabr and Valero (1995)	Aged waste at 19m depth	33
Townsend (1996)	Aged Waste:	
	Gross sample	31.8
	Biodegradable fraction	83
Mehta (2002)	Aged Waste:	
	Control Cell	40.1
	Enhanced Cell	42.6
Gomes (2005)	Aged Waste at 11m depth	56
Hossain and Haque (2009)	Degraded Waste	
	Phase I	94
	Phase IV	41
Reddy (2009)	Fresh MSW	76 - 84

2.2 Decomposition of MSW

Municipal solid waste typically contains 40 to 50% cellulose, 12% hemicellulose, 10 to 15% lignin, and 4% protein on a dry weight basis (Barlaz et al., 1990). Cellulose and hemicellulose are the major biodegradable constituents of MSW and account for 90% of its methane potential. Three major groups of bacteria are involved in methane production from refuse (Barlaz et al., 1990): (1) the hydrolytic and fermentative bacteria, which convert cellulose and hemicelluloses to sugars which are then fermented to carboxylic acids, alcohols, carbon dioxide, and hydrogen; (2) the acetogenic bacteria, which convert carboxylic acids and alcohols to acetate, hydrogen, and carbon dioxide; and (3) the methanogenic bacteria, which convert acetate and hydrogen plus carbon dioxide to methane. The rate of refuse decomposition depends on several factors

including moisture content, pH, temperature, composition of waste, and the addition of nutrients and enzymes.

Numerous studies have been carried out on the anaerobic decomposition of MSW in landfills. Several researchers (Pohland and Harper, 1986; Barlaz et al., 1990; Reinhart and Al-Yousfi, 1996) have characterized the decomposition of MSW in four or five sequential phases between the burial of fresh MSW and well decomposed MSW. According to Barlaz et al. (1990), there are four distinct phases of refuse decomposition. Each phase is characterized by the quality of leachate and the quantity of landfill gas produced as shown in Figure 2.4. It is important to keep in mind that different sections in a landfill can be in different phases of decomposition at the same time, depending on when the waste was landfilled.

Phase 1: Aerobic Phase - In this phase, oxygen (from air trapped in the landfill) and nitrate will be depleted. The sugars present in the fresh waste will be converted to carbon dioxide and water. There is no methane production in this phase and the leachate strength is relatively low.

Phase 2: Anaerobic Acid Phase - In this phase, the oxygen is depleted and anaerobic conditions are established. This phase is characterized by an accumulation of carboxylic acids and a decrease in pH from 7.5 in fresh refuse to between 5.7 and 6.2. There is some cellulose and hemicellulose decomposition in this phase. Also, the methanogen population increases and methane is detected in the landfill gas. The principal gas generated in this phase is carbon dioxide.

Phase 3: Accelerated Methane Production Phase - In this phase, there is a rapid increase in the rate of methane production to some maximum value. Characteristic of this

phase is a methane concentration of 50 to 60%, a decrease in carboxylic acid concentrations, and an increase in the pH (from 6.2 to 7.9). Some additional solids decomposition occurs in this phase.

Phase 4: Decelerated Methane Production Phase - During this phase the methane concentration (about 60%) and pH remain at levels similar to those in phase three. The methane production rate decreases, the acetogen population increases, and carboxylic acids are depleted. The maximum rate of cellulose and hemicellulose decomposition occurs in this phase.

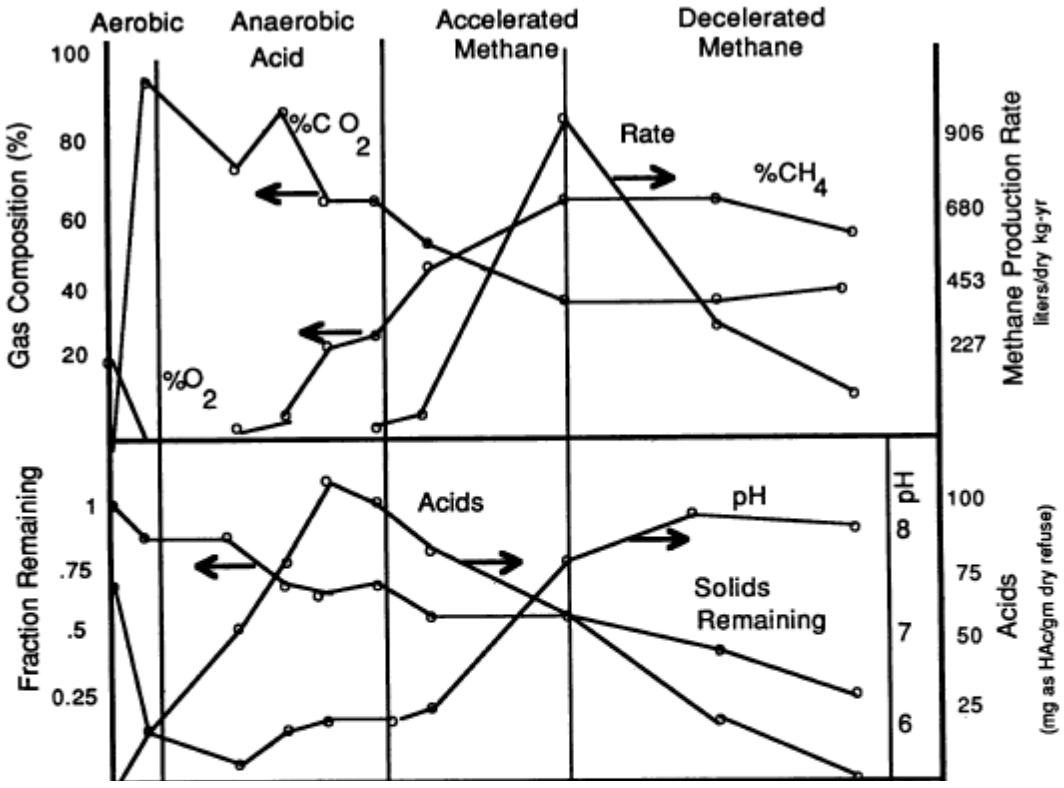

Figure 2.4 Trends in Refuse Decomposition with Leachate Recycle

2.3 Moisture Content Measuring Methods

The fundamental aspect of operating a landfill as a bioreactor landfill is the controlled addition of water and/or the recirculation of leachate into the landfill's waste mass. The main challenge in operating a bioreactor landfill is achieving an optimal and homogenous moisture content throughout the waste. Insufficient amounts of liquid will decrease rate of MSW decomposition. Excess amounts of liquid may cause geotechnical instability, side seeps, and slower gas production rates. The heterogeneity of the waste and the type of daily and intermediate covers used may result in non-uniform leachate distribution and incomplete use of available moisture. Ponding, channeling, and preferential flow paths (Zeiss and Uguccion, 1997; Rosqvist et al., 2005) of leachate are common problems encountered in bioreactor landfills.

At the present time, moisture content of MSW in landfill is commonly determined by using drilling to excavate MSW samples and then measuring the moisture content gravimetrically in the laboratory. This method provides moisture content information at certain points and does not represent a general view of moisture variation within the landfill. Also, the gravimetric method is costly and is not practical for long term monitoring of moisture distribution.

In the last ten years, a lot of effort has been made in the development of instruments to measure moisture content within landfills. Imhoff et al. (2007) summarized six methods that have been used for measuring water/liquids in landfills as follows:

Neutron Probe: The neutron probe emits neutrons from a radioactive source. As these neutrons travel in the medium their velocity is reduced (thermalized) by their collision with other atoms. Hydrogen is extremely effective at thermalizing neutrons. The concentration of the thermalized neutrons is proportional to the hydrogen ion content. When there is no other significant source of hydrogen atoms other than water molecules, the concentration of hydrogen atoms can be related to the moisture content. Limitations of this method include the presence of non- water bound hydrogen in wood and plastic materials in the landfill, the requirement to install aluminum access tubes in the field for entry of the neutron probe, and the expensive and highly regulated storage and disposal of the probe with its radioactive source.

Electrical resistance sensors: Electrical resistance sensors relate the electrical resistance to a current passing through the sensor to the matric potential of surrounding media. Sensors contain a porous medium, and water moves between this porous medium and the refuse until the medium and the refuse are at equilibrium with identical matric potentials. The resistance measured by the sensor is correlated to moisture content by laboratory calibration. Electrical resistance sensors are relatively inexpensive and easy to place in solid waste. Limitations of this method include the fact that sensor readings will be affected by wetting and drying cycles and the sensors tend to deteriorate over time.

Electromagnetic techniques: Several moisture measurement techniques have been developed based on the propagation of electromagnetic waves in porous media, including time domain reflectometry (TDR) and time domain transmissivity (TDT).Both techniques relate the time of travel of electromagnetic waves to the dielectric constant of the waste. This value can in turn be correlated to moisture content because of the significant

differences between the properties of water and other materials. Extracted waste samples are required to establish the relationship between the dielectric constant and the moisture content of waste.

Electrical resistivity tomography / imaging: ERI is based on measurement of the potential distribution arising when electrical current is injected into the ground via electrodes. ERI uses a set of electrodes that provides a large number of measurements. A 2-D or 3-D profile is generated when the data is interpreted. The resistivity variations that occur during leachate recirculation indicate changes in the waste moisture content. ERI holds promise for measuring water distributions, but have not been tested with independent measurements to quantify its accuracy.

Partitioning gas tracers: This method involves the injection and extraction of two tracers under steady gas flow within solid waste: one tracer is inert and non-reactive with refuse and water, while the second partitions into and out of water as it moves due to its affinity for the water phase. The arrival time of these two tracers is measured at a gas collection well, usually using gas chromatography to determine tracer concentrations in gas samples. Because the tracers are separated chromatographically in time due to the influence of water, the difference in mean arrival times is a measure of the fraction of the pore space occupied by water.

Fiber optic sensors: The fiber optic sensing technology is a rapid tool for measuring temperature and the rate of temperature change in solid waste. There are two methods for detecting changes in the volumetric water content or liquid flow in a landfill body. In the first method landfill temperatures and/or temperature changes are monitored. Leakage through sealing materials, side seeps, and unusual liquid flow can be detected by

anomalies in the temperature distribution. The second method combines temperature measurements with heat pulses. The fiber optic cable and nearby refuse are heated with an electrical heating cable. Depending on the local heat conductivity of the surrounding refuse and the flow velocity of the percolating fluid (water or gas), a specific temperature increase over time is measured in response to the heat pulse. As the amount of water in refuse increases, the thermal conductivity increases correspondingly, reducing the rate of temperature increase measured by the fiber optic cable.

2.4 Electrical Resistivity

2.4.1 Theory

Electrical resistivity is a measure of how well a material opposes the flow of electric current. Electrical resistivity is an intrinsic property of a material and is independent of volume, whereas resistance is dependent on the material's volume and geometry. For an element of length L and cross-sectional area A, resistance (R) is proportional to the length and inversely proportional to the cross-sectional area as follow:

$$R = \rho \frac{L}{A} \tag{2.1}$$

where ρ, the electrical resistivity in ohm-m, is the constant of proportionality. The reciprocal of resistivity is electrical conductivity commonly given in Siemens/m. According to Ohm's law, resistance is also defined as the ratio of the potential drop to the applied current:

$$R = \frac{V}{I} \tag{2.2}$$

where R is the resistance in ohms, V is the voltage in volts, and I is the current in amperes

In the resistivity method, artificially generated electric currents are injected into the ground and the resulting potential differences are measured at the surface. Potential

difference patterns provide information on the form of subsurface heterogeneities (Kearey et al., 2002). The injected current flows radially. In a homogenous and isotropic medium, hemispherical equipotentials (contours of equal electric potential) form perpendicular to the current flow lines as shown in Figure 2.5. The current density (J) is the current (I) divided by the area over which the current is distributed ($2\pi r^2$ for a hemisphere) and can be expressed by:

$$J = \frac{I}{2\pi r^2} \tag{2.3}$$

The potential difference can then be expressed by:

$$V = \frac{I\rho}{2\pi r} \tag{2.4}$$

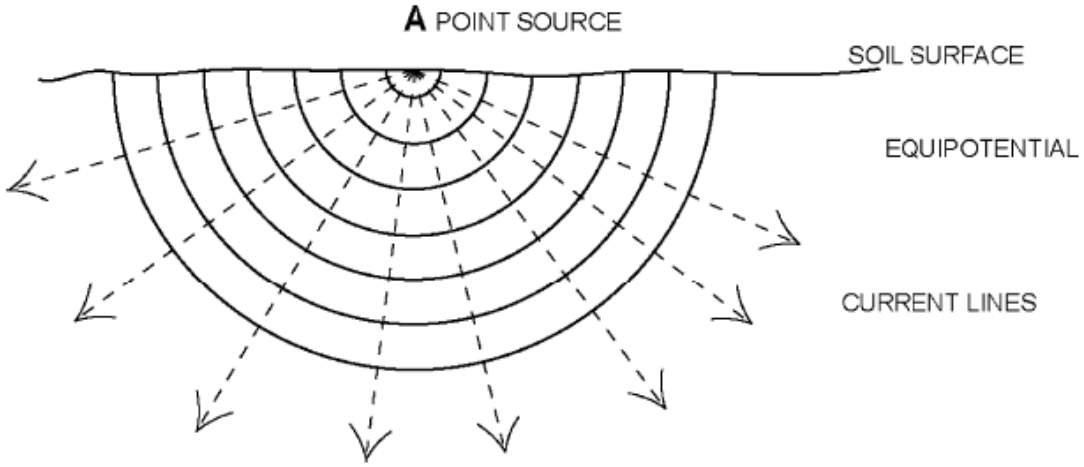

Figure 2.5 Distribution of the Current Flow in a Homogeneous Soil (Samouelian et al., 2005)

Measurement of electrical resistivity requires four electrodes: two current electrodes (A and B) and two potential electrodes (M and N). The potential difference ΔV measured between the electrodes M and N is given by the equation:

$$\Delta V = \frac{\rho I}{2\pi}\left[\frac{1}{AM} - \frac{1}{BM} - \frac{1}{AN} + \frac{1}{BN}\right] \quad (2.5)$$

where AM, BM, AN, and BN is the distance between the electrodes A and M, B and M, A and N, and B and N, respectively. The electrical resistivity is then calculated using:

$$\rho = \left[\frac{2\pi}{\left(\frac{1}{AM}\right) - \left(\frac{1}{BM}\right) - \left(\frac{1}{AN}\right) + \left(\frac{1}{BN}\right)}\right]\frac{\Delta V}{I}$$

$$\rho = K\frac{\Delta V}{I} \quad (2.6)$$

where K is a geometric factor that depends on the arrangement of the four electrodes A, B, M, and N (Samouelian et al., 2005). For an inhomogeneous subsurface, the resistivity calculated using equation (2.6) is no longer the true resistivity and is called the apparent resistivity. The true resistivity of the subsurface is then determined using numerical inversion methods.

2.4.2 Electrical Current Flow in Soil and Rocks

Electrical current flows in soil and rocks through three methods: electronic conduction, electrolytic conduction, and dielectric conduction. In electronic conduction, the electric current is carried by the free electrons in metals. The structure of a metal is can be described as an orderly packing of metal ions surrounded by an atmosphere of valence electrons. The energy needed to move a valence electron from one atom to the next is very small. The high conductivity of metals is explained by the large number of mobile electrons. If the atoms in a metal are perfectly ordered, the electrical resistivity of metals will be nearly zero. However, due to the presence of imperfections in the crystal structure, metals have some resistivity (Keller and Frischknecht, 1966).

For most soil and rocks, conduction is electrolytic and the current is carried by ions in the pore fluid. These ions are produced from the dissociation of salts in water and are distributed through the pore structure of the soil. Since each ion can carry a definite amount of charge, it follows that soils with larger number of ions in the pore fluid (high salinity) will have a higher conductivity (Ward, 1990). In environmental and engineering surveys, electrolytic conduction is the most common method. Electronic conduction is considered only when metallic minerals are present in high quantities.

Dielectric conduction occurs in very weakly conducting materials when an external alternating current is applied, resulting in the atomic electrons being shifted slightly with respect to their nuclei (Reynolds, 1997). At the frequencies used in electrical resistivity imaging (very low frequencies), dielectric conduction is usually disregarded.

2.4.3 Factors Affecting Electrical Resistivity

2.4.3.1 Porosity

Porosity is defined as the ratio of the volume of voids to the total volume of the sample. Pore spaces must be interconnected and partially filled with fluid in order for rocks and soil to conduct electric current. Electrical resistivity and porosity are commonly related by Archie's law (1942), which for saturated clay-free soil is given as:

$$F = \frac{\rho}{\rho_w} = a\phi^{-m} \tag{2.7}$$

where F is the formation factor, ρ is the bulk soil resistivity, ρ_w is the pore fluid resistivity, ϕ is the porosity, and *a* and *m* are constants that depend on the rock type. The constant *m* is known as the cementation factor while the constant *a* is known as the coefficient of saturation. The numerical values for *a* generally fall between 0.5 and 2.5 while those for *m* fall between 1.3 and 2.5 (Reynolds 1997).

Archie found that *m* varies from 1.8 to 2.0 for sandstones while *m* is approximately 1.3 for clean uncemented sands. Jackson et al. (1978) found that the exponent *m* was dependent on the shape of the particles, increasing as they become less spherical, while variations in size and spread of sizes appeared to have little effect. According to Keller and Frischknecht (1966), the value of the constant *a* varies from slightly less than 1 for rocks with intergranular porosity to slightly more than 1 for rocks with joint porosity. The exponent *m* is larger than 2 for cemented and well-sorted granular rocks and less than 2 for poorly sorted and poorly cemented granular rocks. Keller and Frischknecht (1966) summarized the different expressions for Archie's law that have been reported in literature as given in Table 2.2. The authors mentioned that it is necessary to make a large number of measurements of both porosity and resistivity in order to determine the values of *a* and *m* with good degree of reliability. For a first approximation, a value of 1 may be assumed for *a* and a value of 2 may be assumed for *m*.

Table 2.2 Expressions for Archie's Law for Different Geologic Formations (adapted from Keller and Frischnecht, 1966)

Geologic Formation	Porosity Range	Numbers of Measurements	Equation
Frio Sandstone (Oligocene)	0.15 – 0.37	30	$F=0.62\phi^{-2.15}$
Pennsylvanian Sandstone, Oklahoma	0.08 – 0.20	97	$F = 0.65\phi^{-1.91}$
Morrison Sandstone (Jurassic), Colorado	0.14 – 0.23	243	$F = 0.62\phi^{-2.10}$
Clean Miocene Sandstone, Louisiana	0.11 – 0.26	35	$F = 0.78\phi^{-1.92}$
Clean Cretaceous Sandstone, Texas	0.08 – 0.25	50	$F = 0.47\phi^{-2.23}$
Clean Ordovician Sandstone, Oklahoma	0.07 – 0.15	44	$F = 1.3\phi^{-1.71}$
Shaley Sandstone (Eocene), Texas	0.09 – 0.22	72	$F = 1.8\phi^{-1.64}$
Shaley Sandstone (Olegocene), Texas	0.07 – 0.26	63	$F = 1.7\phi^{-1.65}$
Shaley Sandstone (Cretaceous), Texas	0.07 – 0.31	36	$F = 1.7\phi^{-1.80}$
Oolitic Limestone (Cretaceous), Texas	0.07 – 0.19	13	$F = 2.3\phi^{-1.64}$
Oolitic limestone (Jurassic), Arkansas	0.09 – 0.26	42	$F = 0.73\phi^{-2.10}$
Siliceous Limestone (Devonian), Texas	0.07 – 0.30	58	$F = 1.2\phi^{-1.88}$
Limestone (Cretaceous), Texas	0.08 – 0.30	37	$F = 2.2\phi^{-1.65}$

2.4.3.2 Moisture Content

For most soils and rocks, electrical current is carried by the ions in the pore fluid. Thus, electrical current flow depends on the amount of water in the pores and on its quality. In most studies concerning moisture content, the electrical resistivity of the pore fluid is assumed to remain relatively constant.

The original Archie model (equation 2.7) assumed a fully saturated soil. Archie model was later extended to partially saturated porous media (Keller and Frischknecht, 1966), and is given as:

$$\frac{\rho}{\rho_w} = a\phi^{-m}S^{-n} \tag{2.8}$$

where S is the saturation and n is a constant which is usually equal to 2 (Reynolds 1997). Assuming *m* = *n*, Archie's law can be written as:

$$\rho = \rho_w a\theta^{-m} \tag{2.9}$$

where θ is the volumetric moisture content defined as the product of porosity ϕ and saturation S . In order to estimate the volumetric moisture content using Archie's law, the constants (*a* and *m*) has to be first calibrated in the laboratory. Figure 2.6 shows examples of laboratory calibration between the electrical resistivity and the volumetric moisture content for different types of soil (Samouelien et al., 2005). Results showed that electrical resistivity decreases with increasing moisture content.

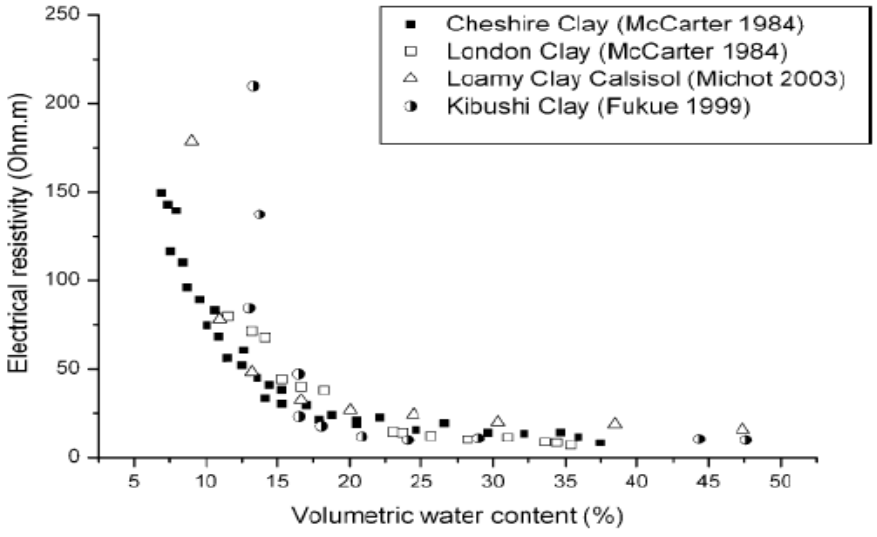

Figure 2.6 Relationship Between the Volumetric Moisture Content and Electrical Resistivity for Different Soil Types (Samouelian et al., 2005)

Abu-Hassanein et al. (1996) studied the variation of electrical resistivity of compacted clay as a function of various soil properties. The author found that resistivity decreased with increasing molding water content. He also found that electrical resistivity is sensitive to compaction conditions, and that lower resistivity values were obtained when soil samples were compacted with a higher compaction effort as shown in Figure 2.7.

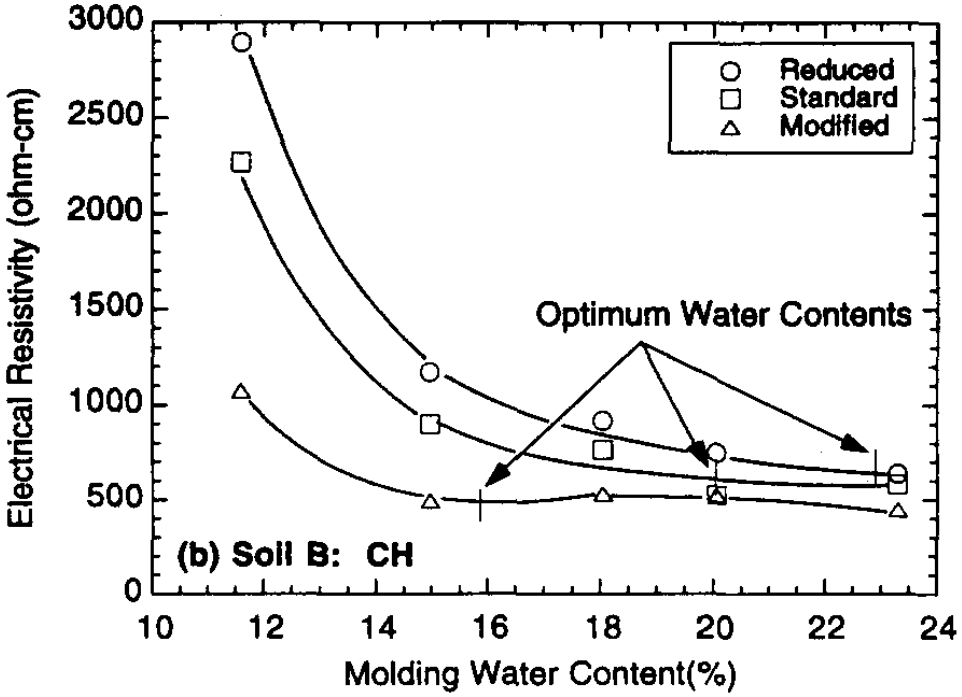

Figure 2.7 Relationship Between Resistivity, Molding Water Content, and Compactive Effort (Abu-Hassanein et al., 1996)

Goyal et al. (1996) suggested the use of an empirical linear relationship between the resistivity and moisture content. The linear dependence of resistivity (ρ) on moisture content (θ), for a depth z and time t, can be written in the form:

$$\rho(z,t) = a + b\theta(z,t) \tag{2.10}$$

where a and b are empirical constants implicitly containing the soil and water characteristics (porosity, temperature, salinity) and are assumed to be constant with time.

2.4.3.3 Pore fluid resistivity

According to Archie's law, the electrical resistivity is directly proportional to the resistivity of the pore fluid. The electrical resistivity of the pore fluid depends on the concentration of salts present in the fluid. When a salt is dissolved in water, the constituent ions in the salt separate and are free to move independently in the solution. When an electric field is applied across the solution, cations will be accelerated toward the negative pole and anions to the positive pole. Soils with pore fluid of high ionic strength are more conductive than soils with low ionic strength pore fluid.

Kalinski and Kelly (1993) estimated the volumetric water content of compacted specimens of a CH soil using three different water solutions with a conductivity of 1, 2, and 3mmho/cm (mS/cm). They found that for a given moisture content, the electrical resistivity decreases when the water conductivity increases (Figure 2.8).

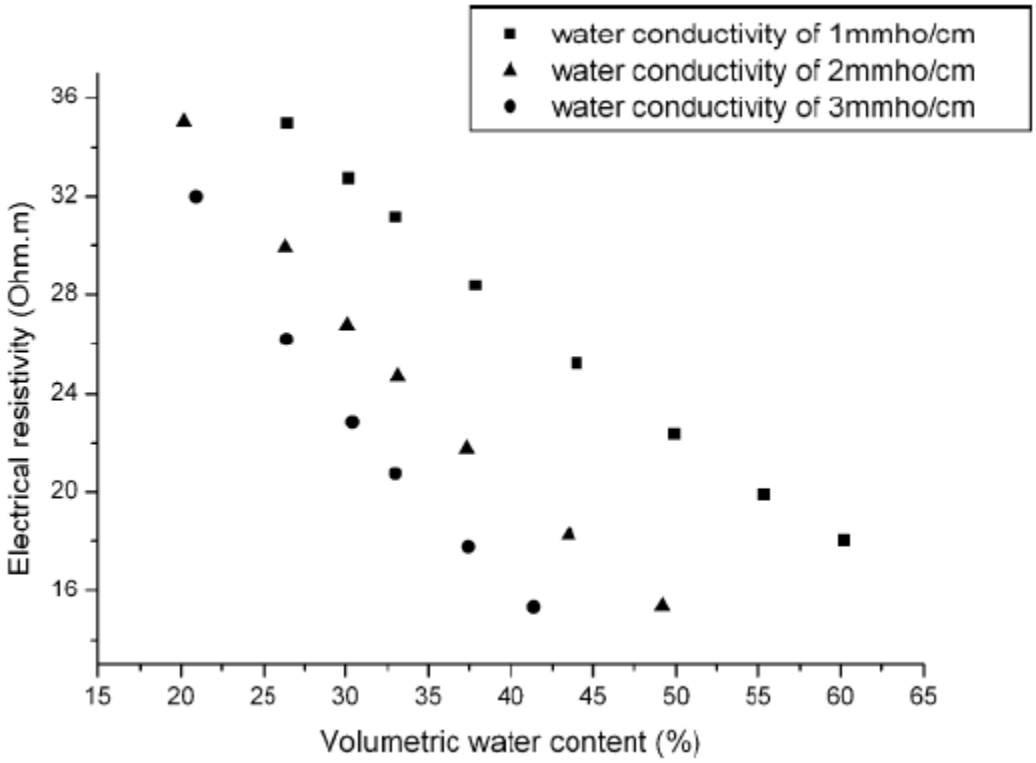

Figure 2.8 Resistivity vs. Water Content for Different Values of Pore-Water Conductivity (Kalinsky and Kelly, 1993)

Yoon and Park (2001) performed laboratory tests on three sandy soils and leachate collected from a landfill in Korea. The authors measured the variations of resistivity by adding 5%, 10%, and 30% by volume leachate mixed with fresh water. At a moisture content of 15%, Figure 2.9 shows that the resistivity of the sample SAND dropped from 4000 to 500 ohm-m by adding 5% of leachate. This was due to increased electrical conduction as a result of the movement of ions in the leachate.

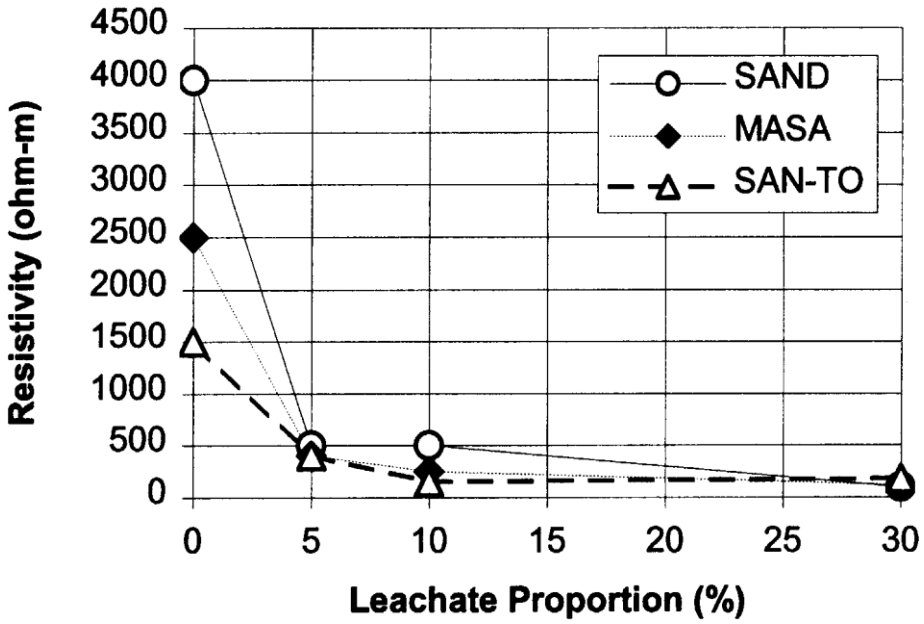

Figure 2.9 Electrical Resistivity Variation with Leachate Proportion (Yoon and Park, 2001)

2.4.3.4 Temperature

An increase in temperature decreases the viscosity of water, causing the ions in the water to become more mobile. Thus, the electrical conductivity increases and the resistivity decrease with increasing temperature. In general, electrical resistivity decreases by about 2% for a temperature increase of 1ºC. According to Keller and Frischknecht (1966),

$$\rho_{t=}\frac{\rho_{18}}{1+\alpha(t-18)} \tag{2.11}$$

where α is the temperature coefficient ($\alpha \approx 0.025$ per ºC), ρ_t is the resistivity at ambient temperature t(ºC), and ρ_{18} is the resistivity at a reference temperature of 18ºC (any other reference temperature may be used).

Extreme ranges in temperature can affect resistivity, particularly if the temperature is high enough to drive water from the rock as steam or low enough to freeze the water in the pores of the rock (Keller and Frischknecht, 1966). At moderate

temperatures, a change in temperature affects the resistivity of rock only if the resistivity of the pore fluid is affected. Abu-Hassanein et al. (1996) studied the effect of temperature on the resistivity of three soil samples. The authors found that a large drop in electrical resistivity occurs as the temperature passes the freezing point (0°C) as shown in Figure 2.10. The α's determined for the three soils were slightly higher than the α suggested by Keller and Frischknecht (1966).

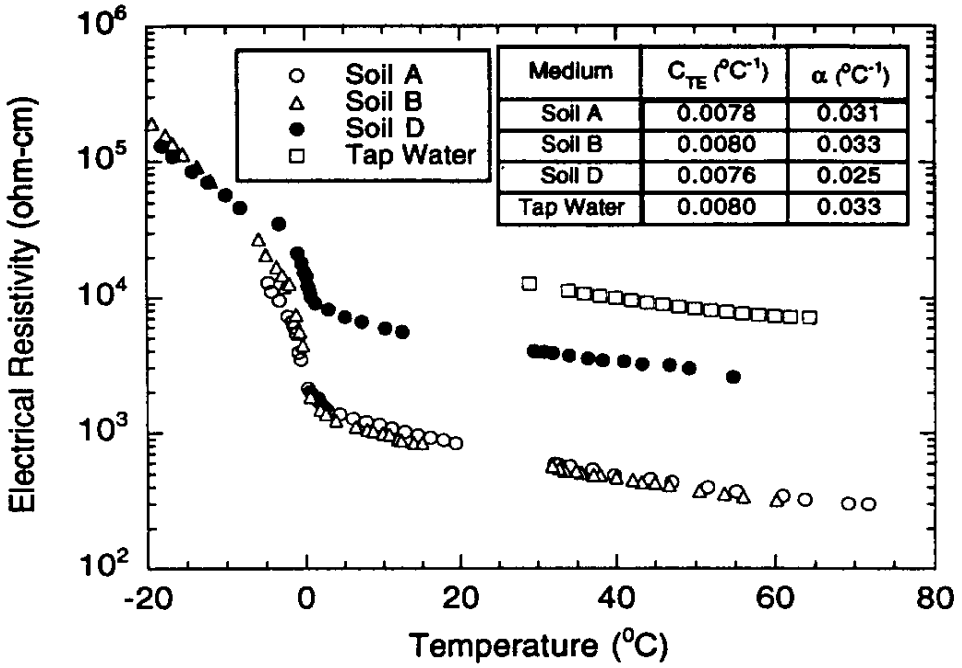

Figure 2.10 Relationship Between Electrical Resistivity and Temperature (Abu-Hassanein et al., 1996)

Grellier et al. (2006) measured the electrical conductivity of two different leachates taken from two bioreactors in France as a function of temperature. The results as shown in Figure 2.11 confirmed the well-known increase in conductivity of about 2% per 1°C. The difference in conductivity between the two leachates at a given temperature

was consistent with the differences in ionic strength. L1 had a higher ionic strength than L2. The authors also emphasized that for a bioreactor landfill, the injected leachate might have a lower temperature than the waste mass. As a result, the expected decrease in resistivity due to the addition of moisture can be masked by the opposite effect resulting from the lower temperature of the injected leachate.

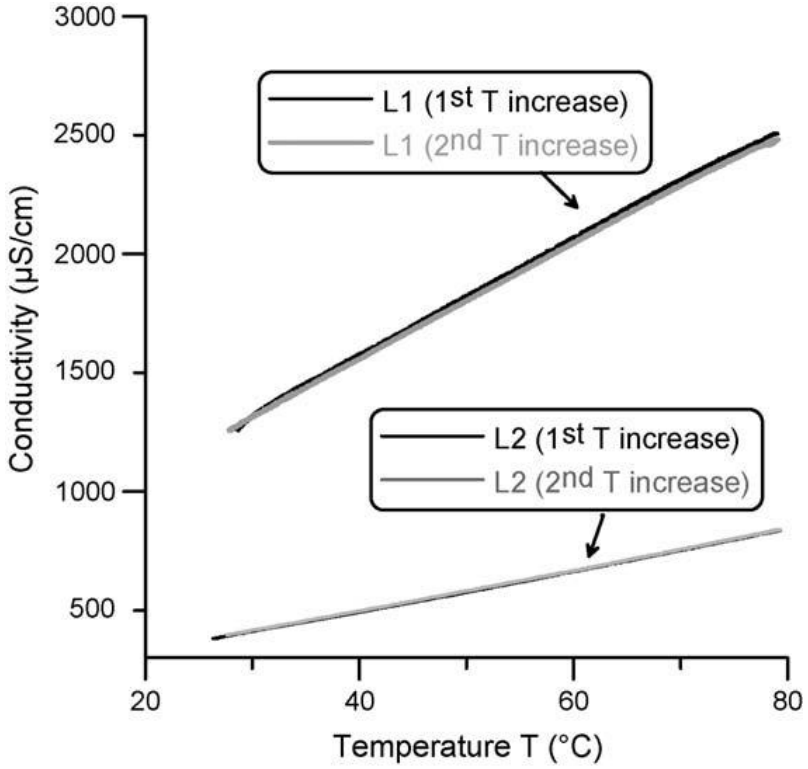

Figure 2.11 Conductivity vs. Temperature for Two Different Leachates (Grellier et al., 2006)

2.4.3.5 Clay Content

A clay particle acts as a separate conducting path in addition to the pore fluid path. The high conductivity (low resistivity) of clay is due to the double layer of exchange cations that form on clay particles as shown in Figure 2.12. The cations are

needed to balance the charge due to substitution within the crystal lattice, and due to broken bonds. The finite size of the cations prevents the formation of a single layer. Therefore, a double layer consisting of a fixed layer and a diffuse layer is formed. The fixed layer is immediately adjacent to the clay surface, while the diffuse layer drops off in density exponentially with distance from the fixed layer (Ward, 1990). For clay-rich soils, surface conductance can be a significant factor affecting the bulk electrical resistivity of the soil. Therefore, parallel resistor models were developed (Waxman and Smits, 1968) to account for conduction through the pore fluid and along the particle surface.

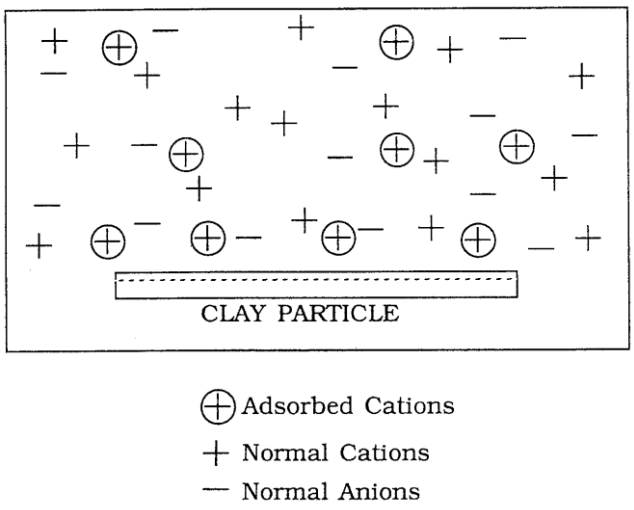

Figure 2.12 Schematic Representation of Ions Adsorbed on Clay Particle (Ward 1990)

The electrical resistivity recorded by Giao et al. (2003) for 25 clay samples collected worldwide ranged from 1 to 12 ohm-m. This range is significantly narrower than the commonly reported range from 1 to 100 ohm-m in literature. Abu-Hassanein et

al. (1996) found that lower electrical resistivity occurs for soils having higher clay content as shown in Figure 2.13.

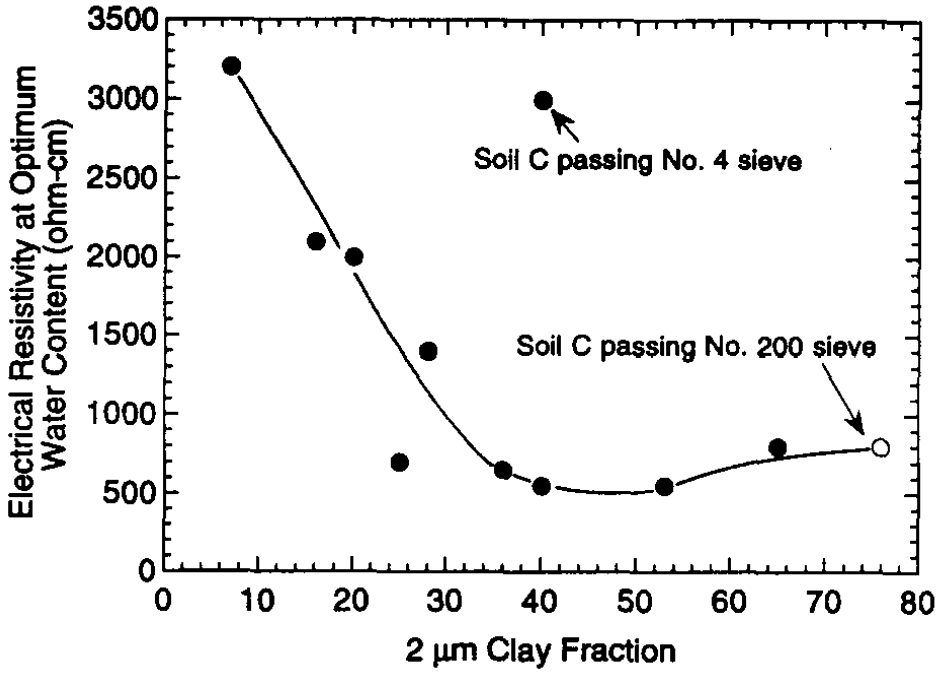

Figure 2.13 Relationship Between Electrical Resistivity at Optimum Water Content and Clay Content (Abu-Hassanein et al., 1996)

2.4.3.6 Type of Solid Constituents

The effect of rock and soil types on electrical resistivity was discussed by several authors (Keller and Frischknecht 1996, Ward 1990, Samoulian et al. 2005). Igneous rocks tend to have the highest resistivity values. The resistivity of these rocks depends mainly on the degree of fracturing, and the percentage of the fractures filled with groundwater. Sedimentary rocks tend to be most conductive, largely due to their high pore fluid content. Metamorphic rocks have intermediate but overlapping resistivity values (Reynolds 1997). Resistivity values of some common earth materials are presented in

Figure 2.14. The electrical resistivity of different types of rocks and soils can vary by several orders of magnitude. The overlap of these ranges makes rock type identification using resistivity difficult.

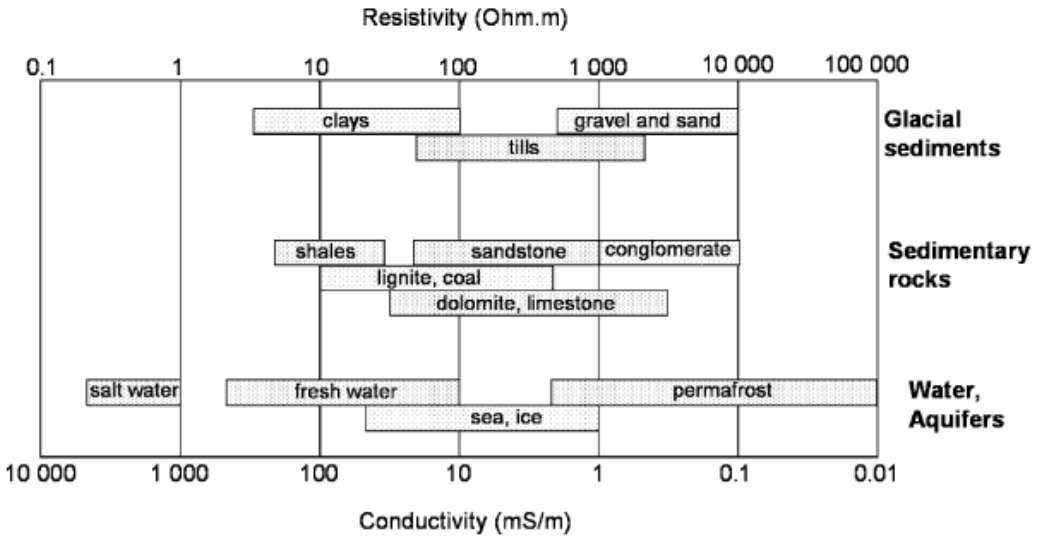

Figure 2.14 Typical Ranges of Electrical Resistivity for Earth Materials (Samouelian et al., 2005)

2.4.4 Measurement of Electrical Resistivity

2.4.4.1 Field Measurement

The purpose of electrical resistivity surveys is to determine the subsurface resistivity distribution. In a 1-D survey, profiling or vertical electrical sounding (VES) is carried out. Profiling is done by moving the electrode array along a straight line and keeping a constant spacing between the electrodes. Profiling is used to detect lateral changes in resistivity. VES is carried out by expanding the spacing between the electrodes around a midpoint. Sounding is used to detect changes in resistivity with depth.

In a 2-D survey, a large number of electrodes (25 or more) are equally spaced along a line on the ground surface. Under software control, four electrodes are selected at a time in a certain configuration until all electrodes in the line have been used. At each step, one measurement is recorded. Then the spacing between the electrodes is increased by a certain factor and the process is repeated until the maximum spacing between the electrodes is reached. The result is a 2-D cross section or image of the subsurface that shows the lateral and vertical variation in resistivity. In a 2-D survey, it is assumed that the resistivity is constant in the direction perpendicular to the survey line.

In a 3-D survey, a grid of electrodes is laid out on the ground surface. The number of electrode combinations that can be measured increases very rapidly with the size of the grid. In theory, a 3-D survey should give the most accurate representation of the subsurface.

2.4.4.2 Laboratory Measurement

Measurement of the electrical resistivity of soil in the laboratory using the four-electrode method is discussed in ASTM G57-06. The soil box is a rectangular box with metal ends and two pins inserted along the length (Figure 2.15). The soil specimen should be thoroughly mixed and be representative of the soil type of interest. Soil specimens compacted in layers into the box, and the metal pins are inserted. The resistivity of the soil specimen is measured by passing an electric current between the end plates and measuring the voltage drop across the pins. The resistivity ρ in ohm-cm is given by:

$$\rho = \frac{RA}{a} \tag{2.12}$$

where R is the resistance in ohms, A is the cross-sectional area of the box perpendicular to the current flow in cm^2, and a is the inner electrode spacing in cm.

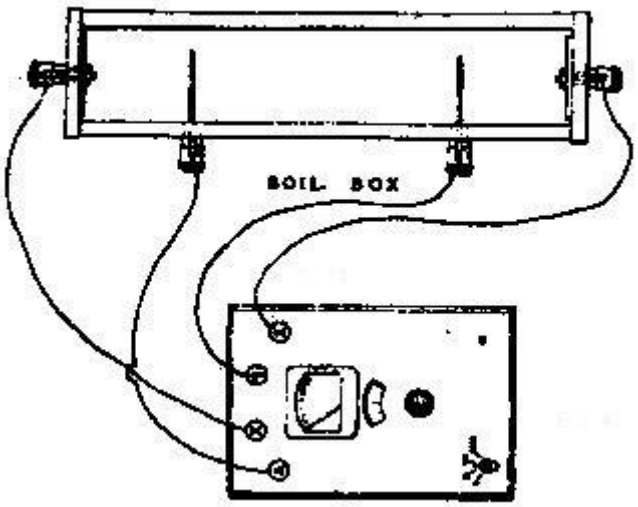

Figure 2.15 Four-Electrode Soil Box (ASTM G57)

Several researchers provided alternatives to the standard soil box to develop relationships between soil resistivity and its hydraulic properties in the laboratory. Kalinski and Kelly (1993) recommended the use of circular four-probe resistivity cells. These are circular cells constructed of a nonconductive material with eight equispaced electrodes inserted through the sides. With the eight-probe configuration, eight separate resistance measurements are made by using each set of four adjacent probes. The average of the eight measured resistances is then used to calculate the resistivity of the specimen.

Abu-Hassanein et al. (1996) measured the electrical resistivity of ten compacted clay samples in the laboratory to relate the resistivity of soil to its hydraulic conductivity. The apparatus used consisted of a PVC cylinder that has the size of a typical compaction mold (Figure 2.16). An electrical field was induced through the specimen via two copper discs pressed against the ends of the specimen. The potential difference was measured between two copper rods placed at the center of the specimen. The specimen was compacted directly in the PVC cylinder.

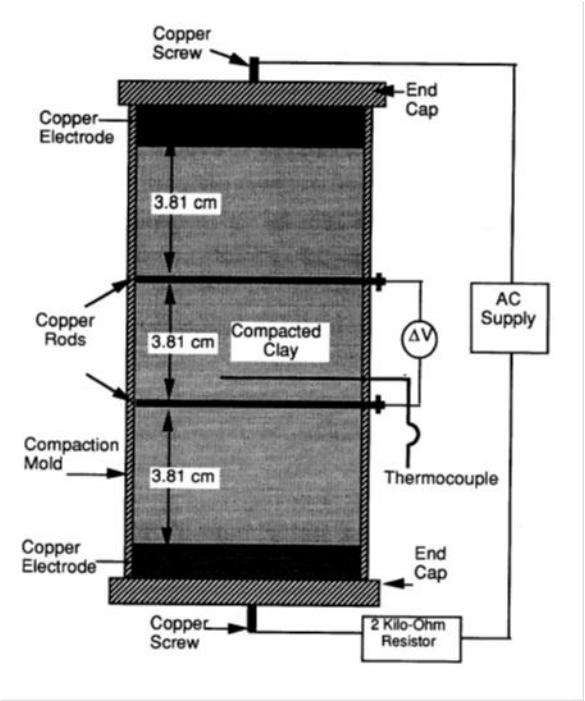

Figure 2.16 Apparatus for Measuring Electrical Resistivity of Compacted Clay (Abu-Hassanein et al., 1996)

Amidu (2008) conducted field and laboratory resistivity measurements to characterize seasonal wetting and drying of soils with high clay content. Three cylindrical soil samples (30.5 cm in diameter) were initially soaked in distilled water for five days. Samples were then drained and four electrodes with 8cm spacing were inserted into the samples as shown in Figure 2.17. Then measurements were made using a Wenner array at different water contents as the samples dried at room temperature.

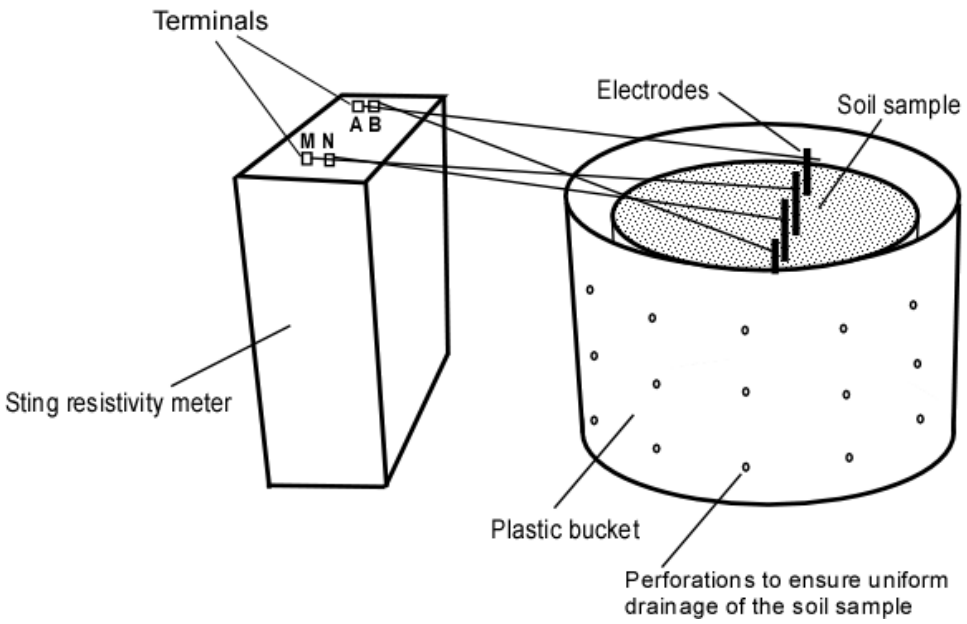

Figure 2.17 Experimental Setup for Resistivity Measurement (Amidu, 2008)

2.5 Previous Resistivity Imaging Studies on MSW

Although electrical resistivity imaging has been widely used in the geotechnical field, ERI is still considered a new tool in the solid waste field. Very few studies have been conducted on MSW utilizing electrical resistivity. Most of these studies used ERI to monitor the spatial distribution of moisture within a landfill, and not to quantify the moisture content of MSW.

Rosqvist et al. (2003) utilized ERI to map leachate plumes at two landfills in South Africa. The authors then compared ERI results to the results of an ongoing groundwater monitoring program. The authors determined that ERI results corresponded well to the groundwater quality results and that ERI was valuable in determining the extent of the leachate plumes.

Grellier et al. (2005) used ERI to monitor leachate recirculation at a bioreactor landfill in Jura, France. Results from the short-term study are presented in Figure 2.18. Liquid movement after leachate injection through the middle horizontal trench was visualized by tracking changes in electrical resistivity. A decrease in resistivity was observed below the leachate injection point. According to the results, there was a large radius of injection influence (15-20 m) and a long period before stabilization (more than 7 days). The increase in resistivity (red regions) observed beneath the right side trench was result of the drying of the refuse following a previous leachate injection through the right side trench.

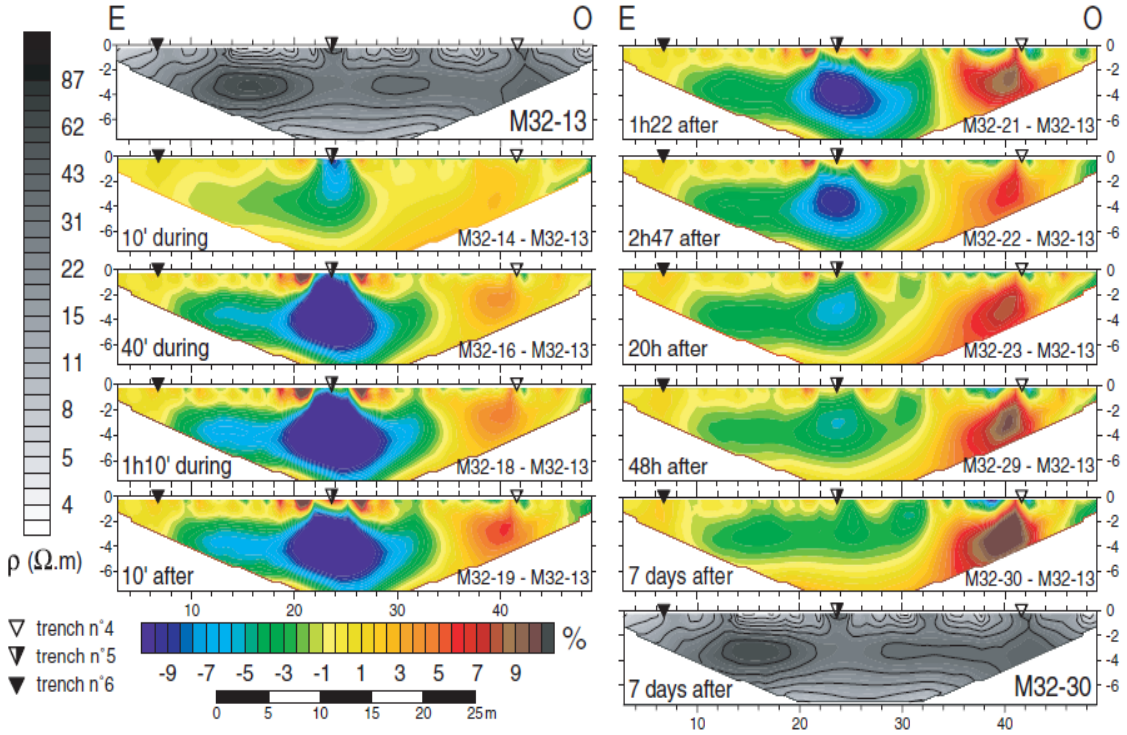

Figure 2.18 Variation of Electrical Resistivity During an Injection through Trench No. 5 (Grellier et al., 2005)

Another ERI study was conducted by Grellier et al. (2006) to monitor the distribution of leachate at Orchard Hills landfill in Illinois. ERI was conducted along and across two horizontal leachate injection trenches to determine the efficiency of the injection system. Figure 2.19 presents variation of resistivity along leachate recirculation line LRL29. The first profile (gray-scale) is the measured resistivity before the beginning of leachate injection and is used as a reference. The color profiles show the relative variation of resistivity during leachate injection. The leachate was injected from the east end of LRL29, and that was reflected by the decrease in resistivity near the injection point. The results also showed that along the last 20m of the recirculation line, the resistivity remained constant, indicating that the injected leachate does not reach the end of the LRL. Based on ERI conducted across LRL29, the authors estimated the zone of influence to be 30m.

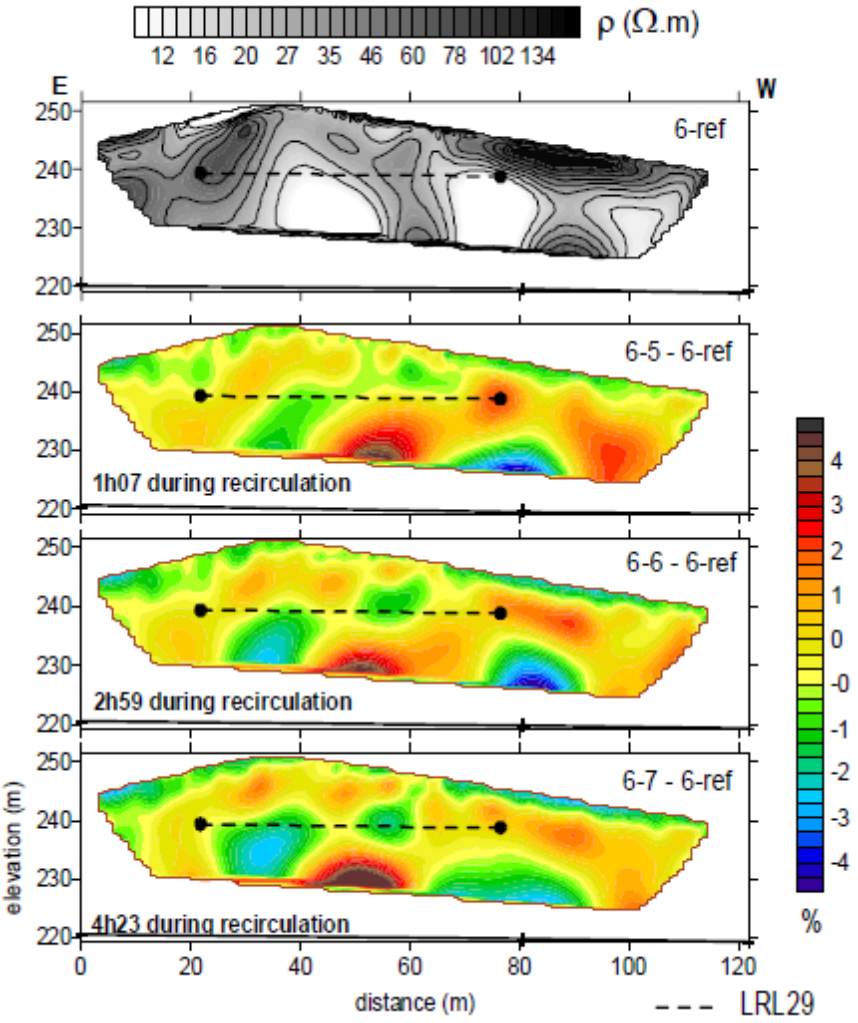

Figure 2.19 Variation of Resistivity during Leachate Recirculation along LRL29 (Grellier et al., 2006)

An attempt was made by Grellier et al. (2007) to develop a direct correlation between electrical resistivity and moisture content. The study was based on field testing program at Orchard Hills landfill (Illinois) that included (1) ERI at three different locations that have been subjected to leachate recirculation and (2) determination of moisture content of waste samples obtained from different depths from boreholes at the same locations where ERI was conducted. Results for samples collected from three

boreholes (GEW14, GEW16, and GEW23) are presented in Figure 2.20. Resistivity values from the field survey were plotted versus the actual moisture content and the data was fitted to Archie's law. Archie's constants were determined to be: a = 0.75 for all samples from the three boreholes, and m = 1.6, 2.15, and 1.8 for samples from GEW14, GEW16, and GEW23, respectively. Using Archie's law, the moisture content was then estimated from the field resistivity values and compared with the actual moisture content values as presented in Figure 2.20. For GEW14, only 1 point out of 7 fits well between the measured and estimated moisture content values. For GEW16, 5 points out of 7 fit well, and for GEW23, 3 points out of 5 fit well. Considering all the points, 9 points out of 19 (47%) fit well (variations less than 13%). The authors concluded that it can be difficult to correlate perfectly electrical resistivity with moisture content without considering the many other factors that affect resistivity.

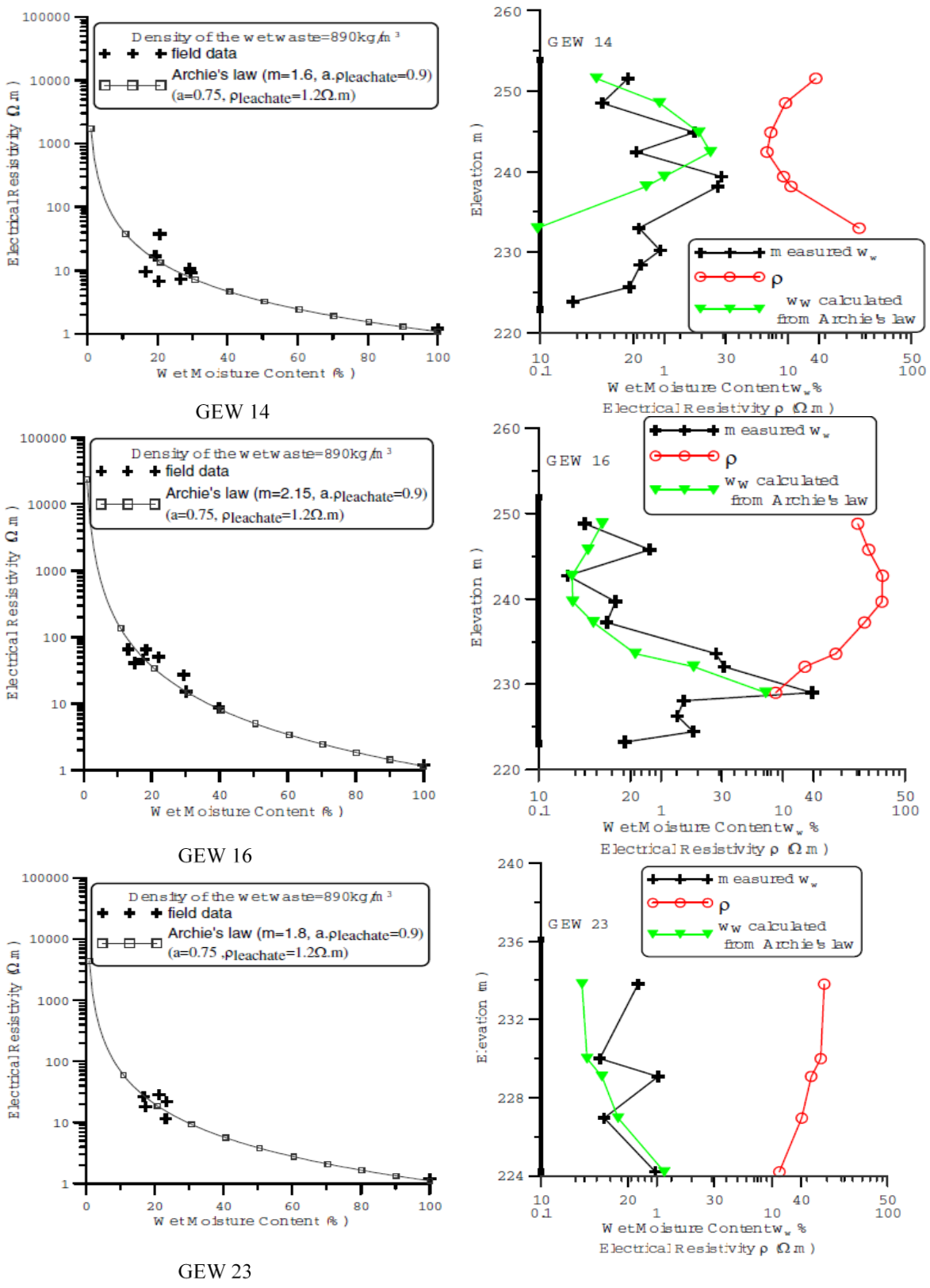

Figure 2.20 Resistivity and Moisture Content Results at Three Borehole Locations (Grellier et al. 2007)

In 2009, Hossain et al. conducted and ERI study at the City of Denton Landfill to monitor the moisture movement within the waste mass. First set of tests were performed along the recirculation pipes to identify the vertical moisture movement through the waste. A second set of tests were performed across the recirculation pipes to determine the zone of lateral moisture movement. Figure 2.21 presents resistivity profiles along recirculation pipe H2. A decrease in resistivity was observed below the recirculation line. However, the decrease in resistivity was not uniform along the pipe, indicating that the flow of leachate through waste is mostly through preferential flow paths due to the heterogeneous nature of the waste.

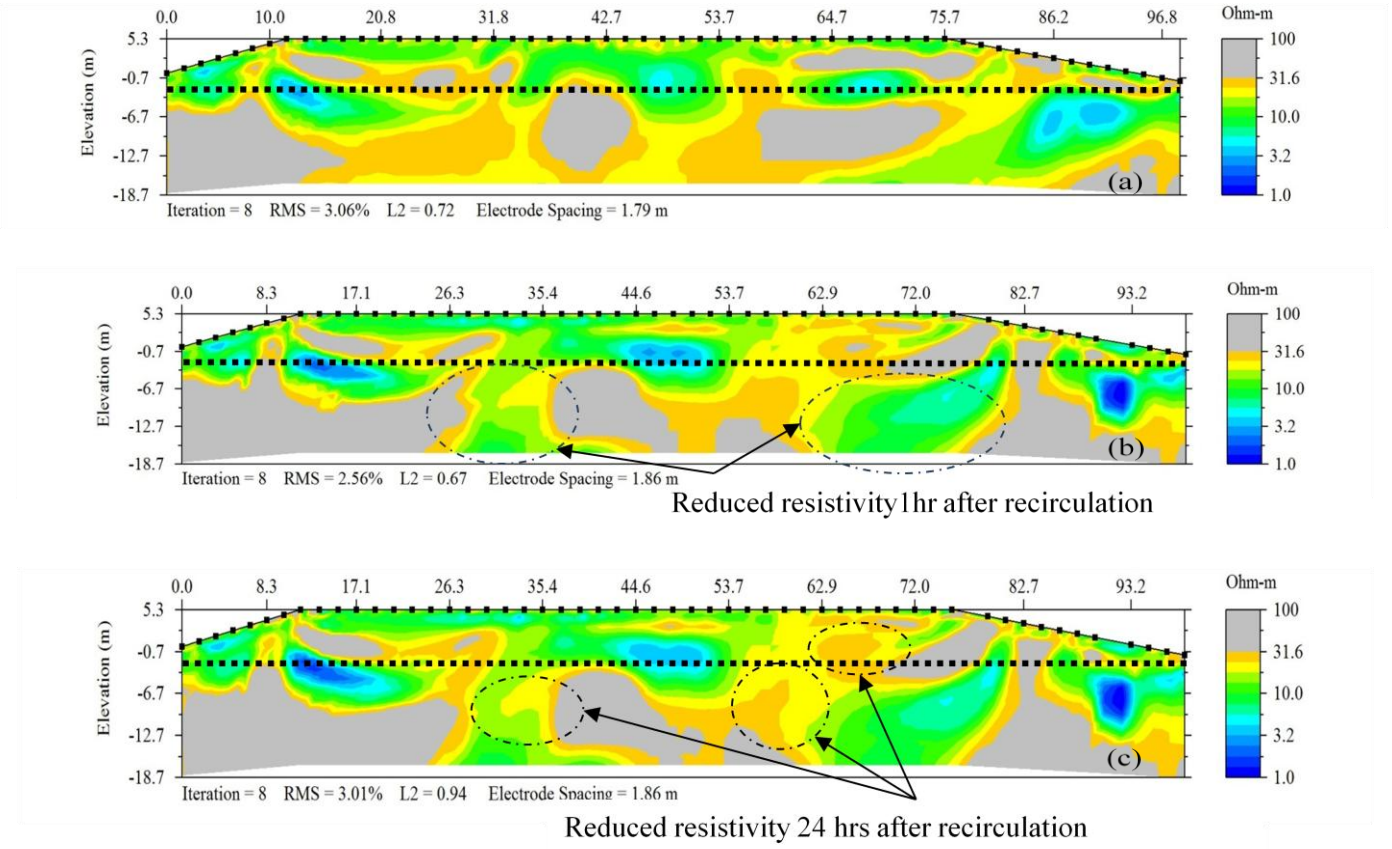

Figure 2.21 Resistivity Profiles along Recirculation Pipe H2: (a) Baseline Study, (b) 1hr after recirculation, and (c) 24hrs after recirculation

CHAPTER 3

MATERIALS AND METHODS

3.1 Introduction

In this chapter, solid waste collection/preparation methodology and procedures followed to determine the physical composition, moisture content, organic content, and unit weight of the MSW samples are first presented. A description of the apparatus used to measure the resistivity of the samples in the laboratory is then presented. Finally, the samples preparation procedures followed to measure the resistivity as a function of moisture content, unit weight, decomposition, temperature, composition of MSW, and composition of the pore fluid are discussed in details.

3.2 Site Description

The city of Denton is located 49 miles northwest of Dallas as presented in Figure 3.1. The City of Denton Landfill is a Type 1 landfill that accepts approximately 550 to 600 tons of waste per day, six days a week. The landfill has a waste footprint of approximately 152 acres. The landfill started its operation in 1984 as a traditional, dry tomb landfill. In May 2009, the landfill started its operation as an enhanced leachate recirculation (ELR) landfill, upgrading the landfill from a waste storage facility to a waste processing facility. The leachate recirculation system consists of a series of six inch diameter perforated HDPE pipes buried in horizontal trenches and backfilled with "select" waste. These horizontal pipes are used for both leachate recirculation and gas

collection. The collected gas is then used to generate electricity using an electric power generator.

Figure 3.1 Location Map of City of Denton

3.3 Solid Waste Collection and Samples Preparation

Both fresh and landfilled solid waste samples were collected as part of the current research. Also, degraded waste samples were prepared using laboratory scale reactors. Samples collection/preparation procedures are presented next.

3.3.1 Fresh MSW Samples

Fresh MSW samples were collected in June 2010 from the working face of the landfill. Five bags of MSW samples were collected, each bag weighing 30 lb to 40 lb. To collect representative samples, the waste was thoroughly mixed, quartered, and then one quarter was randomly selected as presented in Figure 3.2. All samples were brought to

the laboratory and stored at 4^{o}C in an environmental growth chamber (Figure 3.3) to preserve their initial characteristics.

Figure 3.2 Fresh MSW Samples Collection Procedure

Figure 3.3 Environmental Growth Chambers

3.3.2 Landfilled MSW Samples (Partially Degraded)

Landfilled MSW samples were collected twice using a 3ft diameter bucket auger as presented in Figure 3.4. First set of samples were collected in September 2009 for determining the characteristics of the landfilled waste. MSW samples were collected from six boreholes, in conjunction with the drilling of boreholes for installing gas extraction wells. MSW Samples were collected from a depth of 20 ft to 65 ft at 5 ft intervals from each borehole. Ten samples were collected from each borehole, each sample weighing 25 lb to 35 lb. Samples were placed in lidded buckets and stored at 4^{o}C in an environmental growth chamber. The approximate borehole locations and recirculation pipe locations are presented in Figure 3.5. Waste samples from boreholes B45, B47, and B49 (total of 30 samples) were used for this study.

A second set of MSW samples were collected in November 2010 from two boreholes (B70 and B72) for the validation of the developed model. Samples were collected from cell 1590 of the landfill, which is pre-subtitle D with no leachate recirculation. The waste is approximately 20 to 25 years old. Six samples were collected from each borehole from a depth of 10ft up to 60ft at 10ft intervals. The samples weighed approximately between 25 to 35 lbs each. The samples were brought to the laboratory and stored at 4°C in an environmental growth chamber.

Figure 3.4 Borehole Samples Collection Using 3ft Diameter Bucket Auger

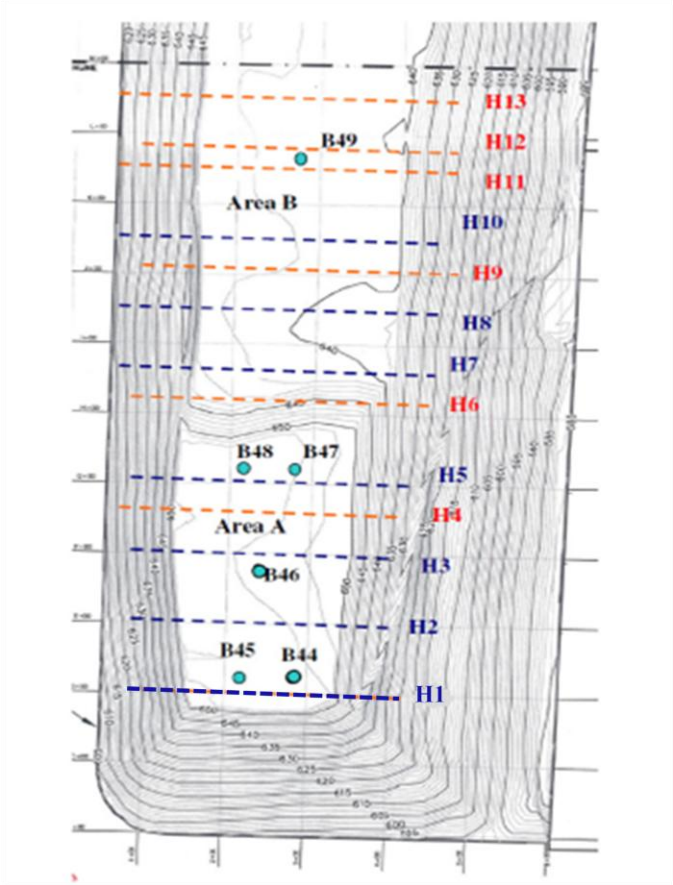

Figure 3.5 Borehole Locations with Respect to Leachate Recirculation Lines

3.3.3 Degraded MSW Samples Preparation

The landfilled MSW samples collected from boreholes B45, B47, and B49 did not show a clear trend of decomposition based on the organic content results. Therefore, the effect of decomposition on electrical resistivity was addressed by preparing degraded waste samples that have been decomposed in laboratory scale reactors.

3.3.3.1 Reactor Setup

MSW samples representing various stages of decomposition were prepared in laboratory scale reactors. Four 6 gallon reactors were filled with fresh MSW collected from the City of Denton Landfill. Approximately 12 to 14 lb of thoroughly mixed waste was placed in each reactor. An inoculum of anaerobic digested sludge was added (20% by weight) to the waste to increase the rate of decomposition. Sufficient amount of water was added to generate 1500 ml of leachate to recirculate. The reactors were then sealed using an O-ring and silicone sealant. A five-layer gas bag and a leachate bag were connected to each reactor. The reactors were operated at a constant temperature of 37°C in an environmental growth chamber for 200 days. A detailed schematic diagram of the reactors is presented in Figure 3.6.

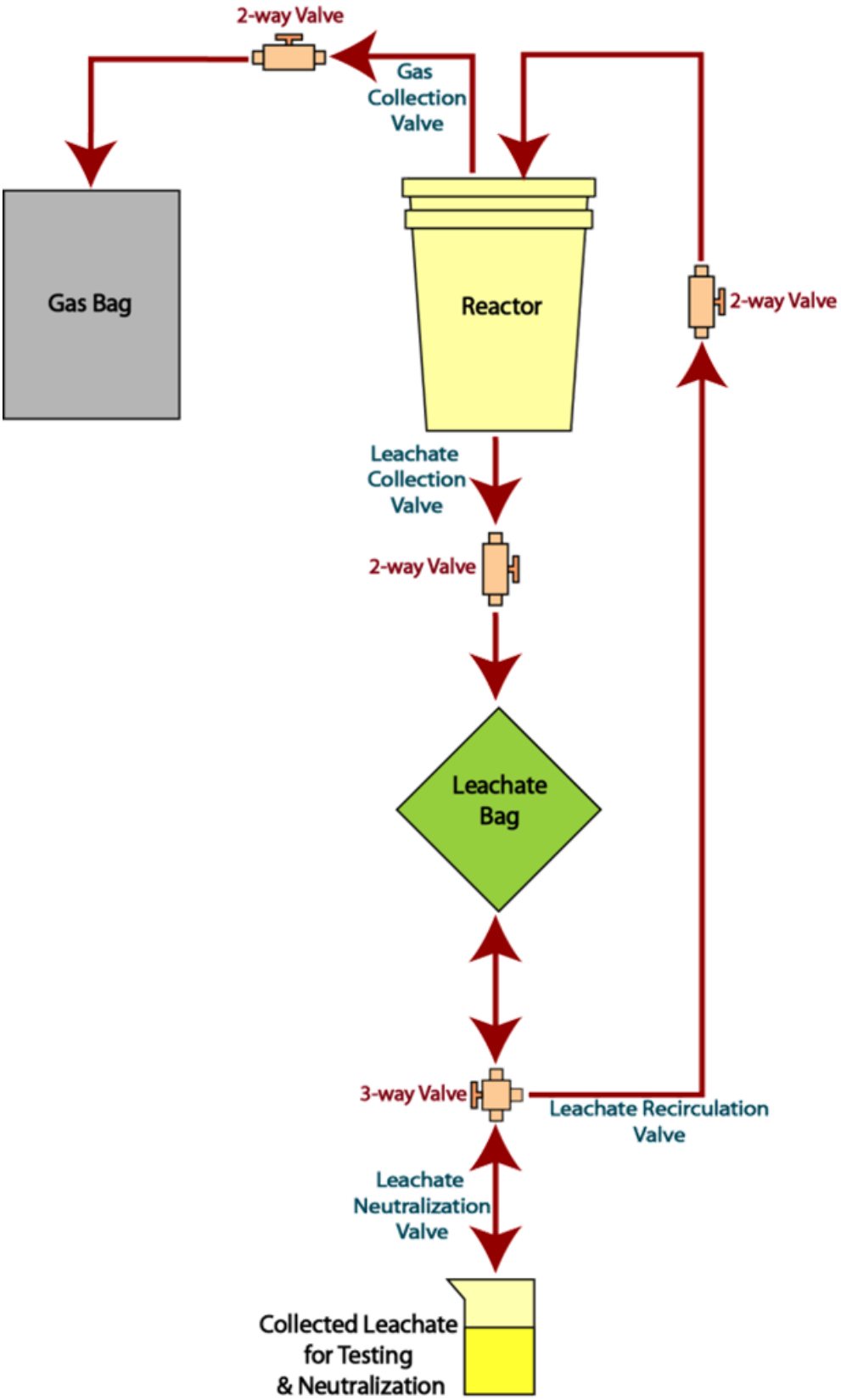

Figure 3.6 Detailed Schematic Diagram of a Laboratory Scale Reactor

3.3.3.1 Reactor Monitoring

The reactors were operated under conditions designed to simulate decomposition in bioreactor landfills by recirculating the generated leachate five times a week as shown in Figure 3.7. Before recirculating the leachate, the pH of the leachate was measured and the leachate was neutralized using potassium hydroxide or hydrochloric acid. Leachate neutralization was done to provide favorable conditions (pH range of 6.8 to 7.4) for the methanogenic bacteria.

The produced gas was collected in five-layer gas bags and the gas volume was measured by pumping it out through a standard SKC air sampler. The composition of the gas (volumetric percentages of CH_4, CO_2, and O_2) was measured using LANDTEC GEM 2000 (Figure 3.8) five times a week. The GEM 2000 is a portable gas analyzer instrumentation that measures CO_2 and CH_4 using a dual wavelength infrared cell with a reference channel, and measures O_2 using an internal electrochemical cell.

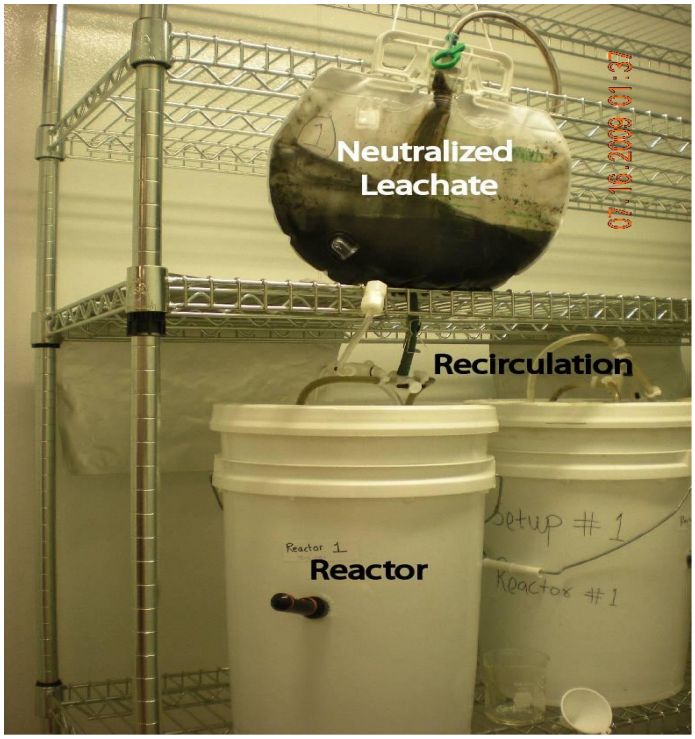

Figure 3.7 Recirculation of Neutralized Leachate

Figure 3.8 Determination of Gas Composition Using GEM 2000

3.3.3.2 Gas and pH Data

The stages of decomposition were determined based on the gas production rate, the gas composition, and the pH of the leachate. Methane production rates and the pH of the leachate are presented in Figure 3.9 and Figure 3.10, respectively.

Based on the methane production curves, day 39 marked the end of the aerobic phase (phase 1) and the onset of the anaerobic acid phase (phase 2), in which methane is detected in the gas. A drop in pH from approximately 5.8 to 5.1 is initially observed, in spite of neutralizing the leachate before recirculation. This is due to the accumulation of volatile fatty acids (VFAs) in the early phases of decomposition. Day 72 marked the beginning of the accelerated methane phase (phase 3), in which there is a rapid increase in the rate of methane production to a maximum value and the pH of leachate is about

neutral. Finally day 98 marked the beginning of the decelerated methane phase (phase 4), in which the methane production rate decreases and then stabilize.

The reactors were destructively sampled at the end of the aerobic phase, anaerobic acid phase, accelerated methane production phase, and decelerated methane production phase and four degraded MSW samples were obtained.

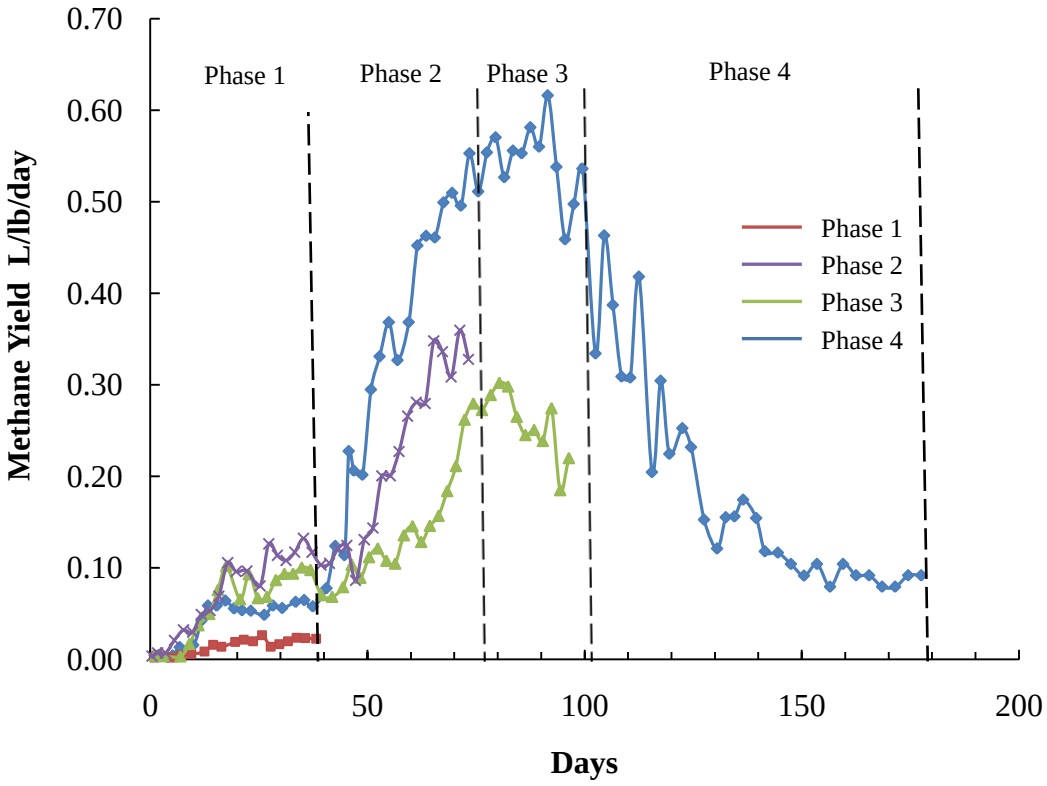

Figure 3.9 Methane Production Rates for Each Phase of Decomposition

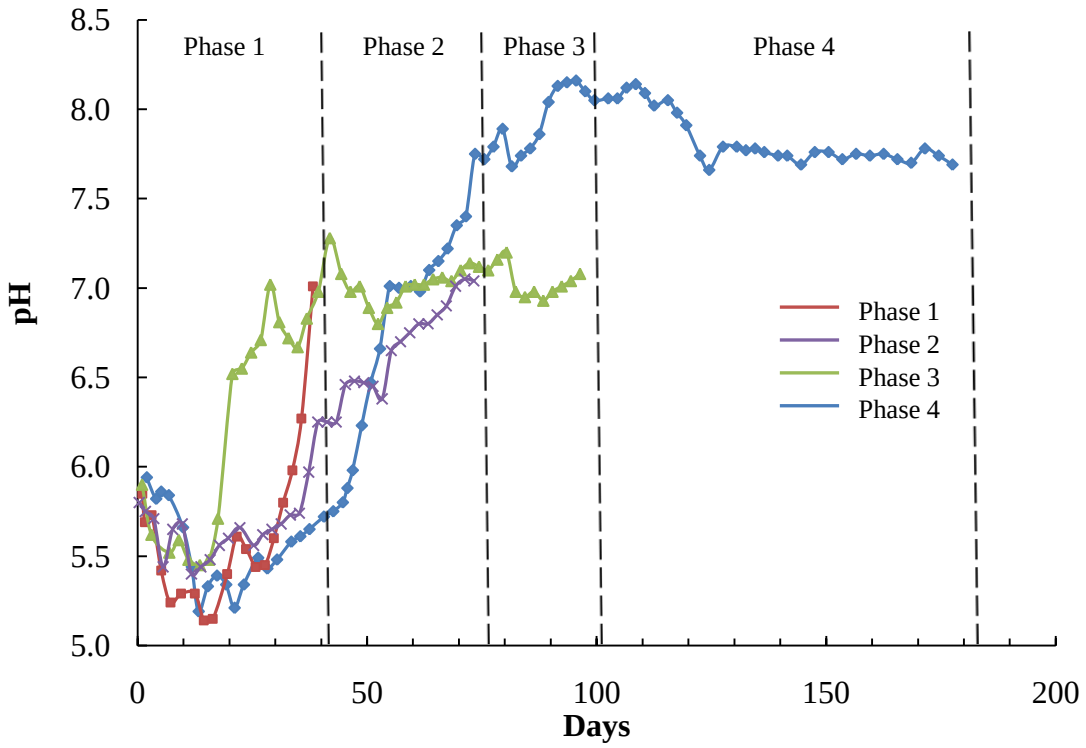

Figure 3.10 Leachate pH Data for Each Phase of Decomposition

3.4 Experimental Program

An extensive experimental program was developed to determine the characteristics of fresh, partially degraded, and degraded MSW samples. Also, the electrical resistivity of fresh, partially degraded, and degraded MSW samples was determined at the laboratory. The experimental program is discussed in details next.

3.4.1 Characteristics of MSW Samples

The characteristics (physical composition, moisture content, organic content, and unit weight) of fresh, partially degraded, and degraded MSW samples were determined as presented in Table 3.1.

Table 3.1 Experimental Program to Determine Characteristics of MSW

Test	Sample	No. of Tests
Physical Composition	Fresh MSW	5
	Partially degraded MSW from boreholes B45, B47, B49	30
	Partially degraded MSW from boreholes B70, B72	12
Moisture Content	Fresh MSW	5
	Partially degraded MSW from boreholes B45, B47, B49	30
	Partially degraded MSW from boreholes B70, B72	12
	Degraded MSW Samples	4
Organic Content	Fresh MSW	5
	Partially degraded MSW from boreholes B45, B47, B49	30
	Degraded MSW Samples	4
Unit Weight	Fresh MSW	5

3.4.1.1 Physical Composition

The physical composition of five fresh MSW samples, thirty landfilled MSW samples (from boreholes B45, B47, and B49), and twelve landfilled MSW samples (from boreholes B70 and B72) was determined by manually sorting the waste components into the following nine categories: paper, plastic, food waste, textile, wood & yard waste, metals, glass, styrofoam & sponge, and others. The "others" category included soil, rocks, and fines that were difficult to identify by visual observation. Figure 3.11 shows one of the borehole samples after sorting. The sorted components were then weighed individually, and weight percentages were determined.

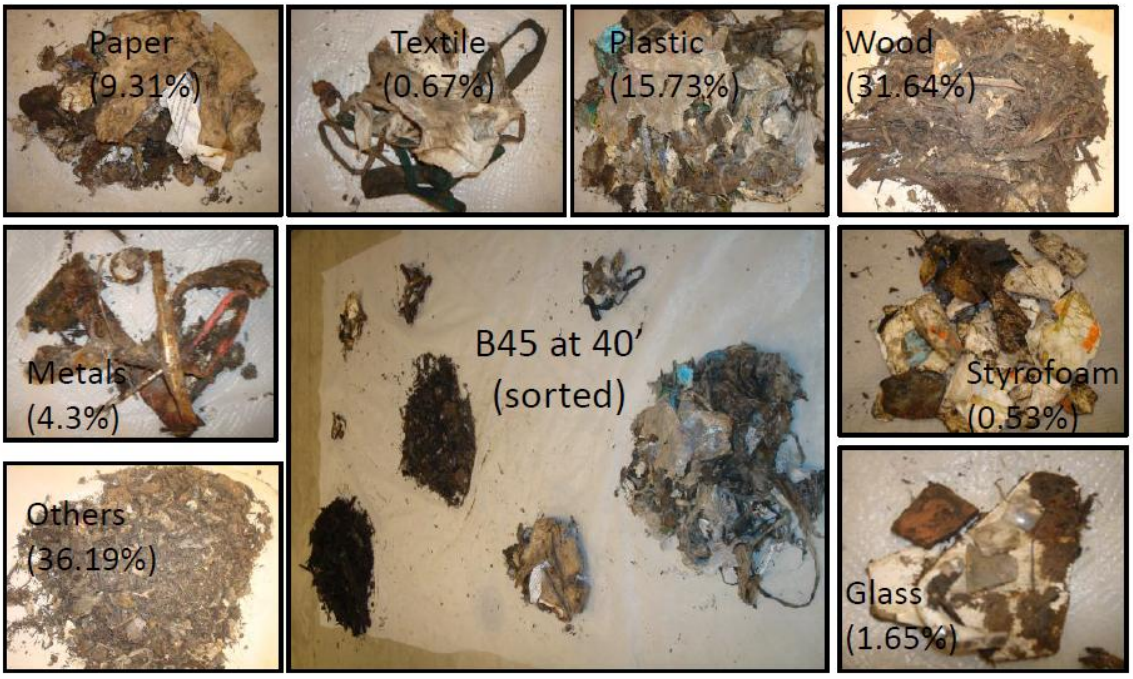

Figure 3.11 Determination of Physical Composition of MSW

3.4.1.1 Moisture Content

The moisture content of five fresh MSW samples, thirty landfilled MSW samples (from boreholes B45, B47, and B49), twelve landfilled MSW samples (from boreholes B70 and B72), and four degraded MSW samples was determined on wet weight basis according to procedure 2540B in Standard Methods (AWWA-APHA, 2005).

Approximately 2 lb of MSW was dried in an oven at 105 ºC for 24 hours until a constant weight was achieved. Moisture content (w_w) on a wet weight basis was determined using:

$$w_w = \frac{M_w}{M_T} \tag{3.1}$$

where M_w is the mass of liquid and M_T is the mass of the total wet sample. w_w has been the traditional parameter used in the MSW field. Electrical resistivity is commonly related to the volumetric moisture content (θ) which is defined by:

$$\theta = \frac{V_w}{V_T} \tag{3.2}$$

where V_w is the volume of liquid and V_T is the volume of the total wet sample. Therefore, it is preferable to use θ to estimate moisture content using electrical resistivity. Volumetric moisture content (θ) is related to the gravimetric moisture content by the following relationship:

$$\theta = \left(\frac{\gamma_m}{\gamma_w}\right) w_w \tag{3.3}$$

where γ_m is the unit weight of the wet sample, γ_w is the unit weight of water, and w_w is the gravimetric moisture content on wet weight basis.

3.4.1.2 Organic Content

Organic content is one of the main indicators of the state of decomposition of MSW. Decomposition results in a decrease in organic content. Organic content, also known as volatile solids (VS) and loss-on-ignition was determined according to procedure 2540E in Standard Methods (AWWA-APHA, 2005). Organic content of five fresh MSW samples, thirty landfilled MSW samples (from boreholes B45, B47, and B49), and four degraded MSW samples was determined. Samples were initially dried at 105ºC before igniting the samples in a muffle furnace at a temperature of 550ºC. Approximately 50 grams of the dried sample was ignited for one hour until a constant weight was achieved. The percent weight lost on ignition is the organic content. The biodegradable portion of MSW (paper, food waste, yard waste) was used to determine the organic content, to minimize the heterogeneities created by the presence of cover soil and

other non-degradable materials. Figure 3.12 shows the muffle furnace used and a waste sample after igniting in a muffle furnace

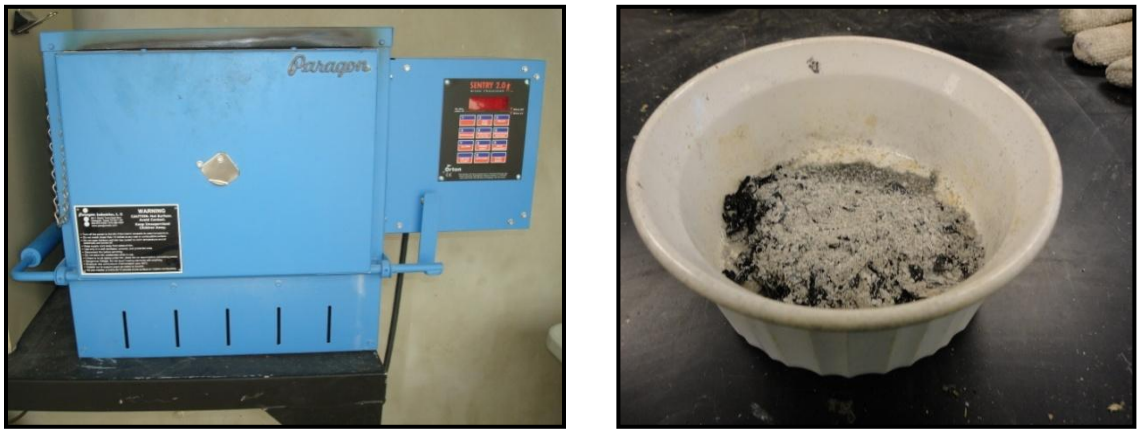

(a) (b)

Figure 3.12 Organic Content Determination: (a) Muffle furnace and (b) Burnt Sample

3.4.1.3 Unit Weight

The unit weight of five fresh MSW samples was determined as per Standard Proctor Compaction. A larger compaction mold than the standard mold was used. The mold has a 6 inch inside diameter and volume of 1/10 cubic feet. A 5.5 lb hammer was dropped 75 times for a fall height of 12 inch on each of three layers to achieve required compaction. Figure 3.13 illustrates the sample preparation for unit weight test. The unit weight is then determined using:

$$Unit\ Weight\ \left(\frac{lb}{ft^3}\right) = \frac{weight\ of\ compacted\ waste\ inside\ the\ mold\ (lb)}{volume\ of\ mold\ (ft^3)} \qquad (3.4)$$

Figure 3.13 Sample Being Compacted for Unit Weight Determination

3.4.2 Electrical Resistivity Tests

The electrical resistivity of fresh MSW samples, landfilled MSW samples, and degraded MSW samples was determined at the laboratory. The following sections discuss the apparatus used for resistivity measurement and the procedures followed to conduct resistivity tests.

An acrylic rectangular box was designed to measure the electrical resistivity of MSW as presented in Figure 3.14a. The test box is based on the four electrode method. The box has two metal ends and two pins inserted across its length. The dimensions of the box are 14.8 cm x 15.5 cm x 29.5 cm. The resistivity of the MSW sample is measured by passing current between the ends and measuring the voltage drop between the interior pins. The basic equation associated with the resistivity box is

$$\rho = \frac{WH}{L} R \tag{3.5}$$

where ρ = specimen resistivity; W = width of the box; H = height of box; R = measured resistance; and L = distance between the inner pins.

The resistivity test box was calibrated using sodium chloride solutions of known electrical resistivity. The solutions were prepared under laboratory conditions using a conductivity meter, which was calibrated itself to standard solutions. Also, the resistivity of highly plastic clay (CH) was measured using the resistivity test box. The resistivity values for highly plastic clay ranged from 2 to 22 ohm-m, which compare well with values found in literature (Abu-Hassanein et al., 1996). The SuperSting R8IP (Figure 3.14b) was used to measure the resistance in ohms.

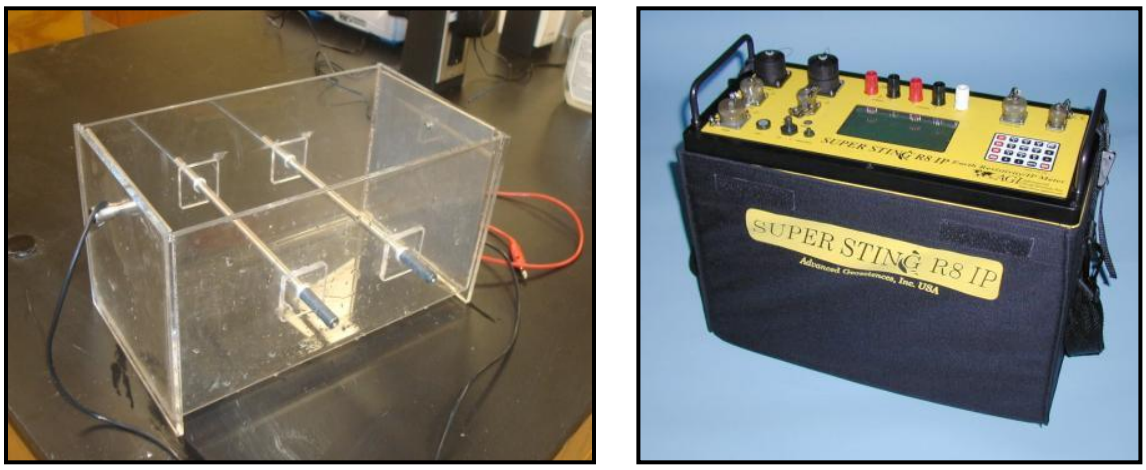

(a) (b)

Figure 3.14 (a) Resistivity Test Box and (b) SuperSting Resistivity Meter

The effect of moisture content, unit weight, decomposition, temperature, composition of MSW, and composition of pore fluid on resistivity of MSW was studied. This was done by varying one variable at a time and controlling the rest of the variables.

The experimental program followed to measure the resistivity of MSW samples is presented in Table 3.2.

Table 3.2 Experimental Program for Resistivity Measurement Tests

Test Variable	Sample	No. of Tests	Comments
Moisture Content	Fresh MSW	5 5	• At field moisture content • Varying m/c from 20% to 55%
	Partially degraded MSW from boreholes B45, B47, B49 MSW from borehole B45	30 3	• At field moisture content • Varying m/c from 20% to 55%
	Degraded MSW	4 4	• At actual moisture content upon reactor dismantling • Varying m/c from 20% to 55%
Unit Weight	Fresh MSW	5 x 3	At unit weight of 35, 45, and 55 lb/ft^3
	Partially degraded MSW from borehole B49	5 x 3	At unit weight of 35, 40, and 45 lb/ft^3
	Degraded MSW	4 x 3	At unit weight of 35, 45, and 55 lb/ft^3
Temperature	Fresh MSW	5	Varying temperature from 60 to 100°F
Composition	Fresh MSW	5	
	Partially degraded MSW from boreholes B45, B47, B49	30	
Pore Fluid Composition	Fresh MSW	5 5	• Using leachate • Using re-use water

3.4.2.1 Effect of Moisture Content

Resistivity tests were initially conducted on five fresh MSW samples, thirty landfilled MSW samples, and four degraded MSW samples at their actual moisture contents as presented in Table 3.2. The samples were compacted to a moist unit weight of 35 lb/ft^3. Taufiq (2010) determined that the moist unit weight of MSW was approximately 35 lb/ft^3 using standard proctor compaction effort. Also the used unit weight is within the range of 30 – 45 lb/ft^3 given be Oweis and Khera (1998) for MSW with moderate to good compaction. MSW samples were compacted in a wooden mold using a standard proctor test hammer. The wooden mold has the same dimensions of the test box and has a detachable base. The wooden mold was used to avoid breaking the acrylic test box. The compacted waste sample was then transferred to the test box and the metal pins were inserted. Then another layer of compacted waste was added. The sample was covered with a plastic wrap to prevent any moisture loss. The sample was left in the test box for at least 24 hours and then the resistivity tests were conducted. The detailed sample preparation procedure is presented in Figure 3.15.

Since the MSW samples at their field moisture contents did not exhibit a wide range of moisture contents, further tests were done on the samples by varying their moisture content. Each of the fresh MSW samples was initially dried completely by placing in an oven at 105 ºC for 24 hours. The oven dried sample was compacted to a dry unit weight of 35 lb/ft^3. The remolded sample was then transferred to the resistivity box. Tap water (resistivity ranging from 30 – 32 ohm-m) was added daily to the sample and the corresponding moisture content was determined. The sample was covered with a plastic wrap to prevent any moisture loss. The sample was left in the test box for at least

24 hours to ensure even moisture distribution and then the resistivity tests were conducted.

Also, further resistivity tests were done on three landfilled MSW samples from B45 collected from depths of 20, 30, and 40 ft. Each of the landfilled MSW samples was oven dried and compacted to a dry unit weight of 21 lb/ft^3. The remolded sample was then transferred to the resistivity box and tap water was added to the sample to vary the moisture content. The sample was left in the test box for at least 24 hours to ensure even moisture distribution and then the resistivity tests were conducted.

Also, further resistivity tests were done on four degraded MSW samples. Each of the degraded MSW samples was oven dried and compacted using the same compaction effort (25 blows on each of 4 layers using standard proctor test hammer). The remolded sample was then transferred to the resistivity box and tap water was added to the sample to vary the moisture content. The sample was left in the test box for at least 24 hours to ensure even moisture distribution and then the resistivity tests were conducted.

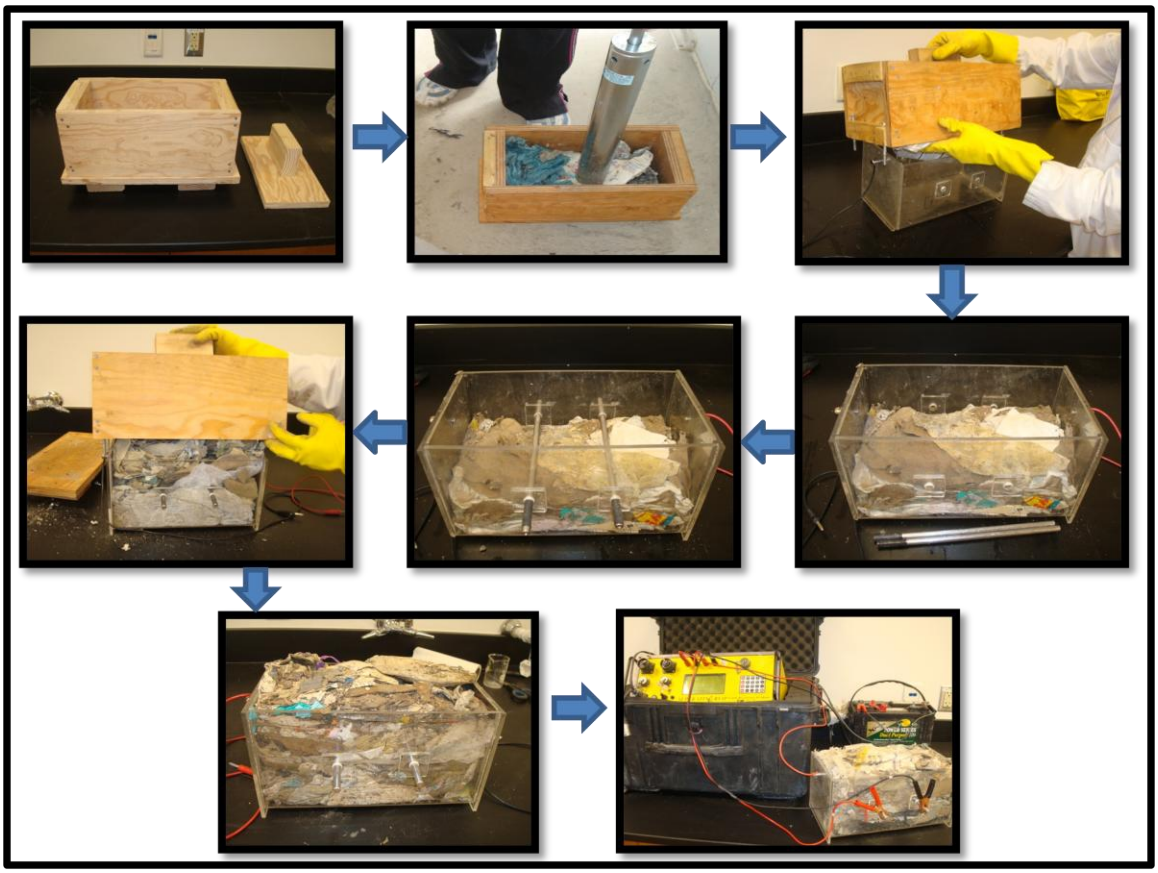

Figure 3.15 Sample Preparation Procedure For Resistivity Test

3.4.2.1 Effect of Unit Weight

To study the effect of unit weight on electrical resistivity, five fresh MSW samples, five landfilled MSW samples, and four degraded MSW samples at their actual moisture content were prepared at 3 different unit weights as presented in Table 3.2.

Five fresh MSW samples at their actual field moisture content were prepared at 35 lb/ft^3, 45 lb/ft^3, and 55 lb/ft^3 by increasing the compaction effort. Compaction was done by applying a load ranging between 1600 to 2000 pounds using a 60 kip tensile-compression machine (Figure 3.16) until the target unit weight was reached. The compression machine was used because it was not possible to reach the higher unit

weights, specially a unit weight of 55 lb/ft^3, using the standard proctor test hammer. The compacted samples were left in the test box for at least 24 hours and then the resistivity tests were conducted.

Also, five landfilled MSW samples from borehole B49 at their actual field moisture content were prepared at 3 different unit weights: 35 lb/ft^3, 40 lb/ft^3, and 45 lb/ft^3 by using a standard proctor test hammer. The compacted samples were left in the test box for at least 24 hours and then the resistivity tests were conducted.

Also, four degraded MSW samples at their actual moisture content upon reactor dismantling were prepared at 3 different unit weights: 35 lb/ft^3, 45 lb/ft^3, and 55 lb/ft^3 by using a standard proctor test hammer. The compacted samples were left in the test box for at least 24 hours and then the resistivity tests were conducted.

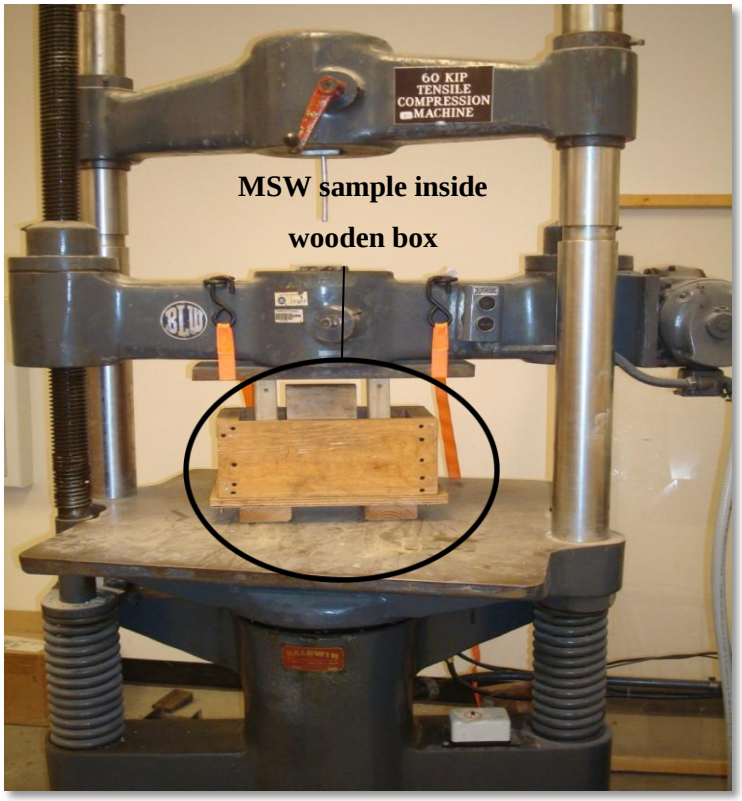

Figure 3.16 Compaction of MSW Sample

3.4.2.2 Effect of Decomposition

Since the landfilled MSW samples (from B45, B47, and B49) were only partially degraded based on organic content test results, four degraded MSW samples were prepared in laboratory scale reactors. Electrical resistivity tests were conducted on the degraded samples at their actual moisture contents upon dismantling the reactors. The degraded samples were compacted using the same compaction effort (25 blows on each of 2 layers using standard proctor test hammer). The compacted samples were left in the test box for at least 24 hours and then the resistivity tests were conducted.

Since the degraded samples had approximately the same moisture content and were compacted using the same compaction effort, any observed difference in resistivity values may be attributed to the effect of decomposition.

3.4.2.3 Effect of Temperature

All laboratory testing was conducted at room temperature (70°F). Before using any correlation that has been developed in the laboratory, the resistivity values obtained from field investigation has to be corrected to a standard temperature (70°F). An increase in temperature decreases the viscosity of water, causing the ions in the water to become more mobile. Therefore, the electrical conductivity of MSW is expected to increases and the resistivity is expected to decrease with increasing temperature.

To study the effect of temperature on the resistivity of MSW, five fresh MSW samples were compacted at their field moisture content to a unit weight of 45 lb/ft^3, placed in the test box, and then placed in a hot room (100 ºF) for 24 hours. Electrical resistivity was then measured as a function of temperature as the sample cooled down to

room temperature. To measure the temperature of the waste sample, a digital thermometer was inserted into the sample as shown in Figure 3.17.

Figure 3.17 Setup for Determining Effect of Temperature on Resistivity

3.4.2.4 Effect of Composition of MSW

Electrical conduction in solid waste is largely electrolytic, taking place in the liquid contained in the pores (Guerin et al., 2004). However, the effect of the composition of the solid waste on the electrical conduction is not clearly understood and has not been studied. In the soil science, it is well known that the type of rock affects electrical resistivity. Typical ranges of resistivities for a number of rock and soil types are well documented. Similarly, it is expected that the solid content of the waste may have an effect on electrical resistivity.

To study the effect of composition of MSW on resistivity, the waste samples in the test box were manually sorted into individual components after conducting the resistivity tests. The weight percentages of the paper and "others" components were determined for five fresh MSW samples and thirty landfilled MSW samples from boreholes B45, B47, and B49. Paper and "others" were selected because they were the dominant components in the waste samples.

3.4.2.5 Effect of Pore Fluid Composition

Electrical conduction in solid waste is largely electrolytic, taking place in the liquid contained in the pores. In a bioreactor landfill, the liquid contained in the pores can be leachate, re-use water, or a combination of both. The composition of the pore fluid is expected to have a significant effect on the electrical resistivity of MSW.

Using Leachate:

Leachate usually contains various inorganic ions (ex: K^+, Na^+, $NH4^+$, Cl^-). More electrical conduction occurs as a result of the movement of these additional ions in the leachate. A significant drop in resistivity is expected for MSW mixed with leachate compared to MSW mixed with water.

To have a better understanding of the effect of pore fluid composition on the resistivity of MSW, the resistivity of the five fresh MSW samples was measured. However, leachate collected from the city of Denton landfill was added to the samples instead of tap water. Leachate was collected in October 2010 from an on-site leachate storage tank as presented in Figure 3.18 (a) and (b).

Each of the fresh MSW samples was initially dried completely, compacted to a dry unit weight of 35 lb/ft^3, and then transferred to the resistivity box. Leachate was

added daily to the sample and the corresponding moisture content was determined. The sample was left in the test box for at least 24 hours to ensure even moisture distribution and then the resistivity tests were conducted. The results obtained from tap water and leachate addition into MSW were compared.

(a) (b)

Figure 3.18 (a) Leachate Storage Tank and (b) Leachate Collection

Using Re-Use Water:

When the amount of leachate produced at the landfill is insufficient, the City of Denton landfill recirculate re-use water into the waste mass. The re-use water is treated waste water effluent from an on-site waste water treatment plant.

The resistivity of the five fresh MSW samples was measured again using re-use water collected in December 2010 from the landfill. Each of the fresh MSW samples was initially dried completely, compacted to a dry unit weight of 35 lb/ft^3, and then transferred to the resistivity box. Re-use water was added daily to the sample and the corresponding moisture content was determined. The sample was left in the test box for at least 24 hours to ensure even moisture distribution and then the resistivity tests were

conducted. The results obtained from tap water and re-use water addition into MSW were compared.

3.5 Multiple Linear Regression Analysis

Multiple linear regression (MLR) analysis was used to develop a model between the electrical resistivity of MSW and the several factors that affect resistivity. Regression analysis is a statistical tool for modeling and analyzing the relationships between several variables. MLR is used to model the relationship between a response variable and two or more predictor variables. MLR is valuable tool for quantifying the effect of various factors simultaneously on a single dependent variable. The assumed linear relationship between the response variable and p-1 predictor variables is given by:

$$Y_i = \beta_0 + \beta_1 X_{i1} + \beta_2 X_{i2} + \ldots + \beta_{p-1} X_{i,p-1} + \varepsilon_i \quad (3.6)$$

where:

$\beta_0, \beta_1, \ldots, \beta_{p-1}$ are unknown model parameters,

$X_1, X_2, \ldots, X_{p-1}$ are predictor variables, and

ε is the random error.

Statistical Analysis System (SAS) software was used for the data analysis. Five predictor variables were considered: moisture content, unit weight, percentage paper, percentage "others" (fines), and organic content. Electrical resistivity was the response variable. SAS was used to fit a preliminary model to the experimental data, to perform residual analysis, to explore interaction terms, and to search for the best model. The best model was selected using backward elimination method, best subsets selection method, and stepwise regression method.

CHAPTER 4

RESULTS AND DISCUSSION

4.1 Introduction

In this chapter, all the experimental results are presented, discussed, and compared with the existing literature. The results of the characteristics of MSW samples (physical composition, moisture content, organic content, and unit weight) are first presented. The results of the resistivity tests are then discussed in details. The resistivity tests results explains the pair-wise effect of moisture content, unit weight, decomposition, temperature, composition of MSW, and composition of the pore fluid on the electrical resistivity of MSW.

4.2 Characteristics of MSW Samples

4.2.1 Physical Composition

4.2.1.1 Fresh MSW samples

For the fresh MSW samples, paper constituted the major portion of MSW in all five bags followed by plastics. The physical composition results show that despite the recycling efforts, a considerable amount of paper and plastic remain in the MSW. The weight percentages of MSW components in each sample are presented in Table 4.1. The average physical composition by weight for all five samples is presented in Figure 4.1. The average weight percentages of paper and plastic are 36.32% and 19.34% respectively. Food waste was a minor component, having an average weight percentage of 2.32% only. This is explained by the increased use of food waste disposal systems in

kitchens in the present days. These physical composition results are consistent with the results determined by Taufiq (2010) in an earlier MSW characterization study on MSW collected from the same landfill.

Table 4.1 Weight Percentages of MSW Components in Each Sample

	Physical Composition (% by Weight)									
Sample	Paper	Plastic	Food waste	Textile	Yard waste	Metals	Glass	Styrofoam	Others	C & D
1	32.75	29.54	1.51	2.25	5.78	5.95	0.4	5.63	12.46	3.72
2	34.2	17.51	2.54	7.76	9.45	2.24	0.43	4.84	17.08	3.94
3	28.45	18.58	1.06	5.64	8.55	20.26	0.32	4.53	11.28	1.33
4	47.63	16.1	4.44	5.31	7.16	2.48	0.69	2.36	13	0.84
5	38.57	14.99	2.07	10.03	13.92	4.47	0.44	1.24	13.47	0.82
Average	36.32	19.34	2.32	6.20	8.97	7.08	0.46	3.72	13.46	2.13
Standard Deviation	7.28	5.86	1.31	2.91	3.10	7.52	0.14	1.84	2.18	1.57

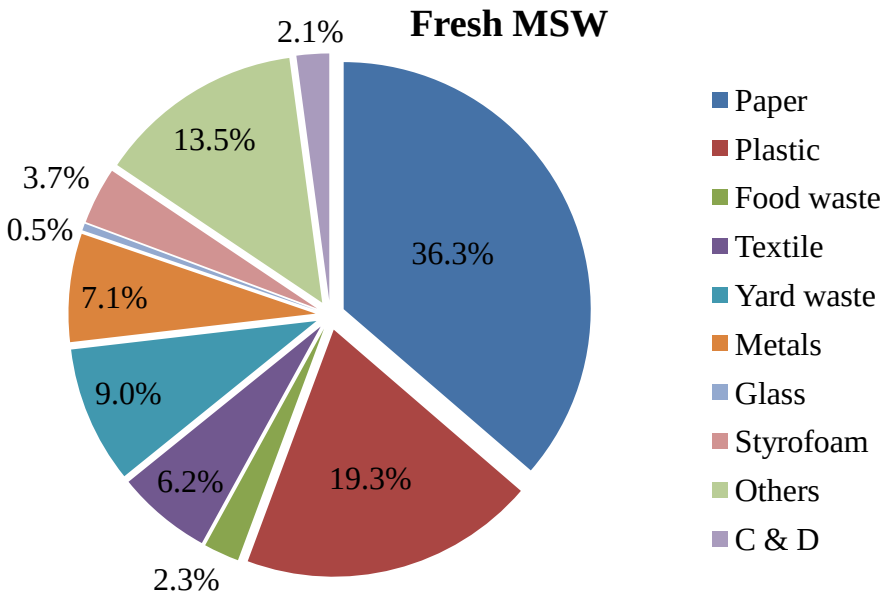

Figure 4.1 Average Physical Composition by Weight for Fresh MSW

4.2.1.2 Landfilled MSW Samples

The first set of landfilled MSW samples (from boreholes B45, B47, and B49) was approximately 2 to 8 years old based on landfill records. The oldest readable material was a newspaper recovered from a depth of 65 ft and was dated April 2002. The weight percentages of MSW components with depth for samples from B45, B47, and B49 are presented in Table 4.2, Table 4.3, and Table 4.4, respectively. The average physical composition by weight for samples from B45, B47, and B49 are presented in Figure 4.2, Figure 4.3, Figure 4.4, respectively.

Paper and "others" constituted the major portion of MSW in the three boreholes. The average weight percentages of paper in boreholes B45, B47, and B49 are 21.43%, 36.32, and 14.76% respectively. The average weight percentages of "others" category in boreholes B45, B47, and B49 are 43.53%, 38.33%, and 61.11% respectively. The high percentages of the "others" category is most likely due to the presence of intermediate soil cover between the solid waste layers. Also, the biodegradable components decompose and disintegrate with time and become unidentifiable. The amount of food waste, glass, and styrofoam were negligible.

Comparing the physical composition of the landfilled MSW samples with that of the fresh MSW samples, a higher “others” content was observed in the landfilled MSW samples. Also, fresh MSW samples contained a small amount of food waste (2.32%), while the landfilled MSW samples contained no food waste.

Table 4.2 Weight Percentages of MSW Components with Depth for Borehole B45

	Physical Composition (% by Weight)								
Depth (ft)	Paper	Plastic	Food waste	Textile	Yard waste	Metals	Glass	Styrofoam	Others
20	28.77	15.13	0.00	1.86	8.95	2.87	0.19	0.16	42.07
25	27.59	16.24	0.00	5.10	1.44	1.46	1.00	0.18	46.98
30	11.72	7.01	0.00	7.19	3.37	11.41	0.56	0.12	58.61
35	35.90	8.97	0.00	1.71	4.66	8.49	0.58	1.32	38.37
40	9.31	15.73	0.00	0.67	31.64	4.30	1.65	0.53	36.19
45	7.19	10.09	0.00	0.51	61.04	0.57	0.44	0.00	20.16
50	30.23	15.52	0.00	1.57	10.10	1.09	0.53	0.00	40.97
55	13.87	8.74	0.00	0.83	10.31	2.70	1.09	0.38	62.09
60	45.73	16.54	7.40	4.00	0.10	3.77	0.10	0.72	21.65
65	4.03	15.73	0.00	5.37	4.01	2.54	0.08	0.04	68.20
Average	21.43	12.97	0.74	2.88	13.56	3.92	0.62	0.34	43.53
Standard Deviation	14.04	3.76	2.34	2.35	18.94	3.45	0.50	0.42	16.01

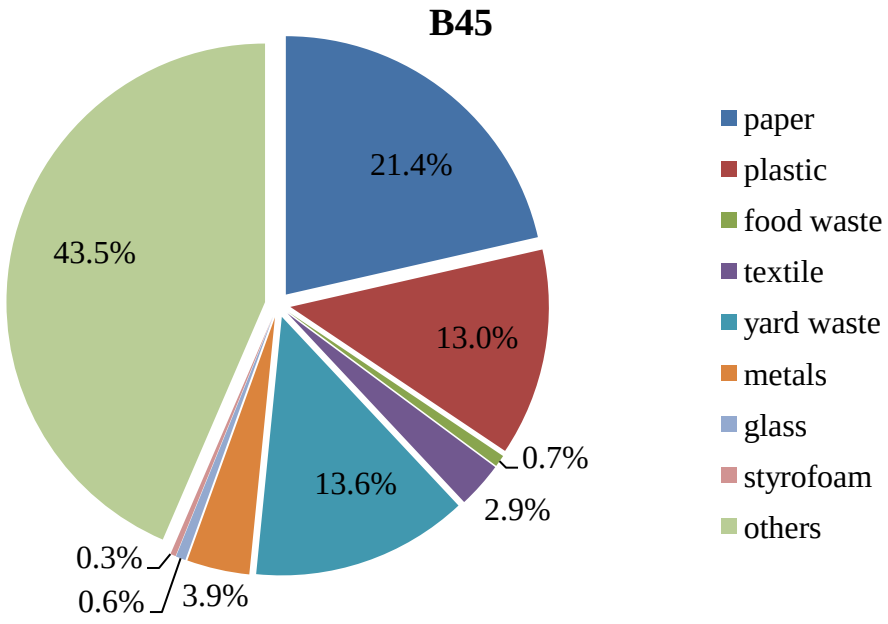

Figure 4.2 Average Physical Composition by Weight for Samples from Borehole B45

Table 4.3 Weight Percentages of MSW Components with Depth for B47

	Physical Composition (% by Weight)								
Depth (ft)	Paper	Plastic	Food waste	Textile	Yard waste	Metals	Glass	Styrofoam	Others
20	42.86	2.84	0.00	14.01	3.95	6.05	1.05	0.06	29.18
25	20.31	6.40	0.00	12.26	14.65	1.14	0.04	0.00	45.19
30	16.01	11.47	0.00	8.59	5.70	1.42	0.24	0.07	56.50
35	4.00	9.22	0.00	0.83	15.73	2.00	0.38	0.06	67.79
40	15.07	6.68	0.00	29.96	8.74	9.32	0.58	0.30	29.36
45	63.43	13.04	0.00	1.06	1.95	2.72	0.12	0.00	17.68
50	50.98	6.51	0.00	2.91	1.27	0.83	0.69	0.00	36.80
55	29.33	5.20	0.04	0.00	0.95	1.66	0.72	0.04	62.07
60	68.33	7.08	3.10	4.97	1.14	1.24	0.51	0.36	13.26
65	52.85	11.46	0.00	1.59	4.44	2.45	1.53	0.21	25.46
Average	36.32	7.99	0.31	7.62	5.85	2.88	0.59	0.11	38.33
Standard Deviation	22.37	3.21	0.98	9.28	5.49	2.71	0.45	0.13	18.85

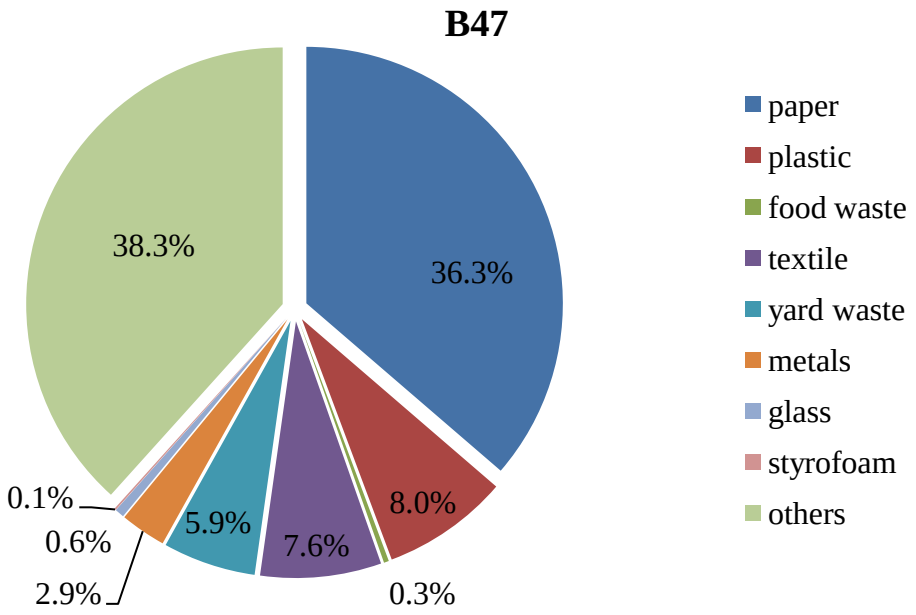

Figure 4.3 Average Physical Composition by Weight for Samples from Borehole B47

Table 4.4 Weight Percentages of MSW Components with Depth for Borehole B49

	Physical Composition (% by Weight)								
Depth (ft)	Paper	Plastic	Food waste	Textile	Yard waste	Metals	Glass	Styrofoam	Others
20	2.36	7.88	0.00	0.39	27.55	1.03	0.30	0.09	60.41
25	15.53	5.34	0.00	2.03	3.37	6.74	0.81	0.15	66.02
30	17.95	5.96	0.00	8.32	0.40	8.54	2.46	0.25	56.13
35	1.49	9.05	0.00	0.81	0.96	0.00	0.08	0.08	87.53
40	15.82	6.85	0.00	8.33	12.17	1.75	0.13	0.26	54.68
45	22.93	20.64	0.00	9.19	3.39	3.13	1.43	0.00	39.30
50	36.45	14.06	0.00	0.93	11.41	2.71	0.52	0.00	33.92
55	10.34	1.79	0.00	0.25	1.08	0.28	0.12	0.01	86.13
60	9.99	5.40	0.00	0.89	15.88	1.88	0.12	0.02	65.83
Average	14.76	8.55	0.00	3.46	8.47	2.89	0.66	0.10	61.11
Standard Deviation	10.73	5.62	0.00	3.91	9.15	2.91	0.81	0.10	18.21

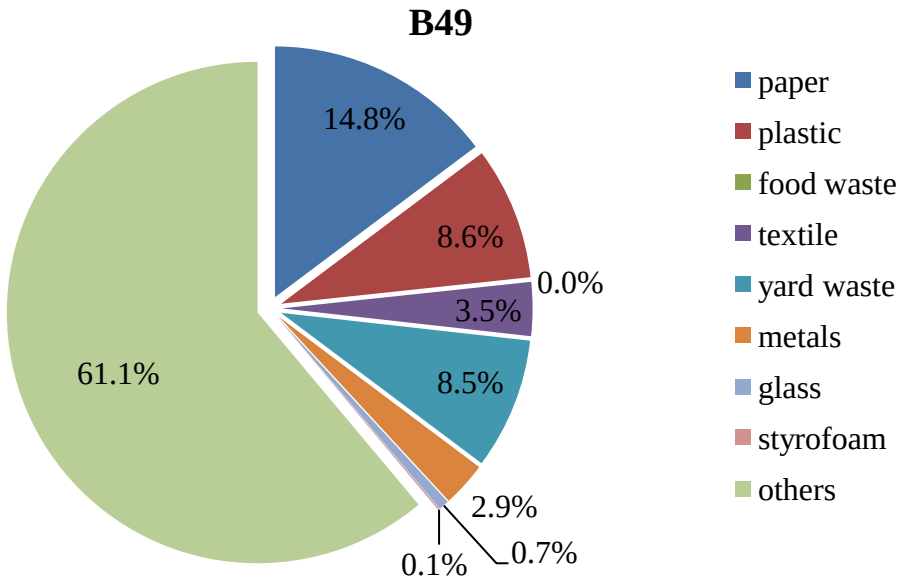

Figure 4.4 Average Physical Composition by Weight for Samples from Borehole B49

The second set of landfilled MSW samples (from boreholes B70 and B72) was collected in November 2010 for validation of the developed model. These samples were approximately 20 to 25 years old based on landfill records. The oldest readable material was a newspaper recovered from a depth of 50 ft and was dated back to 1985. The weight percentages of MSW components with depth for samples from B70 and B72 are presented in Table 4.5 and 4.6, respectively. The average physical composition by weight for samples from B70 and B72 are presented in Figure 4.5 and 4.6, respectively.

Paper constituted the major portion of MSW (43.87%) from borehole B70, while “others” constituted the major portion of MSW (55.83%) from borehole B72. The high percentage of the "others" category is due to presence of high amount of cover soil in samples collected from the top 30ft. MSW sample collected from borehole B72 at 10ft depth was entirely cover soil. The average percentage of paper in samples collected from borehole B72 was only 13.2%. The amount of food, waste, textile, glass, and styrofoam was negligible in MSW samples from both boreholes.

Table 4.5 Weight Percentages of MSW Components with Depth for Borehole B70

	Physical Composition (% by Weight)								
Depth (ft)	Paper	Plastic	Food waste	Textile	Yard waste	Metals	Glass	Styrofoam	Others
10	49.52	15.16	0	2.65	24.97	0.72	0.36	0.06	6.56
20	23.33	8.42	0	0.09	25.92	2.02	0.22	7.76	32.24
30	12.72	4.29	0	4.52	1.17	0.65	0.31	0.22	76.13
40	64.43	12.85	0	6.46	0.36	1.46	6.46	0.67	7.31
50	69.55	4.29	0	0.36	7.48	0.81	0.24	0.20	17.06
60	43.68	1.12	0	0.48	2.35	3.30	2.49	0.78	46.71
Average	43.87	7.69	0	2.43	10.38	1.49	1.68	1.62	31.00
Standard Deviation	22.39	5.46	0	2.62	11.94	1.03	2.50	3.02	26.97

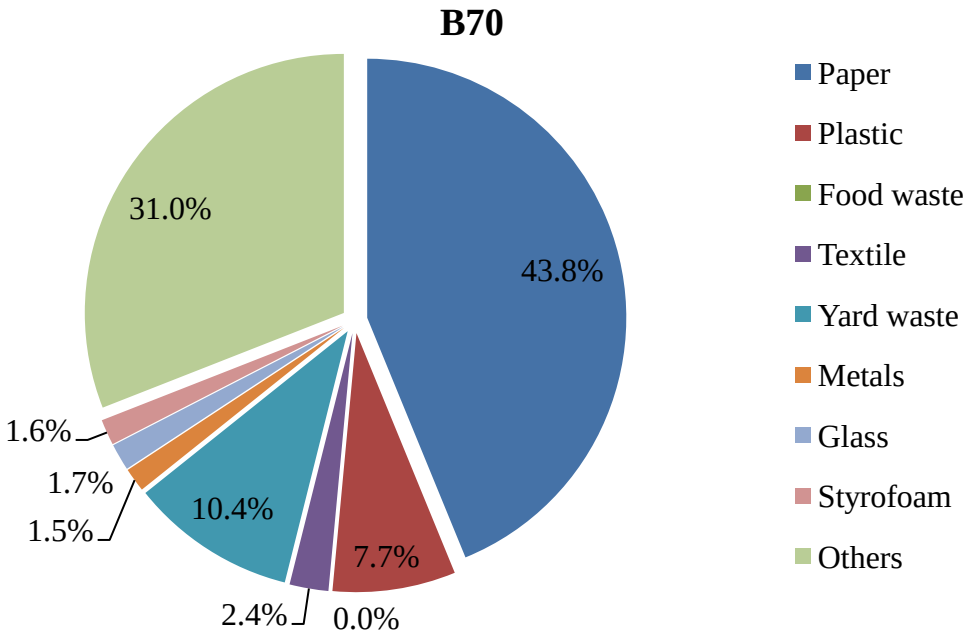

Figure 4.5 Average Physical Composition by Weight for Samples from Borehole B70

Table 4.6 Weight Percentages of MSW Components with Depth for Borehole B72

	Physical Composition (% by Weight)								
Depth (ft)	Paper	Plastic	Food waste	Textile	Yard waste	Metals	Glass	Styrofoam	Others
10	0	0	0	0	0	0	0	0	100
20	2.91	8.41	0	0.62	16.92	1.81	0.8	2.97	65.51
30	12.72	4.29	0	4.52	1.17	0.65	0.31	2.97	76.13
40	21.4	16.02	0	0.15	7.76	1.75	1.66	0.21	48.59
50	1.81	0.38	0	1.04	58.82	0.32	0.49	0.04	37.08
60	40.35	32.82	0	0	0.14	18.53	0.41	0.09	7.66
Average	13.20	10.32	0	1.06	14.14	3.84	0.61	1.05	55.83
Standard Deviation	15.58	12.52	0	1.75	22.84	7.23	0.58	1.49	32.19

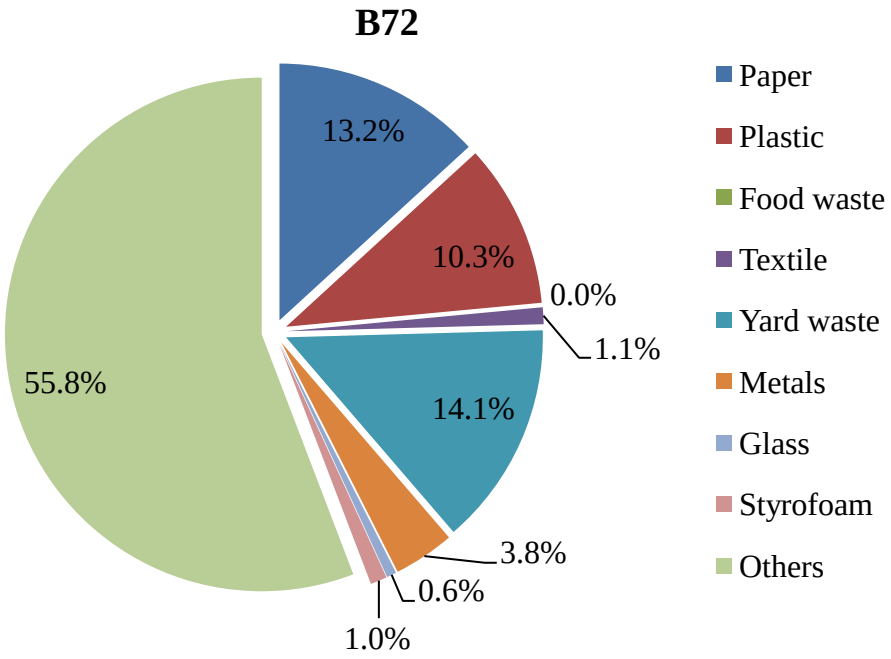

Figure 4.6 Average Physical Composition by Weight for Samples from Borehole B72

4.2.2 Moisture Content

4.2.2.1 Fresh MSW Samples

The moisture content of MSW samples was determined by drying the samples in an oven at 105 ºC for 24 hours as discussed in Chapter 3. For fresh MSW, the moisture content depends on the composition of the waste, the season of the year, and weather conditions. The moisture content results on wet weight basis are presented in Table 4.7 and Figure 4.7. The moisture content of the five fresh MSW samples varied from 24.21 % to 30.21%. The fourth MSW sample had the highest moisture content. From the physical composition results, the fourth sample also had the highest paper and food content. This shows that moisture content of MSW depends on the composition of the waste. Paper products tend to absorb more liquid, and food waste usually has high moisture content. The average moisture content of the five fresh MSW samples is 27.05%. This is within the typical range of 15 to 40 percent given by Tchobanoglous et al. (1993) for fresh MSW.

Table 4.7 Moisture Content Results for Fresh MSW Samples

Sample No.	Moisture Content (%) (Wet Weight Basis)
1	28.27
2	28.03
3	24.21
4	30.21
5	24.53
Average	27.05
Standard Deviation	2.59

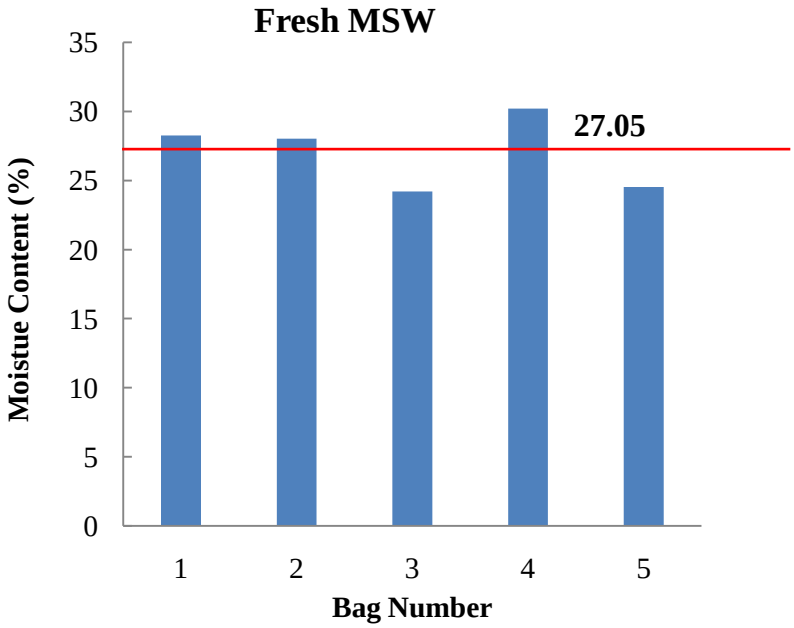

Figure 4.7 Moisture Content Results for Fresh MSW Samples

4.2.2.2 Landfilled MSW Samples

For the first set of landfilled MSW samples, the moisture content on wet weight basis varied from 13.07 % to 46.24%, from 21.4% to 39.47%, and from 11.8 % to 34.6% for samples from boreholes B45, B47, and B49 respectively. The average moisture content of the ten samples from boreholes B45, B47, and B49 are 24.4%, 31.1%, and 25.0 % respectively. The moisture content of MSW samples from the three boreholes are reported in Table 4.8. The moisture content profiles with depth along with the nearest recirculation pipe locations are presented in Figure 4.8, Figure 4.9, and Figure 4.10.

The nearest operating leachate recirculation lines to B45 and B47 are located at a depth of 30ft. This explains why an increase in moisture content is observed immediately below the recirculation lines for B45 and B47. On the other hand, there is no trend of increasing moisture content for B49. This is because the recirculation lines near B49 were

not operating at the time of sample collection. When comparing the average moisture contents of the borehole samples with that of the fresh MSW samples, not much difference is observed.

Table 4.8 Moisture Content of Landfilled MSW Samples from Boreholes B45, B47 and B49

Depth (ft)	Moisture Content (%) (Wet Weight Basis)		
	B45	B47	B49
20	21.74	39.47	11.82
25	25.50	32.83	34.55
30	18.42	28.65	29.37
35	30.13	21.40	20.46
40	46.24	30.14	29.51
45	30.88	27.08	22.79
50	13.07	37.63	31.47
55	13.14	25.65	21.94
60	29.60	29.58	23.10
65	15.72	39.05	
Average	24.45	31.15	25.00
Standard Deviation	10.29	6.04	6.94

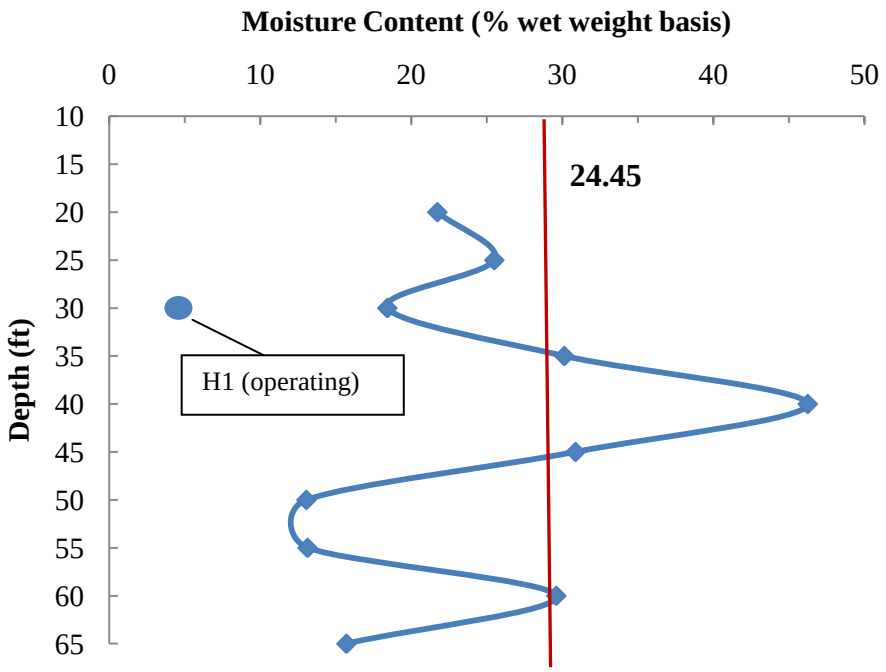

Figure 4.8 Moisture Content Profile with Depth for Borehole B45 with Nearest Recirculation Pipe Location

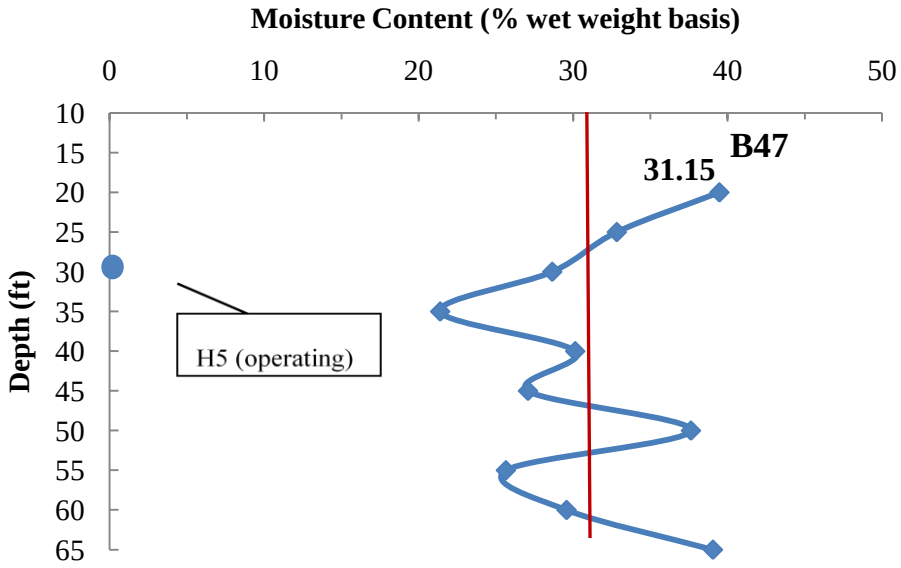

Figure 4.9 Moisture Content Profile with Depth for Borehole B47 with Nearest Recirculation Pipe Location

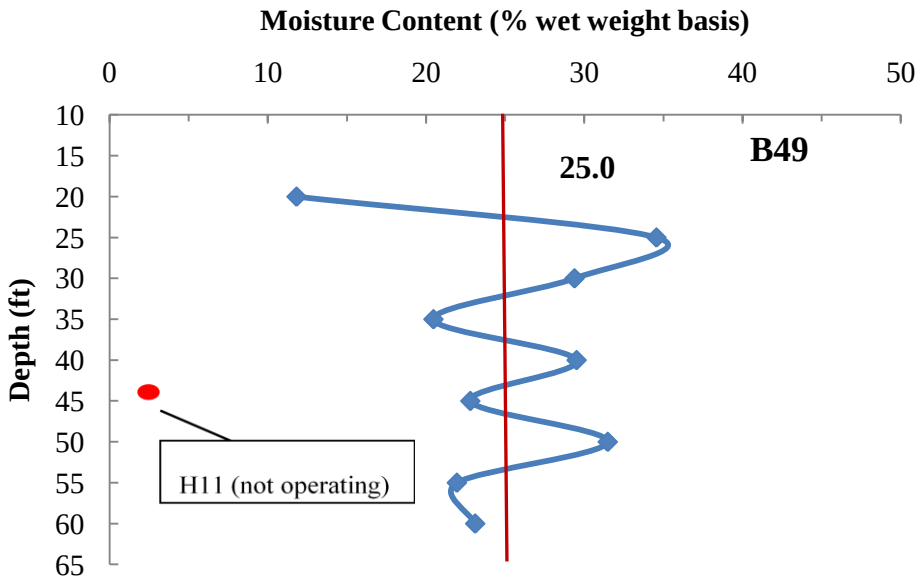

Figure 4.10 Moisture Content Profile with Depth for Borehole B49 with Nearest Recirculation Pipe Location

For the second set of landfilled MSW samples, the moisture content on wet weight basis varied from 17.38 % to 33.94% and from 11.38% to 26.39% for samples from boreholes B70 and B72, respectively. The moisture content of MSW samples from both boreholes is reported in Table 4.9. The moisture content profiles with depth are presented in Figure 4.11 and Figure 4.12.

The average moisture content of the six samples from boreholes B70 and B72 is 28.8% and 18.8%, respectively. The average moisture content of MSW samples from B70 is within the same range as that determined for boreholes B45, B47, and B49. On the other hand, MSW samples from borehole B72 had lower average moisture content. This is due to the presence of high amounts of cover soil and less paper content.

Table 4.9 Moisture Content of Landfilled MSW Samples from Borehole B70 and B72

Depth (ft)	Moisture Content (%) (Wet Weight Basis)	
	B70	B72
10	29.51	11.38
20	17.38	24.37
30	28.61	15.52
40	31.32	26.39
50	32.16	11.94
60	33.94	23.15
Average	28.8	18.8
Standard Deviation	5.92	6.64

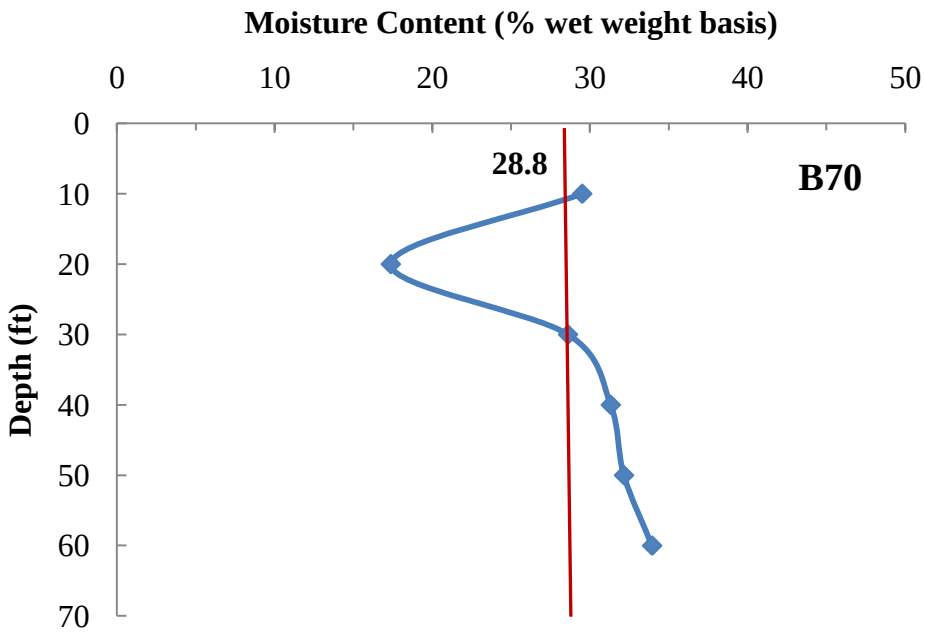

Figure 4.11 Moisture Content Profile with Depth for Borehole B70

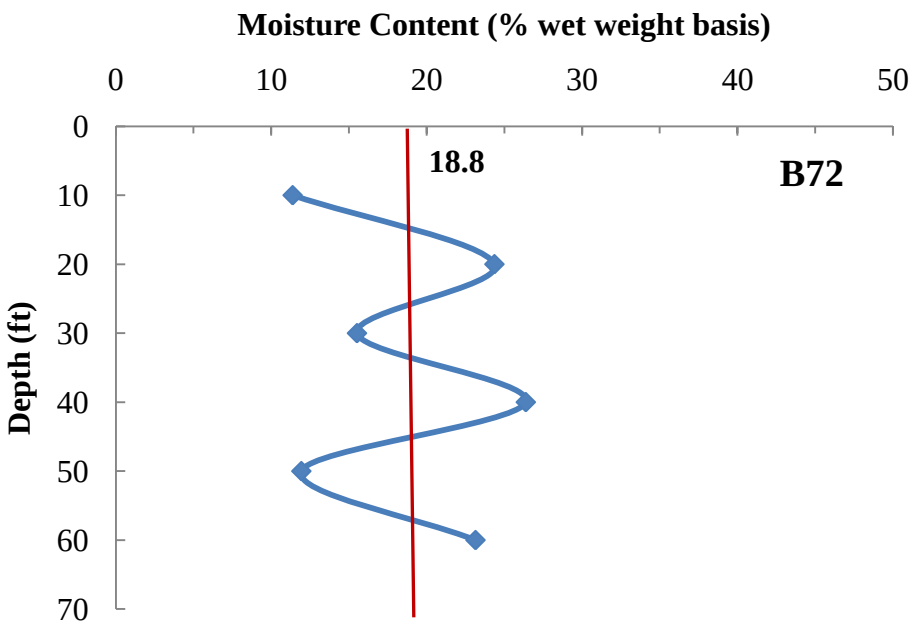

Figure 4.12 Moisture Content Profile with Depth for Borehole B72

4.2.2.3 Degraded MSW Samples

Four degraded samples were prepared in laboratory scale reactors. The moisture content of the degraded samples was determined immediately after dismantling the reactors. The moisture content of the degraded samples ranged from 65.24% to 71.6% on wet weight basis. Moisture content results are presented in Table 4.10 and Figure 4.13. The average moisture content of the degraded samples is 69.37%. The high moisture content values are a result of recirculating the generated leachate.

Table 4.10 Moisture Content of Degraded MSW Samples

Phase	Moisture Content (%) (Wet Weight Basis)
1	71.43
2	65.24
3	69.2
4	71.6
Average	69.37
Standard deviation	2.96

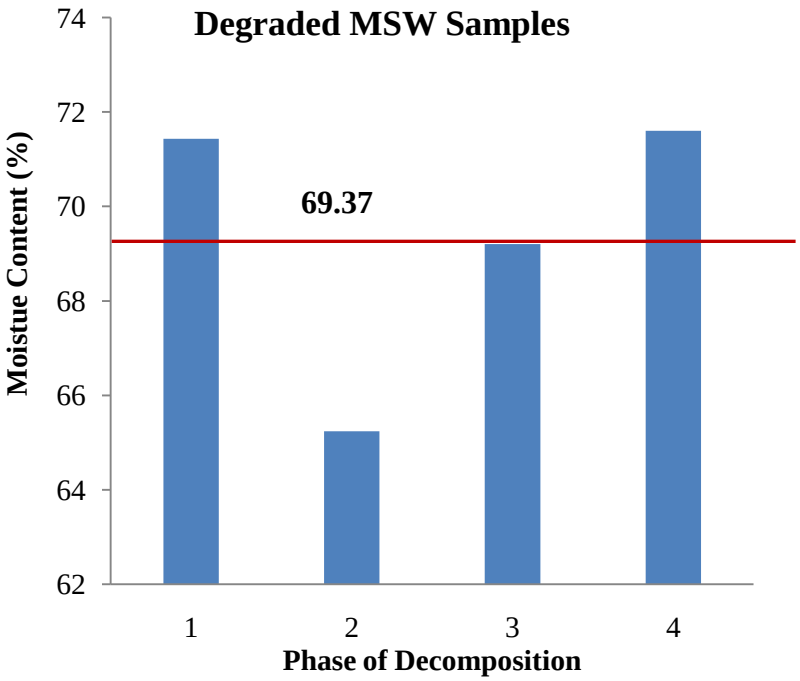

Figure 4.13 Moisture Content of Degraded MSW Samples

4.2.3 Organic Content

4.2.3.1 Fresh MSW Samples

The organic content of MSW samples was determined by igniting the samples in a muffle furnace at a temperature of 550ºC for 1 hour as discussed in chapter 3. For the fresh MSW samples, the organic content varied from 69.0% to 85.2%. The organic content results are presented in Table 4.11 and Figure 4.14. It is important to keep in mind that the biodegradable portion of MSW (paper, food waste, yard waste) was used to determine the organic content .The average organic content of the samples is 76.2%. This value compares well with the organic content value of 79% given by Barlaz et al. (1990) for fresh MSW. Reddy et al. (2009) estimated the organic content of fresh MSW collected from Orchard Hills Landfill in Illinois to range from 76% to 84%.

Table 4.11 Organic Content Results for Fresh MSW Samples

Sample No.	Organic Content (%)
1	77.49
2	69.0
3	74.5
4	74.9
5	85.23
Average	76.2
Standard Deviation	5.91

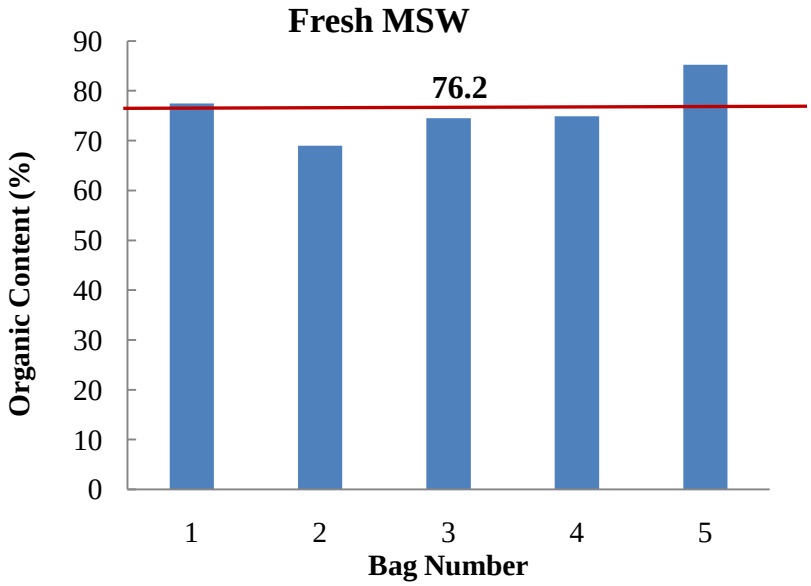

Figure 4.14 Organic Content of Fresh MSW Samples

4.2.3.2 Landfilled MSW Samples

The organic content of the first set of landfilled MSW samples (from boreholes B45, B47, and B49) was determined. The organic content varied from 55.7 % to 80.96%, from 68.0% to 83.3%, and from 65.9% to 83.7% for samples from boreholes B45, B47, and B49 respectively. The average organic content of the ten samples from boreholes B45, B47, and B49 are 71.7%, 73.9%, and 72.1% respectively. The organic content of the landfilled MSW samples is reported in Table 4.12. The organic content profiles with depth are presented in Figure 4.15, Figure 4.16, Figure 4.17. The highest decomposition (organic content = 55.73%) was observed at a depth of 45 ft for borehole B45. The results show that more decomposition occurred near the leachate recirculation lines than at higher depths. The results agree with the fact that more decomposition occurs at increased moisture content. Overall, not much decomposition was observed in the landfilled samples. Comparing the average organic content of the landfilled samples with

that of the fresh MSW samples, the organic content of the landfilled samples was slightly less. This indicates that not much decomposition occurred and that the landfilled samples are only partially degraded.

Table 4.12 Organic Content Results for Borehole Samples

Depth (ft)	Organic Content (%)		
	B45	B47	B49
20	80.00	83.33	83.70
25	63.33	72.00	78.49
30	72.00	76.19	75.89
35	80.96	69.23	65.59
40	62.48	69.23	67.62
45	55.73	76.00	68.27
50	78.42	68.00	65.88
55	75.83	76.92	66.24
60	77.18	76.00	77.27
65	71.43	72.00	--
Average	71.74	73.89	72.11
Standard Deviation	8.54	4.69	6.77

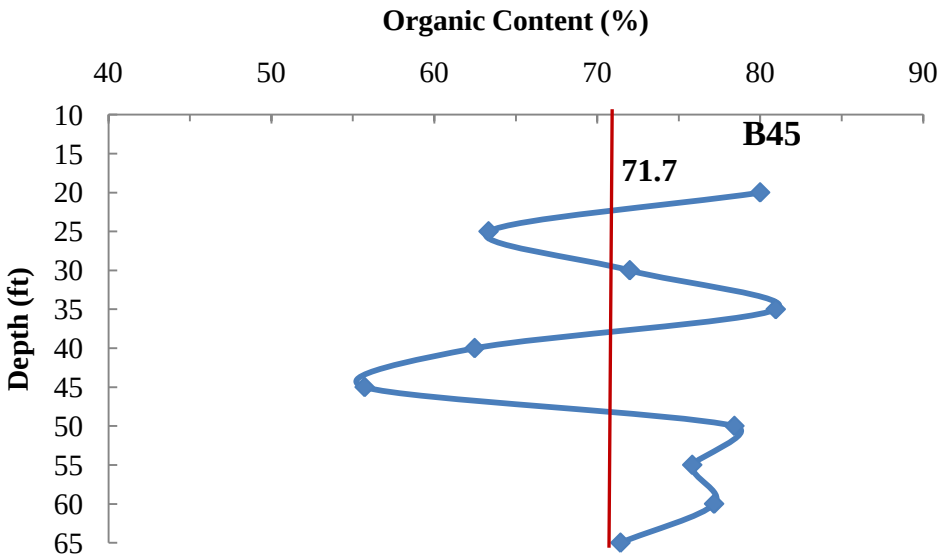

Figure 4.15 Organic Content Profile with Depth for Samples from Borehole B45

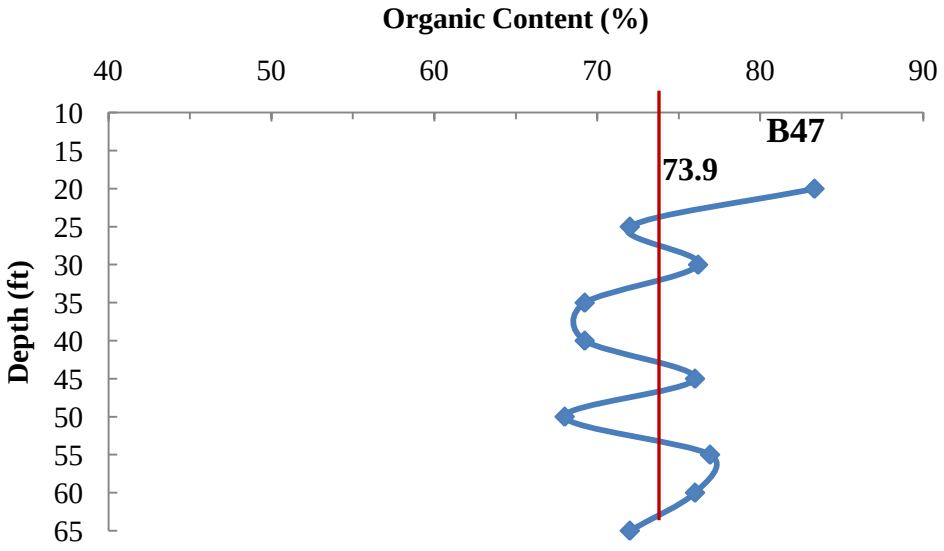

Figure 4.16 Organic Content Profile with Depth for Samples from Borehole B47

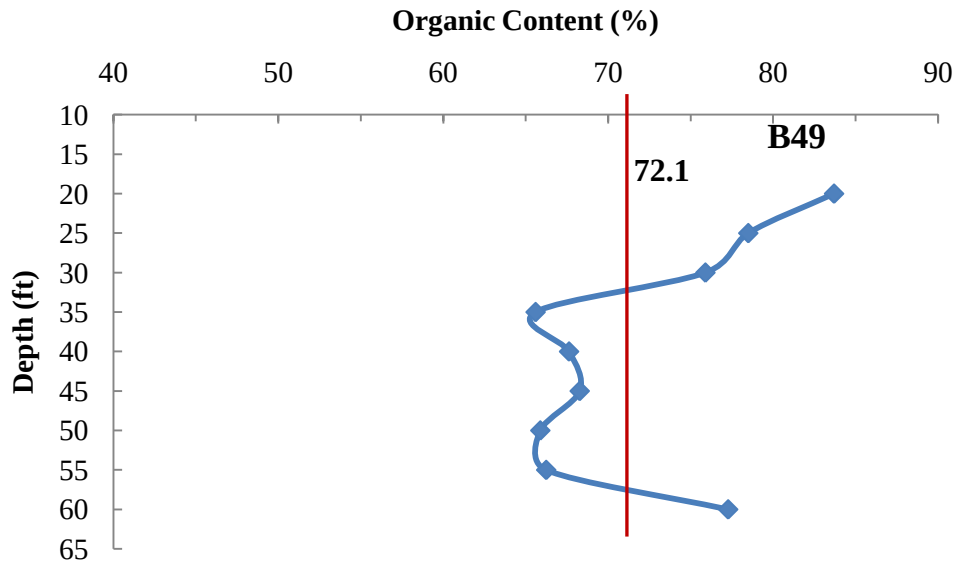

Figure 4.17 Organic Content Profile with Depth for Samples from Borehole B49

4.2.3.3 Degraded MSW Samples

Four degraded samples were prepared in laboratory scale reactors. The organic content of the degraded samples was determined immediately after dismantling the reactors. The organic content of the degraded samples decreased from 63.3% in phase 1 to 44.4% in phase 4. The accelerated decomposition is indicated by the decrease in organic content. Organic content results are presented in Table 4.13 and Figure 4.18. The average organic content of the degraded samples is 52.88%, compared to the average organic content value of 76.2% for fresh MSW samples.

The organic content results compare well with values published in the literature. Gomes et al. (2005) reported an organic content of 56% for aged MSW at 11m depth at a landfill in Portugal. Hossain and Haque (2009) prepared degraded MSW samples in laboratory scale reactors. The authors determined that the organic content of MSW decreased from 94% in phase 1 of decomposition to 41% in phase 4.

Table 4.13 Organic Content of Degraded MSW Samples

Phase	Organic Content (%)
1	63.3
2	50.2
3	53.6
4	44.4
Average	52.88
Standard deviation	7.92

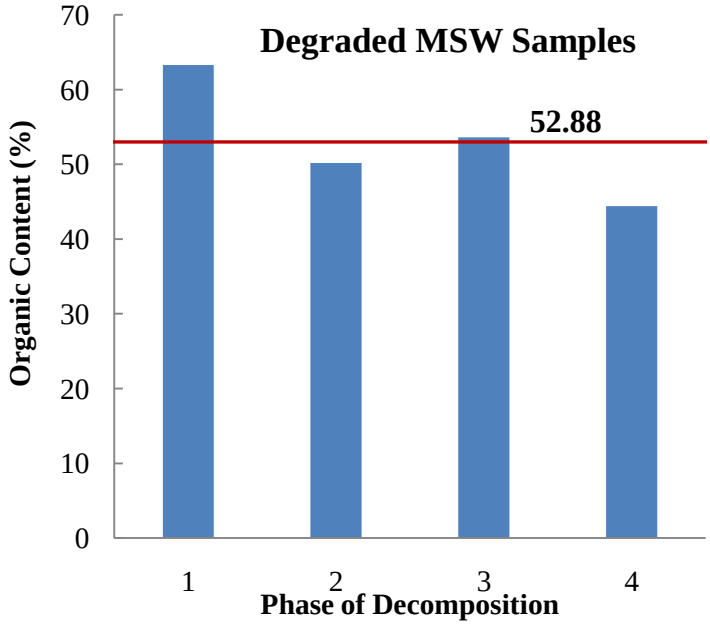

Figure 4.18 Organic Content of Degraded MSW Samples

4.2.4 Unit Weight

The unit weight of five fresh MSW samples compacted by standard proctor compaction effort was determined. The unit weight results are presented in Table 4.14 and Figure 4.19. The unit weight of the fresh MSW samples varied from 33.8 lb/ft^3 to 44.0 lb/ft^3. The average unit weight of the five samples is 38.9 lb/ft^3.

These results compare well with values published in literature. Taufiq (2010) determined that the moist unit weight of fresh MSW was approximately 35 lb/ft^3 using standard proctor compaction effort. Also the used unit weight is within the range of 30 – 45 lb/ft^3 given be Oweis and Khera (1998) for MSW with moderate to good compaction.

Table 4.14 Unit Weight of Fresh MSW Samples

Sample No.	Unit Weight (lb/ft^3)
1	44.0
2	33.8
3	37.4
4	38.8
5	40.5
Average	38.9
Standard Deviation	3.77

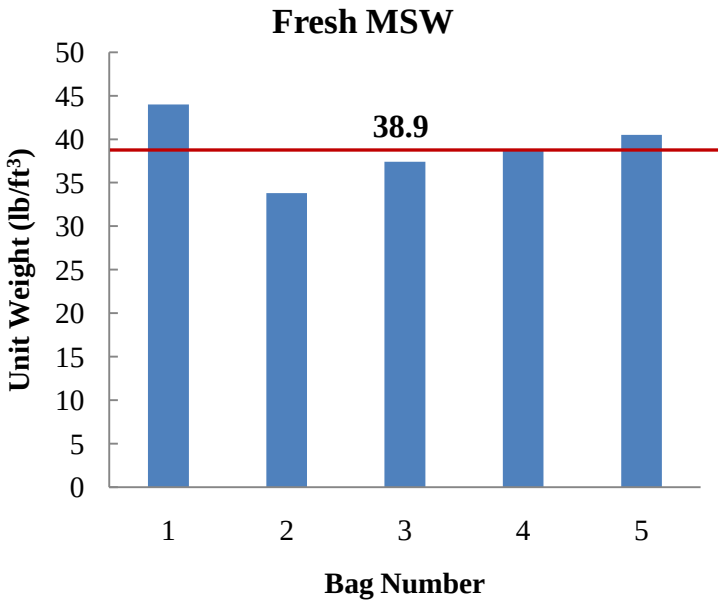

Figure 4.19 Unit Weight of Fresh MSW Samples

4.3 Electrical Resistivity Tests

The electrical resistivity of fresh MSW samples, landfilled MSW samples, and degraded MSW samples was determined at the laboratory. The following sections discuss all experimental results showing the effect of moisture content, unit weight, decomposition, temperature, composition of MSW, and composition of pore fluid on resistivity of MSW.

4.3.1 Effect of Moisture Content

4.3.1.1 Fresh MSW Samples

Electrical resistivity, which is the inverse of conductivity, decreases with an increase in moisture content. The reason behind that is that conduction in MSW is largely electrolytic, and the electrical current is carried by the ions in the pore fluid. More ions in the pore fluid result in increased conductivity. The electrical resistivity of the five fresh MSW samples are plotted versus their corresponding field moisture contents that were

determined by drying the samples at 105ºC for 24 hours in Figure 4.20. Since electrical resistivity is commonly related to the volumetric moisture content, resistivity values are also plotted versus the corresponding volumetric moisture contents. The volumetric moisture contents were determined using equation (3.3).

A decrease in electrical resistivity with increased moisture content was observed. The resistivity of the fresh MSW samples at their field moisture contents ranged from approximately 8 – 60 ohm-m when compacted to a unit weight of 35 lb/ft^3. The measured resistivities are within a reasonable range when compared with values found in literature. A range of 5 to 100 ohm-m was given by Grellier (2007) and 5 to 85 ohm-m by Imhoff et al. (2007).

Since collected MSW samples did not have a wide range of moisture contents, a point corresponding to the resistivity of leachate (moisture content = 100%) was added in order to calibrate Archie's law. A resistivity of 1.35 ohm-m (ρ_w) was used for leachate and was assumed to be constant. Archie's law was fitted to the experimental data and the constants were determined. For the fresh MSW samples the constant 'a' is 0.91 and 'm' is 1.71. These constants are in the same order for soil and rocks.

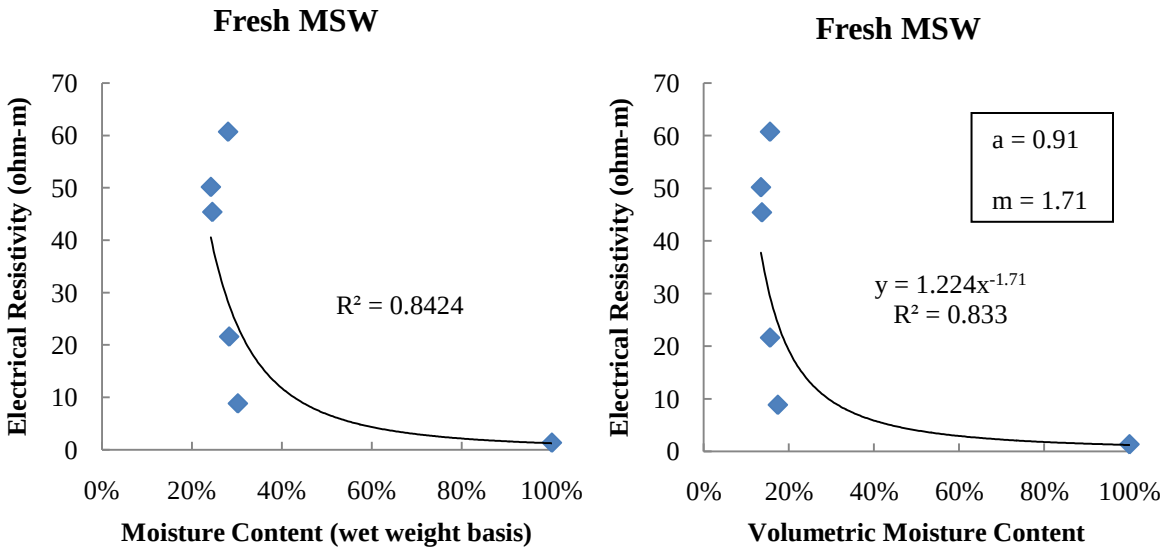

Figure 4.20 Resistivity vs. Moisture Content for Fresh MSW at Field Moisture Content and Unit Weight of 35 lb/ft^3

Further tests were done on the fresh MSW samples by drying each sample and adding tap water to the sample to vary the moisture content from a range of 20% to 55% on a wet weight basis. The results are shown in Figure 4.21 through Figure 4.25. The inverse relationship between resistivity and moisture content is evident. A higher coefficient of determination (R^2) was obtained this time. The better fit is probably due to working with one sample while varying the moisture content only, eliminating the effect of different compositions. Since all five fresh MSW samples were compacted to the same unit weight (γ_d = 35 lb/ft^3), it was expected that all five samples will have the same range of resistivities as a function of moisture content. However, sample 4 (Figure 4.24) had lower resistivity values than the rest of the samples, leading to a conclusion that the composition of MSW also affects resistivity. Sample 4 had a paper composition of 62%

by weight, while the rest of the samples had a paper composition of approximately 40%. The effect of composition is discussed in a later section.

Archie's law constant 'a' varied from 0.87 to 0.96, and the constant 'm' varied from 1.0 to 1.61 for all five samples. The electrical resistivity of the pore fluid was measured at the end of each test by collecting the liquid and measuring its conductivity using a conductivity meter. Due to mineralization, the resistivity of the water dropped from the 30 - 32 ohm-m range to 1.14-1.72 ohm-m range. The resistivity results for the five MSW samples are combined in one plot as presented in Figure 4.26. The data fits reasonably with Archie's law with the constants a = 0.91 and m = 1.45. An average pore fluid resistivity of 1.35 ohm-m was used to determine these constants.

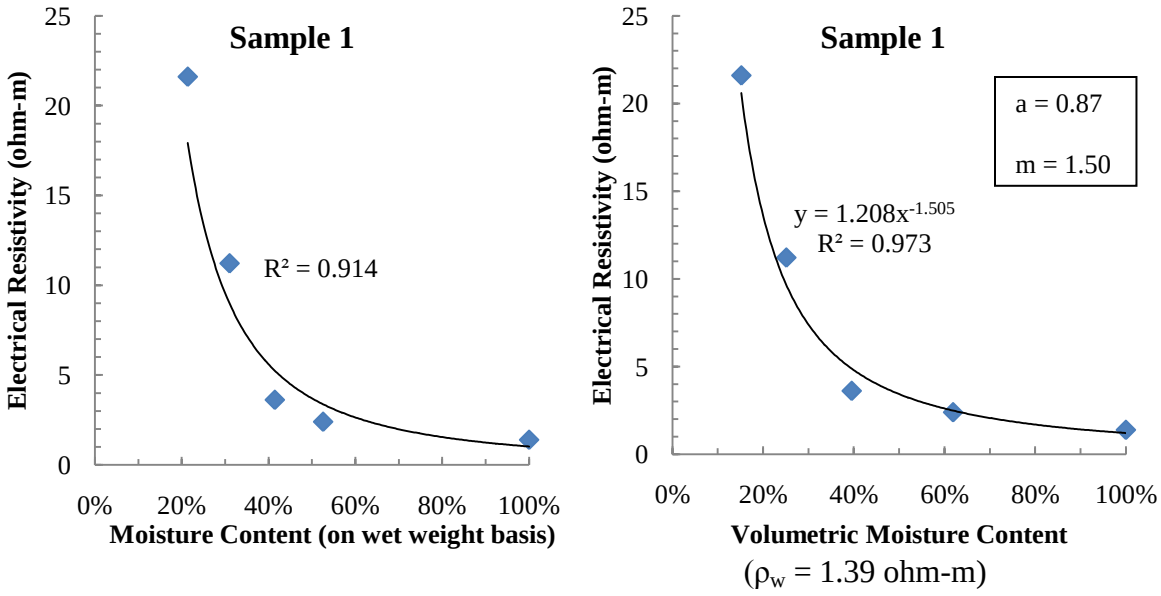

Figure 4.21 Resistivity Variation with Moisture Content for Fresh MSW Sample 1 at Dry Unit Weight of 35 lb/ft^3

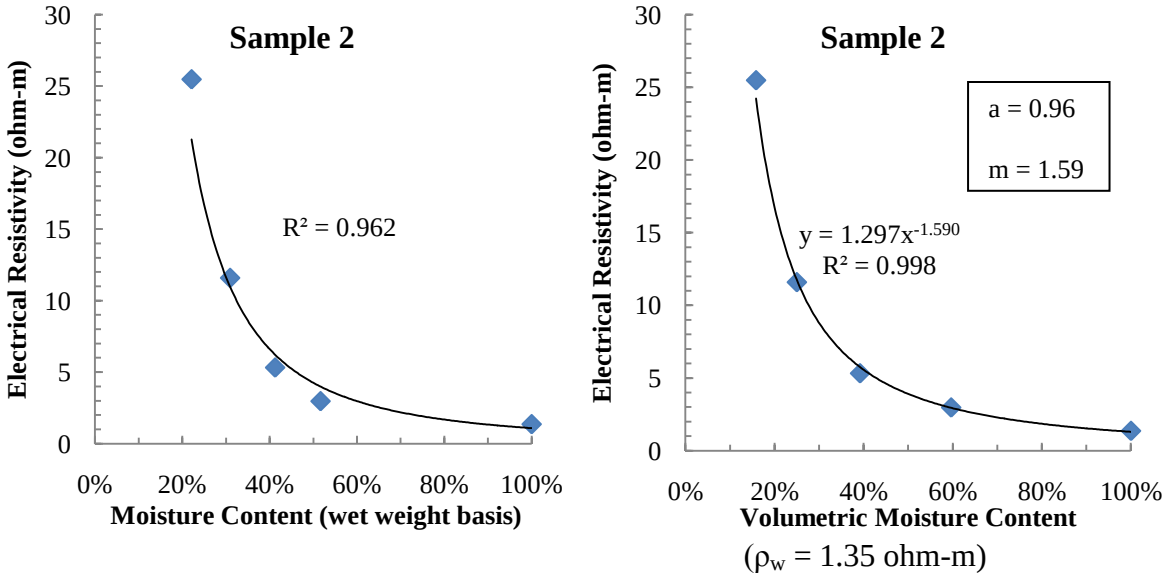

Figure 4.22 Resistivity Variation with Moisture Content for Fresh MSW Sample 2 at Dry Unit Weight of 35 lb/ft^3

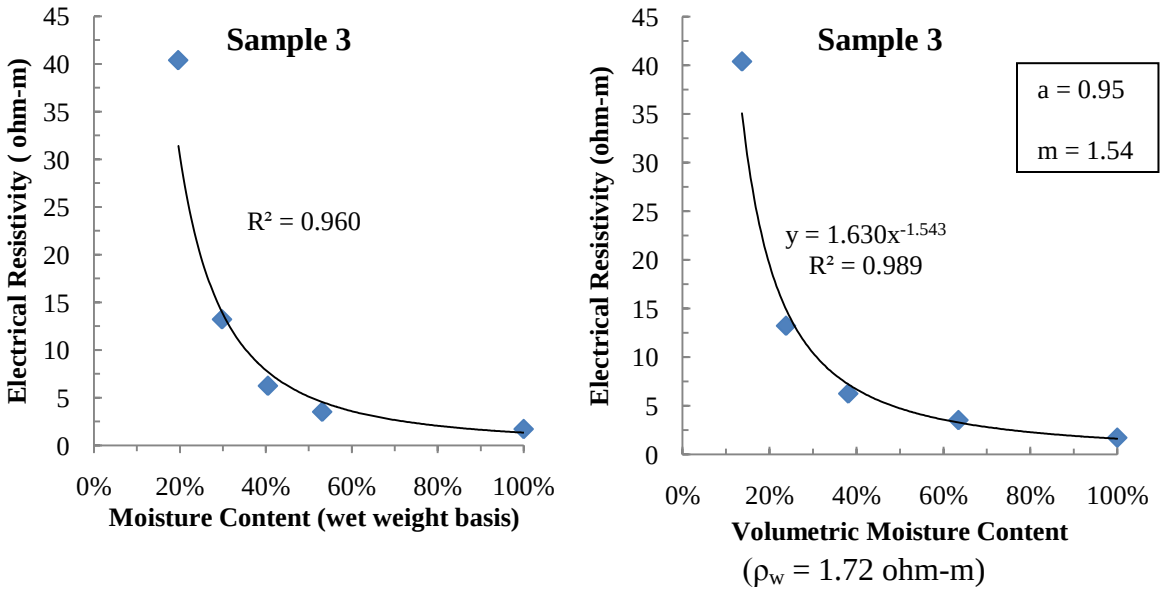

Figure 4.23 Resistivity Variation with Moisture Content for Fresh MSW Sample 3 at Dry Unit Weight of 35 lb/ft^3

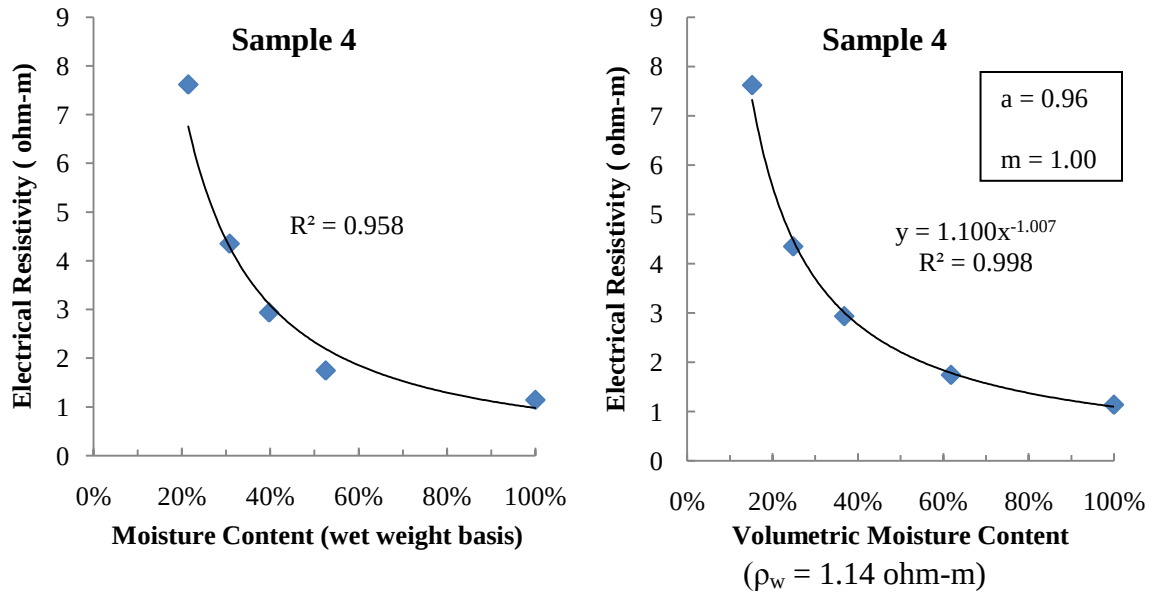

Figure 4.24 Resistivity Variation with Moisture Content for Fresh MSW Sample 4 at Dry Unit Weight of 35 lb/ft^3

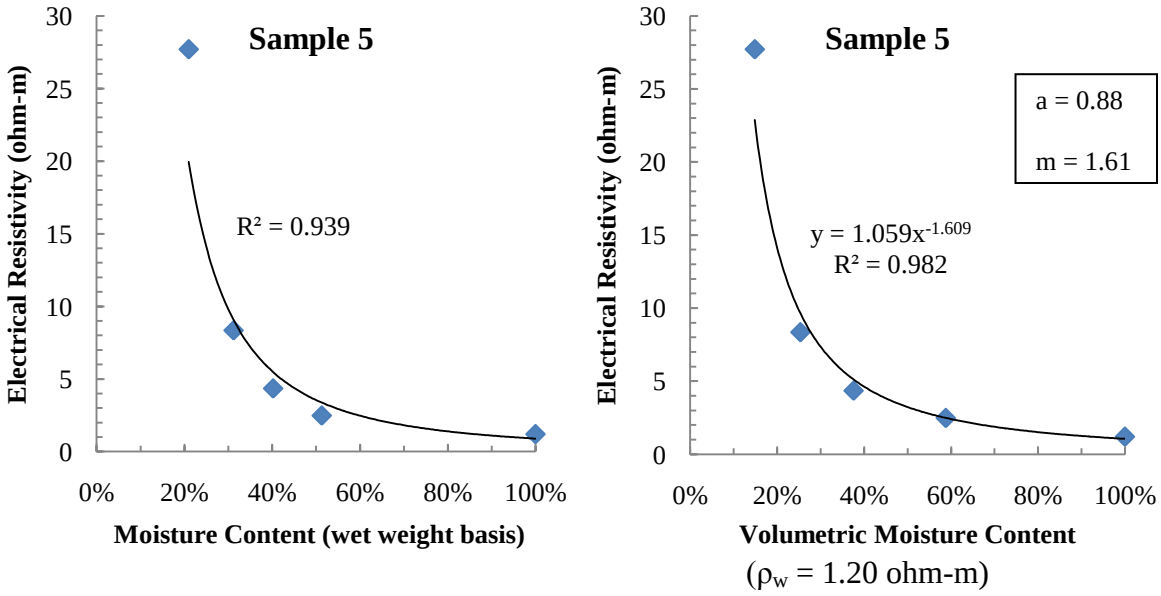

Figure 4.25 Resistivity Variation with Moisture Content for Fresh MSW Sample 5 at Dry Unit Weight of 35 lb/ft^3

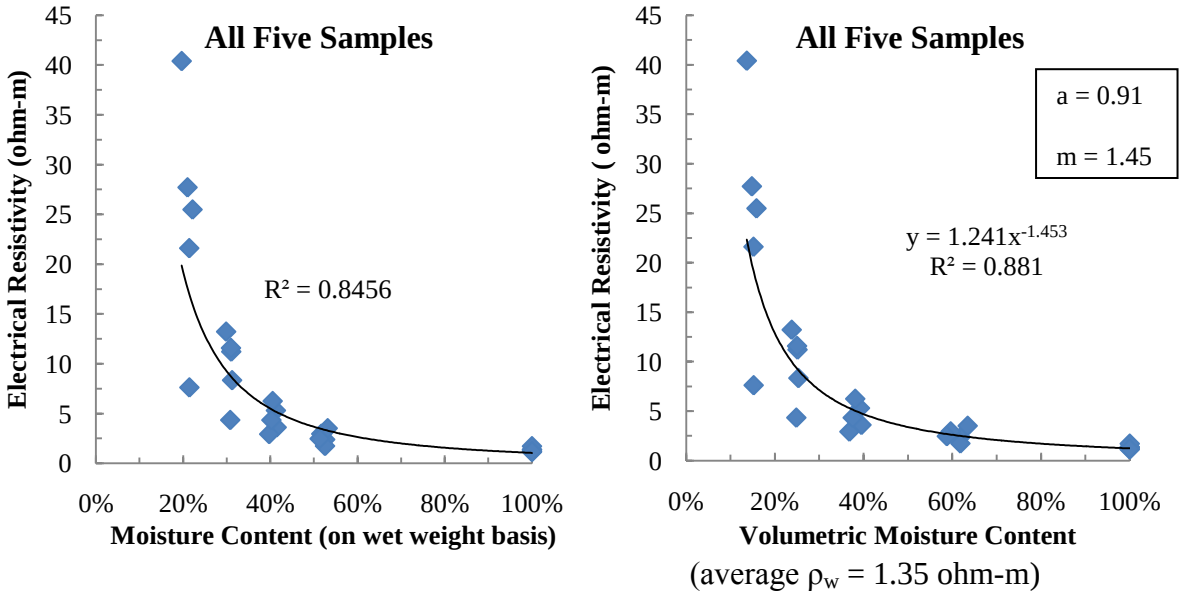

Figure 4.26 Resistivity Variation with Moisture Content for all Five Fresh MSW Samples

4.3.1.1 Landfilled MSW Samples

The electrical resistivity of thirty landfilled MSW samples was first measured at the actual field moisture contents. Figure 4.27 presents a plot of resistivity versus the corresponding field moisture contents for all thirty landfilled samples. A decrease in electrical resistivity with increased moisture content was observed. The resistivity of the landfilled samples at their field moisture contents ranged from approximately 8 – 112 ohm-m when compacted to a unit weight of 35 lb/ft^3. Archie's law was fitted to the experimental data and the constants were determined. The constant 'a' was found to be 1.29 and 'm' was 1.47. Again, these constants are in the same order as soil and rocks.

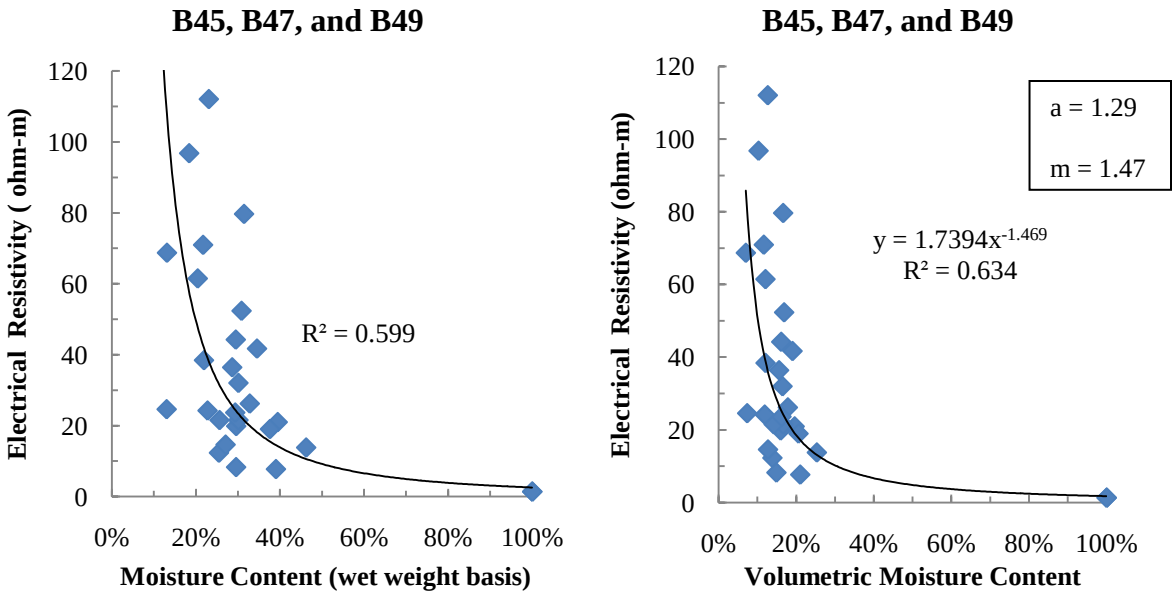

Figure 4.27 Resistivity vs. Moisture Content for Borehole Samples at Field Moisture Content and Unit Weight of 35 lb/ft^3

To better understand the effect of moisture content on resistivity, further resistivity tests were done on three landfilled MSW samples from borehole B45 collected from depths of 20, 30, and 40 ft by drying each sample and adding tap water to the sample to vary the moisture content. The results are presented in Figure 4.28, Figure 4.29, and Figure 4.30. The results showed that the effect of increasing moisture content on electrical resistivity tapers off beyond a certain point (moisture content of approximately 50 to 55%). This can possibly be explained by the fact that at higher values of moisture content, continuous current flow paths through the pores would have already been established. Archie's law constant 'a' varied from 0.72 to 1.77, and the constant 'm' varied from 1.71 to 1.99. The resistivity results for the three landfilled samples are combined in one plot as shown in Figure 4.31. Archie's law constants were determined to be 'a' = 1.0 and 'm' = 1.81.

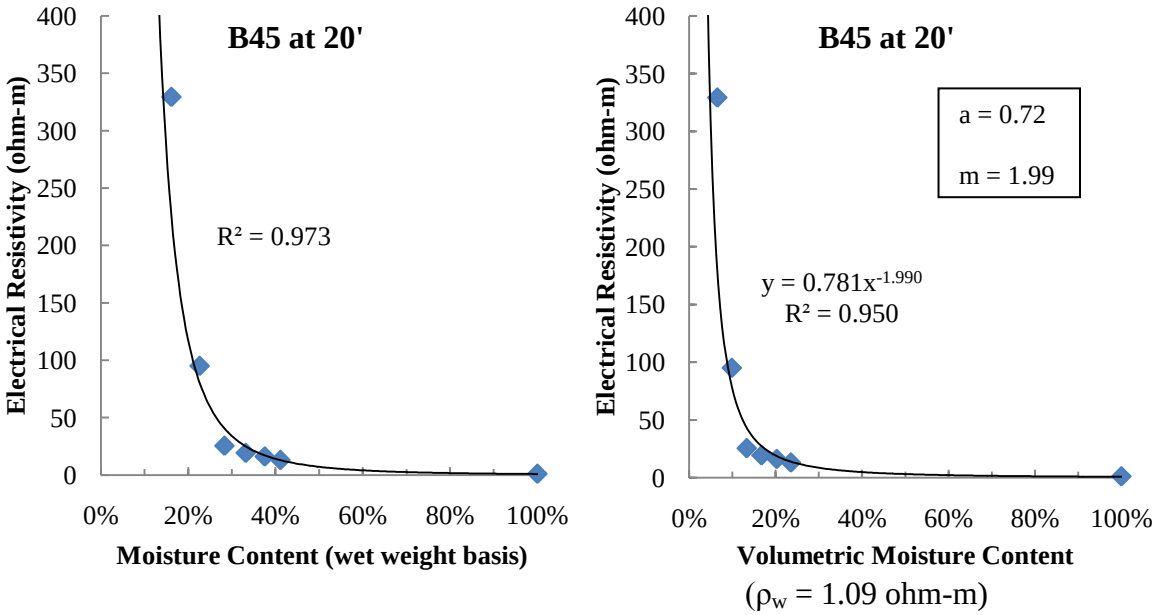

(ρ_w = 1.09 ohm-m)

Figure 4.28 Resistivity Variation with Moisture Content for Sample from Borehole B45 at 20' and Dry Unit Weight of 21 lb/ft^3

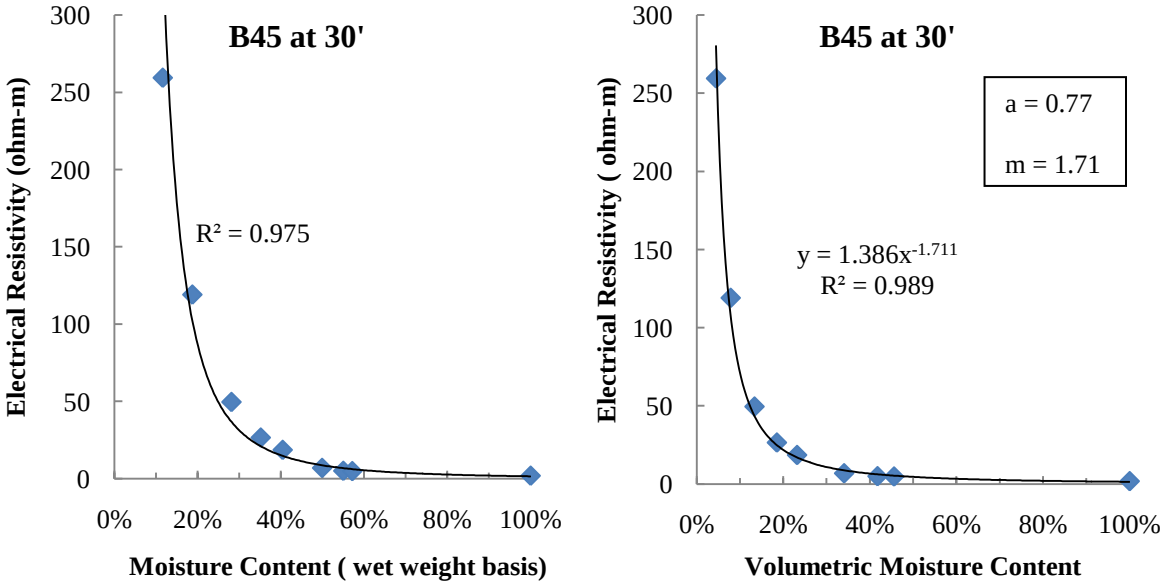

(ρ_w = 1.79 ohm-m)

Figure 4.29 Resistivity Variation with Moisture Content for Sample from Borehole B45 at 30' and Dry Unit Weight of 21 lb/ft^3

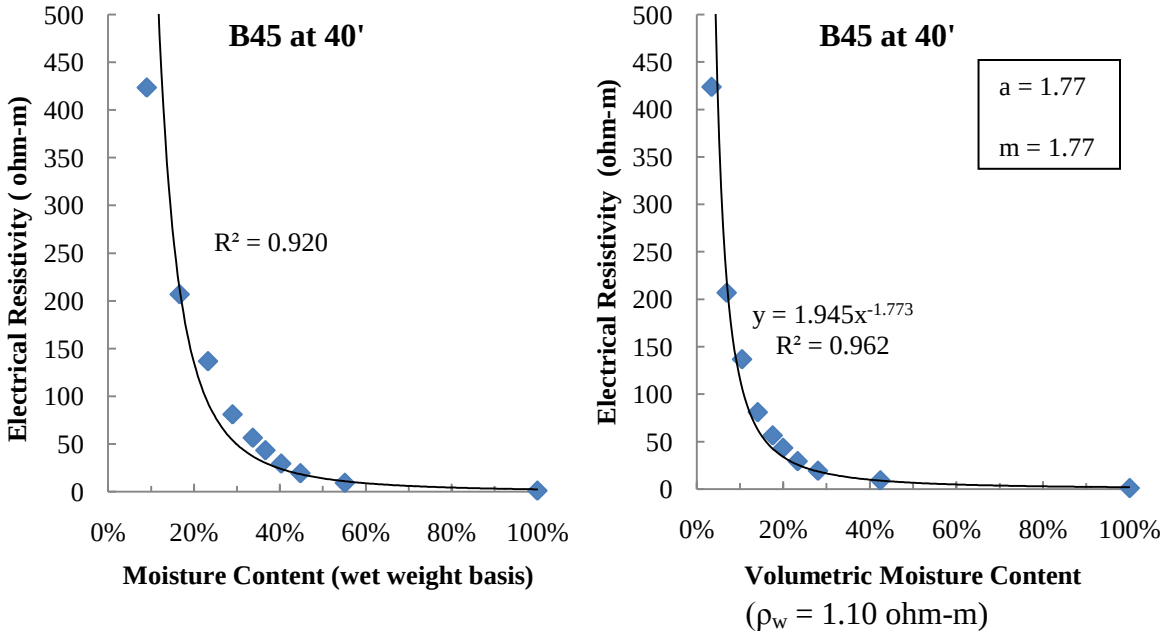

Figure 4.30 Resistivity Variation with Moisture Content for Sample from Borehole B45 at 40' at Dry Unit Weight of 21 lb/ft^3

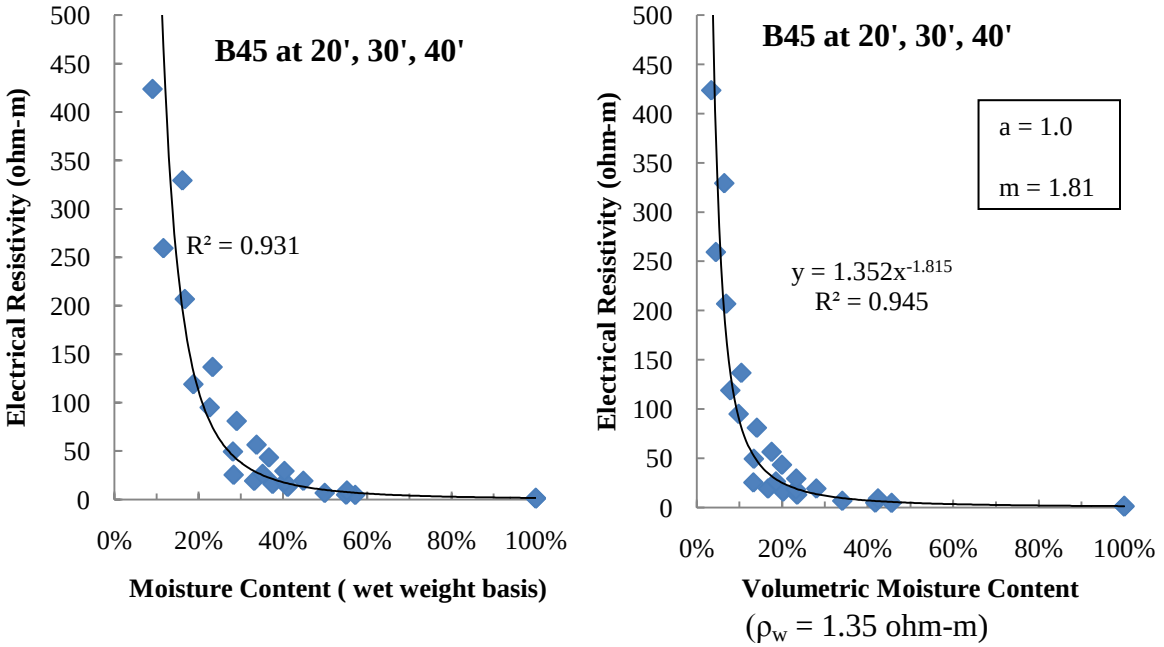

Figure 4.31 Resistivity Variation with Moisture Content for Three Samples from Borehole B45

4.3.1.1 Degraded MSW Samples

Resistivity tests were conducted on four degraded MSW samples by drying each sample and adding tap water to the sample to vary the moisture content. The dried samples were compacted by applying 25 blows on each of 4 layers using a standard proctor test hammer. The results are presented in Figure 4.32 through Figure 4.35. Trends similar to that of fresh MSW and borehole samples were observed. Archie's law was fitted to the experimental results. Archie's law constant 'a' varied from 0.69 to 1.45, and the constant 'm' varied from 1.58 to 2.3. The resistivity results for four degraded samples are combined in one plot as shown in Figure 4.36. Archie's law constants were determined for all degraded samples to be 'a' = 1.08 and 'm' = 1.91.

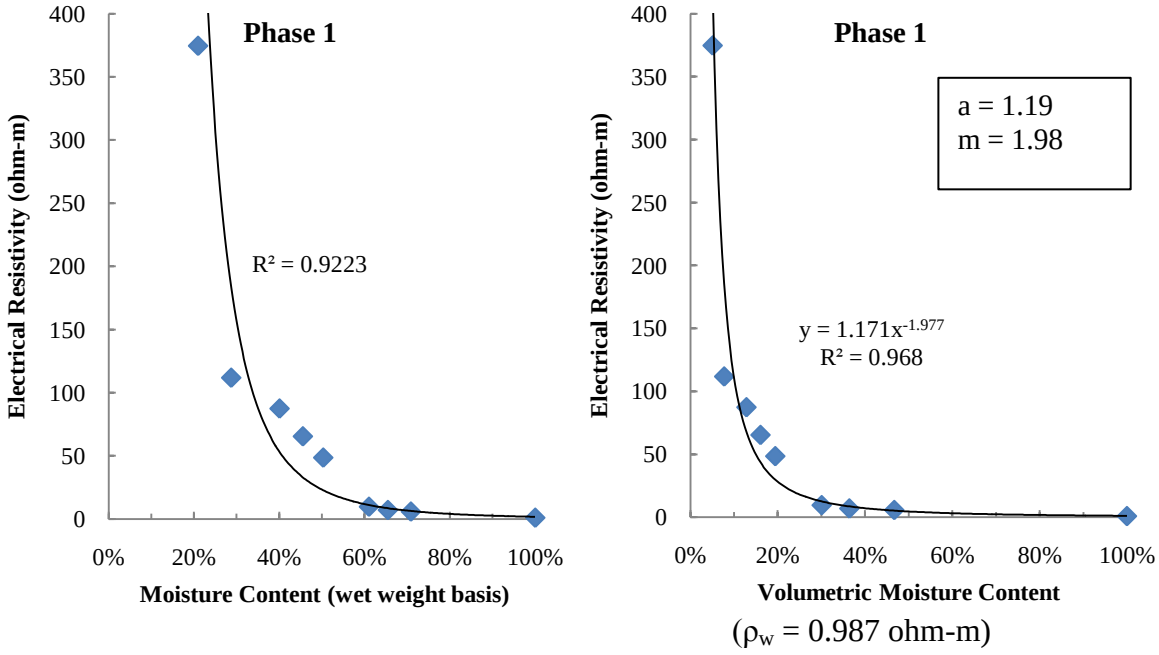

Figure 4.32 Resistivity Variation with Moisture Content for Degraded Sample (Phase 1) and Dry Unit Weight of 12 lb/ft^3

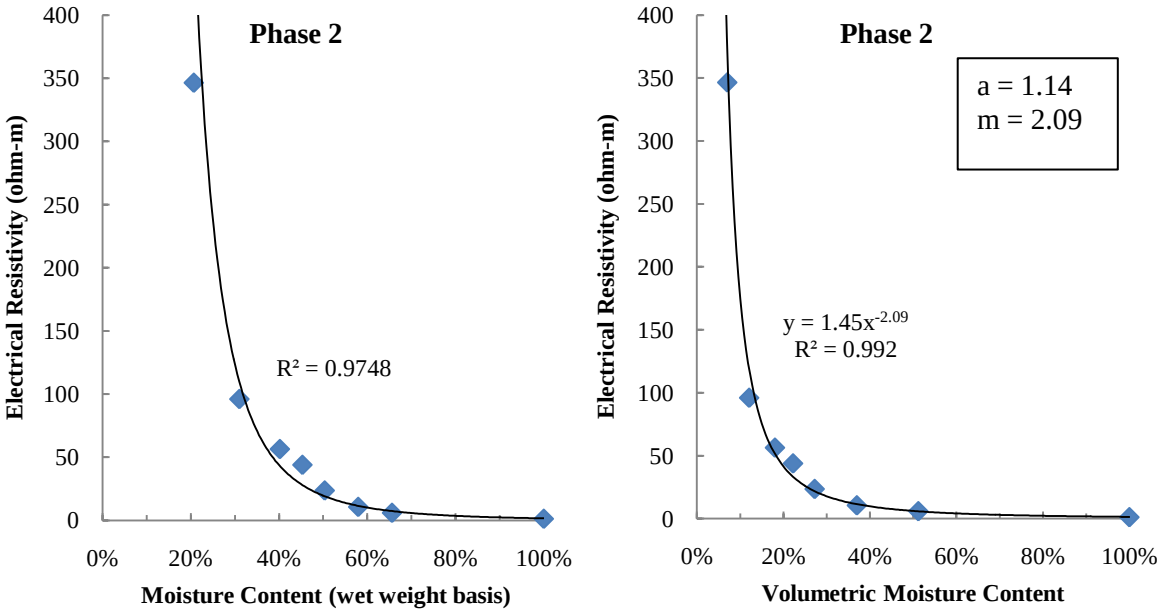

(ρ_w = 1.276 ohm-m)

Figure 4.33 Resistivity Variation with Moisture Content for Degraded Sample (Phase 2) and Dry Unit Weight of 16.7 lb/ft^3

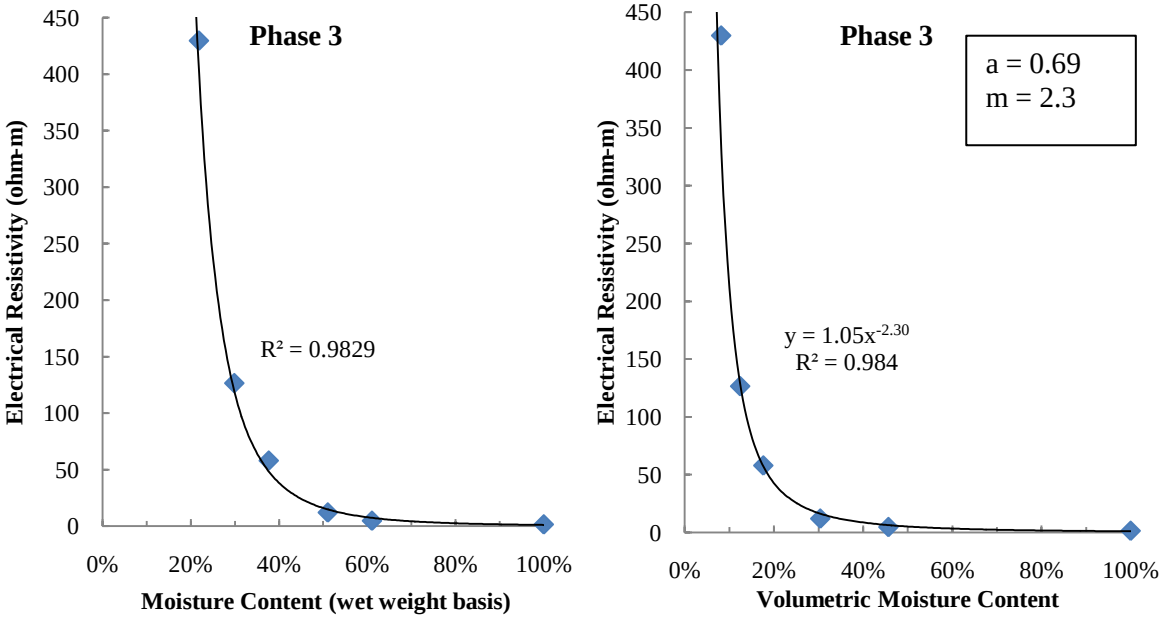

(ρ_w = 1.511 ohm-m)

Figure 4.34 Resistivity Variation with Moisture Content for Degraded Sample (Phase 3) and Dry Unit Weight of 18.2 lb/ft^3

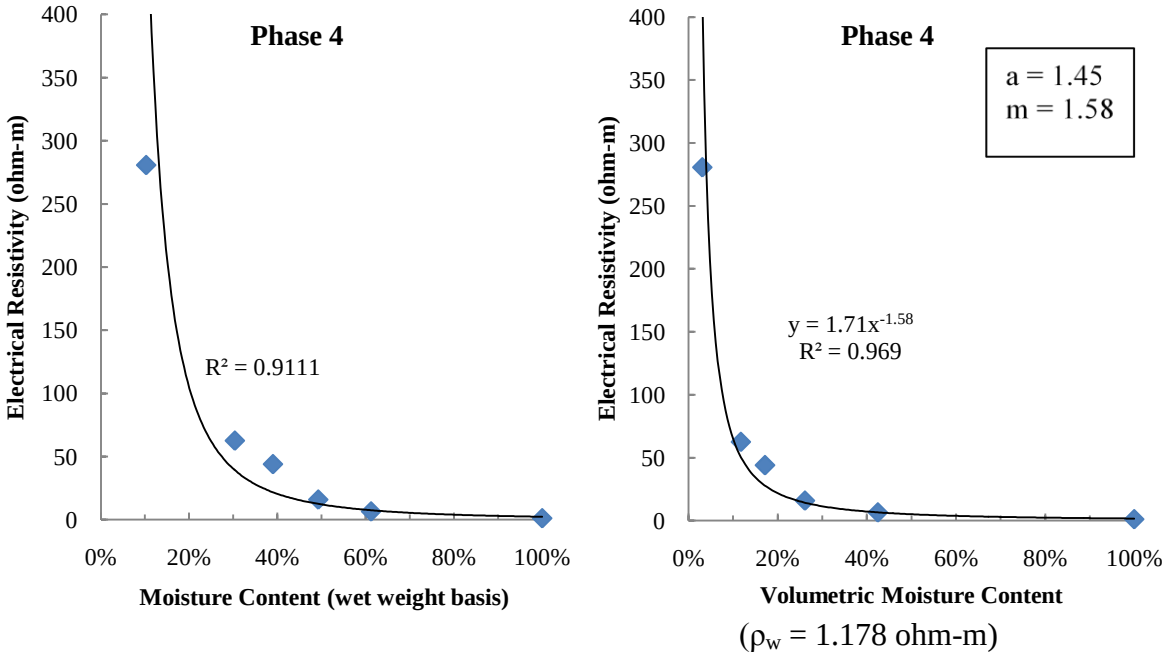

Figure 4.35 Resistivity Variation with Moisture Content for Degraded Sample (Phase 4) and Dry Unit Weight of 16.8 lb/ft^3

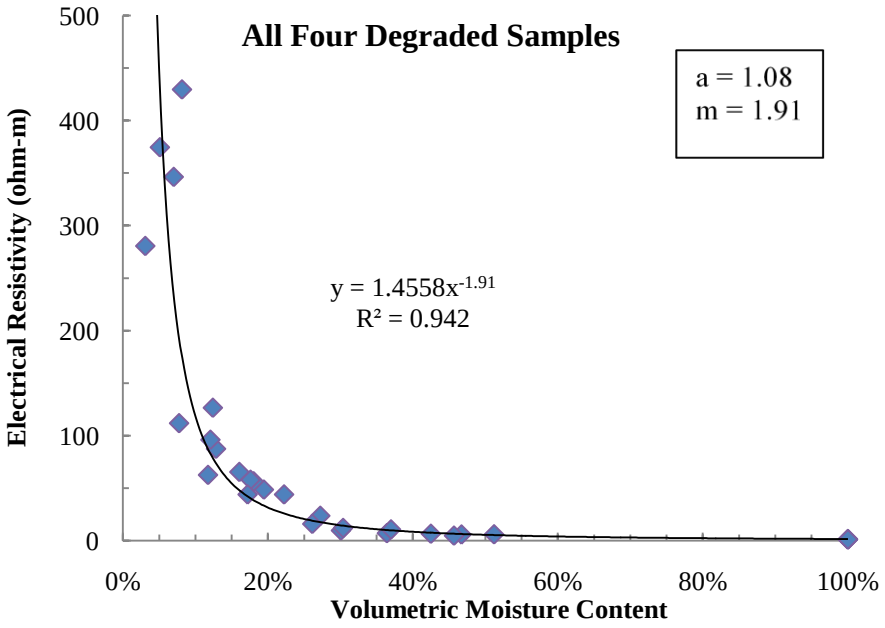

Figure 4.36 Resistivity Variation with Moisture Content for all Degraded Samples

The determined Archie's law constants for fresh, landfilled, and degraded MSW samples are presented in Table 4.15. The constant 'a' varied slightly for fresh, landfilled, and degraded MSW samples. The constant 'm' varied from 1.45 to 1.91. Grellier et al. (2007) determined that 'a' is 0.75 and 'm' ranges from 1.6 to 2.15 for MSW samples from Orchard Hill landfill in Illinois.

These constants are in the same order for soil and rocks. According to Keller and Frischknecht (1966), the value of the constant 'a' varies from slightly less than 1 for rocks with intergranular porosity to slightly more than 1 for rocks with joint porosity. The exponent 'm' is larger than 2 for cemented and well-sorted granular rocks and less than 2 for poorly sorted and poorly cemented granular rocks. Jackson et al. (1978) found that the exponent m was dependent on the shape of the particles, increasing as they become less spherical, while variations in size and spread of sizes appeared to have little effect. It is difficult to make similar conclusions for MSW due to the heterogeneity of the waste.

Table 4.15 Archie's Law Constants for Fresh, Landfilled, and Degraded MSW

Sample	a	m
Fresh MSW	0.91	1.45
Landfilled MSW	1.0	1.81
Degraded MSW	1.08	1.91

4.3.2 Effect of Unit Weight

4.3.2.1 Fresh MSW Samples

Five fresh MSW samples at their field moisture contents were compacted to a unit weight of 35, 45, and 55 lb/ft^3. The variation of electrical resistivity with unit weight for

the five samples is presented in Figure 4.37. The results show that resistivity decreases with increasing unit weight. As the unit weight increases, the air voids are reduced, resulting in an increase in the degree of saturation. An increase in saturation means that more voids are filled with liquid, creating more paths for current flow, and therefore decreasing the electrical resistivity.

It can be seen from Figure 4.37 that samples 1 and 2 had the same moisture contents, but had different resistivity values although the samples were compacted to the same unit weight. This draws attention to the effect of composition. Sample 2 contained 33% "others" (fines) compared to 17% in sample 1. The effect of composition is discussed in subsection 4.3.5.

It must be taken into consideration that the five samples had different moisture contents. To better understand the effect of unit weight on resistivity, the resistivity of the samples prepared at 35, 45, and 55 lb/ft^3 are plotted versus the corresponding gravimetric moisture content of each sample, to capture the effect of both unit weight and moisture content. It can be concluded from Figure 4.38 that the resistivity of MSW decreases with increasing moisture content and increasing unit weight.

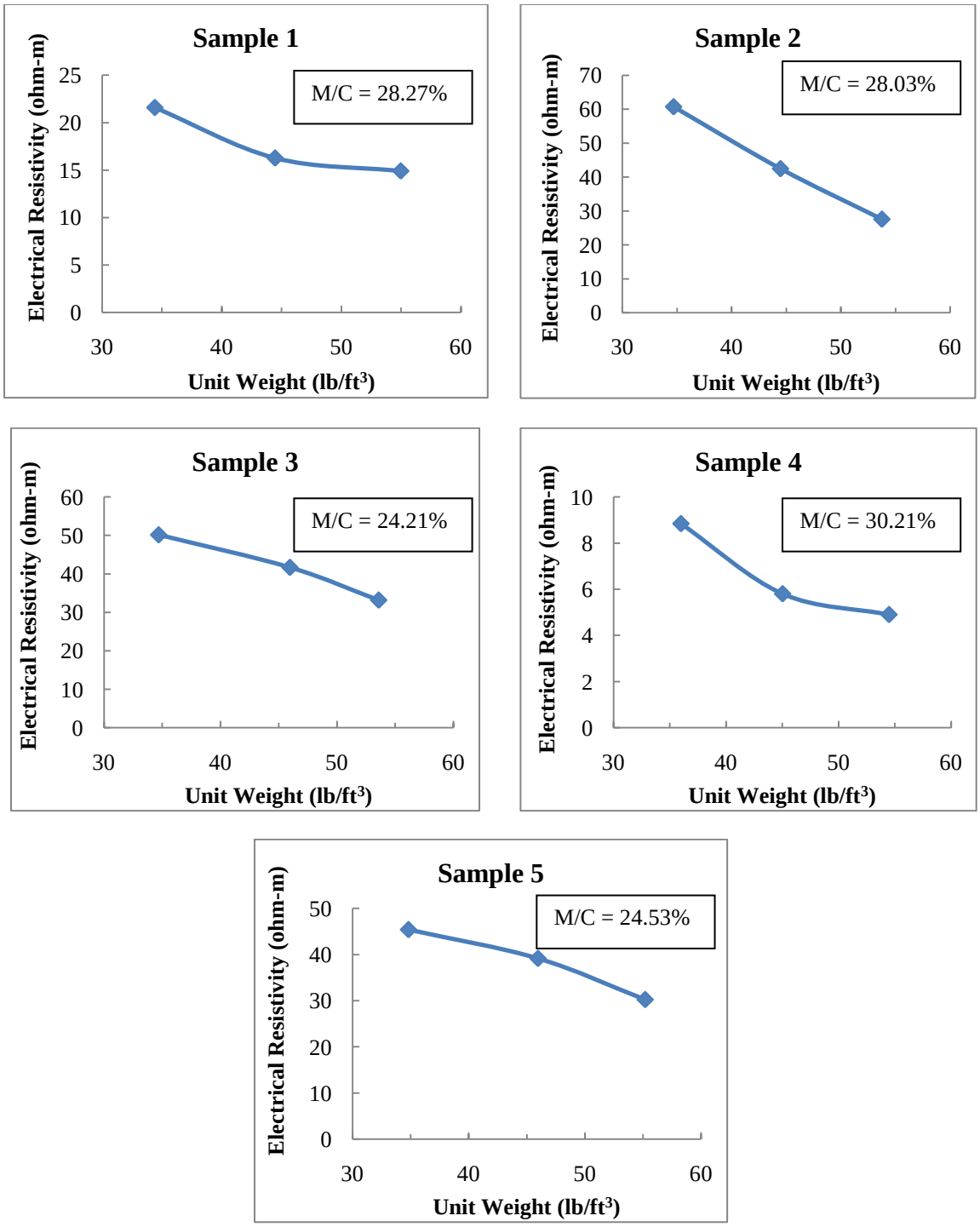

Figure 4.37 Resistivity Variation with Unit Weight for Five Fresh MSW Samples

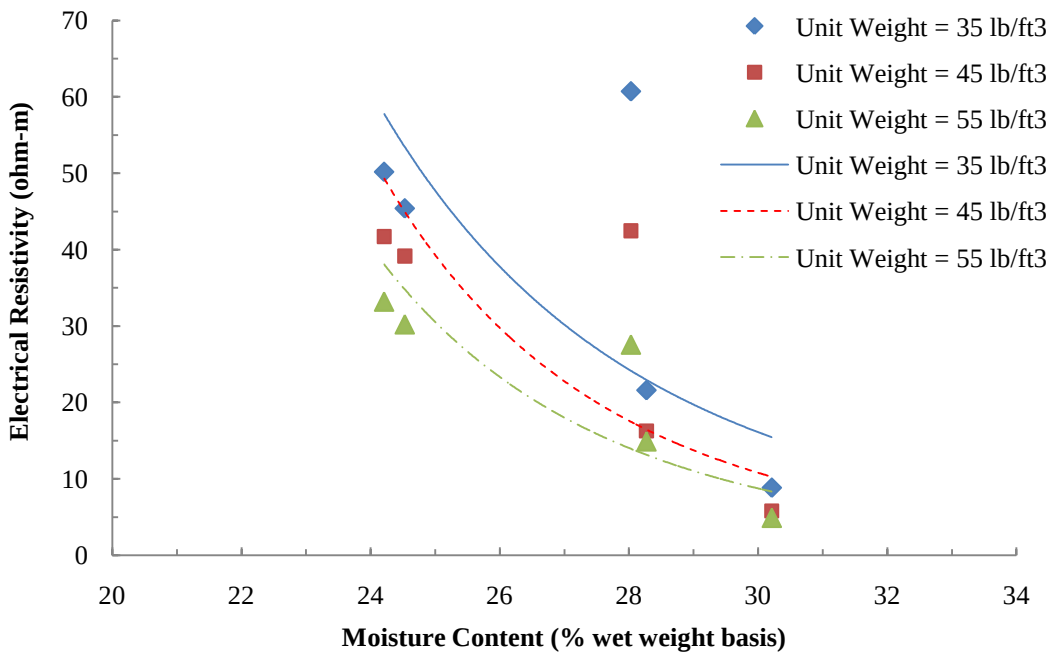

Figure 4.38 Effect of Moisture Content and Unit Weight on Resistivity of Fresh MSW Samples

4.3.2.1 Landfilled MSW Samples

Five landfilled MSW samples from borehole B49 at their field moisture contents were compacted to a unit weight of 35, 40, and 45 lb/ft^3. The variation of electrical resistivity with unit weight for the five samples is presented in Figure 4.39. Again, it is evident from the results that resistivity decreases with increasing unit weight. Figure 4.40 shows the effect of both moisture content and unit weight for the five landfilled samples. Similar to the trend observed for fresh MSW, it can be concluded that resistivity of MSW decreases with increasing moisture content and increasing unit weight.

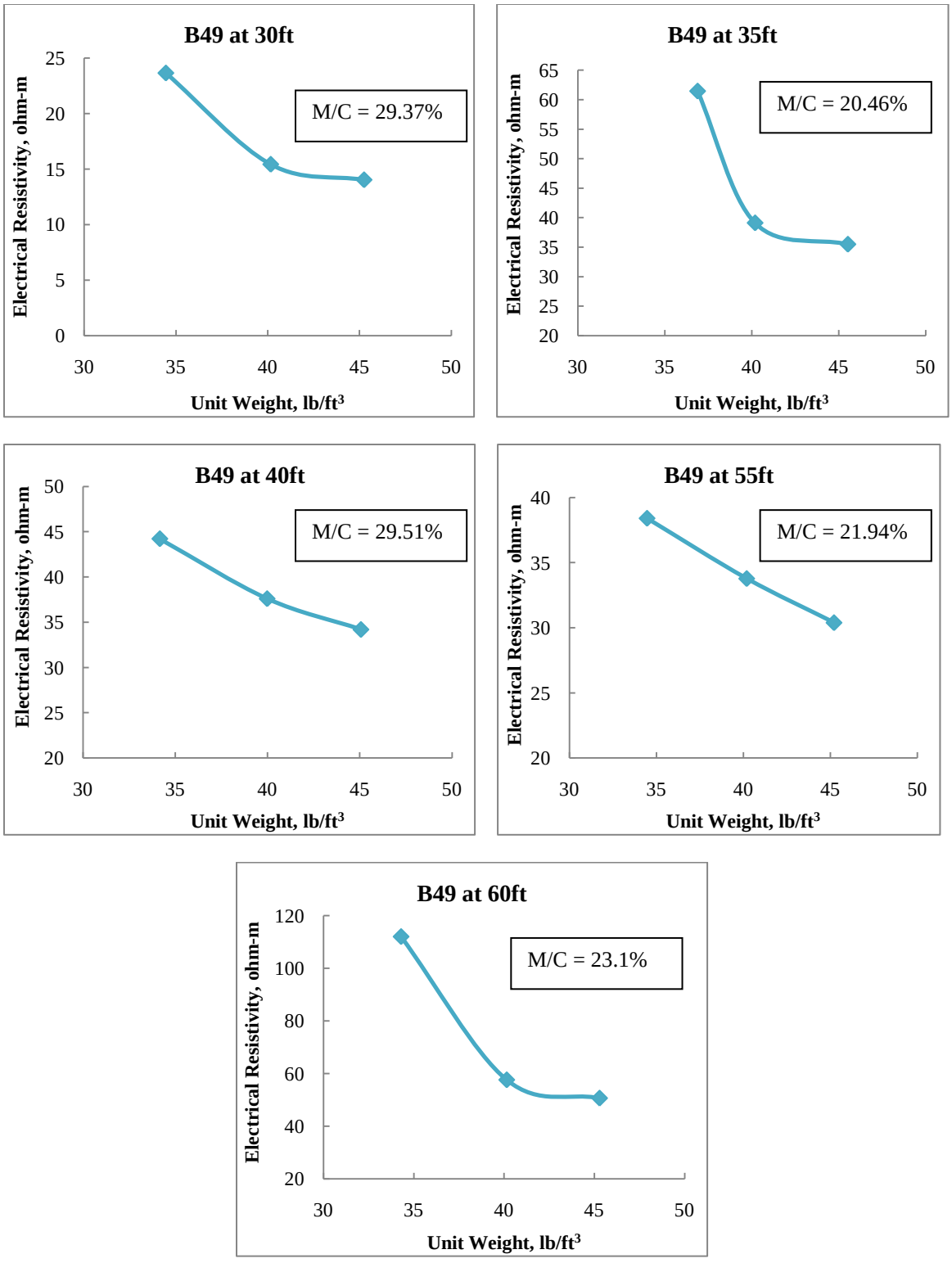

Figure 4.39 Resistivity Variation with Unit Weight for Five Samples from Borehole B49

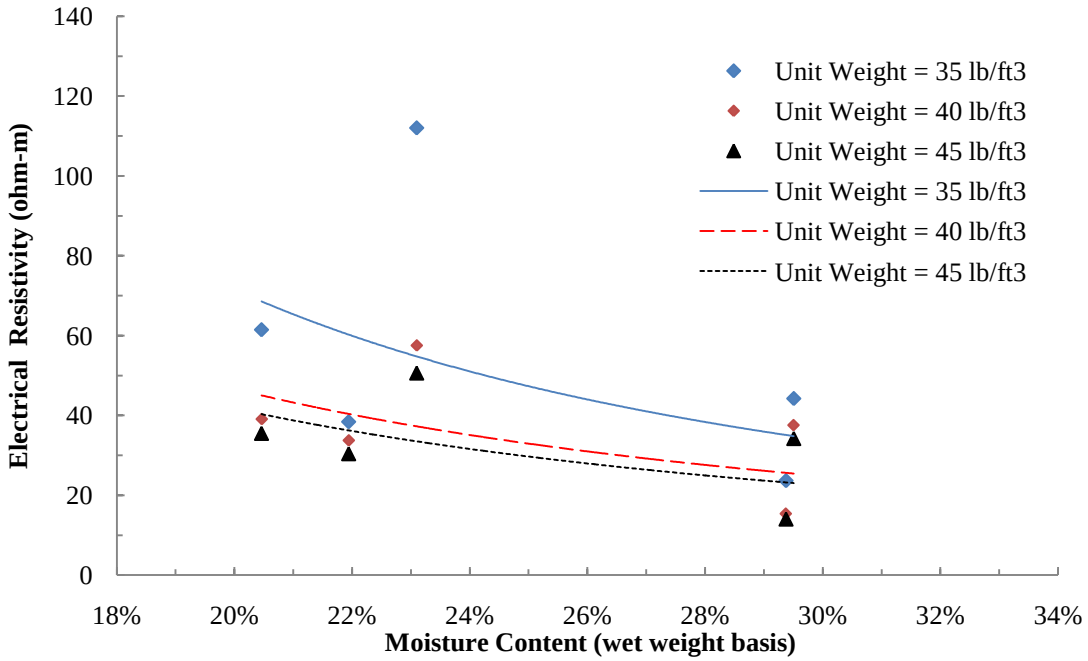

Figure 4.40 Effect of Moisture Content and Unit Weight on Resistivity of Five Landfilled MSW Samples from Borehole B49

4.3.2.2 Degraded MSW Samples

Four degraded MSW samples at their actual moisture content upon reactor dismantling were compacted to an approximate unit weight of 35, 45, and 55 lb/ft^3 using a standard proctor test hammer. The variation of electrical resistivity with unit weight for the four degraded samples is presented in Figure 4.41. Again, it is evident from the results that resistivity decreases with increasing unit weight.

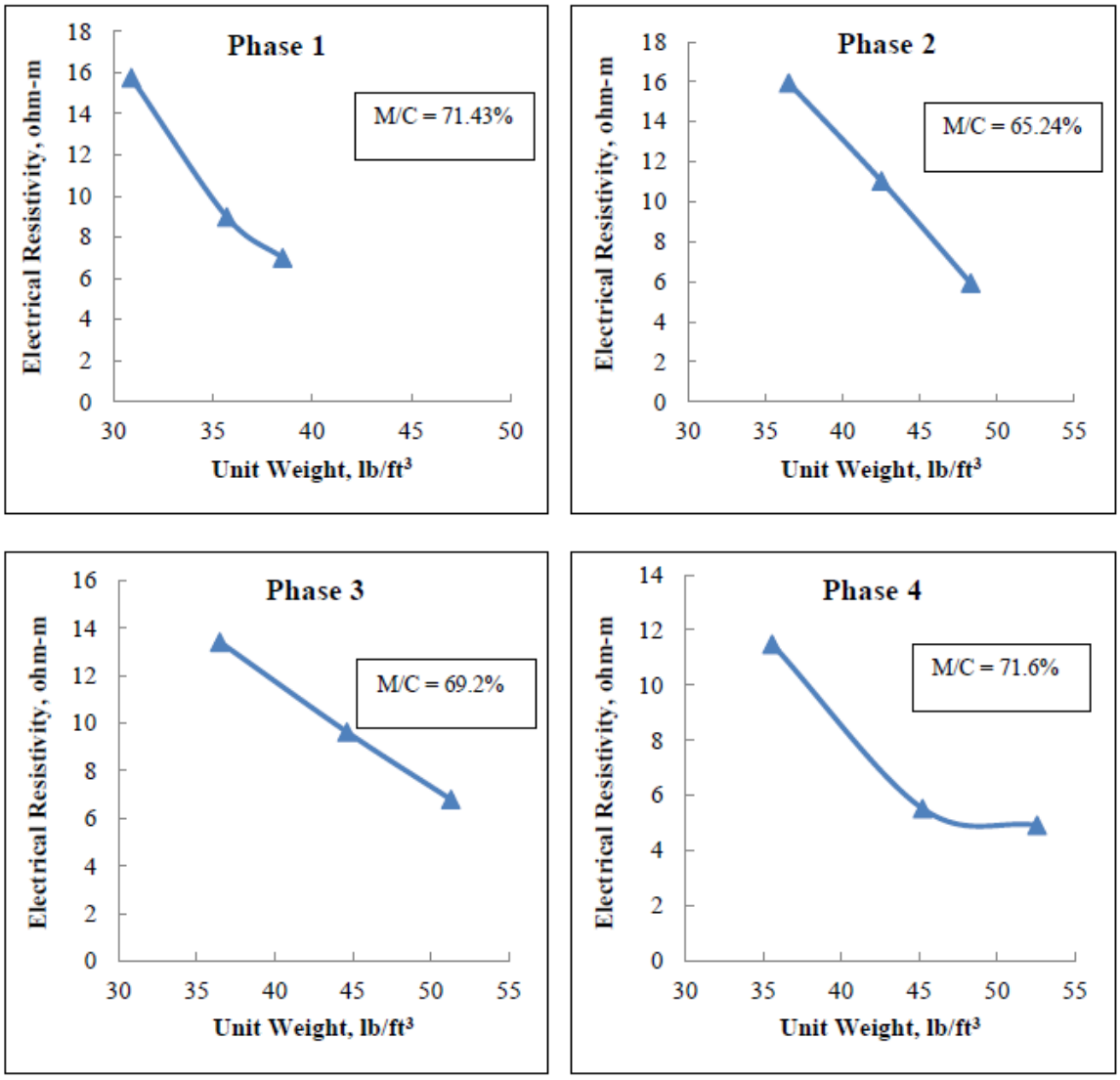

Figure 4.41 Resistivity Variation with Unit Weight for Four Degraded Samples

4.3.3 Effect of Decomposition

Electrical resistivity tests were conducted on the four degraded MSW samples at their actual moisture contents upon dismantling the reactors. Reactor samples were compacted using the same compaction effort (25 blows on each of 2 layers using standard proctor test hammer). The unit weights of samples from phase 1, 2, 3, and 4 were 35.71, 48.31, 51.32, and 52.59 lb/ft^3 respectively, indicating an increase in unit weight with

decomposition. This conclusion is consistent with other results found in literature. According to Dixon and Jones (2005), the bulk unit weight of fresh MSW range from 6 – 7 kN/m^3 while that of degraded waste range from 14 – 20 kN/m^3. Haque (2007) found that the unit weight of MSW increased from 8.5 kN/m^3 in phase 1 of decomposition to 10.7 kN/m^3 in phase 4. This is due to the reduction in particle size with decomposition, resulting in reducing the voids and increasing the mass of solids per unit volume.

The resistivity results, as presented in Figure 4.42, indicate that electrical resistivity decreased with decomposition from 8.98 ohm-m in phase 1 to 4.91 ohm-m in phase 4. This decrease in resistivity is most probably caused by the increase in unit weight as a result of decomposition. According to the organic content results presented in Table 4.13, phase 2 sample was slightly more decomposed than phase 3 sample, and this is reflected in the resistivity results.

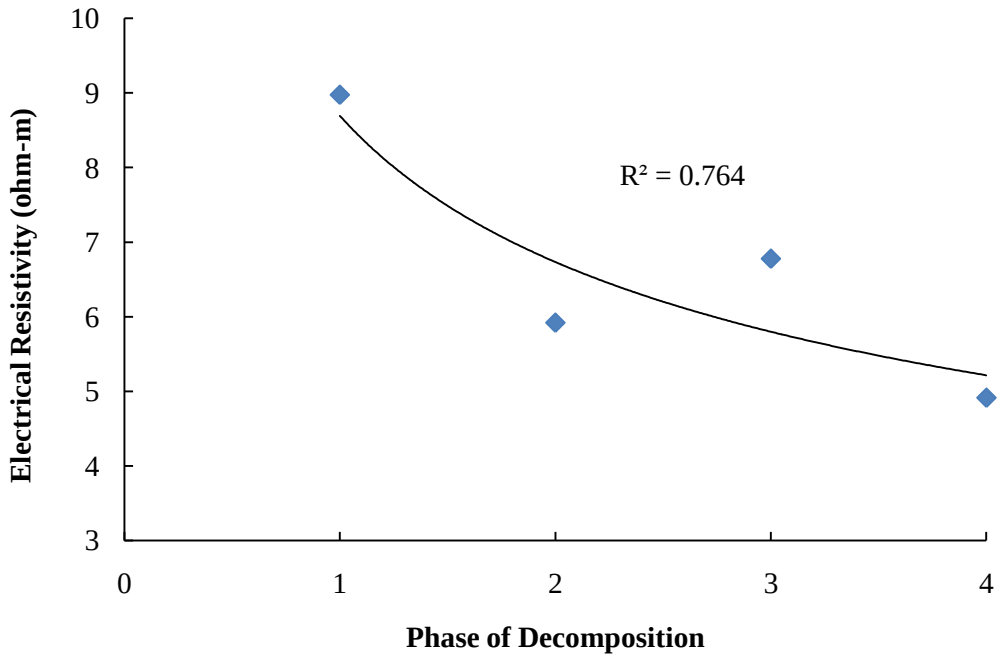

Figure 4.42 Electrical Resistivity of Degraded Samples

As discussed earlier, further resistivity tests were conducted on four degraded MSW samples by drying each sample and adding tap water to the sample to vary the moisture content. The resistivity results for the four degraded samples are combined in one plot in order to understand better the effect of decomposition. As shown in Figure 4.43, there is a clear distinction between the early stage of decomposition (phase 1) and the late stage (phase 4). There is not much difference between the resistivity values of phase 2 and phase 3 samples. It is important to note that the resistivity values are plotted versus the gravimetric moisture content in Figure 4.43.

On the other hand, when the resistivity values are plotted versus the volumetric moisture content (Figure 4.44), there is no clear distinction between the phases of decomposition and most points were fitted to one curve. This is because the volumetric moisture content takes into account the different unit weights of the sample. Therefore, it can be concluded that the observed decrease in resistivity with decomposition is mainly due to the increase in unit weight that happen as a result of decomposition.

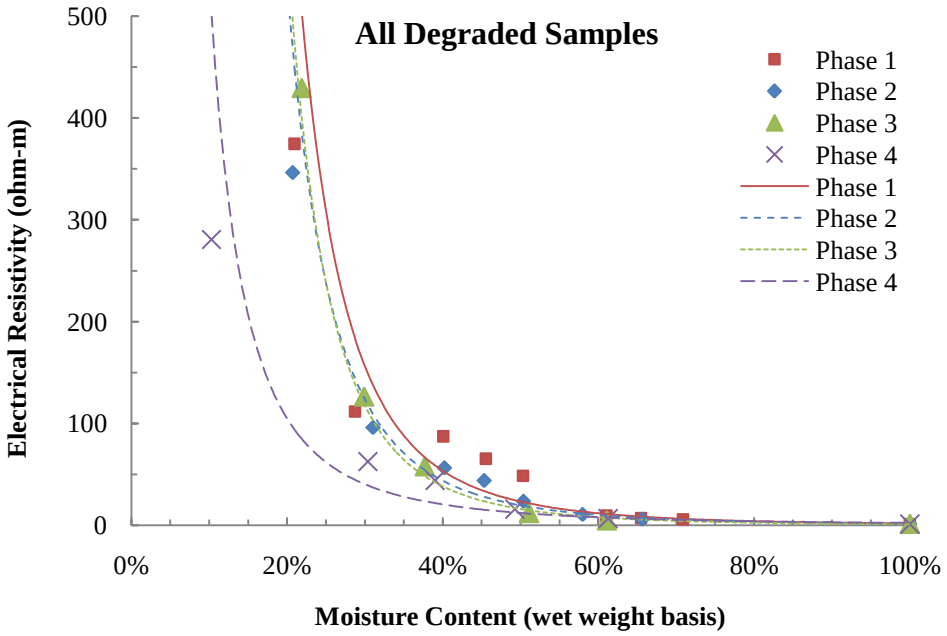

Figure 4.43 Electrical Resistivity Variation with Moisture Content for Degraded Samples

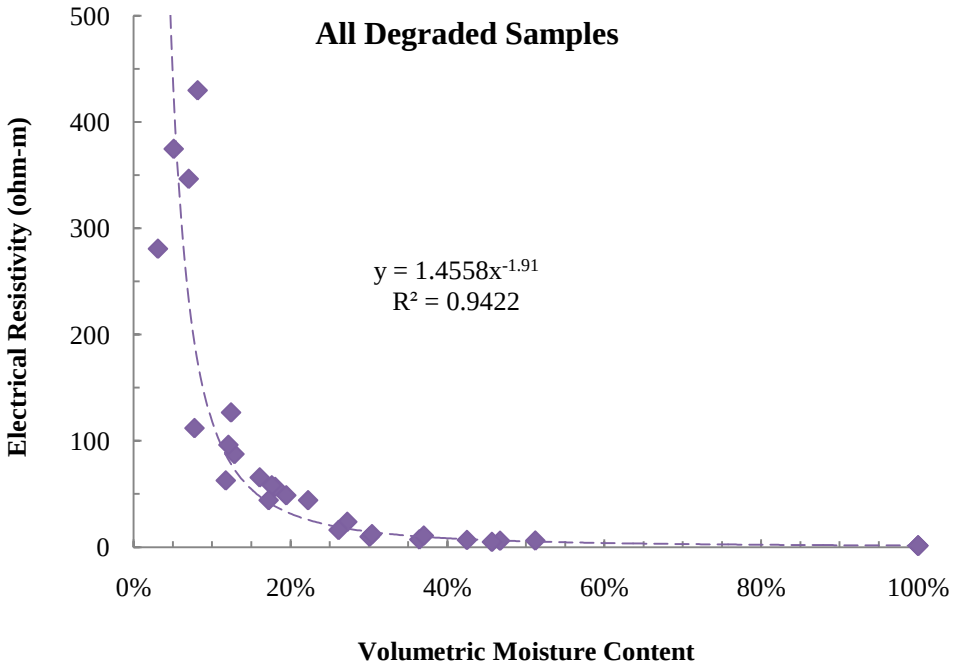

Figure 4.44 Electrical Resistivity Variation with Volumetric Moisture Content for Degraded Samples

4.3.4 Effect of Temperature

Temperature affects the electrical resistivity of MSW because it affects the mobility of the ions in the pore fluid. To investigate the effect of temperature, the resistivity of five fresh MSW samples was measured at different temperatures.

The results for the variation of resistivity with temperature are presented in Figure 4.45 through Figure 4.49. The model suggested by Keller and Frischknecht (1966) (using $\alpha = 0.025$) was also fitted to the data. The model fits the data very well. The temperature coefficient (α) was determined for each sample, and the average temperature coefficient was determined to be 0.020 per degree Celsius, as presented in Table 4.16. These results justify that the Keller and Frischknecht equation (equation 2.11) can be used to correct field resistivity values to a standard temperature (70ºF). The results are also consistent with the findings by Grellier et al. (2005) that the resistivity of leachate decreases by 2% per temperature increase of 1°C.

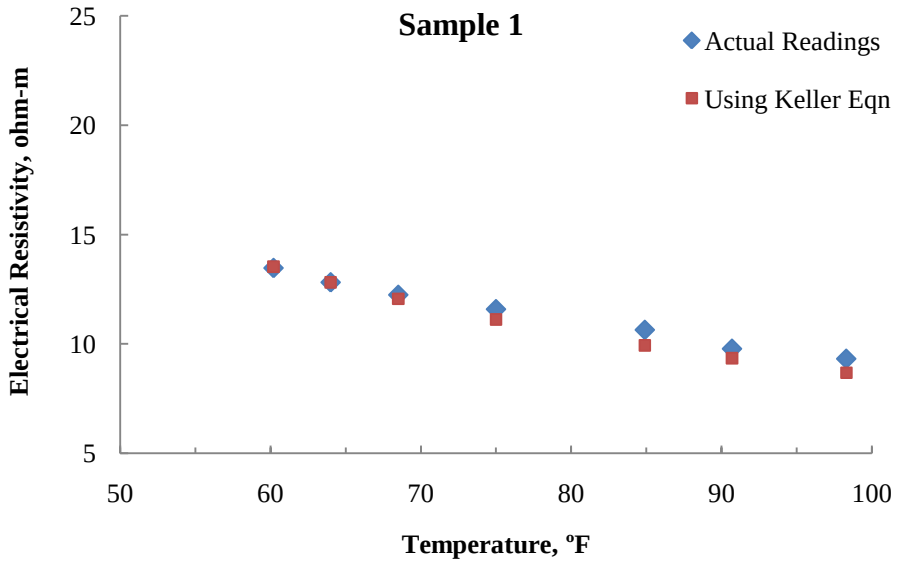

Figure 4.45 Variation of Resistivity with Temperature for Fresh MSW Sample 1

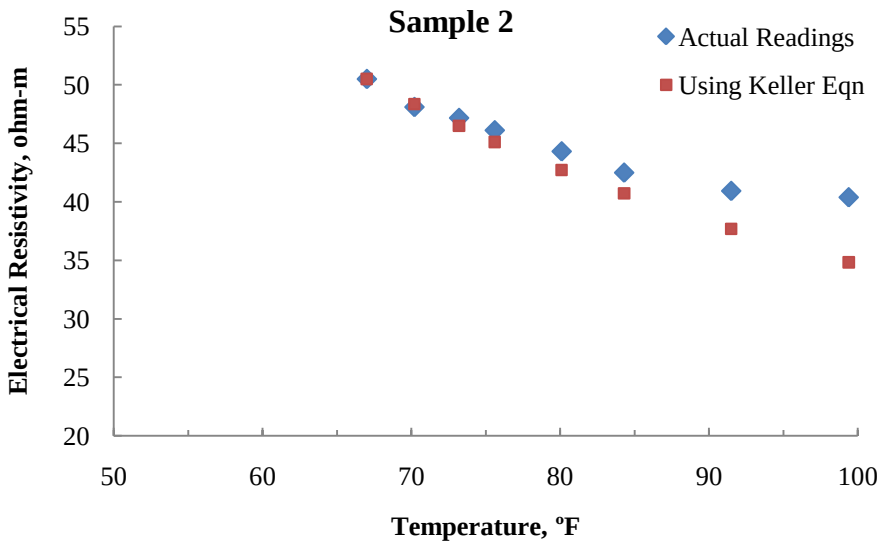

Figure 4.46 Variation of Resistivity with Temperature for Fresh MSW Sample 2

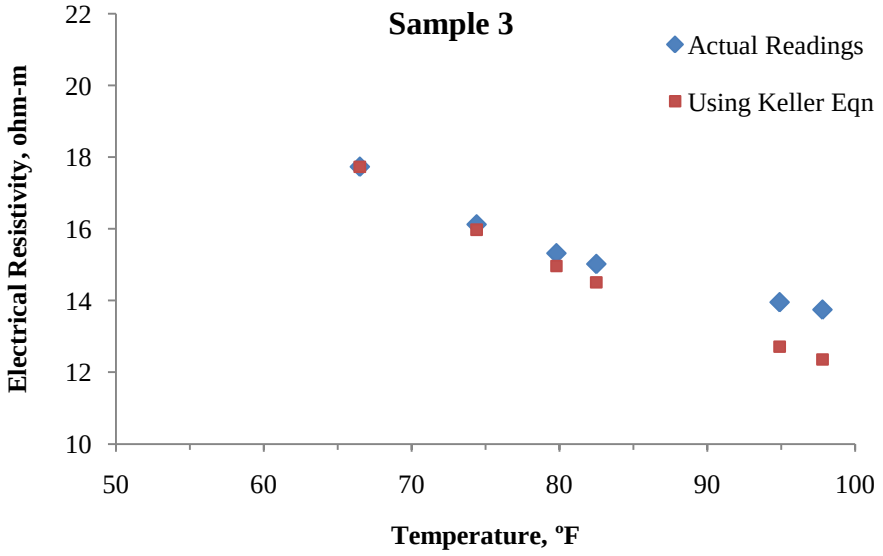

Figure 4.47 Variation of Resistivity with Temperature for Fresh MSW Sample 3

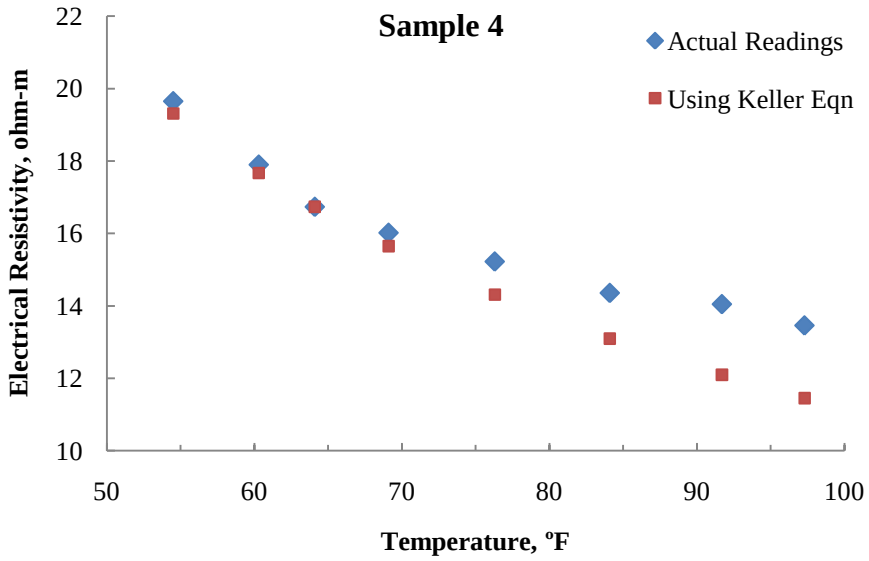

Figure 4.48 Variation of Resistivity with Temperature for Fresh MSW Sample 4

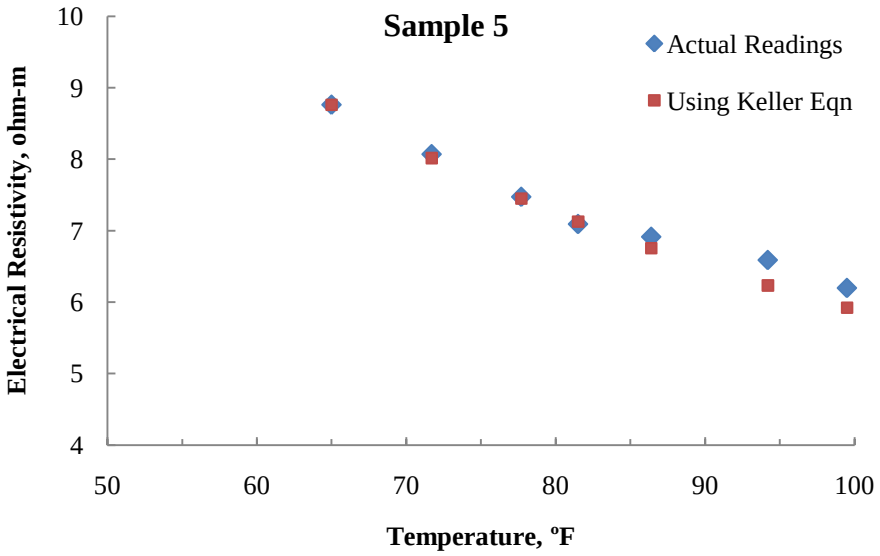

Figure 4.49 Variation of Resistivity with Temperature for Fresh MSW Sample 5

Table 4.16 Temperature Coefficients for Five Fresh MSW Samples

Sample	α (per °C)
1	0.0195
2	0.0198
3	0.0196
4	0.0186
5	0.0229
Average	**0.020**

4.3.5 Effect of Composition

4.3.5.1 Fresh MSW Samples

In order to understand better the effect of the composition of MSW on resistivity, the waste samples in the test box were manually sorted into individual components after conducting the resistivity tests. Table 4.17 presents the composition of MSW in the test box when the samples were compacted to a unit weight of 35 lb/ft^3 at actual field moisture content. The resistivity of each sample was plotted versus its corresponding paper content and "others" content to find any possible trends. Paper and others were selected because they were the dominant components in the waste samples.

Figure 4.50 presents a plot of the electrical resistivity versus the corresponding paper percentage by weight for five fresh MSW samples. A decrease in the electrical resistivity with increasing paper content was observed. This is probably due to the fact that paper products tend to absorb more water, and increases in paper content usually correspond to higher moisture content.

On the other hand, an increase in electrical resistivity with increasing "others" (soil and fines) content was observed as shown in Figure 4.51. This behaviour can be

explained by the fact that an increase in the fines content will decrease the porosity, reducing the amount of voids available for current flow.

Table 4.17 Physical Composition of Fresh MSW Samples in the Test Box

	Physical Composition (% by Weight)						
Sample	Paper	Plastic	Food waste	Textile	Yard waste	Metals	Others
1	46.40	15.94	0	3.25	6.38	11.22	16.82
2	41.21	10.96	0	5.01	5.17	4.45	33.20
3	40.25	10.31	2.75	5.51	8.03	3.28	29.88
4	61.80	14.18	4.07	4.07	3.65	3.76	8.47
5	41.44	15.70	5.38	7.09	8.22	7.34	14.82
Average	46.22	13.42	2.44	4.99	6.29	6.01	20.64
Standard Deviation	9.03	2.64	2.41	1.46	1.93	3.31	10.49

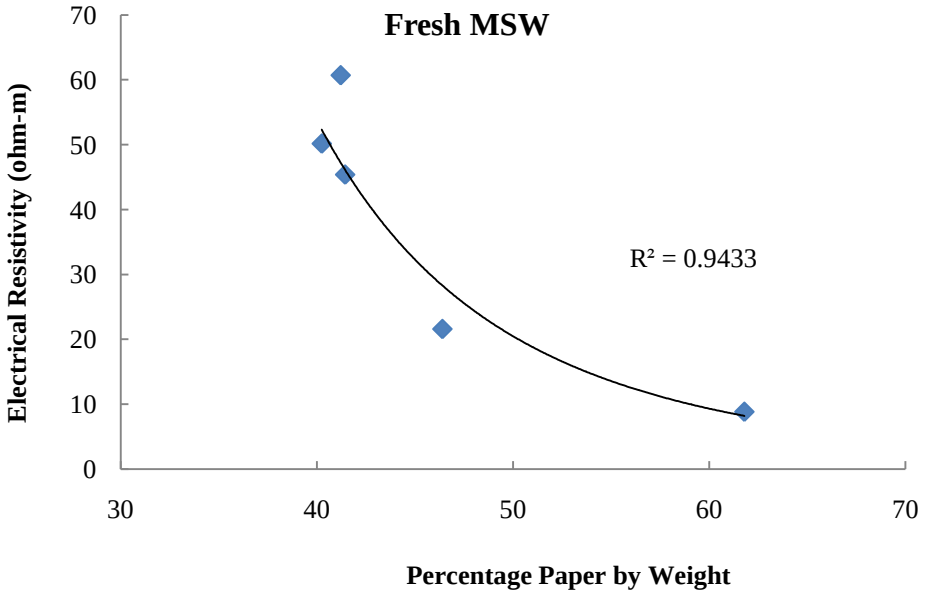

Figure 4.50 Effect of Paper Content on Resistivity of Fresh MSW Samples

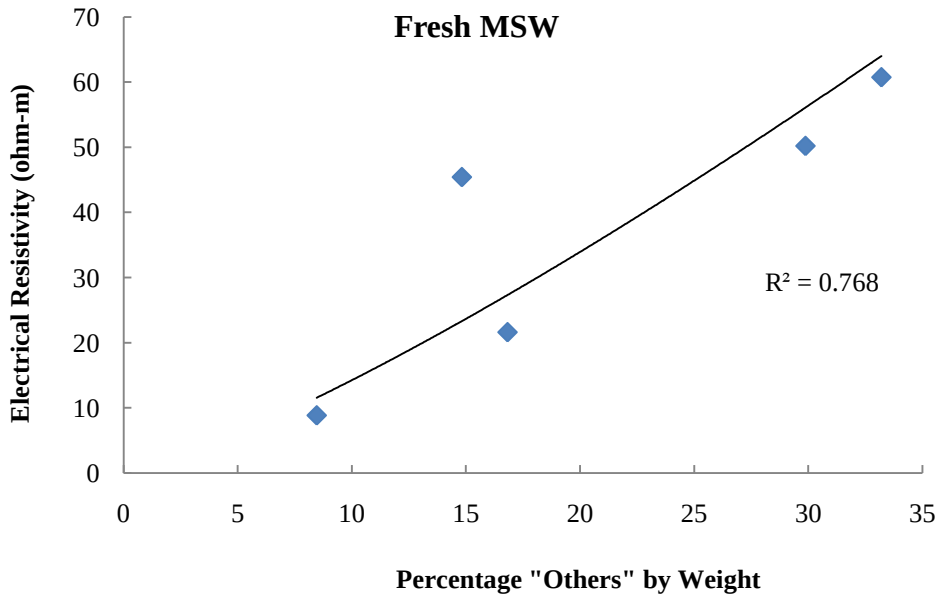

Figure 4.51 Effect of "Others" Content on Resistivity of Fresh MSW Samples

4.3.5.1 Landfilled MSW Samples

After conducting the resistivity tests on the landfilled samples (from boreholes B45, B47, and B49), the waste samples in the test box were manually sorted into individual components. Table 4.18, 4.19, and 4.20 present the composition of MSW in the test box when the samples were compacted to a unit weight of 35 lb/ft^3 at actual field moisture content. The resistivity of each sample was plotted versus its corresponding paper content and "others" content to find any possible trends. Similar trends were observed for the borehole samples. A decrease in the electrical resistivity with increasing paper content was observed (Figure 4.52). Also, an increase in electrical resistivity with increasing "others" (soil and fines) content was observed (Figure 4.53).

Table 4.18 Physical Composition of Samples from Borehole B45 in the Test Box

Borehole No.	Depth (ft)	Physical Composition (% by Weight)					
		Paper	Plastic	Textile	Yard waste	Metals	Others
B45	20	54.65	18.60	0	12.79	0	13.95
	25	60.42	16.51	0	3.34	1.48	18.24
	30	25.85	12.66	0	4.18	3.33	53.98
	35	75.43	14.64	0	3.97	0	5.96
	40	16.67	19.36	1.05	57.02	5.91	0
	45	7.24	7.45	.69	71.52	0	13.1
	50	67.68	19.26	0	0	0	13.06
	55	40.08	7.85	0.88	6.16	6.23	38.79
	60	62.81	14.59	10.15	0	1.82	10.63
	65	7.73	16.42	7.21	3.48	2.32	62.85
	Average	41.86	14.74	2.00	16.25	2.11	23.06
	Standard Deviation	25.82	4.32	3.61	25.79	2.38	21.27

Table 4.19 Physical Composition of Samples from Borehole B47 in the Test Box

Borehole No.	Depth (ft)	Physical Composition (% by Weight)					
		Paper	Plastic	Textile	Yard waste	Metals	Others
B47	20	45.49	9.33	0	3.99	2.27	38.92
	25	41.25	7.22	2.33	8.26	2.63	38.31
	30	49.66	13.34	0	2.35	1.24	33.42
	35	0	9.85	0	43.71	0	46.44
	40	29.82	7.20	1.75	5.2	1.03	54.99
	45	72.68	1.10	0	2.75	0	23.47
	50	62.36	6.67	0	1.77	1.9	27.29
	55	54.98	8.12	0	0	1.23	35.68
	60	100	0	0	0	0	0
	65	76.49	4.70	0	5.45	0	13.37
	Average	53.27	6.75	0.41	7.35	1.03	31.19
	Standard Deviation	27.47	4.00	0.87	13.03	1.01	15.99

Table 4.20 Physical Composition of Samples from Borehole B49 in the Test Box

Borehole No.	Depth (ft)	Physical Composition (% by Weight)					
		Paper	Plastic	Textile	Yard waste	Metals	Others
B49	20	45.49	9.33	0	3.99	2.27	38.92
	25	41.25	7.22	2.33	8.26	2.63	38.31
	30	49.66	13.34	0	2.35	1.24	33.42
	35	0	9.85	0	43.71	0	46.44
	40	29.82	7.20	1.75	5.2	1.03	54.99
	45	72.68	1.10	0	2.75	0	23.47
	50	62.36	6.67	0	1.77	1.9	27.29
	55	54.98	8.12	0	0	1.23	35.68
	60	100	0	0	0	0	0
	65	76.49	4.70	0	5.45	0	13.37
	Average	53.27	6.75	0.41	7.35	1.03	31.19
	Standard Deviation	27.47	4.00	0.87	13.03	1.01	15.99

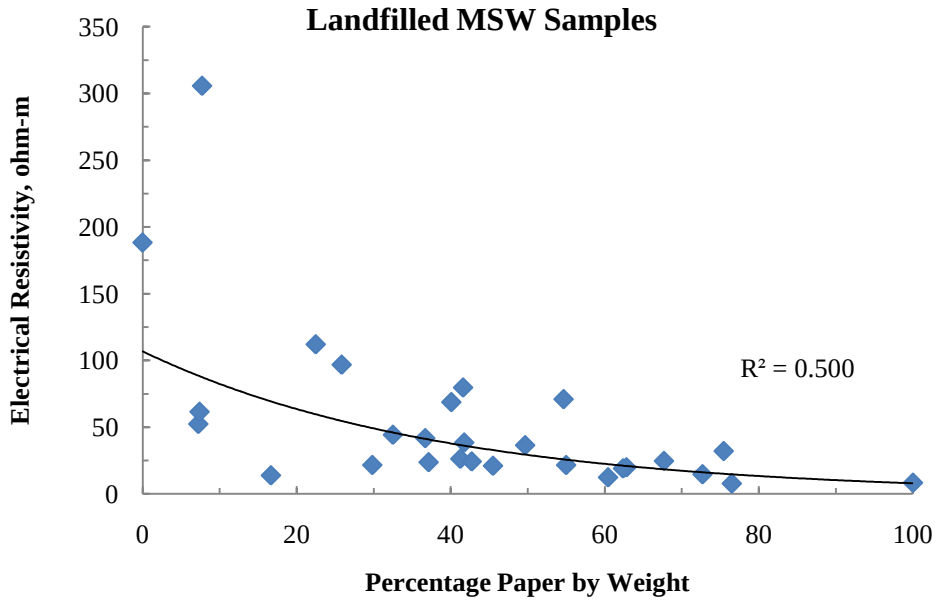

Figure 4.52 Effect of Paper Content on Resistivity of Landfilled Samples

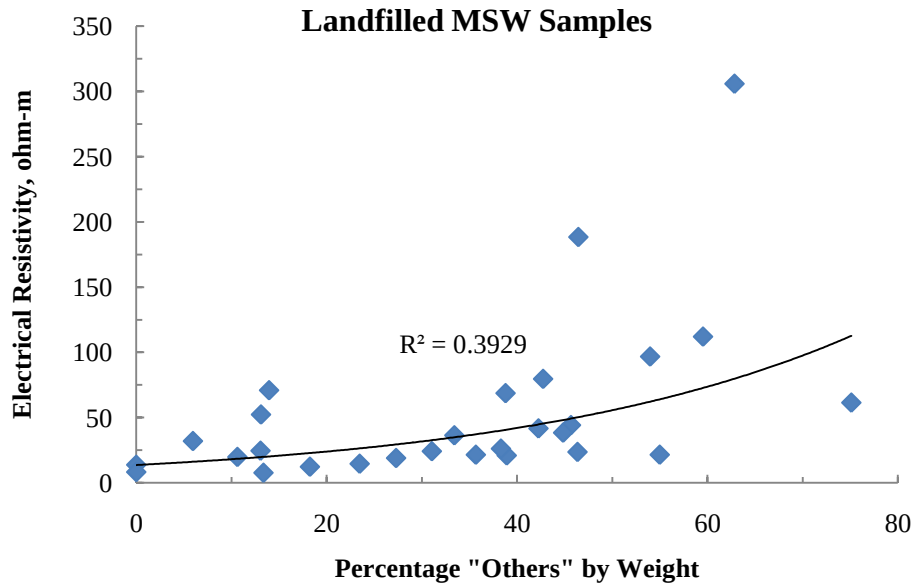

Figure 4.53 Effect of "Others" Content on Resistivity of Landfilled Samples

4.3.6 Effect of Pore Fluid Composition

4.3.6.1 Using Leachate

The resistivity of the five fresh MSW samples was measured again, using leachate as the pore fluid instead of tap water. A significant drop in resistivity values was expected based on similar studies done on soil (Yoon and Park, 2001). According to the authors, the resistivity decreased because of the movement of the high amount of ions present in the leachate.

Figure 4.54 presents resistivity results of the five fresh MSW samples prepared using leachate, compared to earlier results when samples were prepared using tap water. In contrary to what was expected, not much difference was observed. The resistivity values of the samples prepared using leachate were slightly lower than the values obtained when the samples were prepared using tap water. A difference of less than ten percent was observed most of the time.

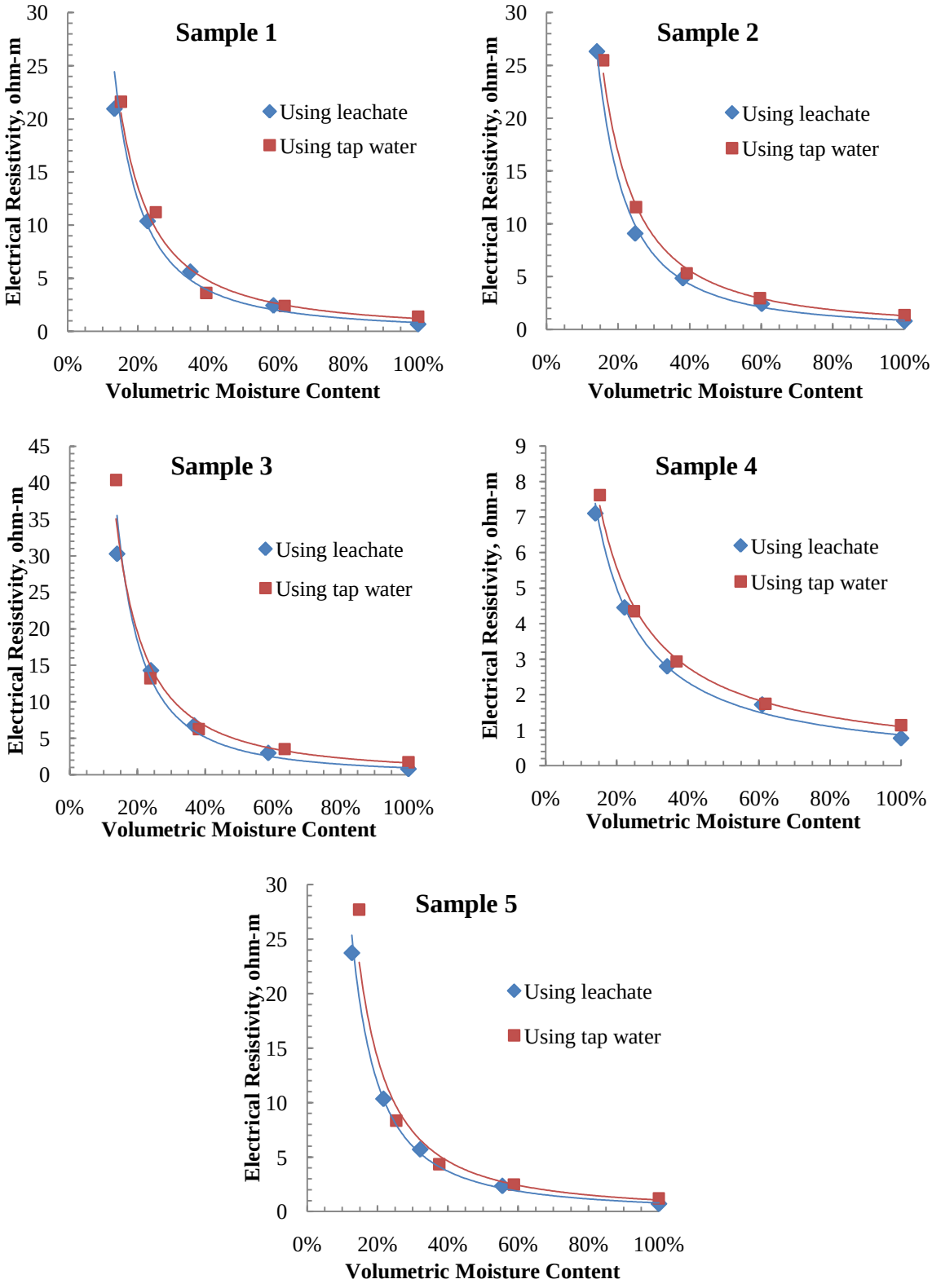

Figure 4.54 Effect of using Leachate as the Pore Fluid on Resistivity of MSW

To explain the results, the resistivity of leachate was measured at the end of each test by collecting the liquid and measuring its conductivity using a conductivity meter. Similarly, the salinity of the leachate was measured before conducting the test, and after the test using a salinity meter. Due to mineralization, the resistivity of the leachate dropped from the 3.5 – 3.7 ohm-m range to the 0.67 – 0.78 ohm-m range as given in Table 4.21. A slight increase in salinity from 0% to 0.6% was observed, indicating that salinity is not a factor that should be considered.

Similarly, when the resistivity tests were conducted on the same samples using tap water, the resistivity of the tap water decreased from the 30 - 32 ohm-m range to 1.1-1.7 ohm-m range. These results indicate that when a liquid is added to a waste sample, the liquid extracts the soluble inorganic and organic compounds present in the waste, and that the resistivity of the liquid stabilizes at some constant value after approximately five days. In other words, due to the presence of high amount of inorganic and organic compounds in the waste itself, the content of the waste is more controlling than the type of fluid in the pores.

Table 4.21 Resistivity and Salinity of Leachate Before and After Mixing with MSW

Liquid	Resistivity (Ωm)	Resistivity after mixing with MSW (Ωm)	Salinity (%)	Salinity after mixing with MSW (%)
Tap water	30 – 32	1.1 – 1.7	0	0.4
Leachate	3.5 – 3.7	0.67 – 0.78	0	0.6

4.3.6.2 Using Re-Use Water

The resistivity of the five fresh MSW samples was measured again, using re-use water as the pore fluid instead of tap water. The re-use water is treated waste water effluent and is used for recirculation when the amount of leachate produced is not sufficient. Figure 4.55 presents resistivity results of the five fresh MSW samples prepared using re-use water, compared to earlier results when samples were prepared using tap water. Again, the resistivity values of the samples prepared using re-use water were almost identical to the values obtained when the samples were prepared using tap water. A difference of less than ten percent was observed most of the time.

The resistivity of the re-use water ranged between 13.8 and 14.0 ohm-m initially before adding it to the waste. This resistivity range is between that of tap water and leachate. After adding the re-use water to the waste and conducting the resistivity tests, the resistivity of the re-use water dropped to the 0.75 – 1.01 ohm-m range as shown in Table 4.22. Also, a slight increase in salinity from 0% to 0.4% was observed, indicating that salinity is not a factor that should be considered.

These results confirm again that due to the presence of high amount of inorganic and organic compounds in the waste itself, the content of the waste is more controlling than the type of fluid in the pores.

Table 4.22 Resistivity and Salinity of Re-use Water Before and After Mixing with MSW

Liquid	Resistivity (Ωm)	Resistivity after mixing with MSW (Ωm)	Salinity (%)	Salinity after mixing with MSW (%)
Tap water	30 – 32	1.1 – 1.7	0	0.4
Re-use water	13.8 – 14.0	0.75 – 1.01	0	0.4

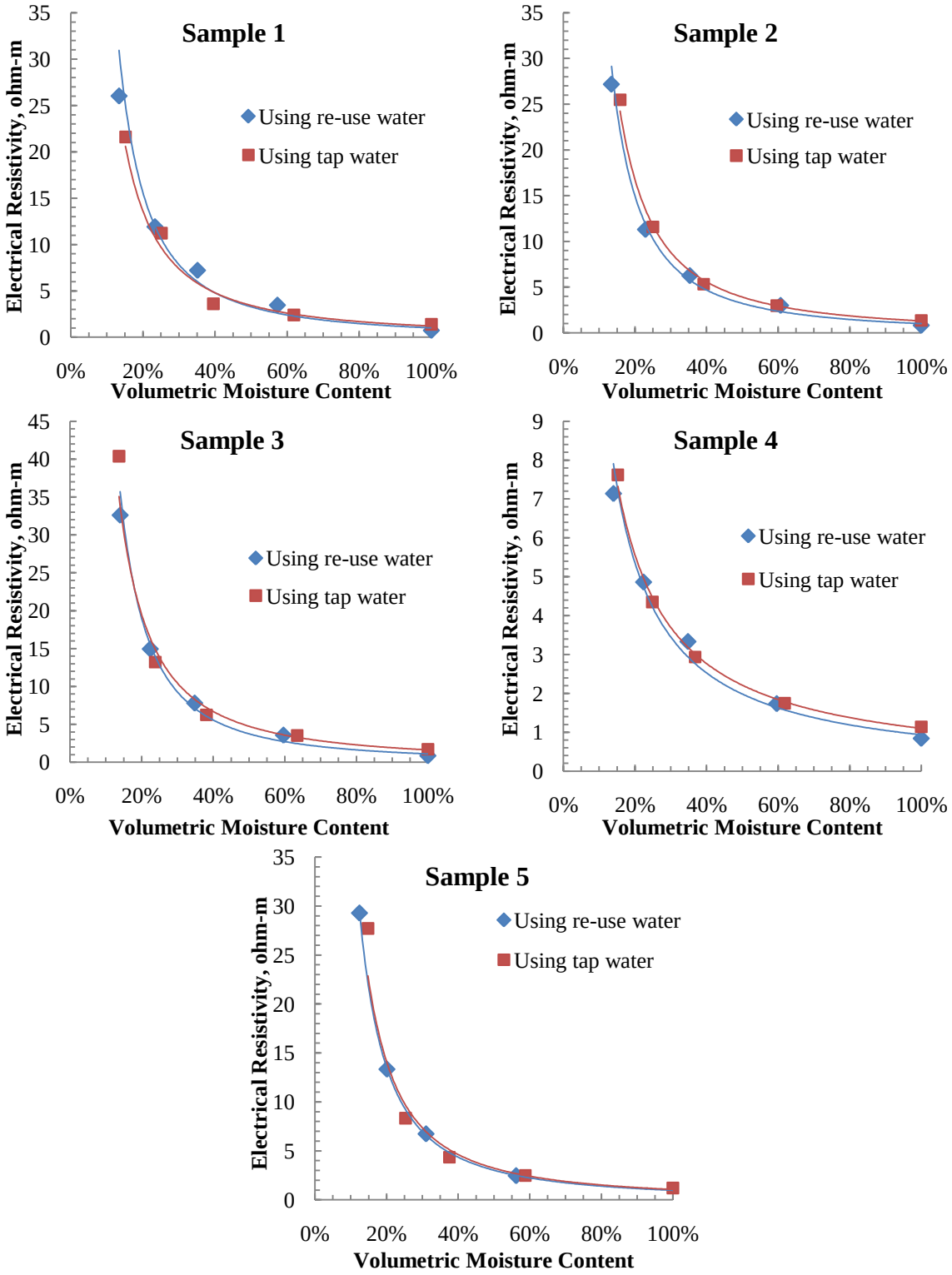

Figure 4.55 Effect of Using Re-use Water as the Pore Fluid on Resistivity of MSW

CHAPTER 5

STATISTICAL MODEL DEVELOPMENT AND VALIDATION

5.1 Introduction

Multiple linear regression (MLR) analysis was used to develop a model between electrical resistivity of MSW and the several factors that affect resistivity. Regression analysis is a statistical tool for modeling and analyzing the relationships between several variables. MLR is used to model the relationship between a response variable and two or more predictor variables. MLR is valuable tool for quantifying the effect of various factors simultaneously on a single dependent variable. The assumed linear relationship between the response variable and p-1 predictor variables is given by:

$$Y_i = \beta_0 + \beta_1 X_{i1} + \beta_2 X_{i2} + \ldots + \beta_{p-1} X_{i,p-1} + \varepsilon_i \quad (5.1)$$

where:

$\beta_0, \beta_1, \ldots, \beta_{p-1}$ are unknown model parameters,

$X_1, X_2, \ldots, X_{p-1}$ are predictor variables, and

ε is the random error.

The response function for the above regression model is a hyperplane, which is a plane in more than two dimensions. It is not possible to picture this response surface. The regression parameters are estimated using the least squares method. It is important to understand the physical meaning of the regression parameters. β_0 is the Y-intercept of the response surface. β_1 indicates the change in the mean response E[Y] per unit increase in X_1 when all other predictor variables in the regression model are held constant, and so on.

The error term ε is assumed to be normally distributed with an expected value of zero and a constant variance.

Statistical Analysis System (SAS) software is used for the data analysis. The steps followed to develop the statistical model are:

1. Data collection and selection.
2. Fitting a preliminary model and checking model assumptions.
3. Performing necessary transformations until essential model assumptions are satisfied.
4. Exploring interaction terms.
5. Searching for the alternate good models.
6. Selecting the best model and interpreting the final results.

5.2 Data Selection

Resistivity tests were conducted on most of the waste samples more than once by varying the moisture content, unit weight, etc. Regression analysis requires the response observations to be uncorrelated. If response observations use the same waste sample, then these observations are linked, and potentially correlated. Therefore, a dataset consisting of 37 observations was selected from the experimental results on different waste samples to cover the following ranges for the predictor variables:

Moisture content (M/C): 13% – 70%

Unit weight: 30 lb/ft^3 – 70 lb/ft^3

Percentage paper: 0% - 100%

Percentage “others”: 0% - 75%

Organic content (O/C): 44% - 85%

Five predictor variables are considered: moisture content, unit weight, percentage paper, percentage "others" (fines), and organic content. The response variable is electrical resistivity. The dataset used in the regression analysis is presented in Table 5.1.

Table 5.1 Data Used in Regression Analysis

Obs.	ρ (ohm-m)	M/C (%)	γ_m (lb/ft^3)	Paper (%)	"Others" (%)	O/C (%)	Sample
	Y	X_1	X_2	X_3	X_4	X_5	
1	21.60	28.27	34.41	46.40	16.82	77.49	Fresh MSW 1
2	42.46	28.03	44.48	41.21	33.20	69.0	Fresh MSW 2
3	33.20	24.21	53.58	40.25	29.88	74.5	Fresh MSW 3
4	2.94	39.71	57.85	61.80	8.47	74.9	Fresh MSW 4
5	2.48	51.287	71.51	41.44	14.82	85.23	Fresh MSW 5
6	16.114	37.52	33.62	54.65	13.95	80.00	B45 at 20'
7	12.31	25.50	33.95	60.42	18.24	63.33	B45 at 25'
8	6.842	49.90	42.59	25.85	53.98	72.00	B45 at 30'
9	31.99	30.13	34.14	75.43	5.96	80.96	B45 at 35'
10	9.264	55.17	47.97	16.67	0.0	62.48	B45 at 40'
11	52.32	30.88	34.16	7.24	13.10	55.73	B45 at45'
12	24.58	13.07	35.23	67.68	13.06	78.42	B45 at 50'
13	68.69	13.14	33.41	40.08	38.79	75.83	B45 at 55'
14	19.82	29.60	33.74	62.81	10.63	77.18	B45 at 60'
15	305.80	15.72	34.351	7.73	62.85	71.43	B45 at 65'
16	20.96	39.47	31.00	45.49	38.92	83.33	B47 at 20'
17	26.18	32.83	33.93	41.25	38.31	72.00	B47 at 25'
18	36.39	28.65	33.97	49.66	33.42	76.19	B47 at 30'
19	188.34	21.40	34.29	0.00	46.44	69.23	B47 at 35'
20	21.54	30.14	34.48	29.82	54.99	69.23	B47 at 40'
21	14.61	27.08	29.37	72.68	23.47	76.00	B47 at 45'
22	18.99	37.63	34.16	62.36	27.29	68.00	B47 at 50'
23	21.52	25.65	34.62	54.98	35.68	76.92	B47 at 55'
24	8.26	29.58	31.46	100.00	0.00	76.00	B47 at 60'
25	7.70	39.05	33.64	76.49	13.37	72.00	B47 at 65'
26	41.680	34.55	34.44	36.69	42.25	78.49	B49 at 25'
27	14.024	29.37	45.25	37.13	46.35	75.89	B49 at 30'
28	35.492	20.46	45.52	7.40	75.12	65.59	B49 at 35'
29	34.201	29.51	45.06	32.50	45.67	67.62	B49 at 40'
30	24.206	22.79	32.57	42.73	31.05	68.27	B49 at 45'

Table 5.1 – *Continued*

31	79.637	31.47	33.01	41.61	42.74	65.88	B49 at 50'
32	30.393	21.94	45.21	41.75	44.84	66.24	B49 at 55'
33	50.604	23.10	45.29	22.48	59.54	77.27	B49 at 60'
34	8.98	71.43	35.71	43.31	18.92	63.3	Reactor Ph1
35	5.92	65.24	48.31	49.97	28.70	50.2	Reactor Ph2
36	6.78	69.2	51.32	41.59	27.53	53.6	Reactor Ph3
37	4.91	71.6	52.59	2.06	2.50	44.4	Reactor Ph4
AVG	36.53	34.44	39.73	42.75	30.02	70.65	
Std. Dev.	55.79	15.44	9.21	22.26	18.70	9.03	

5.2.1 Raw Data Scatter Plots

To get a preliminary evaluation of the suitability of using MLR for analyzing the data, it is useful to plot the response variable versus each predictor variable, and also plot each predictor variable versus the other predictor variables. Figure 5.1 presents the matrix scatter plot of the response vs. predictor plots as well as the predictor vs. predictor plots.

5.2.1.1 Response-Predictor Scatter Plots

From the scatter plots of resistivity vs. moisture content, resistivity vs. unit weight, and resistivity vs. percentage paper, a slightly curvilinear downward trend is observed. A slightly upward trend is observed in the resistivity versus percentage others plot. No trend is observed in the resistivity versus organic content trend.

5.2.1.2 Predictor-Predictor Scatter Plots

The predictor versus predictor scatter plots are checked for possible multicollinearity issues among the predictor variables. There is a downward trend in the moisture content versus organic content plot. This confirms the fact that at higher moisture content, more decomposition occurs and a reduction in the organic content is observed. There is a downward trend in the percentage paper versus the percentage others

plot. Also, there is an upward trend in the percentage paper versus organic content plot. Other than that, there are no strong trends among the rest of the predictor variables.

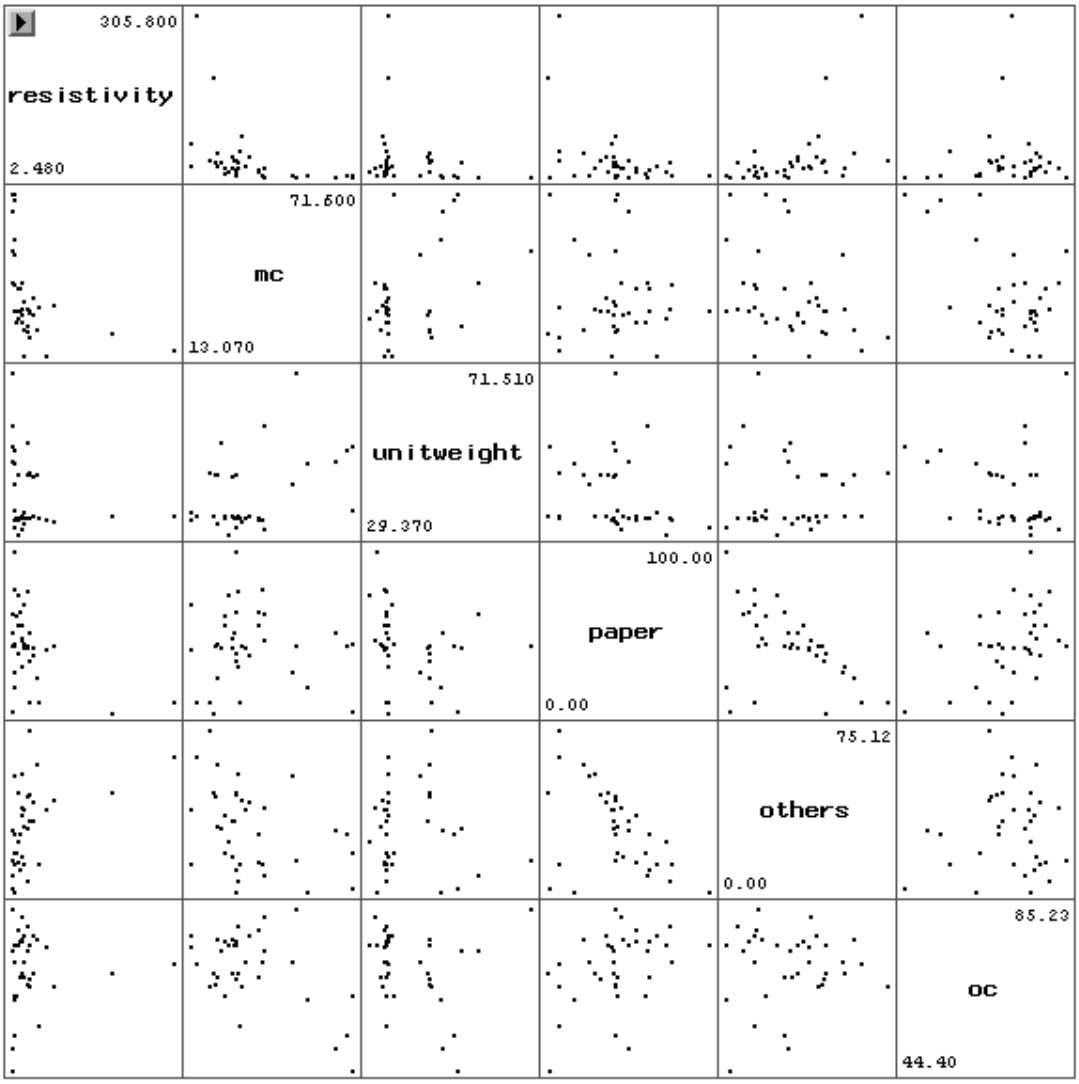

Figure 5.1 Scatter Plot Matrix of Response and Predictor Variables

5.2.2 Correlation Matrix of Response and Predictor Variables

Another measure of the correlation among variables is the correlation coefficient (*r*). The correlation coefficient ranges from -1 to 1. Values of *r* near 1 indicate a strong positive linear relationship, while values of *r* near -1 indicate a strong negative linear relationship. Values of *r* near zero indicate little or no relationship between the variables. Table 5.2 presents the correlation matrix for the response-predictor and predictor-predictor pairwise correlations.

5.2.2.1 Response-Predictor Correlation

r_{y1} = -0.41238 indicates that resistivity and moisture content are somewhat negatively correlated.

r_{y2} = -0.22732 indicates that resistivity and unit weight are slightly negatively correlated.

r_{y3} = -0.4508 indicates that resistivity and percentage paper are somewhat negatively correlated.

r_{y4} = 0.44631 indicates that resistivity and percentage “others” are somewhat positively correlated.

r_{y5} = 0.03201 indicates that resistivity and organic content are not correlated.

5.2.2.2 Predictor-Predictor Correlation

r_{12} = 0.4266 indicates that moisture content and unit weight are somewhat positively correlated.

r_{13} = -0.08511 indicates that moisture content and percentage paper are not correlated.

r_{14} = -0.37078 indicates that moisture content and percentage “others” are somewhat negatively correlated.

r_{15} = -0.52352 indicates that moisture content and organic content are somewhat negatively correlated.

r_{23} = -0.26683 indicates that unit weight and percentage paper are slightly negatively correlated.

r_{24}= -0.06494 indicates that unit weight and percentage "others" are not correlated.

r_{25} = -0.1845 indicates that unit weight and organic content are slightly negatively correlated.

r_{34} = -0.50233 indicates that percentage paper and percentage "others" are somewhat negatively correlated.

r_{35} = 0.41937 indicates that percentage paper and organic content are somewhat positively correlated.

r_{45} = 0.06191 indicates that there is very low correlation between percentage "others" and organic content.

Since none of the correlation coefficients are higher than 0.7, then there are no serious multicollinearity issues among the predictor variables.

Table 5.2 Correlation Coefficients of Response and Predictor Variables

Pearson Correlation Coefficients, N = 37
Prob > |r| under H0: Rho=0

	resistivity	mc	unitweight	paper	others	oc
resistivity	1.00000	-0.41238 0.0112	-0.22732 0.1760	-0.45080 0.0051	0.44631 0.0056	0.03201 0.8508
mc	-0.41238 0.0112	1.00000	0.42660 0.0085	-0.08511 0.6165	-0.37078 0.0239	-0.52352 0.0009
unitweight	-0.22732 0.1760	0.42660 0.0085	1.00000	-0.26683 0.1104	-0.06494 0.7026	-0.18450 0.2743
paper	-0.45080 0.0051	-0.08511 0.6165	-0.26683 0.1104	1.00000	-0.50233 0.0015	0.41937 0.0098
others	0.44631 0.0056	-0.37078 0.0239	-0.06494 0.7026	-0.50233 0.0015	1.00000	0.06191 0.7158
oc	0.03201 0.8508	-0.52352 0.0009	-0.18450 0.2743	0.41937 0.0098	0.06191 0.7158	1.00000

5.3 Preliminary Model

5.3.1 Fitting a Preliminary Model

Regressing electrical resistivity (Y) on all five predictor variables, the regression coefficients were determined using SAS to be (Table 5.3):

b_0 = 165.8117, b_1 = -1.18329, b_2 = -1.33399, b_3 = -1.34216, b_4 = 0.11625 and b_5 = 0.25989. So the preliminary regression model is:

$$\hat{y} = 165.8117 - 1.18329x_1 - 1.33399x_2 - 1.34216x_3 + 0.11625x_4 + 0.25989x_5$$

where:

y is the electrical resistivity in ohm-m,

x_1 is the moisture content in percentage (on wet weight basis),

x_2 is the unit weight in lb/ft^3,

x_3 is the paper composition in percentage,

x_4 is the "others" composition in percentage, and

x_5 is the organic content in percentage.

Table 5.3 Regression Parameter Estimates

Parameter Estimates

Variable	DF	Parameter Estimate	Standard Error	t Value	Pr > |t|	Type I SS	Variance Inflation
Intercept	1	165.81168	89.69788	1.85	0.0741	49383	0
mc	1	-1.18329	0.67752	-1.75	0.0906	19055	1.96576
unitweight	1	-1.33399	0.94619	-1.41	0.1685	361.86983	1.36296
paper	1	-1.34216	0.47732	-2.81	0.0085	30238	2.02671
others	1	0.11625	0.53130	0.22	0.8282	126.91110	1.77198
oc	1	0.25989	1.11060	0.23	0.8165	109.80095	1.80489

5.3.2 Checking Model Assumptions

Residual analysis is used to verify the regression model assumptions. The residual (e) is defined as the difference between the observed value Y and the fitted value $\hat{Y}$. The regression model is based on the following assumptions:

1. A linear model is reasonable.
2. The residuals have constant variance.
3. The residuals are normally distributed.
4. The residuals are uncorrelated.

A residual plot can clearly show if there is any deviation from the above assumptions. For example, curvilinearity in a residual plot (Figure 5.2a) indicates that the current model form is not adequate, and a funnel shape (Figure 5.2b) indicates that the constant variance assumption is not satisfied.

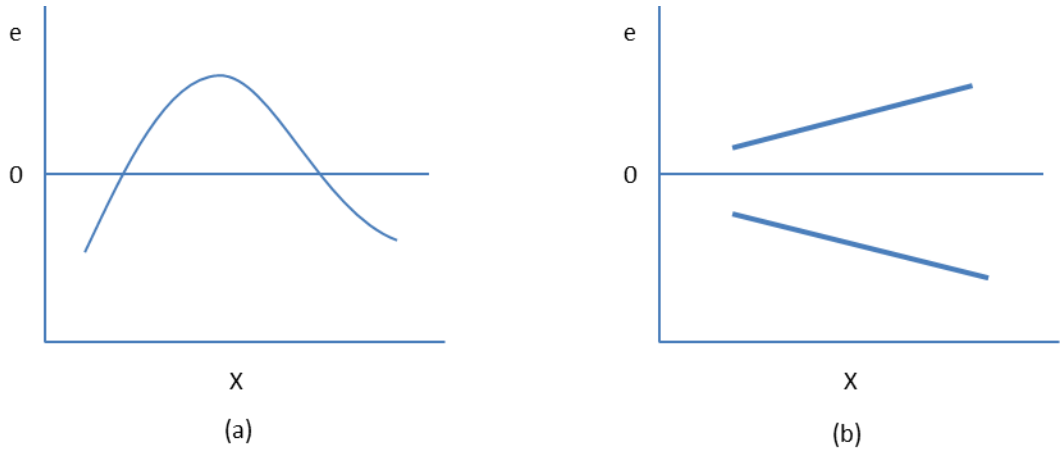

Figure 5.2 Prototype Residual Plots: (a) Curvature and (b) Funnel Shape

5.3.2.1 MLR Model Form

To verify the adequacy of the current MLR model form, the plots of the residuals versus the predictor variables are checked for any curvature. The residual plots are presented in Figure 5.3. Curvature is observed in the plots of residuals vs. moisture content, residuals vs. unit weight, and residuals vs. percentage paper. Slight curvature can also be seen in the relationships between resistivity and these predictor variables in Figure 5.1. Therefore, the current model form is not adequate and some transformations should be investigated to rectify the problem.

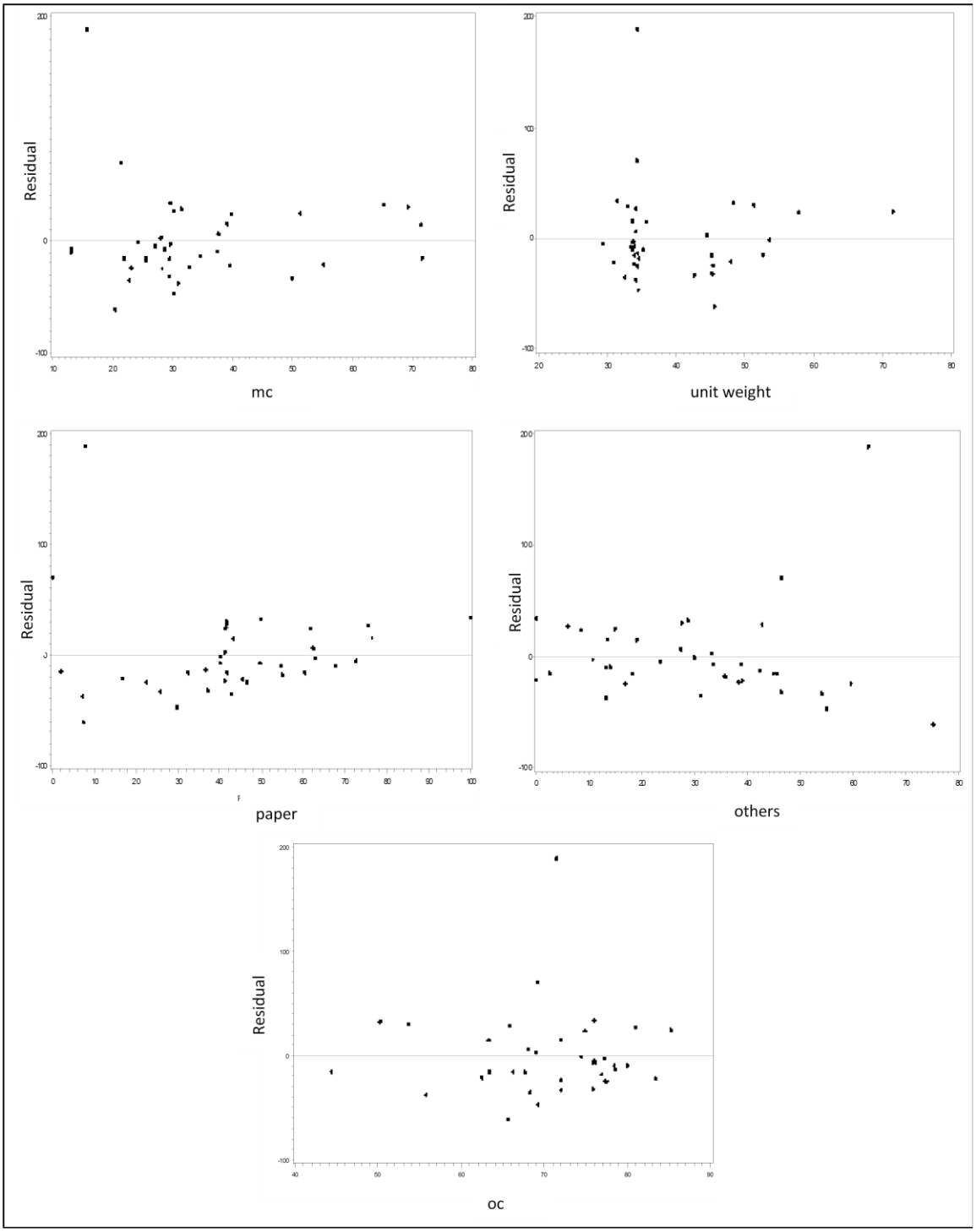

Figure 5.3 Residual vs. Predictor Variables Plots

5.3.2.2 Constant Variance

To verify the constant variance assumption, the plot of the residuals versus the predicted value of resistivity (Figure 5.4) is checked for a funnel shape. No clear funnel shape is observed in Figure 5.4; however there seems to be a possible nonconstant variance issue due to the wider spread of points for higher predicted value of resistivity. The constant variance assumption will be checked again after performing a transformation to correct curvature.

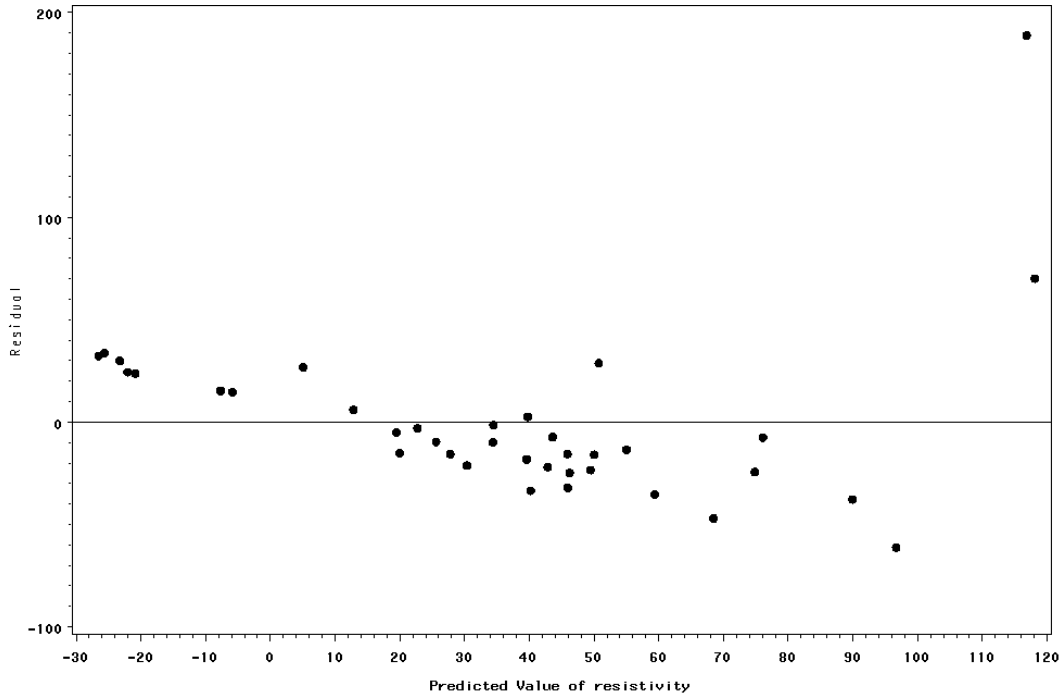

Figure 5.4 Plot of Residuals versus Predicted Value of Resistivity

5.3.2.3 Normality

The normality of the error terms is checked using a normal probability plot. In a normal probability plot, each residual is plotted against its expected value under normality. A plot that is nearly linear suggests agreement with normality, while a plot

that departs substantially from linearity suggests that the error distribution is not normal. Figure 5.5 shows the normal probability plot for the preliminary model. It can be seen that the error term distribution is skewed to the right, possibly due to the presence of an outlier. Therefore, normality of the error terms is not satisfied. Normality will be checked again after performing a transformation.

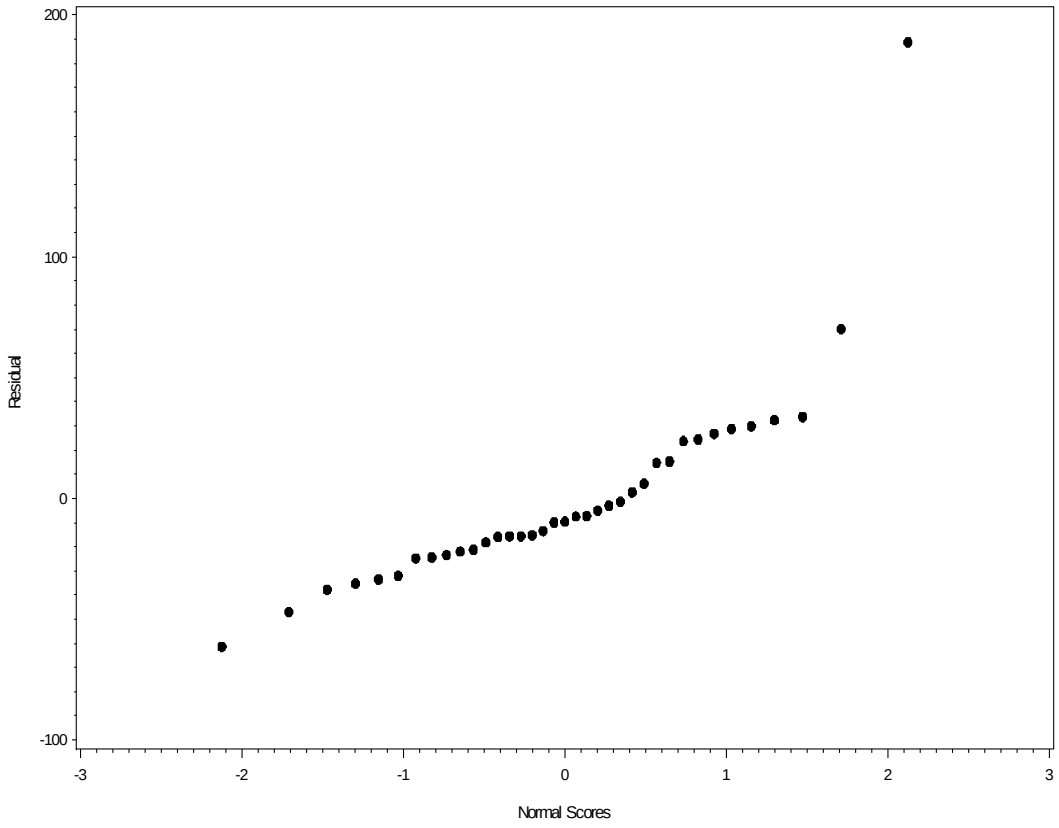

Figure 5.5 Normal Probability Plot for Preliminary Model

5.3.2.4 Uncorrelated Errors

Since the data was collected over time, a time series plot of the residuals was prepared (Figure 5.6). The purpose of plotting the residuals against time or observation number is to see if there is any correlation between error terms that are near each other in

the sequence. From Figure 5.6, the residuals are fluctuating in a random pattern around the base line zero. Therefore, it is concluded that serial correlation is not an issue.

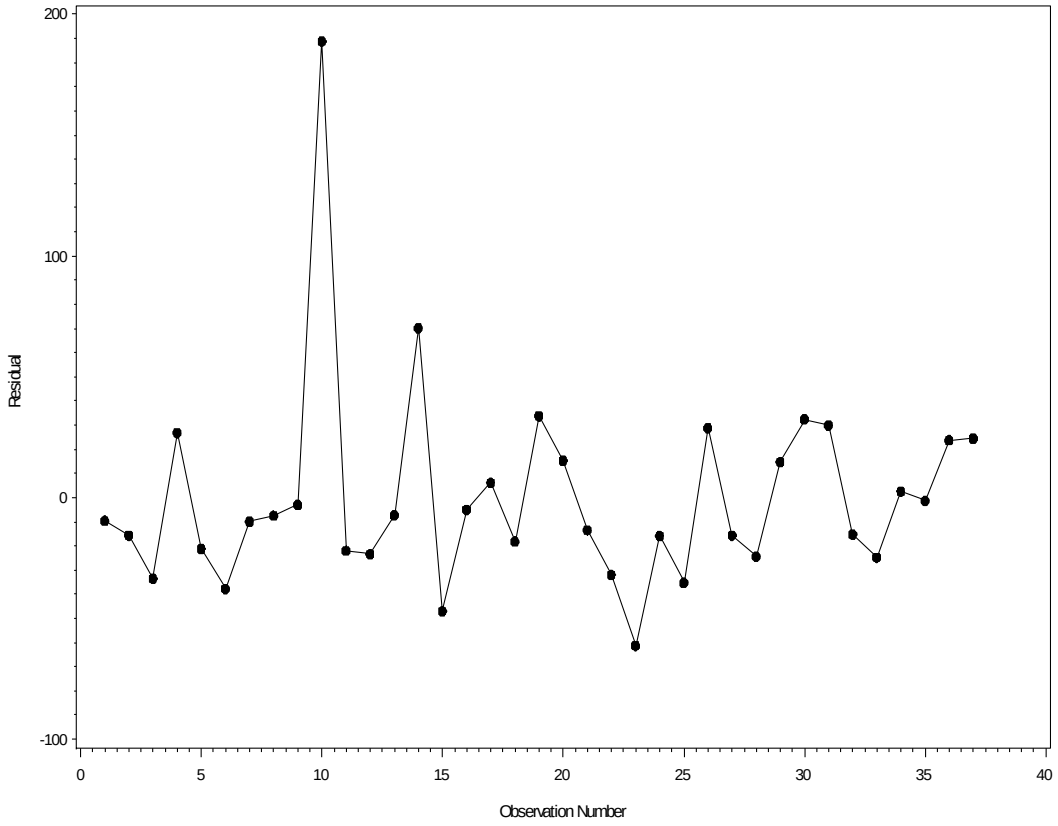

Figure 5.6 Time Series Plot

5.4 Transformations

Since curvature was observed in the plots of residuals versus moisture content, residuals versus unit weight, and residuals vs. percentage paper (Figure 5.3), it is necessary to perform some kind of transformation to satisfy the linear model form requirement. Given the non-normality and the particular trend of the curvature seen in response-predictor plots (Figure 5.1), it is advisable to compress high values of Y. Therefore, a logarithmic (base 10) transformation was performed on resistivity (Y). It should be noted that this transformation will affect all five predictors.

5.4.1 Transformed Model

Regressing the logarithm of electrical resistivity (log Y) on all five predictor variables, the regression coefficients were determined using SAS to be (Table 5.4):

$b_0 = 3.02966$, $b_1 = -0.01549$, $b_2 = -0.01906$, $b_3 = -0.00936$, $b_4 = 0.00218$ and $b_5 = -0.00123$. The regression model after performing the log transformation is:

$$\widehat{\text{Log } y} = 3.02966 - 0.01549x_1 - 0.01906x_2 - 0.00936x_3 + 0.00218\,x_4 - 0.00123x_5$$

Table 5.4 Parameters Estimates for Transformed Model

Parameter Estimates

Variable	DF	Parameter Estimate	Standard Error	t Value	Pr > |t|	Type I SS	Variance Inflation
Intercept	1	3.02966	0.44142	6.86	<.0001	64.20087	0
mc	1	-0.01549	0.00333	-4.65	<.0001	3.36455	1.96576
unitweight	1	-0.01906	0.00466	-4.09	0.0003	0.37397	1.36296
paper	1	-0.00936	0.00235	-3.98	0.0004	1.84789	2.02671
others	1	0.00218	0.00261	0.83	0.4105	0.03200	1.77198
oc	1	-0.00123	0.00547	-0.23	0.8232	0.00247	1.80489

5.4.2 Re-checking Model Assumptions

5.4.2.1 MLR Model Form

To verify the adequacy of the current MLR model form, the plots of the residuals versus the predictor variables are checked again for any curvature. The residual plots are presented in Figure 5.7. The log transformation resolved the curvature issue, and curvature is not observed in any of the residual plots. It should be noted here that although curvature was not observed for predictor variables percentage others and organic content, the transformation has accommodated what appeared to be outliers previously. The current MLR model form is now adequate.

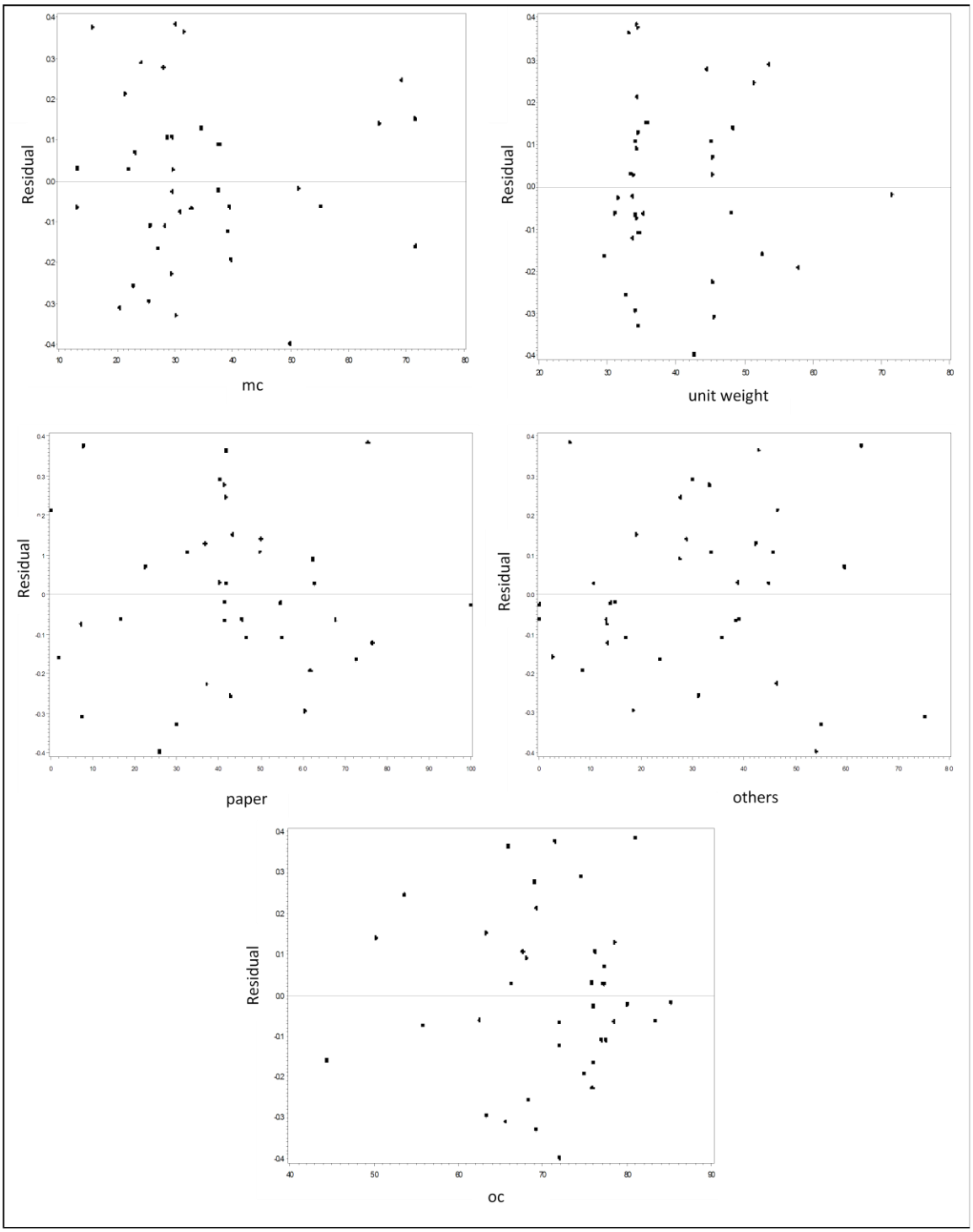

Figure 5.7 Residuals versus Predictor Variables (After Transformation)

5.4.2.2 Constant Variance

To verify the constant variance assumption, the plot of the residuals versus the predicted value of log resistivity (Figure 5.8) is checked for a funnel shape. No funnel shape is observed in Figure 5.8.Therefore, the constant variance assumption is satisfied.

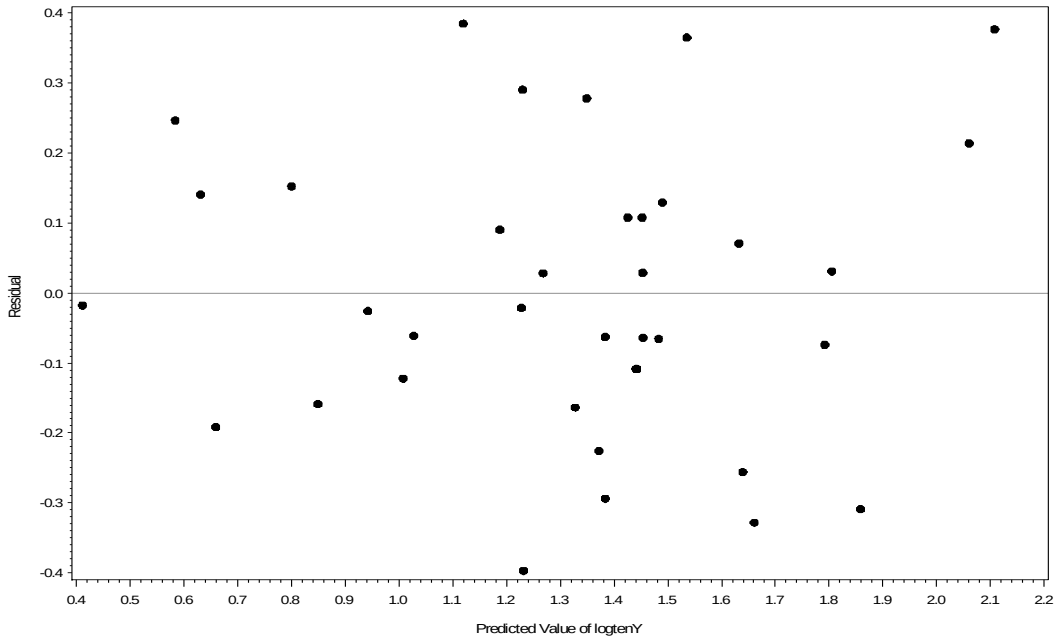

Figure 5.8 Plot of Residuals versus Predicted Value of Log Resistivity

5.4.2.3 Normality

The normal probability plot for the transformed model is presented in Figure 5.9. It can be seen that the normality improved after performing the log transformation. The normal probability plot is mostly straight, and it is reasonable to conclude that the residuals are close to following a normal distribution.

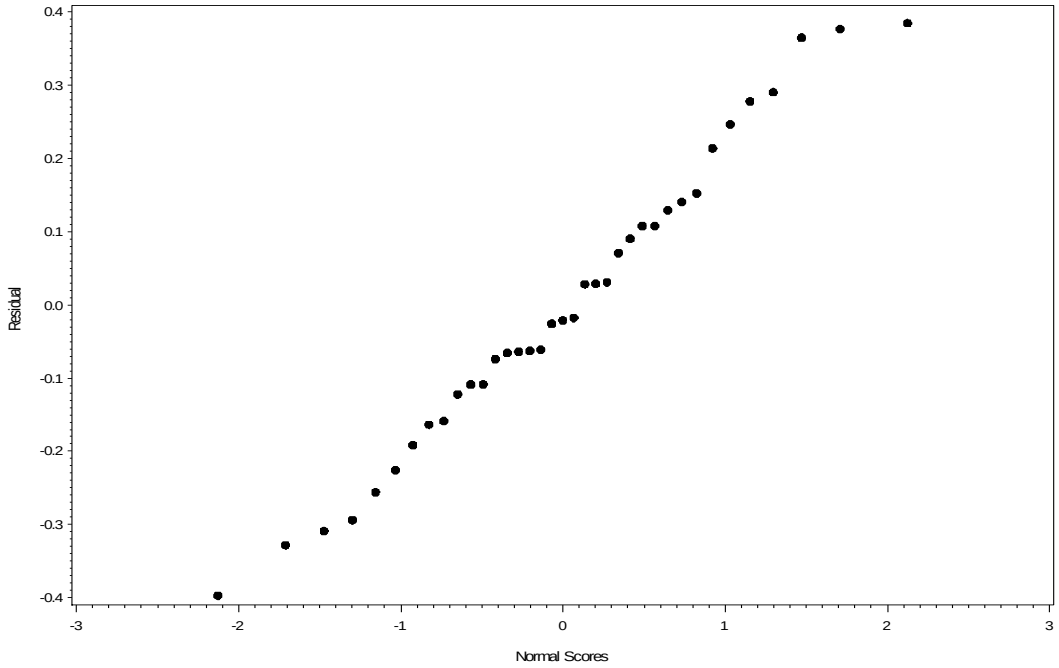

Figure 5.9 Normal Probability Plot for Transformed Model

5.4.3 Checking Model Diagnostics

5.4.3.1 X-Outliers

Leverage values (h_{ii}) values are used to check whether x-outliers exist or not.

Guideline: if h_{ii}>2p/n= 2*6/37 = 0.3243 (where p is the number of parameters), then observation *i* is x-outlying and has high leverage. From Table 5.5, observations #6, #32, and #37 have leverage values exceeding the cutoff. Therefore, it is concluded that 3 observations are x-outliers and there is a need to assess their influence on the regression.

5.4.3.2 Y-Outliers

Bonferroni outlier test is used to check for y-outliers.

*Guideline:*If $|t_i| > t\left(1-\frac{\alpha}{2n}; n-p-1\right)$, then conclude observation *i* is a y-outlier.

Bonferroni: $t\left(1-\frac{\alpha}{2n};n-p-1\right)=t\left(1-\frac{0.10}{2*37};37-6-1\right)=t(0.9986,30)$

$=3.2563$

From Table 5.5, none of the observations have Rstudent values exceeding the cutoff. Therefore, it is concluded that no y-outliers exist

5.4.3.3 Influence

To assess the influence of observations #6, #32, and #37 on the regression, two criteria will be used:

Influence on the Fitted Values (DFFITS):

Guideline: if $|\text{DFFITS}|>2\sqrt{\frac{p}{n}}=2\sqrt{\frac{6}{37}}=0.8054$, then outlier has high influence on the estimated regression equation and fitted values. From Table 5.5, none of the x-outliers identified earlier are influential according to this criteria.

Cook's Distance:

Guideline: if D*i* >F(0.50; p, n-p) = F(0.50; 6, 37- 6) = 0.991,then that outlier has high influence on the estimated regression equation and fitted values. From Table 5.5, none of the x-outliers identified earlier are influential according to this criteria.

Table 5.5 Diagnostics for Best Model

Obs	Residual	Rstudent	hii	DFFITS	Cook D
1	-0.0209	-0.0998	0.1241	-0.0376	0.00024
2	-0.2937	-1.4711	0.1484	-0.6141	0.06057
3	-0.3968	-2.0976	0.1821	-0.9897	0.14711
4	0.3854	1.9493	0.1225	0.7283	0.08109
5	-0.0609	-0.3149	0.2521	-0.1828	0.00574
6	-0.0737	-0.4040	0.3333	-0.2857	0.01398
7	-0.0637	-0.3092	0.1505	-0.1302	0.00291
8	0.0314	0.1465	0.0838	0.0443	0.00034
9	0.0287	0.1339	0.0850	0.0408	0.00029
10	0.37773	1.9531	0.1619	0.8583	0.11256
11	-0.0625	-0.3167	0.2202	-0.1683	0.00486
12	-0.0653	-0.2991	0.0479	-0.0671	0.00077
13	0.1083	0.4970	0.0468	0.1101	0.00207
14	0.2143	1.0872	0.1949	0.5349	0.0474
15	-0.3279	-1.5991	0.0903	-0.5038	0.04028
16	-0.1632	-0.7740	0.0962	-0.2525	0.01076
17	0.0907	0.4230	0.0792	0.1241	0.00264
18	-0.1082	-0.4984	0.0524	-0.1172	0.00234
19	-0.0255	-0.1296	0.2290	-0.0706	0.00086
20	-0.1218	-0.5779	0.1050	-0.1979	0.00667
21	0.1298	0.6170	0.1073	0.2139	0.00778
22	-0.2255	-1.0653	0.0730	-0.2989	0.01483
23	-0.3088	-1.6448	0.2343	-0.9097	0.13075
24	0.1082	0.5035	0.0724	0.1406	0.00338
25	-0.2557	-1.2113	0.0684	-0.3281	0.01768
26	0.3654	1.7835	0.0746	0.5065	0.03995
27	0.0291	0.1408	0.1450	0.058	0.00058
28	0.0713	0.3417	0.1300	0.1321	0.00299
29	0.1528	0.8131	0.2804	0.5076	0.04342
30	0.1410	0.7656	0.3111	0.5144	0.0447
31	0.2469	1.3040	0.2449	0.7425	0.08986
32	-0.1584	-0.9258	0.3996	-0.7552	0.09551
33	-0.1085	-0.5099	0.0902	-0.1605	0.0044
34	0.2785	1.3187	0.0594	0.3313	0.01787
35	0.2910	1.4627	0.1551	0.6268	0.06315
36	-0.1915	-0.9782	0.2122	-0.5077	0.04302
37	-0.0173	-0.1133	0.5367	-0.122	0.00256

In summary, the data set contains three x-outliers (#6, #32, and #37) and no y-outliers. None of the three x-outliers was found to be influential. Since there is no justification (typo error, measurement error, etc.) to delete these observations from the data set, it is decided to proceed with the best model selection process.

5.4.4 Analysis of Variance (ANOVA)

The ANOVA table for the preliminary model is presented in Table 5.6. The total variability in electrical resistivity prior to considering any predictor variables is the total sum of squares (SSTO), which is equal to 7.13. The variability in electrical resistivity that is explained by the current MLR model is the regression sum of squares (SSR), which is equal to 5.62. The variability in electrical resistivity that is unexplained by the model is the error sum of squares (SSE), which is equal to 1.50. The ratio of explained variability to total variability, SSR/SSTO, assesses the quality of the current model fit. In the ANOVA table, this is the coefficient of determination, $R^2 = 0.7888$, which indicates that 78.9% of total variability in electrical resistivity is explained by the regression model with predictors moisture content, unit weight, percentage paper, percentage "others", and organic content.

Table 5.6 Analysis of Variance (ANOVA) for Preliminary Model

Analysis of Variance

Source	DF	Sum of Squares	Mean Square	F Value	Pr > F
Model	5	5.62087	1.12417	23.15	<.0001
Error	31	1.50530	0.04856		
Corrected Total	36	7.12618			

Root MSE	0.22036	R-Square	0.7888
Dependent Mean	1.31725	Adj R-Sq	0.7547
Coeff Var	16.72868		

5.5 Exploration of Interaction Terms

Interaction terms are terms formed by a cross-product of two predictor variables. For the five predictor variables considered, ten potential interaction terms (x_1x_2, x_1x_3, x_1x_4, x_1x_5, x_2x_3, x_2x_4, x_2x_5, x_3x_4, x_3x_5, and x_4x_5) can be added to the model. Since adding excessive terms can overcomplicate the regression analysis, it is desirable to identify in advance the interaction terms that are most likely to influence the response variable. Partial regression plots may be used to identify possibly useful interaction terms. Partial regression plots are formed by:

1. Determining the residuals from regressing the response variable on all five predictor variables.
2. Determining the residuals from regressing each interaction term on all five predictor variables.
3. Plotting the residuals from (1) versus the residuals from (2)

If a trend is observed in a partial regression plot, the interaction term should be considered. On the other hand, if scattered points without any particular trend are observed in a partial regression plot, then the interaction term should not be considered.

Figure 5.10 and 5.11 present the partial regression plots for the ten interaction terms. An upward trend is observed for x_1x_3. A downward trend is observed for x_3x_5. Therefore, it is concluded to consider the interaction terms x_1x_3 (moisture content × percentage paper) and x_3x_5 (percentage paper × organic content) in the model. Remaining plots show scattered points, so the rest of the interaction terms are not considered in the model.

When interaction terms are added to the model, high multicollinearity may exist between the interaction terms and the predictor variables. A correlation coefficient

greater than 0.7 indicates that predictor variables and interaction terms are highly correlated. Table 5.7 presents the correlation coefficients for the two added interaction terms. The two added interaction terms are highly correlated to the predictor variable percentage paper.

Table 5.7 Correlation Coefficients for Interaction Terms

Pearson Correlation Coefficients, N = 37						
	logtenY	mc	unitweight	paper	other	oc
x1x3	-0.63289	0.50553	0.0315	0.74541	-0.48056	0.07124
x3x5	-0.32854	-0.16425	-0.27692	0.98014	-0.50013	0.55812

To reduce multicollinearity, the interaction terms are standardized by centering the mean to zero (subtracting by the mean) and scaling the variance to one (dividing by the standard deviation). Table 5.8 presents the correlation coefficients for the standardized interaction terms. It can be seen that the correlation coefficients have decreased and that the interaction terms are no longer highly correlated to percentage paper.

Table 5.8 Correlation Coefficients for Standardized Interaction Terms

Pearson Correlation Coefficients, N = 37						
	logtenY	mc	unitweight	paper	other	oc
stdx1x3	0.49482	-0.40632	-0.14531	-0.11362	0.57346	0.25694
stdx3x5	-0.16125	0.24195	0.05418	-0.17869	-0.46648	-0.37259

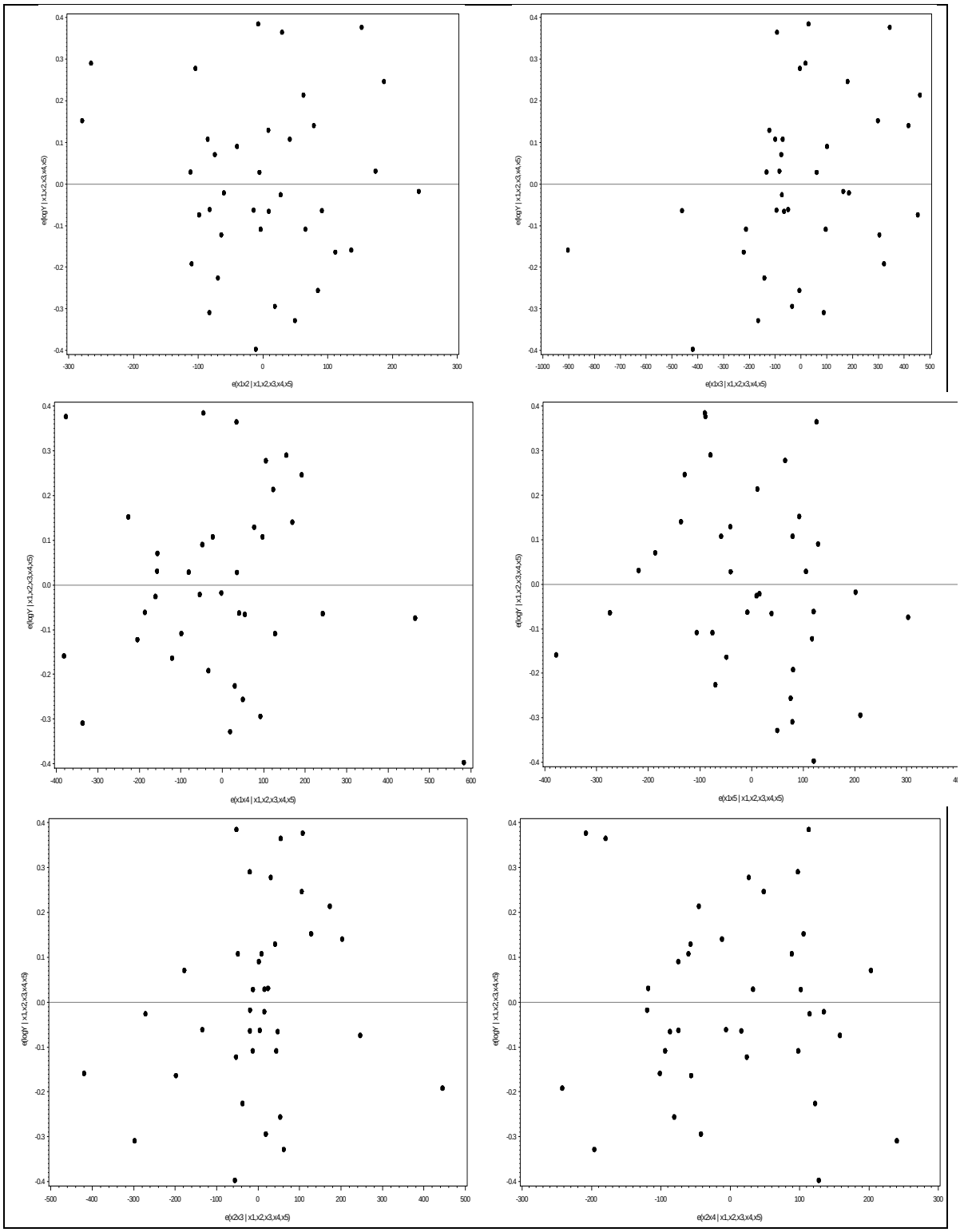

Figure 5.10 Partial Regression Plots

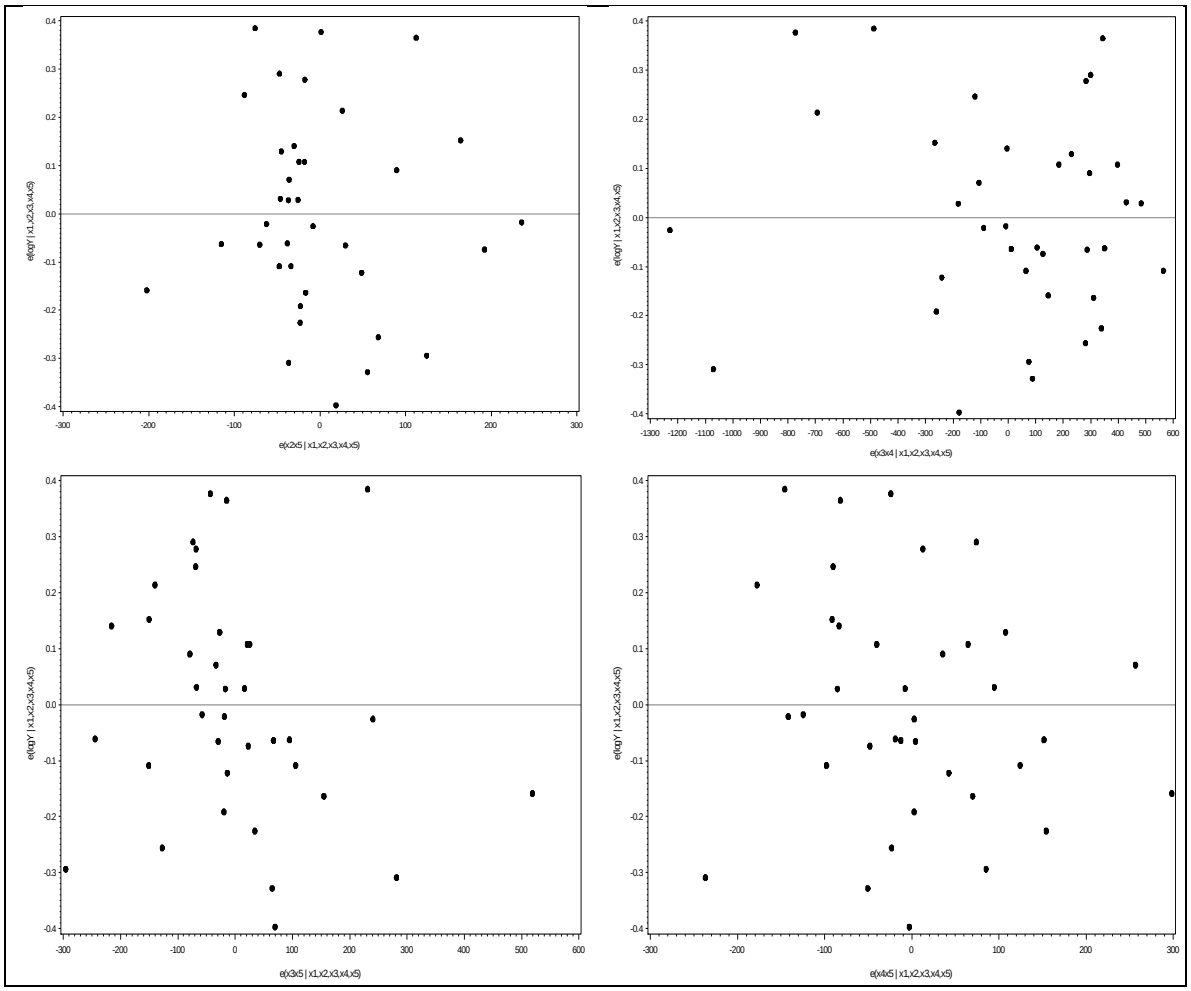

Figure 5.11 Partial Regression Plots

5.6 Model Search

Searching for the "best potential model" is a critical step in MLR analysis. Unnecessary predictor variables are removed in this step. Three methods are used to select the best model: backward elimination, best subsets selection, and stepwise regression. The model selection methods are discussed next.

5.6.1 Backward Elimination

This method begins by including all predictor variables in the model. The variable with the largest *p*-value exceeding the specified α cutoff value (selected as 0.05) is removed from the model because the variable is statistically insignificant. The process continues until no remaining predictor variables have *p*-values above the specified cutoff. This method gives one potentially good model.

Table 5.9 shows the SAS output for the backward elimination method. One potentially good model is left in which all the variables are significant at α = 0.05 level. The model contains four predictor variables: moisture content, unit weight, percentage paper, and $stdx_1x_3$.

Table 5.9 SAS Output for Backward Elimination Method

Backward Elimination: Step 0

All Variables Entered: R-Square = 0.8126 and C(p) = 8.0000

Analysis of Variance

Source	DF	Sum of Squares	Mean Square	F Value	Pr > F
Model	7	5.79040	0.82720	17.96	<.0001
Error	29	1.33577	0.04606		
Corrected Total	36	7.12618			

Variable	Parameter Estimate	Standard Error	Type II SS	F Value	Pr > F
Intercept	3.17373	0.50511	1.81847	39.48	<.0001
mc	-0.01473	0.00338	0.87535	19.00	0.0001
unitweight	-0.01900	0.00459	0.78800	17.11	0.0003
paper	-0.00979	0.00263	0.63725	13.83	0.0009
others	-0.00049765	0.00332	0.00104	0.02	0.8818
oc	-0.00218	0.00544	0.00741	0.16	0.6912
stdx1x3	0.09010	0.05605	0.11902	2.58	0.1188
stdx3x5	0.00298	0.05751	0.00012387	0.00	0.9590

Table 5.9 – *Continued*

Backward Elimination: Step 1

Variable stdx3x5 Removed: R-Square = 0.8125 and C(p) = 6.0027

Analysis of Variance

Source	DF	Sum of Squares	Mean Square	F Value	Pr > F
Model	6	5.79028	0.96505	21.67	<.0001
Error	30	1.33590	0.04453		
Corrected Total	36	7.12618			

Variable	Parameter Estimate	Standard Error	Type II SS	F Value	Pr > F
Intercept	3.18681	0.43032	2.44217	54.84	<.0001
mc	-0.01478	0.00321	0.94159	21.15	<.0001
unitweight	-0.01904	0.00446	0.81215	18.24	0.0002
paper	-0.00986	0.00226	0.84395	18.95	0.0001
others	-0.00057886	0.00288	0.00180	0.04	0.8418
oc	-0.00224	0.00526	0.00804	0.18	0.6739
stdx1x3	0.08844	0.04534	0.16941	3.80	0.0605

Backward Elimination: Step 2

Variable others Removed: R-Square = 0.8123 and C(p) = 4.0419

Analysis of Variance

Source	DF	Sum of Squares	Mean Square	F Value	Pr > F
Model	5	5.78848	1.15770	26.83	<.0001
Error	31	1.33770	0.04315		
Corrected Total	36	7.12618			

Variable	Parameter Estimate	Standard Error	Type II SS	F Value	Pr > F
Intercept	3.15649	0.39680	2.73061	63.28	<.0001
mc	-0.01464	0.00309	0.96770	22.43	<.0001
unitweight	-0.01899	0.00438	0.81049	18.78	0.0001
paper	-0.00961	0.00187	1.13667	26.34	<.0001
oc	-0.00230	0.00517	0.00858	0.20	0.6587
stdx1x3	0.08395	0.03886	0.20140	4.67	0.0386

Table 5.9 – *Continued*

Backward Elimination: Step 3

Variable oc Removed: R-Square = 0.8111 and C(p) = 2.2282

Analysis of Variance

Source	DF	Sum of Squares	Mean Square	F Value	Pr > F
Model	4	5.77989	1.44497	34.35	<.0001
Error	32	1.34628	0.04207		
Corrected Total	36	7.12618			

Variable	Parameter Estimate	Standard Error	Type II SS	F Value	Pr > F
Intercept	3.00221	0.19200	10.28627	244.50	<.0001
mc	-0.01396	0.00265	1.16479	27.69	<.0001
unitweight	-0.01936	0.00425	0.87485	20.79	<.0001
paper	-0.01001	0.00162	1.61749	38.45	<.0001
stdx1x3	0.08136	0.03794	0.19348	4.60	0.0397

All variables left in the model are significant at the 0.0500 level.

5.6.2 Best Subsets Selection

This method finds a specified number of best models containing one, two, three variables and so on, up to the model containing all of the variables. The criteria used for the best model selection are:

- High R^2, the coefficient of multiple determination. R^2 represents the total variation in Y that is explained by the regression model. Adding more X variables to the model always increases R^2.
- High R_{adj}^2, the adjusted coefficient of multiple determination. R_{adj}^2 is a better measure than R^2 because it is adjusted for the number of X variables in the model.
- Low Mallow's C_p. This criterion estimates the total mean squared error of the *n* fitted values for each subset regression model.

- Low AIC (Akaike's Information Criterion) and SBC (Schwarz' Bayesian Criterion). These two criteria penalize models having large number of predictors.

Table 5.10 shows the SAS output for the best subsets method. Only two best models from each subset size are shown. It can be seen that R_{adj}^2 starts to decrease when there are five variables in the model. The highlighted model in Table 5.10 is selected as the best potential model because it met the following criteria:

- Highest R_{adj}^2 value ($R_{adj}^2 = 0.7875$)
- Lowest C_p value ($C_p = 2.2282$)
- Lowest AIC value (AIC = -112.6021)
- Lowest SBC value (SBC = -104.5475)

The best model selected from this method is consistent with the one obtained using the backward elimination method.

Table 5.10 SAS Output for Best Subsets Selection Method

Number in Model	Adjusted R-Square	R-Square	C(p)	AIC	SBC	Variables in Model
1	0.4571	0.4721	48.6661	-80.5844	-77.36260	mc
1	0.2829	0.3028	74.8620	-70.2905	-67.06870	others
2	0.6402	0.6602	21.5681	-94.8840	-90.05125	mc paper
2	0.5483	0.5734	35.0016	-86.4639	-81.63119	mc others
3	0.7643	0.7839	4.4288	-109.6336	-103.18995	mc unitweight paper
3	0.6600	0.6883	19.2214	-96.0774	-89.63371	mc paper stdx1x3
4	0.7875	0.8111	2.2282	-112.6021	-104.54750	mc unitweight paper stdx1x3
4	0.7689	0.7946	4.7798	-109.5054	-101.45079	mc unitweight paper stdx3x5
5	0.7820	0.8123	4.0419	-110.8388	-101.17326	mc unitweight paper oc stdx1x3
5	0.7810	0.8114	4.1773	-110.6666	-101.00109	mc unitweight paper others stdx1x3
6	0.7750	0.8125	6.0027	-108.8887	-97.61228	mc unitweight paper others oc stdx1x3
6	0.7749	0.8124	6.0225	-108.8634	-97.58701	mc unitweight paper oc stdx1x3 stdx3x5

5.6.3 Stepwise Regression

This method combines backward elimination and forward selection methods. This method begins with no predictor variables in the model. Variables are added or deleted one at a time to the model, as long as the p-value is between a specified α_{in} and α_{out}. Stepwise regression method gives only one potentially good model.

Table 5.11 shows the SAS output for the stepwise regression method. One potentially good model is left in which all the variables are significant at $\alpha = 0.05$ level. The selected model is consistent with the one obtained using the backward elimination and best subsets method.

Table 5.11 SAS Output for Stepwise Regression

Stepwise Selection: Step 1

Variable mc Entered: R-Square = 0.4721 and C(p) = 48.6661

Analysis of Variance

Source	DF	Sum of Squares	Mean Square	F Value	Pr > F
Model	1	3.36455	3.36455	31.31	<.0001
Error	35	3.76163	0.10748		
Corrected Total	36	7.12618			

Variable	Parameter Estimate	Standard Error	Type II SS	F Value	Pr > F
Intercept	1.99900	0.13323	24.19381	225.11	<.0001
mc	-0.01980	0.00354	3.36455	31.31	<.0001

Stepwise Selection: Step 2

Variable paper Entered: R-Square = 0.6602 and C(p) = 21.5681

Analysis of Variance

Source	DF	Sum of Squares	Mean Square	F Value	Pr > F
Model	2	4.70483	2.35242	33.03	<.0001
Error	34	2.42135	0.07122		
Corrected Total	36	7.12618			

Variable	Parameter Estimate	Standard Error	Type II SS	F Value	Pr > F
Intercept	2.40765	0.14365	20.00524	280.91	<.0001
mc	-0.02086	0.00289	3.71003	52.10	<.0001
paper	-0.00870	0.00201	1.34028	18.82	0.0001

Table 5.11 – *Continued*

Stepwise Selection: Step 3

Variable unitweight Entered: R-Square = 0.7839 and C(p) = 4.4288

Analysis of Variance

Source	DF	Sum of Squares	Mean Square	F Value	Pr > F
Model	3	5.58641	1.86214	39.91	<.0001
Error	33	1.53977	0.04666		
Corrected Total	36	7.12618			

Variable	Parameter Estimate	Standard Error	Type II SS	F Value	Pr > F
Intercept	3.09739	0.19672	11.56694	247.90	<.0001
mc	-0.01615	0.00258	1.82939	39.21	<.0001
unitweight	-0.01944	0.00447	0.88158	18.89	0.0001
paper	-0.01057	0.00168	1.84789	39.60	<.0001

Stepwise Selection: Step 4

Variable stdx1x3 Entered: R-Square = 0.8111 and C(p) = 2.2282

Analysis of Variance

Source	DF	Sum of Squares	Mean Square	F Value	Pr > F
Model	4	5.77989	1.44497	34.35	<.0001
Error	32	1.34628	0.04207		
Corrected Total	36	7.12618			

Variable	Parameter Estimate	Standard Error	Type II SS	F Value	Pr > F
Intercept	3.00221	0.19200	10.28627	244.50	<.0001
mc	-0.01396	0.00265	1.16479	27.69	<.0001
unitweight	-0.01936	0.00425	0.87485	20.79	<.0001
paper	-0.01001	0.00162	1.61749	38.45	<.0001
stdx1x3	0.08136	0.03794	0.19348	4.60	0.0397

All variables left in the model are significant at the 0.0500 level.

No other variable met the 0.0500 significance level for entry into the model.

5.6.4 Verifying Model Assumptions for the Selected Model

5.6.4.1 MLR Model Form

To verify the adequacy of the current MLR model form for the best model, the plots of the residuals versus the predictor variables moisture content, unit weight,

percentage paper, and $stdx_1x_3$ are checked for any curvature. The residual plots are presented in Figure 5.12. No curvature is observed in any of the residual plots. Therefore, the current model form is adequate.

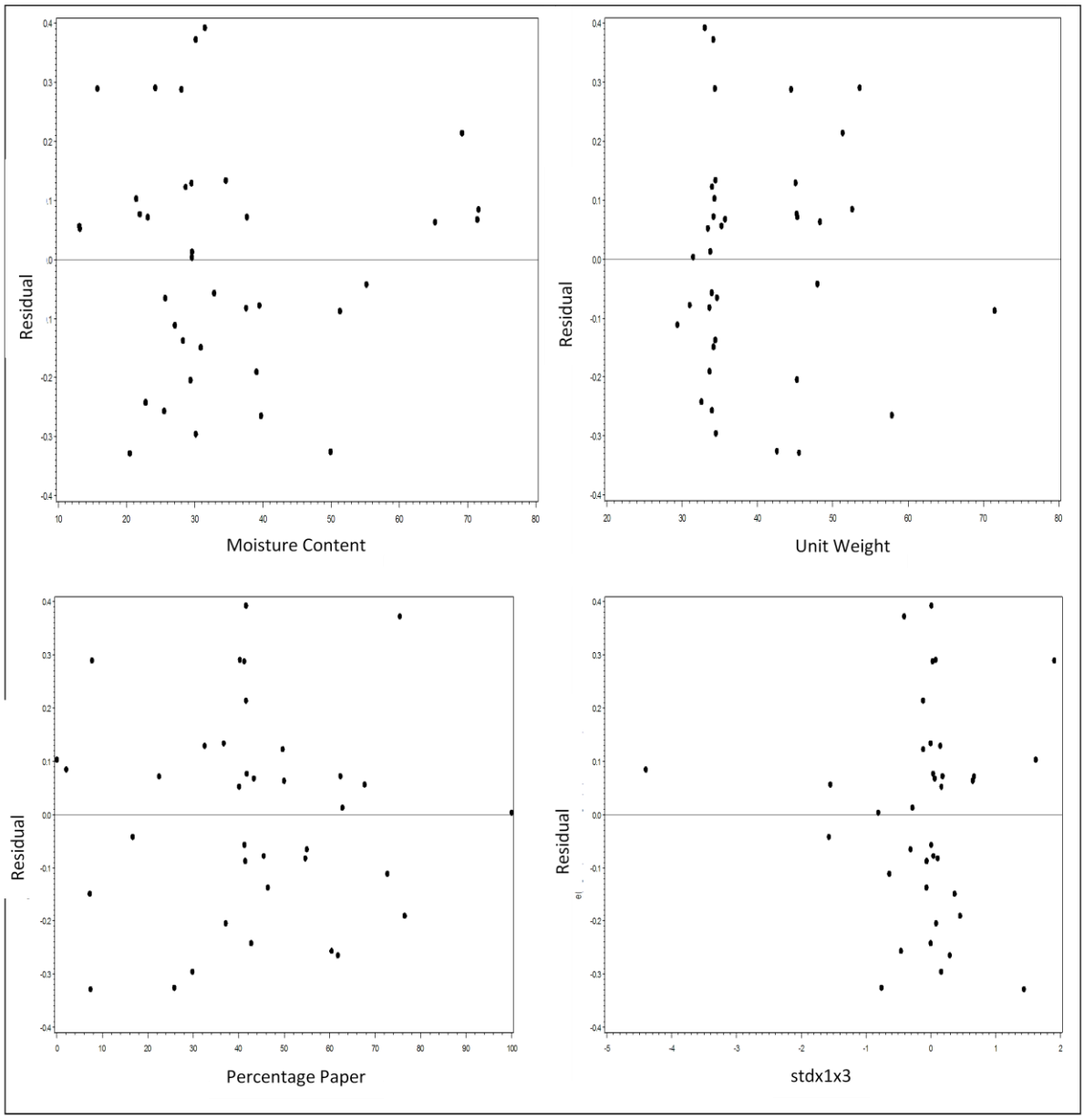

Figure 5.12 Residual Plots for Best Model

5.6.4.2 Constant Variance

To verify the constant variance assumption, the plot of the residuals versus the predicted value of log resistivity (Figure 5.13) is checked for a funnel shape. No funnel shape is observed in Figure 5.13. Therefore, the constant variance assumption is satisfied. The Modified Levene test is done to confirm this conclusion.

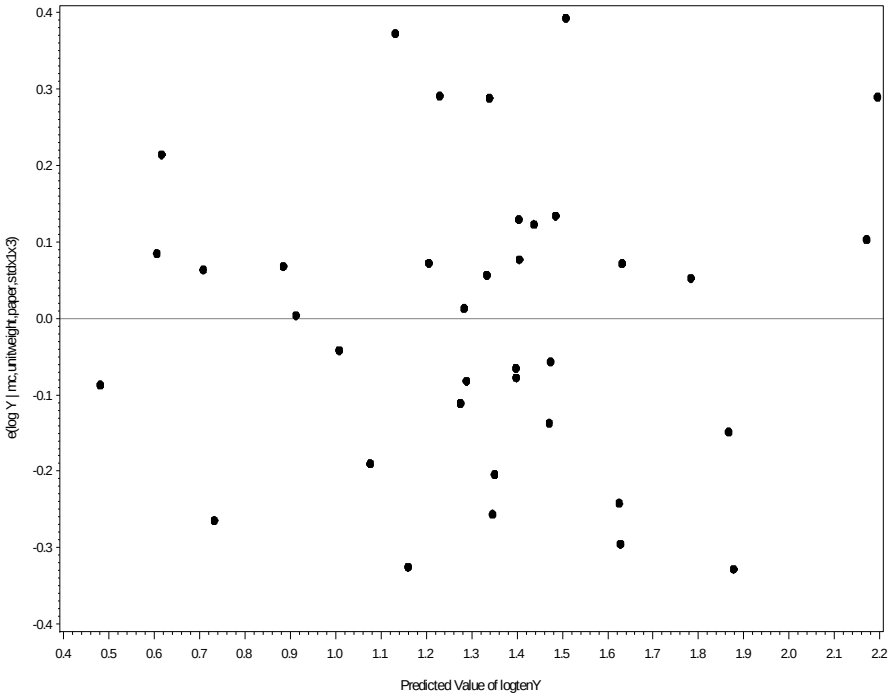

Figure 5.13 Residuals versus Predicted Value of Log Resistivity

Modified Levene Test:

To conduct this test, the data is divided into two groups of about the same number of observations. The cutoff value "1.35" was used. Group 1 has 19 observations and group 2 has 18 observations (Table 5.12). The steps followed to conduct this test are:

1. Calculate absolute deviations of the residuals around their group medians:

   $d_{i1} = 0.1509$ $d_{i2} = 0.1628$

2. Test variance of 2 groups: d_{i1} and d_{i2} ($\alpha = 0.1$)

   Hypothesis: H_0: Variances of $d_{i1}$and $d_{i2}$are equal.

   H_1: Variances of $d_{i1}$and $d_{i2}$are not equal.

   Decision rule if P-Value (F-test) < 0.1 then rejects H_0

   From SAS output, 0.6212 > 0.1 then fail to reject H_0

   Conclusion: variances of two groups are equal

3. Conduct two-sample *t*-test on the d_{i1} and d_{i2} ($\alpha = 0.1$)

   Hypothesis: H_0: Means of d_{i1} and d_{i2} populations are equal.

   H_1: Means are not equal.

   Decision rule if P-Value (t-test) < 0.1 then rejects H_0

   From SAS output, 0.7489> 0.1 then fail to reject H_0

   Conclusion: Means of two groups are equal

Therefore, we are 90% confident that the constant variance assumption is satisfied.

Table 5.12 Modified Levene Test for Best Model

group	N	Mean	Std Dev	Std Err	Minimum	Maximum
1	19	0.1509	0.1178	0.0270	0	0.3598
2	18	0.1628	0.1043	0.0246	0.0547	0.3950
Diff (1-2)		-0.0118	0.1115	0.0367		

group	Method	Mean	95% CL Mean		Std Dev	95% CL Std Dev	
1		0.1509	0.0941	0.2077	0.1178	0.0890	0.1742
2		0.1628	0.1109	0.2146	0.1043	0.0783	0.1564
Diff (1-2)	Pooled	-0.0118	-0.0863	0.0626	0.1115	0.0904	0.1454
Diff (1-2)	Satterthwaite	-0.0118	-0.0860	0.0624			

Method	Variances	DF	t Value	Pr > |t|
Pooled	Equal	35	-0.32	0.7489
Satterthwaite	Unequal	34.851	-0.32	0.7481

Equality of Variances

Method	Num DF	Den DF	F Value	Pr > F
Folded F	18	17	1.27	0.6212

5.6.4.3 Normality

The normal probability plot for the best model is presented in Figure 5.14. The normal probability plot is mostly straight and indicates normality is reasonably close. The normality test is used to verify the results from the normal probability plot.

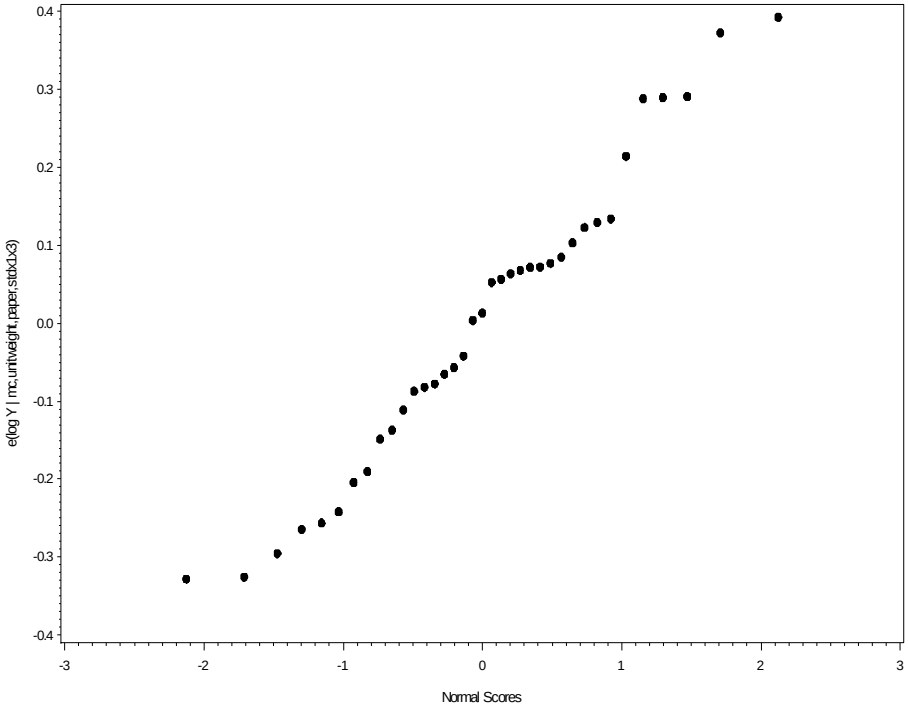

Figure 5.14 Normal Probability Plot for Best Model

Normality Test:

Hypothesis H_0: Normality is satisfied.

H_1: Normality is violated.

Decision rule if sample correlation between residuals and normal score (ρ) is less than cutoff $c(\alpha, n)$, then reject H_0

Use $\alpha = 0.1$; $c\ (0.1, 37) = 0.977$;

$\rho = 0.98908$ (from Table 5.13) >0.977

Therefore, fail to reject (FTR) H_0

Hence, given the results of the plot and the test, it is reasonable to conclude that the residuals are close to following a normal distribution.

Table 5.13 Normality Test for Best Model

Pearson Correlation Coefficients, N = 37 Prob > |r| under H0: Rho=0		
	e2	enrm2
e2	1.00000	0.98908
e(log Y | mc,unitweight,paper,stdx1x3)		<.0001
enrm2	0.98908	1.00000
Normal Scores	<.0001	

5.7 Best Model

The best model can be expressed as:

$$\widehat{\log y} = 3.00221 - 0.01396x_1 - 0.01936x_2 - 0.01001x_3 + 0.08136stdx_1x_3$$

where:

y is the electrical resistivity in ohm-m,

x_1 is the moisture content in percentage (on wet weight basis),

x_2 is the unit weight in lb/ft^3,

x_3 is the paper composition in percentage, and

$stdx_1x_3$ is the moisture content × percentage paper (standardized) interaction.

As mentioned earlier, interaction terms are commonly standardized to reduced multicollinearity among predictor variables. Standardization is done by centering the mean to zero (subtracting by the mean) and scaling the variance to one (dividing by the standard deviation):

$$stdx_1x_3 = \left(\frac{x_1 - \overline{x_1}}{S_{x_1}}\right)\left(\frac{x_3 - \overline{x_3}}{S_{x_3}}\right)$$

$$stdx_1x_3 = \left(\frac{x_1 - 34.44}{15.44}\right)\left(\frac{x_3 - 42.75}{22.26}\right)$$

$$= 0.002909x_1x_3 - 0.124416x_1 - 0.008146x_3 + 0.34835$$

Substituting the standardized interaction term with the above expression, the final regression model can be expressed as:

$$\widehat{\log y} = 3.35056 - 0.0240825x_1 - 0.01936x_2 - 0.018156x_3 + 0.00023668x_1x_3$$

Since the purpose of the developed model is to estimate moisture content from resistivity, the model is re-arranged to:

$$x_1 = \frac{3.35056 - logy - 0.01936x_2 - 0.018156x_3}{0.0240825 - 0.00023668x_3} \quad (5.2)$$

5.7.1 Discussion on Best Model

It can be seen from Table 5.14 that the developed model has all predictors significant at the α = 0.05 level. The predictor variables percentage "others" and organic content are no longer in the model because it was determined that they are not statistically significant. Also, there is no serious multicollinearity among the predictors because the variance inflation factors (VIFs) are not much higher than 1.0 (where VIFs of 1.0 indicate no multicollinearity).

Table 5.14 Parameter Estimates for Best Model

Parameter Estimates

Variable	DF	Parameter Estimate	Standard Error	t Value	Pr > |t|	Variance Inflation
Intercept	1	3.00221	0.19200	15.64	<.0001	0
mc	1	-0.01396	0.00265	-5.26	<.0001	1.43637
unitweight	1	-0.01936	0.00425	-4.56	<.0001	1.30816
paper	1	-0.01001	0.00162	-6.20	<.0001	1.10597
stdx1x3	1	0.08136	0.03794	2.14	0.0397	1.23043

The ANOVA table for the best model is presented in Table 5.15. The total variability in the logarithm of electrical resistivity is the total sum of squares (SSTO), which is equal to 7.13. The variability in the logarithm of electrical resistivity that is explained by the model is the regression sum of squares (SSR), which is equal to 5.78. The variability in the logarithm of electrical resistivity that remains unexplained by the model is the error sum of squares (SSE), which is equal to 1.35. The ANOVA table also shows the coefficient of determination, $R^2 = 0.8111$, which indicates that 81.1% of total variability in the logarithm of electrical resistivity is explained by the regression model with predictors moisture content, unit weight, percentage paper, and stdx_1x_3.

Table 5.15 Analysis of Variance (ANOVA) for Best Model

Analysis of Variance

Source	DF	Sum of Squares	Mean Square	F Value	Pr > F
Model	4	5.77989	1.44497	34.35	<.0001
Error	32	1.34628	0.04207		
Corrected Total	36	7.12618			

Root MSE	0.20511	R-Square	0.8111
Dependent Mean	1.31725	Adj R-Sq	0.7875
Coeff Var	15.57126		

5.7.2 Plots of Best Model

Plots of the best model are presented in this section. Since the best model is a 4-D model that is difficult to imagine, one variable (percentage paper) was fixed, and a 3-D plot was prepared using MATLAB. Figure 5.15 and Figure 5.16 present surface plots of the model for a paper composition of 20% and 40%, respectively. Similar plots can be prepared for other compositions.

Also, 2D plots (set of curves) were prepared by fixing the two variables: unit weight and percentage paper. The plots were prepared for unit weights of 45, 55, and 65 lb/ft^3 as presented in Figure 5.17 and Figure 5.18. The unit weight of MSW in a landfill depends primarily on the compaction practices used in the field, the depth of the sample (overburden pressure), the age of the waste, and the composition of the waste. Studies have shown that the unit weight of MSW increases with depth and decomposition. Also, the presence of high amounts of soil and fines tend to increase the unit weight of MSW. All these factors have to be considered in order to estimate the unit weight of MSW.

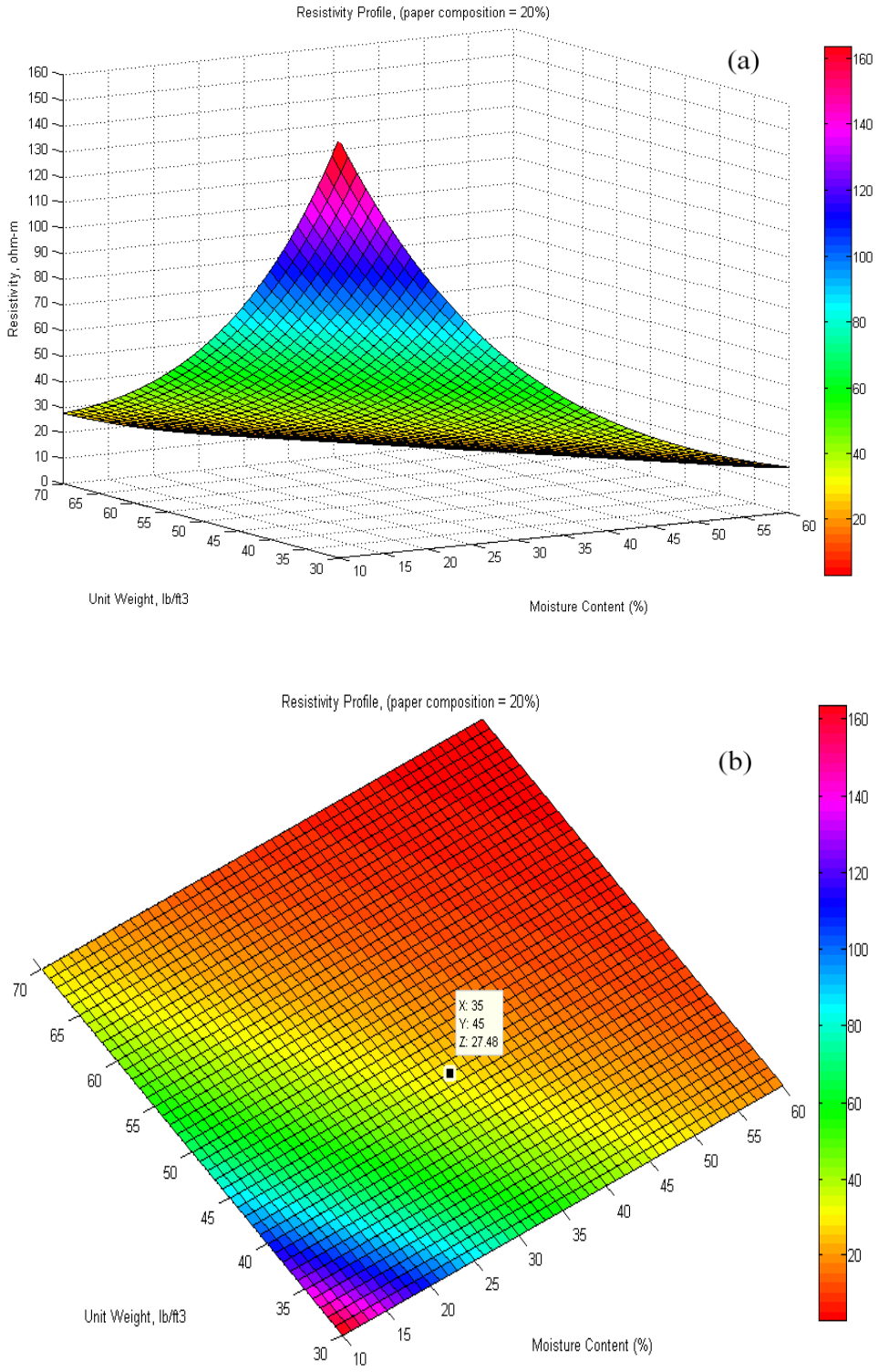

Figure 5.15 Plot of Best Model for Paper Composition = 20%
(a) Surface Plot; (b) Rotated View

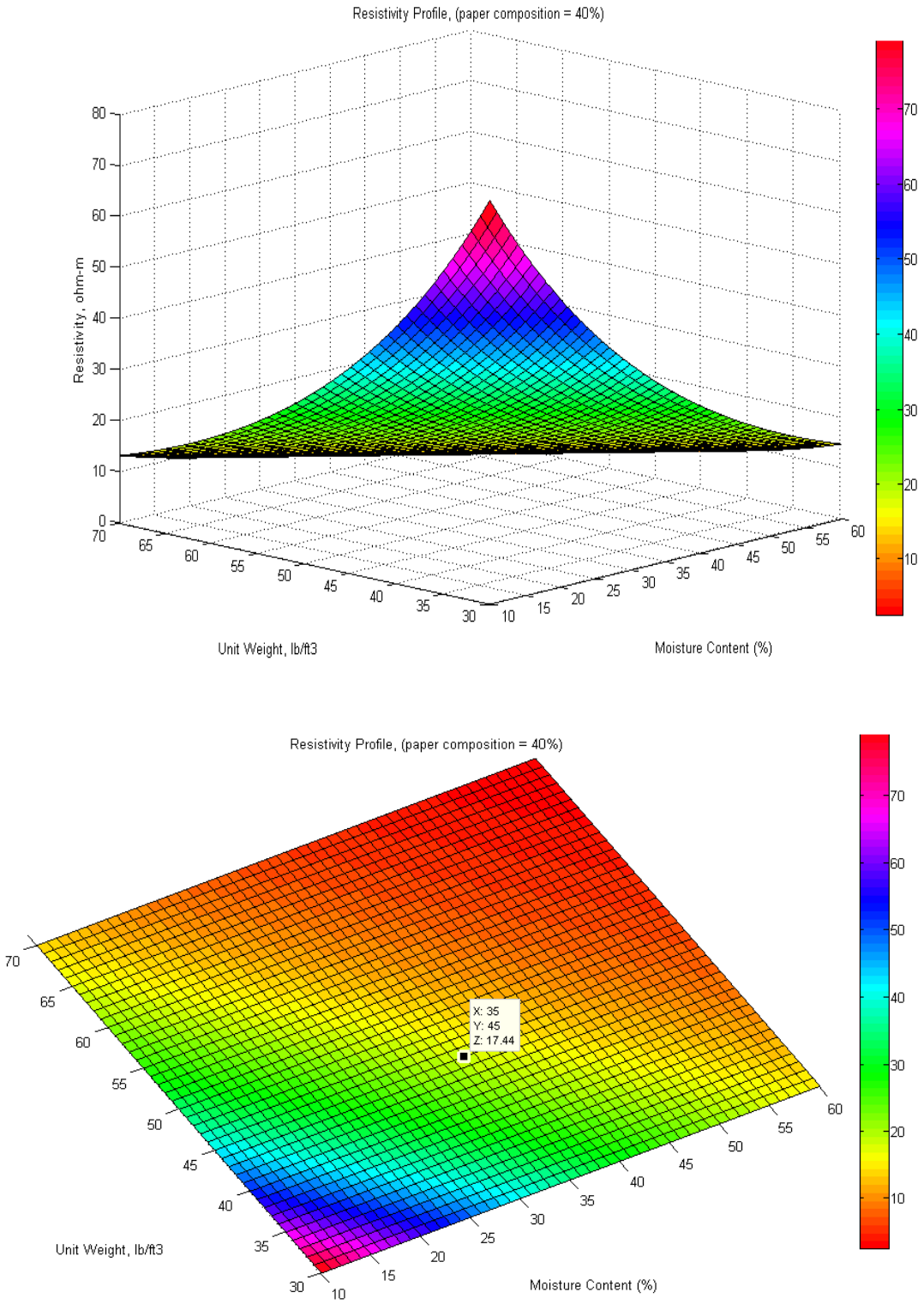

Figure 5.16 Plot of Best Model for Paper Composition = 40%
(a) Surface Plot; (b) Rotated View

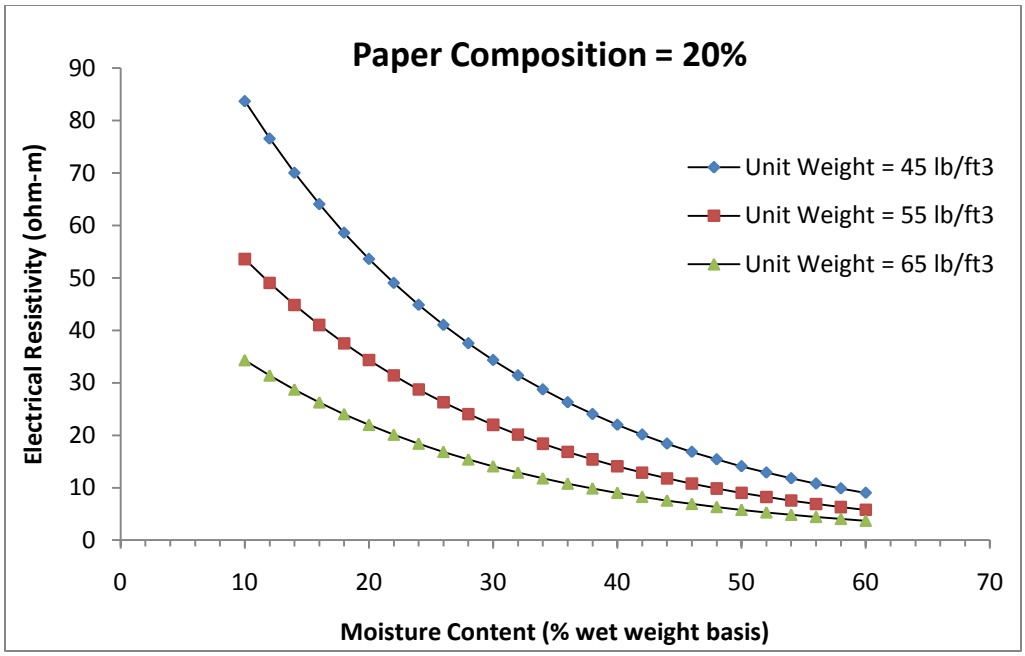

Figure 5.17 Plot of Best Model for Paper Composition = 20% for Different Values of Unit Weight

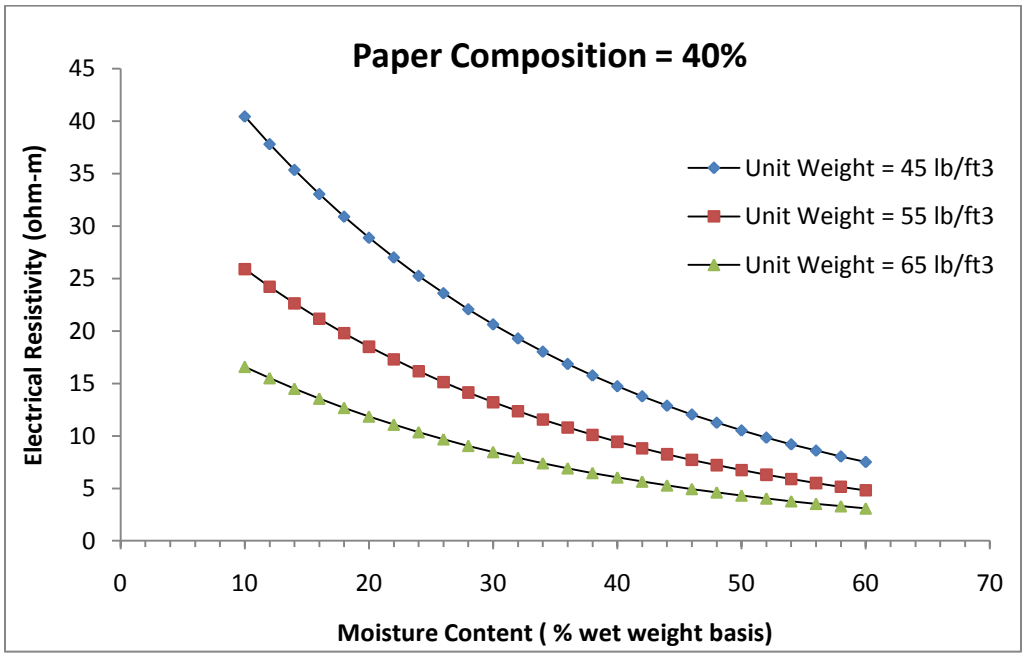

Figure 5.18 Plot of Best Model for Paper Composition = 40% for Different Values of Unit Weight

5.8 Model Validation

In this section, an attempt is made to validate the developed model with resistivity values from the field. A second set of landfilled MSW samples was collected from the City of Denton Landfill as discussed in Chapter 3 and was used for model validation. The moisture content and physical composition of the collected samples were determined in the laboratory. Electrical resistivity imaging was conducted at the same location from which the samples were collected. Using the field resistivity values and the developed model, the moisture content was estimated. The estimated moisture content was then compared with the actual measured moisture content. Details are discussed next.

5.8.1 Resistivity Imaging

Two dimensional (2D) resistivity imaging was conducted at the landfill between the two boreholes B70 and B72 in March 2011 (Figure 5.19). Fifty six electrodes at 6ft spacing were utilized in a dipole-dipole array. A programmable eight channel SuperSting R8/IP resistivity meter was used. The collected data was processed using Earth Imager 2D software. This software uses a forward modeling subroutine to calculate apparent resistivity values, which is then inverted using a nonlinear least squares optimization technique. The resistivity profile between B70 and B72 is presented in Figure 5.20.

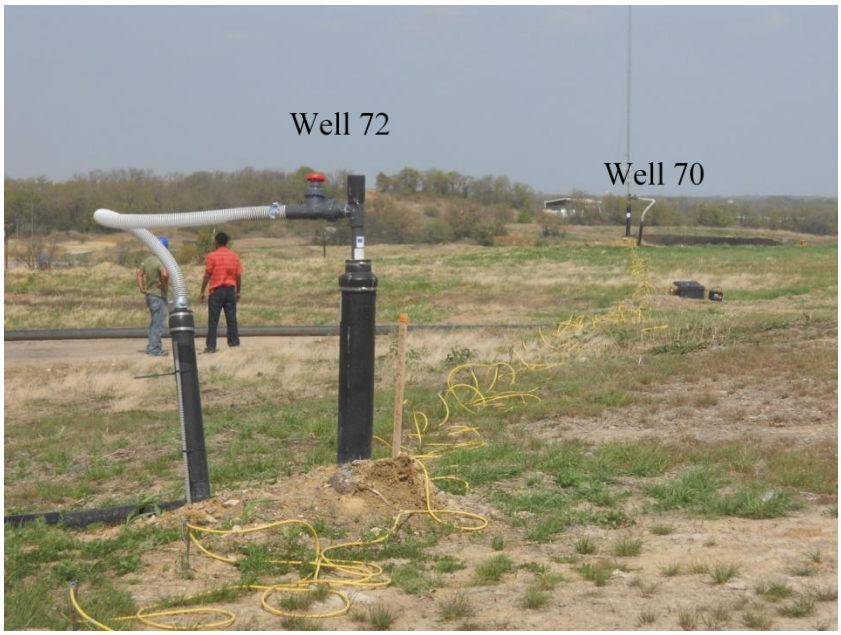

Figure 5.19 Resistivity Imaging Line between Well 70 and Well 72

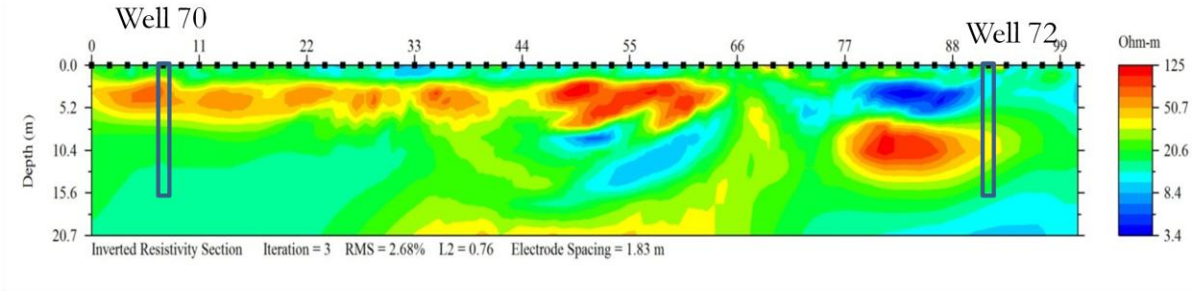

Figure 5.20 Resistivity Profile between Well 70 and Well 72

5.8.2 Moisture Content Estimation

In this section, resistivity values from the field will be used to estimate the moisture content using the developed model:

$$x_1 = \frac{3.35056 - logy - 0.01936x_2 - 0.018156x_3}{0.0240825 - 0.00023668x_3}$$

Resistivity values from the field have to first be corrected to a standard temperature of 70ºF. The resistivity survey was conducted on March 25th, 2001. On that day, the low daily temperature was 49ºF, the high daily temperature was 71ºF, and the mean daily temperature was 60ºF. These temperatures represent the ambient air temperature and do not necessarily represent the waste temperature at different depths. Temperature within the waste mass is expected to increase with depth.

The temperature profile within the waste is estimated following the method used by Yesiller et al. (2005) and Liu (2007). According to the authors, baseline waste temperatures can be estimated using the analytical formulation for sinusoidal fluctuation of temperature with depth:

$$T_{(x,t)} = T_m - A_s e^{-x\sqrt{\pi/365s\alpha}} cos\left[\frac{2\pi}{365s}\left(t - t_0 - \frac{x}{2}\sqrt{\frac{365s}{\pi\alpha}}\right)\right] \quad (5.3)$$

where

$T_{(x,t)}$ = temperature (ºF) at depth *x* and time *t*

T_m = mean annual earth temperature (ºF)

A_s = amplitude of surface temperature wave (ºF)

x = depth below surface (m)

s = 86,400 sec

α = thermal diffusivity (m^2/day)

t = time of year in days (where 0 = midnight December 31)

t_0 = phase constant = 34.6 days = 2,989,440 sec

These baseline waste temperatures represent seasonal temperature variations in the waste but neglects the internal heat generation due to waste decomposition. According to Hanson et al. (2010), the temperature of the waste initially increases with

depth, reaching a peak value at middle depth, and then starts to decrease slightly. A study done on waste of different age (Figure 5.21) showed that the temperature profiles shifted to the left with age, indicating that most of the heat generation occurs during the early years of waste placement.

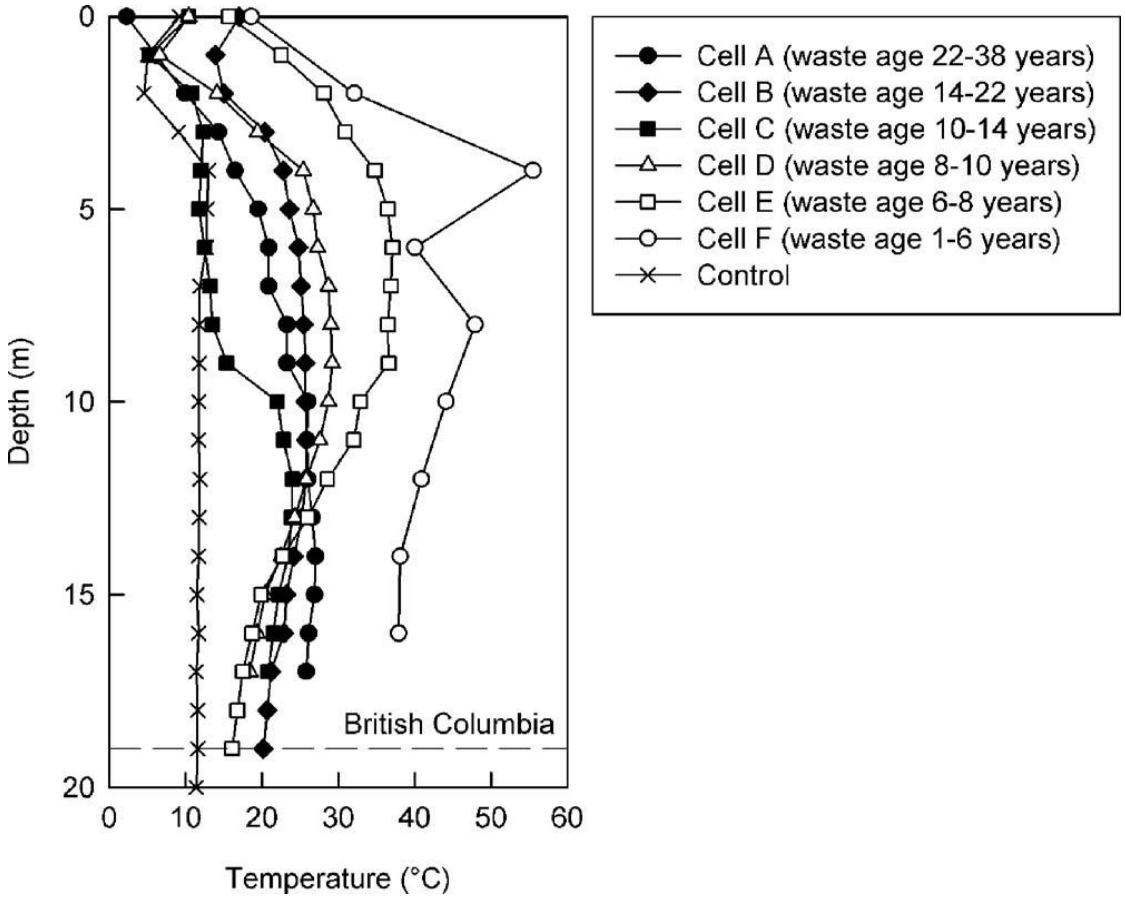

Figure 5.21 Effect of Waste Age on Waste Temperature (Hanson et al., 2010)

Since the resistivity survey was done on a closed section of the landfill in which the waste was approximately 20 to 25 years old, it is reasonable to estimate the temperature profile using equation (5.3), neglecting the heat generation by the waste. A mean annual earth temperature of 67ºF was used for the Dallas-Fort Worth area. An amplitude of surface temperature wave of 59ºF (15ºC) and a thermal diffusivity of 5 x10^{-7}

m^2/s were used as suggested by Liu, 2007. The resulting temperature profile is presented in Figure 5.22.

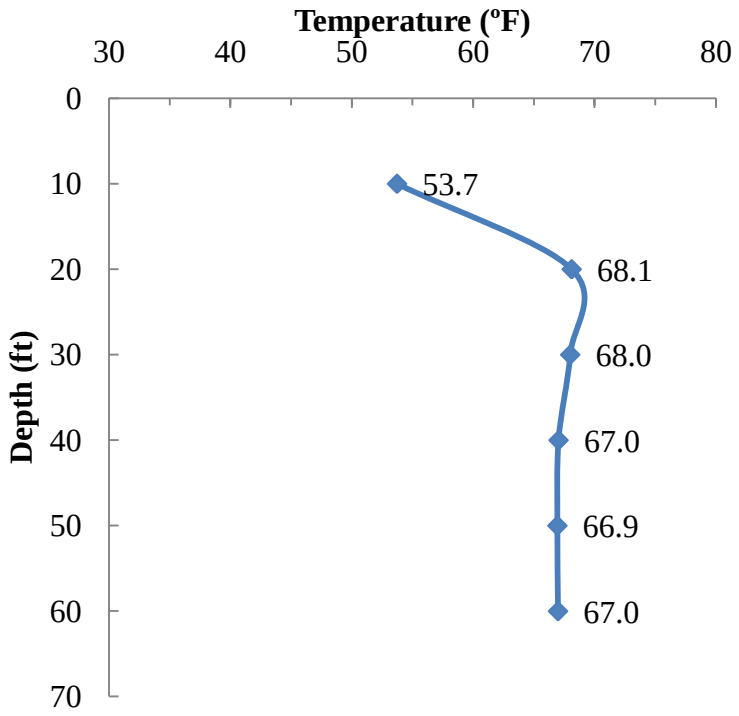

Figure 5.22 Temperature Profile with Depth (March 25, 2011)

The samples collected from the first 20ft will not be considered in the validation step. The reason behind that is that the waste samples were collected in November 2010 while the resistivity imaging was done at the landfill in March 2011. During these four months, the moisture content of the waste in the top 20ft might have changed due to weather and rainfall events. The moisture content of the waste at higher depths (30 to 60ft) is expected to remain constant. From the temperature profile presented in Figure 5.22, the temperature ranged from 68ºF at 30ft depth to 67ºF at 60ft depth. Therefore, it is concluded that the effect of temperature on resistivity is not significant for this study.

To estimate the moisture content of MSW using the field resistivity values, an average percentage of paper of 43.9% and 15.8% (from physical composition results) were used for samples from B70 and B72 respectively. The unit weight of the samples was estimated according to the compaction practices followed at the landfill. According to landfill personnel, an average unit weight of 1000 lb/yd^3 (40 lb/ft^3) is typical for fresh waste in the top layers of the landfill. For B70, a unit weight of 40 lb/ft^3 was used for samples from the top layers. Higher unit weights were used for samples at higher depths to account for the effect of overburden pressure. For B72, a unit weight of 60 lb/ft^3 was used for samples from the top layers. That is because samples from B72 were mostly cover soil and contained less paper products; thus a higher unit weight was used to account for increased fines content.

The moisture contents predicted using the model were compared with the measured moisture contents and the percentage error was determined. Good agreement was found between the estimated moisture contents and the measured ones. Results are presented in Table 5.16 and 5.17 for B70 and B72, respectively. As mentioned earlier, samples from the top 20 ft will not be considered. The percentage error ranged from 4.9 to 10.2 percent and from 0.5 to 13.8 percent for samples from B70 and B72, respectively. Figure 5.23 and Figure 5.24 present the predicted and measured moisture content profiles with depth for MSW samples from boreholes B70 and B72, respectively. Also, a plot of the predicted versus the measured moisture contents for all samples is presented in Figure 5.25.

Table 5.16 Predicted Moisture Content of Samples from Borehole B70

Sample #	Depth (ft)	Depth (m)	Paper (%)	Moisture Content (%)	Unit Weight (lb/ft^3)	Resistivity (ohm-m)	M/C from resistivity (%)	% error
1	10	3.0	43.9	29.51	40	58.3	0.98	-96.7
2	20	6.1	43.9	17.38	40	41.1	12.07	-30.6
3	30	9.1	43.9	28.61	45	18.4	30.49	6.6
4	40	12.2	43.9	31.32	45	16.2	34.53	10.2
5	50	15.2	43.9	32.16	46	15.2	35.14	9.3
6	60	18.3	43.9	33.94	48	13.7	35.60	4.9

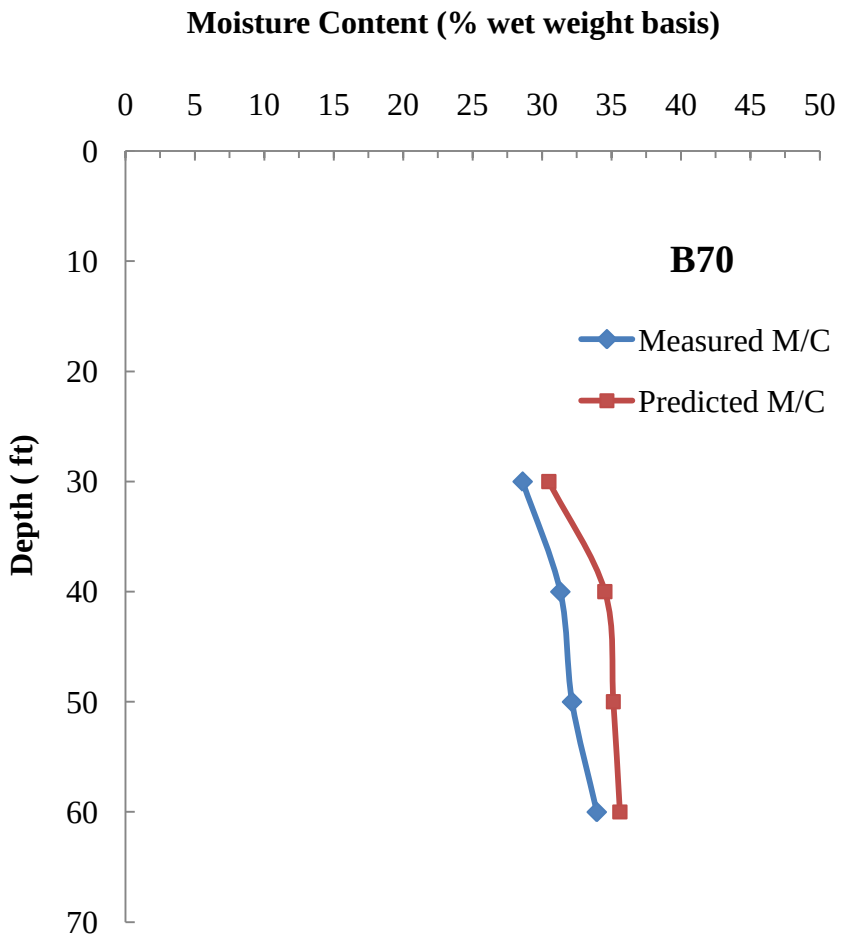

Figure 5.23 Predicted and Actual Moisture Content Profile for Borehole B70

Table 5.17 Predicted Moisture Content of Samples from Borehole B72

Sample #	Depth (ft)	Depth (m)	% Paper	Moisture Content (%)	Unit Weight (lb/ft^3)	Resistivity, ohm-m	M/C from resistivity (%)	% error
1	10	3.0	0	11.38	120	13.5	-4.28	-137.6
2	20	6.1	15.8	24.37	60	19.6	29.98	23.0
3	30	9.1	15.8	15.52	60	34.9	17.66	13.8
4	40	12.2	15.8	26.39	60	25.9	24.03	-9.0
5	50	15.2	15.8	11.94	80	18.1	12.64	5.9
6	60	18.3	15.8	23.15	80	11	23.28	0.5

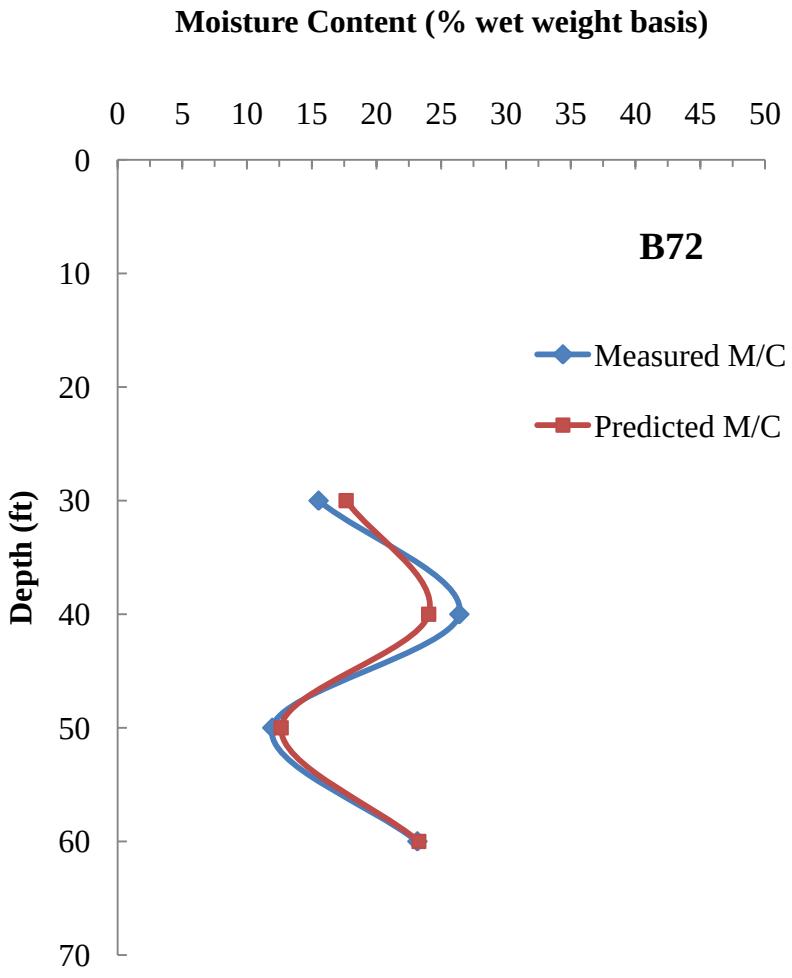

Figure 5.24 Predicted and Actual Moisture Content Profile for Borehole B72

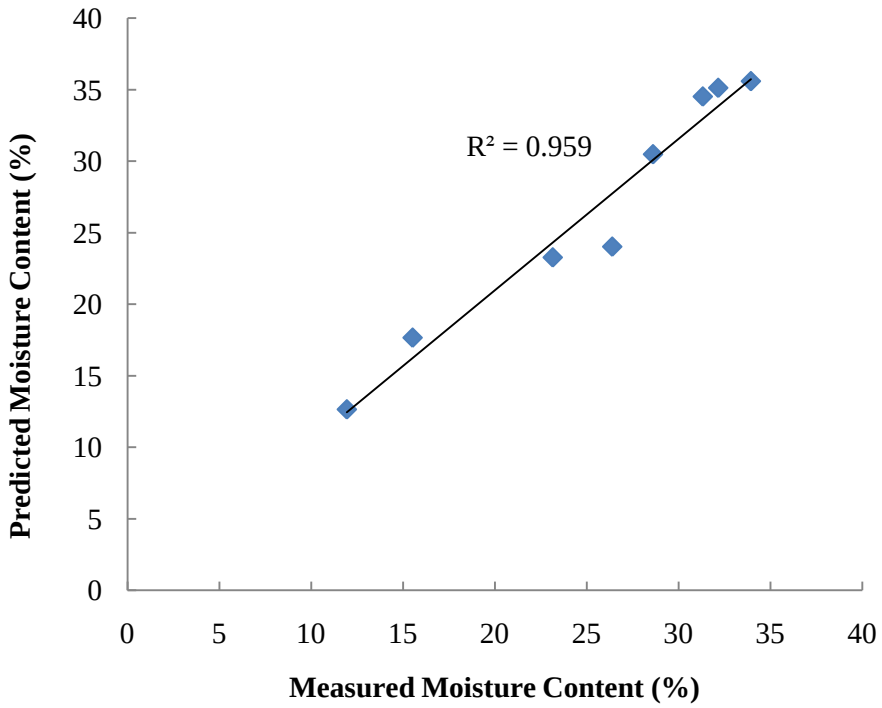

Figure 5.25 Predicted vs. Actual Moisture Contents for all Samples

The moisture content of the landfilled samples from boreholes B70 and B72 was also estimated using Archie's law. The constants 'a' = 1.0 and 'm' = 1.81 were used as determined by resistivity tests conducted on landfilled MSW samples in the laboratory. A resistivity of 1.35 ohm-m was used for the pore fluid resistivity. The moisture contents estimated using Archie's law were compared with the measured moisture contents and the percentage error was determined. Results are presented in Tables 5.18 and 5.19 for B70 and B72, respectively. Figures 5.26 and 5.27 present the moisture content profiles with depth for MSW samples from boreholes B70 and B72, respectively. The percentage error ranged from 6.47 to 14.47 percent and from 5.74 to 55.70 percent for samples from B70 and B72, respectively. These results show that the developed model can predict

moisture content with a better accuracy than Archie's law. This is because Archie's law does not account for the effect of composition of MSW.

Table 5.18 Predicted Moisture Content (Using Archie's Law) of Samples from Borehole B70

Sample #	Depth (ft)	Depth (m)	Moisture Content (%)	Unit Weight (lb/ft^3)	Resistivity (ohm-m)	M/C using Archie's law (%)	% error
1	10	3.0	29.51	40	58.3	19.48	-33.98
2	20	6.1	17.38	40	41.1	23.63	35.98
3	30	9.1	28.61	45	18.4	32.75	14.47
4	40	12.2	31.32	45	16.2	35.14	12.19
5	50	15.2	32.16	46	15.2	35.60	10.71
6	60	18.3	33.94	48	13.7	36.14	6.47

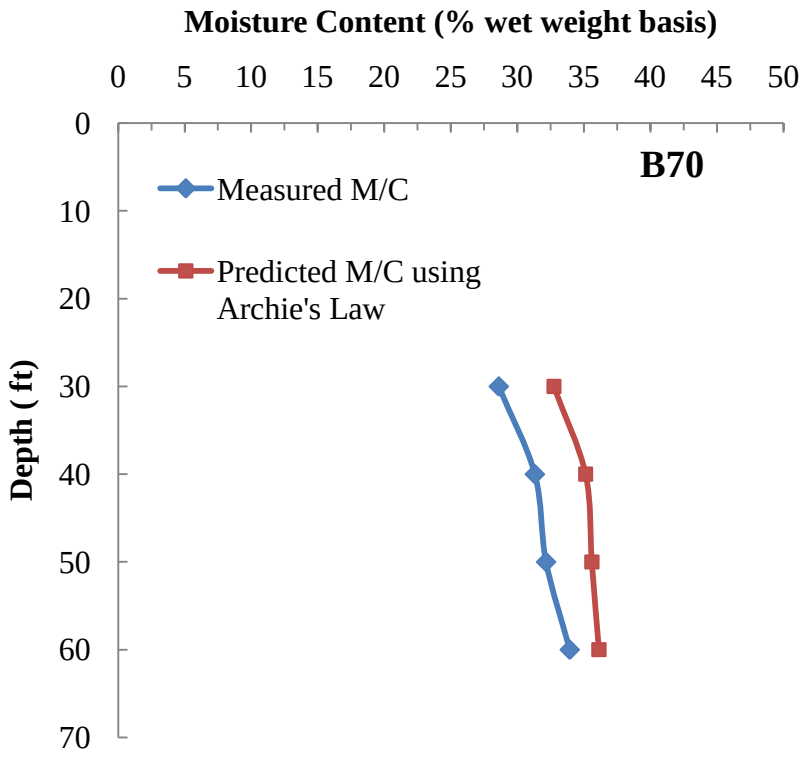

Figure 5.26 Predicted (Using Archie's Law) and Actual Moisture Content Profile for Borehole B70

Table 5.19 Predicted Moisture Content (Using Archie's Law) of Samples from Borehole B72

Sample #	Depth (ft)	Depth (m)	Moisture Content (%)	Unit Weight (lb/ft^3)	Resistivity, ohm-m	M/C using Archie's law (%)	% error
1	10	3.0	11.38	120	13.5	14.57	28.06
2	20	6.1	24.37	60	19.6	23.72	-2.67
3	30	9.1	15.52	60	34.9	17.25	11.12
4	40	12.2	26.39	60	25.9	20.33	-22.95
5	50	15.2	11.94	80	18.1	18.59	55.70
6	60	18.3	23.15	80	11	24.48	5.74

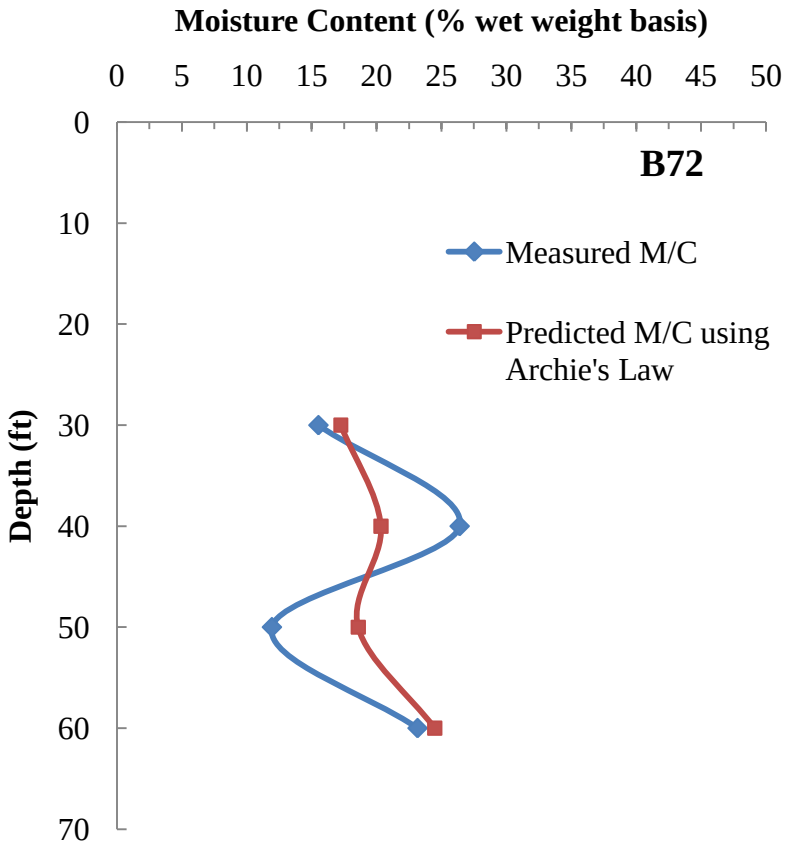

Figure 5.27 Predicted (Using Archie's Law) and Actual Moisture Content Profile for Borehole B72

CHAPTER 6

CONCLUSIONS AND RECOMMENDATIONS

The fundamental aspect in the operation of a bioreactor landfill is the controlled addition of water and/or the recirculation of leachate into the landfill's waste mass. Understanding the moisture distribution within a bioreactor landfill is essential for the design and operation of the leachate recirculation system. In the recent years, there has been a huge interest in using electrical resistivity imaging as a non-destructive tool to monitor the moisture distribution within a bioreactor landfill. However, few studies used electrical resistivity imaging in the solid waste field to provide the spatial distribution of moisture within a landfill and did not give quantitative information about the moisture content of the waste. The overall objective of this research was to develop a correlation between electrical resistivity and moisture content of waste, in order to be able to determine the moisture content of MSW without any direct sampling and laboratory testing.

6.1 Summary and Conclusions

The following results and conclusions are based on the findings of this study:

1. Fresh MSW samples were comprised mainly of paper. The average percentage of paper was 36.32%. Landfilled MSW samples were comprised mainly of "others" (soil and fines). The average percentage of "others" in the landfilled MSW samples collected from five boreholes was 45.96%.

2. The average moisture content of fresh MSW samples was 27.05%. The average moisture content of the landfilled MSW samples collected from five boreholes was 25.64%. The average moisture content of the degraded samples was approximately 70%.
3. The average organic content of fresh MSW samples was 76.2%. The average organic content of the landfilled MSW samples collected from three boreholes was 72.6%. The average organic content of the degraded samples was 52.9%.
4. The average unit weight of five fresh MSW samples compacted by standard proctor compaction effort was 38.9 lb/ft^3.
5. The electrical resistivity of MSW is a complex property that depends on moisture content, unit weight, degree of decomposition, temperature and, composition of the waste.
6. Resistivity decreases with an increase in moisture content. For example, the resistivity of fresh MSW sample #1 decreased from 21.6 ohm-m at moisture content of 21.4% to 2.4 ohm-m at moisture content of 52.6%. The reason behind that is that the electrical current is carried by the ions in the pore fluid. When there is more liquid in the pores, there will be more ions available to carry the current, and therefore conductivity increases and resistivity decreases. Also, results showed that the effect of increasing moisture content on electrical resistivity tapers off beyond a certain point (moisture content of approximately 50 to 55%). This can possibly be explained by the fact that at higher values of moisture content, continuous current flow paths through the pores would have already been established.

7. Electrical resistivity of MSW and volumetric moisture content can be related by Archie's law. The volumetric moisture content term accounts for the effect of unit weight. However, Archie's law does not take into consideration the effect of the stage of decomposition and the effect of the composition of the waste. The constants 'a' and 'm' are specific to the type of MSW and will need to be calibrated for MSW with different composition.
8. From the experimental results, the Archie's law constants 'a' and 'm' were determined to be 0.91 and 1.45 respectively for the fresh MSW samples. For the landfilled MSW samples, the Archie's law constants 'a' and 'm' were determined to be 1.0 and 1.81 respectively. For the degraded MSW samples, the Archie's law constants 'a' and 'm' were determined to be 1.08 and 1.91 respectively. These constants are in the same order for soils and rocks.
9. Electrical resistivity decreases with increasing unit weight of MSW. For example, the resistivity of fresh MSW sample #1 decreased from 21.6 ohm-m at unit weight of 35 lb/ft^3 to 14.9 ohm-m at unit weight of 55 lb/ft^3. As the unit weight increases, the air voids are reduced, resulting in an increase in the degree of saturation. An increase in saturation means that more voids are filled with liquid, creating more paths for current flow, and therefore decreasing the electrical resistivity.
10. Electrical resistivity tests conducted on degraded MSW samples indicate some decrease in resistivity with decomposition. At a moisture content of approximately 71%, the resistivity of degraded samples decreased from 8.98 ohm-m (phase 1) to 4.91 ohm-m (phase 4). This decrease in resistivity is most probably caused by the increase in unit weight as a result of decomposition. Unit weight of

MSW typically increases with decomposition. This is because as larger particles are broken down to smaller particles, the air voids are reduced resulting in an increase in unit weight.

11. Electrical resistivity of MSW decreases with increasing temperature. For example, the resistivity of fresh MSW sample #1 decreased from 13.47 ohm-m at temperature of 60.2°F to 9.32 ohm-m at temperature of 98.3°F. An increase in temperature decreases the viscosity of liquid in the pores, causing the ions in the liquid to become more mobile. Thus, the electrical conductivity increases and the resistivity decrease with increasing temperature. Field resistivity values have to be corrected to a standard temperature to account for the effect of temperature. Laboratory tests done on five fresh MSW samples confirmed that Keller and Frischknecht (1966) equation can be used for temperature correction using a temperature coefficient of 0.02 per degree Celsius. In other words, the results showed that resistivity of MSW decreases by 2% per temperature increase of 1°C.
12. Based on the experimental results, the composition of MSW affects the resistivity. MSW samples having same moisture content and same unit weight had different resistivity values, indicating that the composition of the waste itself affects resistivity. A decrease in electrical resistivity with increasing paper content was observed. This is probably due to the fact that paper products tend to absorb more water, and increases in paper content usually correspond to higher moisture content. On the other hand, an increase in electrical resistivity with increasing "others" (soil and fines) content was observed. This behaviour can be explained

by the fact that an increase in the fines content will decrease the porosity, reducing the amount of voids available for current flow.

13. Based on the experimental results, the effect of the pore fluid composition on the resistivity of MSW is not significant. Same MSW samples had close resistivity values (difference of less than ten percent most of the time) when prepared using tap water, leachate, or re-use water. This is because when a liquid is added to a waste sample, the liquid extracts the soluble inorganic and organic compounds present in the waste, and the resistivity of the liquid stabilizes at some constant value. In other words, due to the presence of high amount of inorganic and organic compounds in the waste itself, the content of the waste is more controlling than the type of fluid in the pores.

14. Multiple linear regression analysis was used to quantify the effect of the several factors that affect resistivity. Five predictor variables were considered: moisture content, unit weight, percentage paper, percentage "others" (fines), and organic content. The best model, which was selected using backward elimination method, best subsets selection method, and stepwise regression method, has an adjusted R^2 value of 0.7875. The best model is given by:

$$\widehat{\log y} = 3.00221 - 0.01396x_1 - 0.01936x_2 - 0.01001x_3 + 0.08136stdx_1x_3$$

where y is the electrical resistivity in ohm-m, x_1 is the moisture content in percentage (on wet weight basis), x_2 is the unit weight in lb/ft^3, x_3 is the paper composition in percentage. The predictor variables percentage "others" and organic content are no longer in the model because it was determined that they are not statistically significant.

15. Since the purpose of the developed model is to estimate moisture content from resistivity, the model is re-arranged to:

$$\hat{x}_1 = \frac{3.35056 - \log y - 0.01936x_2 - 0.018156x_3}{0.0240825 - 0.00023668x_3}$$

This model can be used to estimate the moisture content of MSW using field resistivity values.

16. The developed model was validated using a second set of landfilled MSW samples. The moisture content and physical composition of the collected samples were determined in the laboratory. Electrical resistivity imaging was conducted at the same location from which the samples were collected. Using the field resistivity values and the developed model, the moisture content was estimated. The estimated moisture content was then compared with the actual measured moisture content. Good agreement was found between the estimated moisture contents and the measured ones. The percentage error ranged from 4.9 to 10.2 percent and from 0.5 to 13.8 percent for samples from B70 and B72, respectively.

6.2 Recommendations for Future Studies

Based on this study, the following are recommendations are given for future studies:

1. Some improvements can be done to the resistivity test box. Instead of using a separate mold to compact MSW samples and then transfer the samples to the resistivity test box, it is recommended to compact the samples directly in the resistivity test box. This can be done by using a test box made of an insulating material such as polyvinyl chloride (PVC). PVC is durable to high compaction

efforts and will not affect the resistivity readings because it is an electrical insulator.

2. It is recommended to prepare two or more degraded MSW samples by using laboratory scale reactors to confirm the effect of decomposition on resistivity of MSW.
3. The effect of the composition of MSW on resistivity can be further investigated. The model considered only the percentage of paper and the percentage of ‘others” because these were the dominant components in the studied waste. It will be interesting to determine how high percentage of food waste for example affects resistivity. This can be achieved by preparing waste samples of different compositions at the laboratory.
4. Understanding the temperature profile within the waste with depth is important in order to correct the field resistivity values to a standard temperature. It is recommended to install temperature sensors within the waste to understand better the internal heat generation due to waste decomposition and the effect of the recirculated leachate on temperature.
5. For the model validation step, it is recommended to collect MSW samples within a short time period after conducting the resistivity survey in the field. This ensures that the moisture content of the waste at the field did not change due to weather or rainfall events.
6. It is recommended to collect more MSW samples from different sites of the landfill, and from different landfills to validate the model and to determine how accurately the model can be used to estimate moisture content.

REFERENCES

1. Abu-Hassanein, Z. S., Benson, C. H., & Blotz, L. R. (1996). "Electrical resistivity of compacted clays." *Journal of Geotechnical Engineering*, 397-406.
2. Amidu, S. (2008). "Electrical Resistivity Imaging for Characterizing Dynamic Hydrologic Systems." PhD Dissertation, Baylor University.
3. Archie, G. E. (1942). "The electrical resistivity log as an aid in determining some reservoir characteristics." *Transactions American Institute of Mining Metallurgical and Petroleum Engineers, 146*, 54-67.
4. ASTMG57. (2006). "Standard Test Method for Field Measurement of Soil Resistivity Using the Wenner Four-Electrode Method."
5. AWWA, APHA, & WEF. (2005). "Standard Methods for the Examination of Water and Wastewater."
6. Barlaz, M. A., Ham, R. K., & Schaefer, D. M. (1990). "Methane Production from Municipal Refuse: a Review of Enhancement Techniques and Microbial Dynamics." *Critical Reviews in Environmental Control, 19*(6), 557-584.
7. Brunet, P., Clement, R., & Bouvier, C. (2010). "Monitoring soil water content and deficit using Electrical Resistivity Tomography (ERT) - A case study in the Cevennes area, France." *Journal of Hydrology, 380*, 146-153.
8. Carpenter, P. J., Calkin, S. F., & Kaufmann, R. S. (1991). "Assessing a fractured landfill cover using electrical resistivity and seismic refraction techniques." *Geophysics, 56*(11), 1896-1904.

9. Clement, R., Descloitres, M., Gunther, T., Oxarango, L., Morra, C., Laurent, J., et al. (2010). "Improvement of Electrical Resistivity Tomography for Leachate Injection Monitoring." *Waste Management, 30*, 452-464.
10. Dahlin, T. (2001). "The Development of DC Resistivity Imaging Techniques." *Computers and Geociences*, 1019-1029.
11. Drahor, M. (2006). "Application of Electrical Resistivity Tomography Technique for Investigation of Landslides: a case from Turkey." *Environmental Geology, 50*, 147-155.
12. EPA. (2009). "Municipal Solid Waste Generation, Recycling, and Disposal in the United States: Fact and Figures for 2009."
13. Fassett, J. B., Leonards, G. A., & Repetto, P. C. (1994). "Geotechnical Properties of Municipal Solid Wastes and their Use in Landfill Design." *Proceedings, Waste Tech '94 Conference* . Charleston, S.C.
14. Gabr, M. A., & Valero, S. N. (1995). "Geotechnical Properties of Municipal Solid Waste." *Geotechnical Testing Journal, 18*(2), 241-251.
15. Gomes, C., Lopes, M. L., & Lopes, M. G. (2005). "A study of MSW Properties of a Portuguese Landfill." *Proceedings of International Workshop on Hydro-Physico Mechanics of Landfills.* Lirigm, France.
16. Goyal, V. C., Gupta, P. K., Seth, S. M., & Singh, V. N. (1996). "Estimation of Temporal Changes in Soil Moisture Using Resistivity Method." *Hydrological Processes, 10*, 1147-1154.
17. Grellier, S., Bouye, J., Guerin, R., Robain, H., & Skhiri, N. (2005). "Electrical Resistivity Tomography (ERT) applied to moisture measurements in bioreactor:

principles, in situ measurements and results." *International Workshop "Hydro-Physico-Mechanics of Landfills.* Grenoble, France.

18. Grellier, S., Guerin, R., Robain, H., Bobachev, A., Vermeersch, F., & Tabbagh, A. (2008). "Monitoring of Leachate Recirculation in a Bioreactor Landfill by 2-D Electrical Resitivity Imaging." *Journal of Environmental and Engineering Geophysics, 13*(4), 351-359.
19. Grellier, S., Reddy, K. R., Gangathulasi, J., Adib, R., & Peters, C. C. (2007). "Correlation between Electrical Resistivity and Moisture Content of Municipal Solid Waste in Bioreactor Landfill." *Geotechnical Special Publication No.163*.
20. Grellier, S., Reddy, K., Gangathulasi, J., Adib, R., & Peters, A. (2006). "Electrical Resistivity Tomography Imaging of Leachate Recirculation in Orchard Hills Landfill." *Proceedings of the SWANA Conference.* Charlotte.
21. Grellier, S., Robain, H., Bellier, G., & Skhiri, N. (2006). "Influence of Temperature on the Electrical Conductivity of Leachate from Municipal Solid Waste." *Jounral of Hazardous Materials*, 612-617.
22. Guerin, R., Munoz, M. L., Aran, C., Laperrelle, C., Hidra, M., Drouart, E., et al. (2004). "Leachate Recirculation: Moisture Content Assessment by means of a Geophysical Technique." *Waste Management, 24*, 785-794.
23. Gupta, S. C., & Hanks, R. J. (1972). "Influence of water content on electrical conductivity of the soil." *Soil Science Society of America Proceedings*, (pp. 855-857).

24. Hanson, J., Yesiller, N., & Oettle, N. (2010). "Spatial and Temporal Temperature Distributions in Municipal Solid Waste Landfills." *Journal of Environmental Engineering, 136*(8), 804-814.

25. Haque, A. (2007). "Dynamic Characteristics and Stability Analysis of MSW in Bioreactor Landfills." Ph.D Dissertation, University of Texas at Arlington.

26. Hobbs, B. (1999). "Investigating Brownfield Sites with Electrical Resistivity." *Physics Education, 34*(4), 192-198.

27. Hossain, M. S., & Haque, M. A. (2009). "The Effects of Daily Cover Soils on Shear Strength of Municipal Solid Waste in Bioreactor Landfills." *Waste Management, 29,* 1568-1576.

28. Hossain, M. S., Kemler, V., Dugger, D., & Penmethsa, K. (2010). "Monitoring Moisture Movement withing Municipal Solid Waste in Enhanced Leachate Recirculation Landfill Using Resistivity Imaging." *Proceedings of the 1st International Conference on Final Sinks, Sep 23-25.* Vienna, Austria.

29. Imhoff, P. T., Reinhart, D. R., Englund, M., Guerin, R., Gawande, N., Han, B., et al. (2007). "Review of state of the art methods for measuring water in landfills." *Waste Management, 27,* 729-745.

30. ITRC. (2008). "Characterization, Design, Construction, and Monitoring of Bioreactor Landfills."

31. Jackson, P. D., Taylor, S. D., & Stanford, P. N. (1978). "Reistivity-Porosity Particle Shape Relationships for Marine Sands." *Geophysics, 43*(6), 1250-1268.

32. Kalinski, R. J., & Kelly, W. E. (1993). "Estimating Water Content of Soils from Electrical Resistivity." *Geotechnical Testing Journal, 16*(3), 323-329.

33. Kavazanjian, E. J. (2001). "Mechanical Properties of Municipal Solid Waste." *Proceedings of 8th International Landfill Symposium.* Sardina, Italy.

34. Kavazanjian, E. J., Matasovic, N., Stokoe, K., & Bray, J. (1996). "In Situ Shear Wave Velocity of Solid Waste from Surface Wave Measurements." *Environmental Geotechnics, 1*, 97-102.

35. Kearey, P., Brooks, M., & Hill, I. (2002). *An Introduction to Geophysical Exploration.* Blackwell Science.

36. Keller, G. V., & Frischknecht, F. C. (1966). *Electrical Methods in Geophysical Prospecting.* Oxford, Pergamon Press.

37. Landva, A. O., & Clark, J. I. (1990). "Geotechnics of Waste Fill." *Geotechnics of Waste Fill-Theory and Practice*, ASTM STP 1070.

38. Liu, W. (2007). "Thermal Analysis of Landfills." PhD Dissertation, Wayne State University, Michigan.

39. Manassero, M., Van Impe, W. F., & Bouazza, S. (1996). "Waste Disposal and Containment." *Proceedings of the Second International Congress on Environmental Geotechnics*, (pp. 1425 -1474). Japan.

40. McCarter, W. J. (1984). "The Electrical Resistivity Characteristics of Compacted Clays." *Geotechnique, 34*, 263-267.

41. Mehta, R., Barlaz, M., Yazdani, R., Augenstein, D., Bryars, M., & Sinderson, L. (2002). "Refuse Decomposition in the Presence and Absence of Leachate Recirculation." *Journal of Environmental Engineering*, 228-236.

42. Pacey, J., Augenstein, D., Morck, R., Reinhart, D., & Yazdani, R. (1999). "Bioreactive landfill." *MSW Management*, 53-60.

43. Pohland, F. G. (1975). "Sanitary landfill stabilization with leachate recycle and residential treatment." EPA Grant No. R-801397, U.S.E.P.A. Cincinnati: National Environmental Research Center.

44. Pohland, F. G., & Harper, S. R. (1986). "Critical Review and Summary of Leachate and Gas Production from Landfills." EPA/600/2-86/073, OH, USA.

45. Reddy, K. (2006). "Geotechnical Aspects of Bioreactor Landfills." *IGC 2006*, (pp. 79-94). Chennai, India.

46. Reddy, K. R., Hettiarachchi, H., Parakalla, N. S., Gangathulasi, J., & Bogner, J. E. (2009). "Geotechnical Properties of Fresh Municipal Solid Waste at Orchard Hills Landfill, USA." *Waste Management, 29*(2), 952-959.

47. Reinhart, D. R., & Townsend, T. G. (1998). *Landfill bioreactor design and operation.* New York, Lewis.

48. Reinhart, D., & Al-Yousfi, B. (1996). "The Impact of Leachate Recirculation on Municipal Solid Waste Landfill Operating Characteristics." *Waste Management and Research*, 337-346.

49. Reinhart, D., & Townsend, T. (2007). "Update on Florida NRRL Bioreactor Landfill Demonstration Project." Presented at the Illinois Recycling & Solid Waste Conference and Trade Show.

50. Reynolds, J. M. (1997). *An Introduction to Applied and Environmental Geophysics.* New York, John Wiley & Sons Ltd.

51. Rosqvist, H., Dahlin, T., Fourie, A., Rohrs, L., Bengtsson, A., & Larsson, M. (2003). "Mapping of Leachate Plumes at Two Landfill Sites in South Africa

Using Geoelectrical Imaging Techniques." *Proceedings Sardinia, Ninth International Waste Management and Landfill Symposium* . Cagliari, Italy.

52. Rosqvist, N. H., Dollar, L. H., & Fourie, A. B. (2005). "Preferential Flow in Municipal Solid Waste and Implications for Long-term Leachate Quality: Valuation of Laboratory-Scale Experiments." *Waste Management and Research, 23*, 367-380.
53. Sadek, M. (1993). "A comparative Study of the Electrical and Hydraulic Conductivities of Compacted Clays." Ph.D dissertation, Department of Civil Engineering, University of Californai at Berkeley.
54. Samouelian, A., Cousin, I., Tabbagh, A., Bruand, A., & Richard, G. (2005). "Electrical Resistivity Survey in Soil Science: a review." *Soil & Tillage Research, 83*, 173-193.
55. Schwartz, B., Schreiber, M., & Yan, T. (2008). "Quantifying Field-Scale Soil Moisture Using Electrical Resistivity Imaging." *Journal of Hydrology, 362*, 234-246.
56. Taufiq, T. (2010). "Characteristics of Fresh Municipal Solid Waste." Masters Thesis, University of Texas at Arlington.
57. Tchbanoglaus, G., Theisen, H., & Vigil, S. (1993). *Integrated Solid Waste Management.* New York, NY, McGraw-Hill.
58. Townsend, T. G., Miller, W. L., Lee, H., & Earle, J. F. (1996). "Acceleration of Landfill Stabilization Using Leachate Recycle." *Journal of Environmental Engineering*, 263-268.

59. Turesson, A. (2006). "Water Content and Porosity Estimated from Ground-Penetrating Radar and Resistivity." *Journal of Applied Geophysics, 58*, 99-111.

60. Ward, S. H. (1990). "Resistivity and Induced Polarization Methods." *Geotechnical and Environmental Geopysics, 1*, 147-190.

61. Warith, M. (2002). "Bioreactor landfills: experimental and field results." *Waste Management*, 7-17.

62. Yesiller, N., Hanson, J., & Liu, W. (2005). "Heat Generation in Municipal Solid Waste Landfills." *Journal of Geotechnical and Geoenvironmental Engineering, 131*(11), 1330-1344.

63. Yoon, G. L., & Park, J. B. (2001). "Sensitivity of Leachate and Fine Contents on Electrical Resistivity Variation of Sandy Soils." *Journal of Hazardous Materials*, 147-161.

64. Zeiss, C., & Uguccioni, M. (1997). "Modified flow parameters for leachate generation." *Water Environment Research, 69*(3), 276-285.

65. Zekkos, D., Bray, J., Kavazanjian, E., Matasovic, N., Rathje, E., Riemer, M., et al. (2006). "Unit Weight of Municipal Solid Waste." *Journal of Geotechnical and Geoenvironmental Engineering, 132*(10), 1250-1261.

66. Zomberg, J. G., Jernigan, B. L., Sanglerat, T. H., & Cooley, B. H. (1999). "Retention of Free Liquid in Landfill Undergoing Vertical Expansion." *Journal of Geotechnical and Geoenvironmental Engineering, 125*(7), 583-594.

BIOGRAPHICAL INFORMATION

Huda Shihada received her Bachelor's degree in Chemical Engineering from the American University of Sharjah in 2001. She worked as Process Engineer for one year at Petrofac Limited (Sharjah, UAE) before moving to the U.S. to pursue her graduate studies. She received her Master's degree in Civil Engineering in 2003 from Florida Atlantic University with emphasis on water resources and environmental engineering and worked for one year at the South Florida Water Management District.

In 2006, she was admitted to the doctoral program in the Civil & Environmental Engineering department at the University of Texas at Arlington. During her graduate program, she worked as a graduate teaching assistant for undergraduate courses in the Civil Engineering department. She also worked as a graduate research assistant for Dr. Hossain. She is a member of Chi Epsilon, the national civil engineering honor society. Her research interests include electrical resistivity imaging, bioreactor landfills, landfill gas, and wastewater treatment.